



An *In Situ* Permeable Reactive Barrier for the Treatment of Hexavalent Chromium and Trichloroethylene in Ground Water: Volume 1 Design and Installation



An *In Situ* Permeable Reactive Barrier for the Treatment of Hexavalent Chromium and Trichloroethylene in Ground Water: Volume 1 Design and Installation

David W. Blowes¹
Robert W. Gillham¹
Carol J. Ptacek¹
Robert W. Puls²
Timothy A. Bennett¹
Stephanie F. O'Hannesin¹
Christine J. Hanton-Fong¹
Jeffrey G. Bain¹

¹Department of Earth Sciences
University of Waterloo
Waterloo, Ontario, Canada

²Subsurface Protection and Remediation Division
National Risk Management Research Laboratory
U.S. Environmental Protection Agency
Ada, OK 74820

Cooperative Agreement No. CR-823017

Project Officer
Robert W. Puls
Subsurface Protection and Remediation Division
National Risk Management Research Laboratory
Ada, OK 74820

National Risk Management Research Laboratory
Office of Research and Development
U.S. Environmental Protection Agency
Cincinnati, OH 45268

Notice

The U.S. Environmental Protection Agency through its Office of Research and Development partially funded and collaborated in the research described here under Cooperative Agreement No. CR 823017 to the University of Waterloo. It has been subjected to the Agency's peer and administrative review and has been approved for publication as an EPA document. Mention of trade names or commercial products does not constitute endorsement or recommendation for use.

All research projects making conclusions or recommendations based on environmentally related measurements and funded by the Environmental Protection Agency are required to participate in the Agency Quality Assurance Program. This project was conducted under an approved Quality Assurance Project Plan. The procedures specified in this plan were used without exception. Information on the plan and documentation of the quality assurance activities and results are available from the Principal Investigator.

Foreword

The U.S. Environmental Protection Agency is charged by Congress with protecting the Nation's land, air, and water resources. Under a mandate of national environmental laws, the Agency strives to formulate and implement actions leading to a compatible balance between human activities and the ability of natural systems to support and nurture life. To meet these mandates, EPA's research program is providing data and technical support for solving environmental problems today and building a science knowledge base necessary to manage our ecological resources wisely, understand how pollutants affect our health, and prevent or reduce environmental risks in the future.

The National Risk Management Research Laboratory (NRMRL) is the Agency's center for investigation of technological and management approaches for reducing risks from threats to human health and the environment. The focus of the Laboratory's research program is on methods for the prevention and control of pollution to air, land, water, and subsurface resources; protection of water quality in public water systems; remediation of contaminated sites and ground water; and prevention and control of indoor air pollution. The goal of this research effort is to catalyze development and implementation of innovative, cost-effective environmental technologies; develop scientific and engineering information needed by EPA to support regulatory and policy decisions; and provide technical support and information transfer to ensure effective implementation of environmental regulations and strategies.

Environmental scientists are generally familiar with the concept of barriers for restricting the movement of contaminant plumes in ground water. Such barriers are typically constructed of highly impermeable emplacements of materials such as grouts, slurries, or sheet pilings to form a subsurface "wall." The goal of such installations is to eliminate the possibility that a contaminant plume can move toward and endanger sensitive receptors such as drinking water wells or discharge into surface waters. Permeable reactive barrier walls reverse this concept of subsurface barriers. Rather than serving to constrain plume migration, permeable reactive barriers (PRB's) are designed as preferential conduits for the contaminated ground-water flow. A permeable reactive subsurface barrier is an emplacement of reactive materials where a contaminant plume must move through it as it flows, typically under natural gradient, and treated water exits on the other side. The purpose of this document is to provide detailed design, installation and performance monitoring data on a full-scale PRB application which successfully remediated a mixed waste (chromate and chlorinated organic compounds) ground-water plume. It was also the first full-scale installation of this technology to use a trencher to install a continuous reactive wall to intercept a contaminant plume. The information will be of use to stakeholders such as implementors, state and federal regulators, Native American tribes, consultants, contractors, and all other interested parties. There currently is no other site which has used this innovative technology and reported on its performance to the extent detailed in this report. It is hoped that this will prove to be a very valuable technical resource for all parties with interest in the implementation of this innovative, passive, remedial technology.

Clinton W. Hall, Director
Subsurface Protection and Remediation Division
National Risk Management Research Laboratory

Abstract

A 46 m long, 7.3 m deep, and 0.6 m wide permeable subsurface reactive wall was installed at the U.S. Coast Guard (USCG) Support Center, near Elizabeth City, North Carolina, in June 1996. The reactive wall was designed to remediate hexavalent chromium [Cr(VI)] contaminated ground water at the site, in addition to treating portions of a larger overlapping trichloroethylene (TCE) ground-water plume which has not yet been fully characterized. The wall was installed in approximately 6 hours using a continuous trenching technique, which simultaneously removed aquifer sediments and installed the porous reactive medium. The reactive medium was composed entirely of granular iron, with an average grain size (d_{50}) of 0.4 mm. The reactive medium was selected from various mixtures on the basis of reaction rates with Cr(VI), TCE and degradation products, hydraulic conductivity, porosity, and cost.

The continuous wall configuration was chosen over a Funnel-and-Gate configuration, based on three-dimensional computer simulations of ground-water flow and contaminant transport, and cost. The simulations indicated that both configurations could be designed to achieve the same capture areas and residence times with the same volume of reactive material. However, initial cost comparisons suggested that a reactive wall would have a lower material and installation cost than a Funnel-and-Gate. For this site, the installation and material cost was approximately \$7550 U.S./linear meter for a 46 m long, 7.3 m deep and 0.6 m wide continuous reactive wall. The minimum required width of the granular iron wall was determined from simulations of TCE decay within the barrier, rather than Cr(VI) reduction because Cr(VI) reaction rates are significantly faster. Simulations of contaminant transport within the granular iron wall indicate that 10,000 $\mu\text{g/L}$ TCE, 900 $\mu\text{g/L}$ cis-dichloroethylene (cDCE) and 101 $\mu\text{g/L}$ vinyl chloride (VC) are reduced to less than maximum contaminant level (MCL) values of 5, 70, and 2 $\mu\text{g/L}$ respectively, within 0.3 m of travel through the wall under the maximum flow velocities expected at the site.

The total project cost, including site assessment, reactive barrier design, installation, soil treatment and follow-up, was approximately \$985,000 U.S. The U.S. Coast Guard anticipates that using this reactive barrier will result in a saving of \$4 million U.S. in operation and maintenance costs over a 20 year period, compared to a pump-and-treat system.

Table of Contents

Abstract	iv
Table of Contents	v
List of Tables	vii
List of Figures	viii
List of Appendices	x
Introduction	1
Background	2
Site History	2
Geologic Setting	2
Conceptual Model of Plume Development	3
Remediation Strategy	3
Design Methodology	5
Introduction	5
Materials	5
Ground Water	5
Zero Valent Iron	5
Aquifer Materials	5
Methodology	5
Laboratory Batch Tests	5
Laboratory Column Tests	6
Analytical Procedures	6
Organic Analysis	6
Inorganic Analysis	7
Geochemical Modeling	7
Flow and Reactive-Transport Modeling	7
Model Description	7
Model Limits and Grid	8
Hydraulic Parameters	8
Boundary Conditions	8
Reactive Barrier Configurations	8
Reactive-Transport Parameters	9
Results and Discussion	10
Column and Batch Tests	10
Batch Results	10
Organic	10
Inorganic	10
Geochemical Modeling – Inorganic Data	10
Column Results	11
Organic	11
High Flow Velocity Tests	12
Low Flow Velocity Tests	12
Inorganic Results	13
Chromium	13
Cations and Anions	13

Eh, pH and Alkalinity	13
Geochemical Modeling	13
Determination of Reaction Parameters: Cr(VI)	15
Determination of Reaction Parameters: Halogenated Hydrocarbons	15
Reactive Barrier Designs	16
Final Selection of a Reactive Barrier	17
Final Reactive Barrier Design	17
Barrier Installation	18
Configuration	18
Site Preparation	18
Installation	18
Post-Installation Work	18
Barrier Costs and Performance	19
Conclusions	20
References	21

List of Tables

Table 1.	Horizontal Hydraulic Gradients and Water Levels Observed in Monitoring Wells Screened Between 3 and 4.5 m Below Ground Surface	26
Table 2.	First-order Rate Constants for the Dehalogenation of TCE, DCE Isomers, and VC (after Johnson <i>et al.</i> , 1996)	26
Table 3.	Reactive Mixtures Used in Batch Experiments	26
Table 4.	Reactive Mixtures Used in Column Experiments	26
Table 5.	Column Flow Velocities and Hydraulic Properties of Reactive Mixtures Used (after O'Hannesin <i>et al.</i> , 1995)	27
Table 6.	Method Detection Limits (MDL)	28
Table 7.	Changes in TCE Concentration in Batch Experiments Over Time, for Reaction and Control Vials. Three Reaction Vials and One Control Vial Were Sampled at Each Time. Only TCE Was Analyzed.	29
Table 8.	Summary of Cr Removal in Batch Tests	30
Table 9.	Inorganic Concentrations of All Columns for Both Influent and Effluent Samples at Steady State Conditions.	30
Table 10.	First Detection of Cr at the 2.5 cm Sample Port in Each Column. Predicted Breakthrough Volumes Calculated from These Data Are Shown.	31
Table 11.	First Order Rate Constants in Various Reactive Iron Mixtures (Rate Constants Not Normalized to Surface Area)	31
Table 12.	Hydraulic Properties and First-order Rate Constants for Peerless and Master Builders Granular Iron.	31
Table 13.	Hydraulic Conductivity Values Used in Ground-water Flow Simulations to Compare Relative Capture Areas and Residence Times of Two Barrier Designs.	32
Table 14.	Capture Areas for the Funnel-and-Gate Under Varying Aquifer Hydraulic Conductivity Conditions.	32
Table 15.	Capture Areas for the Continuous Wall Configuration Under Varying Aquifer Hydraulic Conductivity Conditions.	32
Table 16.	Ground-water Velocities and Residence Times within the Reactive Material Zones of the Funnel-and-Gate and the Continuous Wall.	33
Table 17.	Hydraulic Parameters (<i>Source</i> of Values Indicated in Brackets) Used in Ground-water Flow Modeling to Determine Minimum Barrier Dimensions.	33
Table 18.	Reactive-transport Parameters, Source Concentrations, and Minimum Distance within Reactive Barrier before Contaminant Falls Below MCL.	33
Table 19.	Barrier Installation Project Costs in U.S.\$ (Jim Vardy, Pers. Comm.).	34

List of Figures

Figure 1. Location map showing U.S. Coast Guard Support Center, Elizabeth City, North Carolina	36
Figure 2. Plan view map showing total Cr concentrations (mg/L), and inferred 0.05 and 1 mg/L contours	36
Figure 3. Plan view map showing approximate locations of temporary wells, cone penetrometer tests, river sampling, and deep wells (after Parsons Engineering Science, 1994)	37
Figure 4. (a) Cross-section B-B', and (b) cross-section A-A' indicating total chromium concentrations (mg/L), and inferred 0.05 mg/L and 1.00 mg/L contours in June 1994	37
Figure 5. Cr concentration profiles (mg/L) at multilevel samplers in the approximate locations of piezometer bundles ML11, ML21, and ML31, upgradient of proposed Reactive Barrier (April 1996)	38
Figure 6. Plan view map showing TCE concentrations ($\mu\text{g/L}$), and inferred 5 and 100 $\mu\text{g/L}$ contours	38
Figure 7. (a) Cross-section B-B', and (b) cross-section A-A' indicating TCE concentrations ($\mu\text{g/L}$), and inferred 5 $\mu\text{g/L}$ and 100 $\mu\text{g/L}$ contours in June 1994	39
Figure 8. TCE concentration profiles (mg/L) at multilevel samplers in the approximate locations of piezometer bundles ML11, ML21, and ML31, upgradient of proposed Reactive Barrier (April 1996)	39
Figure 9. Cross-sections extrapolated from borehole log data	40
Figure 10. Geologic cross-section A-A' extrapolated from cone penetrometer test data	40
Figure 11. Geologic cross-section B-B' extrapolated from cone penetrometer test data	41
Figure 12. Water levels in wells screened 3 to 4.5 m below ground surface (ft.a.s.l.)	41
Figure 13. Conceptual model diagram	42
Figure 14. (a) Reductive β -elimination, and (b) hydrogenolysis reaction steps in degradation of TCE (after Arnold and Roberts, 1997)	43
Figure 15. Schematic of the apparatus used in the column experiments	44
Figure 16. Model domain dimensions, with Funnel-and-Gate barrier shown (all dimensions in m)	45
Figure 17. Model boundary conditions, with Funnel-and-Gate barrier shown	45
Figure 18. (A) Funnel-and-Gate, and (B) permeable wall configurations used in flow simulations [all dimensions in meters]	46
Figure 19. TCE concentration versus time in each of the four batch test mixtures	47
Figure 20. Batch test inorganic geochemistry for all mixtures, versus time	48
Figure 21. Cr(VI) concentration vs. time in each of the four batch test mixtures	49
Figure 22. Mineral saturation indices for batch tests, calculated with MINTEQA2	50
Figure 23. TCE concentration versus distance along all six columns at the first flow velocity (FV1), approximately 61 cm/day (2 ft/day).	51

Figure 24. TCM concentration versus distance along all six columns at the first flow velocity (FV1), approximately 61 cm/day (2 ft/day).	51
Figure 25. cDCE concentration versus distance along all six columns at the first flow velocity (FV1), approximately 61 cm/day (2 ft/day).	52
Figure 26. VC concentration versus distance along all six columns at the first flow velocity (FV1), approximately 61 cm/day (2 ft/day).	52
Figure 27. TCE concentration versus distance along three columns at the second flow velocity (FV2), approximately 30 cm/day (1 ft/day).	53
Figure 28. TCM concentration versus distance along three columns at the second flow velocity (FV2), approximately 30 cm/day (1 ft/day).	53
Figure 29. cDCE concentration versus distance along three columns at the second flow velocity (FV2), approximately 30 cm/day (1 ft/day).	54
Figure 30. VC concentration versus distance along three columns at the second flow velocity (FV2), approximately 30 cm/day (1 ft/day).	54
Figure 31. Inorganic results for column 50MBSSAQ at FV1.	55
Figure 32. Inorganic results for column 50MBSS at FV1.	56
Figure 33. Inorganic results for column 100MB at FV1 and FV2.	57
Figure 34. Inorganic results for column 100PL at FV1 and FV2.	58
Figure 35. Inorganic results for column 50PLSSAQ at FV1 and FV2.	59
Figure 36. Inorganic results for column 48PL/52AQ at FV1.	60
Figure 37. Cr detection at the 2.5 cm sample port.	61
Figure 38. Mineral saturation indices for column 50MBSSAQ at FV1.	62
Figure 39. Mineral saturation indices for column 50MBSS at FV1.	63
Figure 40. Mineral saturation indices for column 100MB at FV1 and FV2.	64
Figure 41. Mineral saturation indices for column 100PL at FV1 and FV2.	65
Figure 42. Mineral saturation indices for column 50PLSSAQ at FV1 and FV2.	66
Figure 43. Mineral saturation indices for column 48PL/52AQ at 78.4 PV and FV1.	67
Figure 44. Experimental and calculated TCE concentration profiles in column	68
Figure 45. Experimental and calculated cDCE concentration profiles in column	68
Figure 46. Experimental and calculated VC concentration profiles in column	69
Figure 47. (A) Ground-water flow divergence in vicinity of a Funnel-and-Gate, and (B) Capture area	70
Figure 48. Vertical ground-water flow divergence around a Funnel-and-Gate	71
Figure 49. Horizontal ground-water flow divergence around a Funnel-and-Gate	71
Figure 50. Ground-water flow divergence around a continuous wall	72
Figure 51. Predicted TCE, cDCE, and VC concentration profiles through the iron-filings wall	72
Figure 52. (a) Plan view, and (b) cross-sectional view of reactive barrier	73
Figure 53. Picture showing storage of granular iron at the site	74
Figure 54. Picture showing erosion control measures during installation	74
Figure 55. Picture showing trenching machine	75
Figure 56. Picture showing excavated aquifer sediments forming a soil slurry	75
Figure 57. Picture showing collapse of concrete	76

List of Appendices

Appendix A: Grain size distribution curves	79
Appendix B: Elemental and TCLP analyses	80
Appendix C: Bromide tracer test data (lab columns)	82
Appendix D: Batch test inorganic data	84
Appendix E: Batch test mineral saturation indices	85
Appendix F: Reactive column organic data	86
Appendix G: Reactive column inorganic data	103
Appendix H: Reactive column mineral saturation indices	107
Appendix I: Analytical laboratory procedures	111

Introduction

Ground water at the U.S. Coast Guard Support Center, Elizabeth City, NC (Figure 1), contains hexavalent chromium [Cr(VI)] and trichloroethylene (TCE) derived from historical electroplating and degreasing operations. Site investigations conducted since 1991 have shown maximum ground-water concentrations of greater than 10 mg/L Cr and 19,000 µg/L TCE; (Puls *et al.*, 1994; Parsons Engineering Science, 1993, 1995, 1997). These concentrations exceed the maximum contaminant level (MCL) values of 0.05 mg/L for Cr and 5 µg/L for TCE. The Cr and TCE ground-water plumes overlap, and discharge to the Pasquotank River which borders the northern extent of the USCG Support Center.

The traditional method to remediate contaminated ground water is often a variant of a pump-and-treat system. These systems pump both contaminated and uncontaminated ground water to an above-ground treatment facility where large volumes of ground water are treated and discharged. Ground-water contaminant concentrations can be reduced to less than MCL values with this method, but experience has shown that contaminant source zones can persist for very long time periods due to mass transfer limitations (Mackay and Cherry, 1989). Inherent in the pump-and-treat method are several disadvantages such as: long treatment times, large volumes of ground water to treat and discharge, operation and maintenance costs, and loss of land-use. The limitations and disadvantages of the pump-and-treat method have prompted questions regarding remediation goals, and alternative remediation methods (Mackay *et al.*, 1993).

One alternative remediation technique that avoids the limitations of pump-and-treat is the use of passive *in situ* reactive barriers (McMurty and Elton, 1985; Gillham and Burris, 1992; Gillham and O'Hannesin, 1992; Blowes and Ptacek, 1992). *In situ* reactive barriers are composed of a permeable reactive material that passively removes contaminants from flowing ground water. These barriers are installed in the subsurface, allowing continued use of the land. The barriers do not require on-going maintenance or energy input, and above ground treatment and disposal of ground water is not required. Blowes *et al.* (1995) describe a variety of contaminants which can be treated using subsurface permeable reactive walls. In order to successfully remediate a plume, the reactive wall must be large enough that the entire ground-water plume passes through it. An alternative reactive barrier design is the Funnel-and-Gate (Starr and Cherry, 1994). The Funnel-and-Gate barrier utilizes cutoff walls to focus or funnel ground-water flow through a smaller *in situ* reactive material zone.

A passive *in situ* barrier, composed of granular iron, was proposed as an innovative ground-water remediation technology to treat both dissolved Cr(VI) and TCE in ground water at the USCG Support Center. Previous laboratory and field studies indicated that reactive mixtures composed of granular iron can successfully remediate ground water contaminated with Cr(VI) (Blowes and Ptacek, 1992; Puls *et al.*, 1995; Blowes *et al.*, 1997) and TCE (O'Hannesin and Gillham, 1992; O'Hannesin, 1993; Gillham and O'Hannesin, 1994; Focht *et al.*, 1996). Patents held by the University of Waterloo cover the removal of dissolved metals from ground water through the *in situ* precipitation of harmless, insoluble reduced metal phases in a permeable reactive mixture placed in the path of the contaminated ground water (U.S. Patents 5,362,394 and 5,514,279). A patent held by the University of Waterloo covers the *in situ* removal of dissolved halogenated organic contaminants from water using zero valent iron installed in the pathway of the contaminated ground water (U.S. Patent 5,266,213).

Laboratory batch and column tests were conducted using materials from the USCG Elizabeth City site to determine the granular iron mixture which would be the best suited for simultaneously treating Cr(VI) and TCE contaminated ground water. The reaction rates, hydraulic properties and cost of these mixtures were included in the selection criteria. Peerless™ granular iron was selected for the reactive barrier.

Three-dimensional ground-water flow simulations were conducted to assess the relative efficiency of a Funnel-and-Gate versus a continuous wall (Bennett, 1997). Simulations of contaminant transport through the reactive barrier under the maximum flow conditions expected at the USCG site were conducted to determine the minimum barrier thickness required to remediate contaminant concentrations, similar to those observed at the site, to less than MCL values.

The site preparation, trenching installation, follow-up soil treatment, and overall project costs, using the selected reactive material and barrier configuration are described.

Background

Site History

The U.S. Coast Guard Support Center, Elizabeth City, NC, has been the focus of numerous studies since the discovery of a leak of acidic chromium solution beneath a former electroplating shop in 1988. The plating shop was in operation for 30 years, prior to its closure in 1984. Sediments beneath the plating shop floor were found to contain up to 14,500 mg/kg Cr. The contaminated sediments were removed at that time. A subsequent site investigation indicated that a plume of ground water containing Cr(VI) in excess of the MCL value extended from the electroplating shop, in Hangar 79, toward the Pasquotank River (Figure 2) (Parsons Engineering Science, 1993, 1994, 1995). Sampling results from a monitoring network of more than 40 wells indicated that the Cr(VI) plume was approximately 35 meters wide, and extended 65 meters from the hangar to the river. A series of water samples was taken from cone penetrometer test (CPT) locations (Figure 3). The CPT ground-water samples indicate that the core of the Cr plume exists between approximately 4.5 - 6.1 m below ground surface. The bottom fringe of the plume, defined by the MCL value of 0.05 mg/L, extends to a depth of approximately 7 m, as the plume nears the Pasquotank River (Figure 4). Multilevel sampling wells installed in the vicinity of the proposed reactive barrier similarly indicated that the Cr(VI) plume predominates between depths of 4.5 and 6.5 m (Figure 5). Very low Cr(VI) concentrations were detected in two deep wells, MW21 and MW22, screened between 12 m and 15 m below ground surface. The maximum observed Cr(VI) concentration exceeds 10 mg/L (Puls *et al.*, 1994).

In 1991, TCE was detected in ground-water samples collected during the Cr(VI) delineation program. The source of the TCE is speculated to be an existing sewer manhole located adjacent to the electroplating shop (Parsons Engineering Science, 1993). The TCE may be associated with the historical plating operations in Hangar 79, as TCE is commonly used to degrease parts prior to chrome plating (Greenwood, 1971; Dennis and Such, 1972). The extent of the TCE in the ground water has not been completely delineated to the west, south, and east of the apparent source area (Parsons Engineering Science, 1993). The TCE plume overlaps the Cr(VI) plume, and is larger in lateral extent (Figure 6). Ground-water samples taken during cone penetrometer testing indicate that a TCE plume exists between 4.5 and greater than 7.6 m below ground surface. The plume also extends to the west, where higher concentrations, and concentrations greater than MCL exist at 9.1 m depth (Figure 7). Multilevel sampling wells installed in the vicinity of the proposed reactive barrier similarly indicate that the TCE is heterogeneously distributed with depth (Figure 8). The full vertical extent of the TCE has yet to be determined, but TCE concentrations of up to 580 µg/L have been observed in wells at 12 m depth below ground surface (Parsons Engineering Science, 1993).

TCE concentrations that exceed MCL were detected in temporary wells installed near the riverbank (T1, T2, T3, T4, T5, T6), with the highest concentrations of 2,400 µg/L observed in T1. TCE concentrations which exceed the MCL and approach 8 µg/L were also observed in river water samples (R2, R11, R12, R21, R22) indicating that the TCE plume impacts the river. The highest TCE concentration reported in sampling events since 1991 was 19,200 µg/L.

Geologic Setting

The contaminated surficial aquifer at the USCG site consists of Atlantic coastal plain sediments. Borehole log data (Parsons Engineering Science, 1993) (Figure 9) indicate that the surficial aquifer is complex and heterogeneous, composed of varying amounts of fine sands and silty clays. In general, the upper 2 m of the aquifer are sandy silty clays which pinch out toward the north, toward the Pasquotank River, where fill sands have been added. Fine sands, with varying amounts of silt and clay, and silty clay lenses form the lower portion of the shallow aquifer. Cone penetrometer tests also indicate that the surficial aquifer is very heterogeneous with fine sands interfingering with silty clay lenses. The thickness of these lenses varies from 0.3 m to more than 3 m (Figures 10 and 11). The aquifer is underlain at approximately 18 meters depth by dense clay of the Yorktown Confining Unit.

Water level measurements indicate that the ground-water flows northwards toward the Pasquotank River (Figure 11). In five monitoring events over a three year period, the general ground-water flow field downgradient of the plating shop varied in direction from approximately N30° W to N10° E (Figure 12). Water levels measured in the monitoring wells fluctuate between approximately 1.5 and 2.1 m below ground surface. The calculated average horizontal hydraulic gradient varies between 0.0011 and 0.0033 (Table 1).

Slug tests were conducted on monitoring wells with 1.5 m long, 2.05 cm diameter screened intervals between 3 m and 6 m below ground surface. Hydraulic conductivity values calculated from these tests vary from 0.1 m/day to 4.8 m/day (Parsons Engineering Science, 1993).

A multiple borehole tracer test in wells screened between 3.9 to 5.9 m depth below ground surface was conducted by Puls *et al.* (1995). Ground-water velocities of 0.13 m/day and 0.18 m/day were measured in this test. Assuming an average gradient of 0.0023 and a porosity of 0.38, these velocities correspond to an average hydraulic conductivity of approximately 26 m/day.

Conceptual Model of Plume Development

The chromium plume exists in the ground water as a result of leakage from a chromic acid tank located in an old plating shop in Hangar 79. The dissolved Cr(VI) water moves with the ground water. The general ground-water flow direction varies between N30°W and N10°E, and the aqueous chromium plume extends northward toward the Pasquotank River. The chromium plume is predominantly located in the silty-clayey fine sand unit, which underlies the surficial clay, because hydraulic conductivities and thus ground-water velocities are the highest within this sandy unit (Figure 13a).

TCE exists in the ground water as a result of the release of pure-phase TCE into the subsurface. TCE is a dense nonaqueous phase liquid (DNAPL) that is relatively immiscible with water, and has a relatively low solubility of 1,100 mg/L (Pankow and Cherry, 1996). Once released into the subsurface, pure-phase TCE migrates downward as a result of its higher density than water. TCE will pond and spread laterally on lenses where small-scale variations in entry pressure exist, due to differences in grain size or clay content. The sensitivity of TCE migration to fine scale structure of sands has been previously documented (Poulsen and Kueper, 1992; Pankow and Cherry, 1996). Pondered TCE zones can form multiple sources, and can be extremely difficult to delineate due to the random migration pathways which result from its density and immiscibility.

Aqueous TCE plumes which extend from residual source zones will flow with the ground water. Dissolved TCE concentrations within these plumes can be orders of magnitude greater than the MCL value of 5 µg/L. The larger lateral extent of the TCE plume probably arises from the spreading and ponding of TCE, or possibly from multiple release locations. The presence of TCE at depths of greater than 12 m most likely results from the downward migration of pure-phase TCE due to its higher density (Figure 13b).

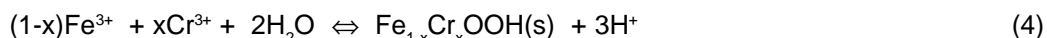
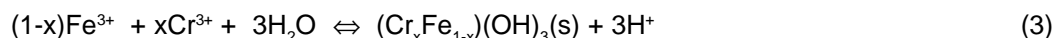
Remediation Strategy

Hexavalent chromium [Cr(VI)] is the oxidized valence state of chromium, and is a strong oxidant. The reduction of Cr(VI) to the less soluble and therefore less mobile Cr(III) valence state by a variety of reductants is thermodynamically favorable and kinetically rapid (Schroeder and Lee, 1975; Hem, 1977; Eary and Rai, 1988; Palmer and Wittbrodt, 1991; Palmer and Puls, 1994; Wittbrodt and Palmer, 1997). Reductants that are commonly found in soils include ferrous iron-bearing minerals and organic matter. Laboratory experiments indicate that the reduction of Cr(VI) by aqueous ferrous iron and ferrous salts under acidic conditions can be very rapid, reaching equilibrium within a matter of minutes (Eary and Rai, 1988; Buerge and Hug, 1997). However, the reduction of Cr(VI) by ferrous iron bearing minerals involves the dissolution of ferrous iron and can be significantly slower, taking tens of minutes to tens of hours depending on the pH and the ferrous mineral (Eary and Rai, 1989; Eary and Rai, 1991). Blowes and Ptacek (1992) suggested that iron bearing solids such as elemental iron (Fe⁰) and pyrite could be used in a porous subsurface reactive wall to reduce and remove Cr(VI) from ground water under intermediate pH conditions. Their laboratory experiments indicated that the rate of Cr(VI) removal by fine grained iron is greater than that for coarse grained iron and pyrite. Cr(VI) concentrations decreased from 25 mg/L to less than 0.05 mg/L within a matter of hours with high purity granular iron (0.5 - 1 mm diameter), as opposed to tens of hours for iron chips or pyrite. Their results suggested that the reaction was surface area and pH dependent. A similar surface area and pH dependence was found by Gould (1982), who determined a rate expression for the reduction of Cr(VI) by Fe⁰:

$$\frac{d[Cr^{VI}]}{dT} = -k[Cr^{VI}]^{0.5}[H^+]^{0.5} A \quad (1)$$

where A is the surface area of zero-valent iron (cm²/L), and the rate constant k has a value of 5.45 x 10⁻⁵ L cm⁻² min⁻¹.

The reduction of Cr(VI) by Fe⁰ produces ferric iron [Fe(III)] and Cr(III) and (eqn. 2). Chromium may be removed through the precipitation or co-precipitation of mixed Fe(III)-Cr(III) hydroxide solid solution (eqn. 3; Eary and Rai, 1988; Puls *et al.*; 1994; Powell *et al.*, 1995; Blowes *et al.*, 1997) or mixed Fe(III)-Cr(III) (oxy)hydroxide solid (eqn. 4; Schwertmann, 1989):



Goethite (FeOOH) and Cr(III) substituted goethite containing up to 27 mass % Cr(OH)₃ have been identified as the principal precipitates in this reaction (Blowes *et al.*, 1997; Pratt *et al.*, 1997). The substitution and incorporation of Cr(III) into ferric oxyhydroxides is similar to the findings of Eary and Rai (1988) who report a 3:1 stoichiometry for Fe/Cr in a mixed hydroxide precipitate. These hydroxides have a minimum solubility between pH 7 and 10 (Rai *et al.*, 1987; Sass and Rai, 1987). In this pH range, Cr(III) concentrations in equilibrium with Cr(III) and mixed Cr(III)-Fe(III) hydroxides are

less than the MCL. Thus, the reduction of Cr(VI) by zero-valent iron provides a method of treating Cr(VI) contaminated ground water.

Elemental iron has also been found to promote the relatively rapid degradation of a wide range of halogenated aliphatics, including TCE, dichloroethylene (DCE) and vinyl chloride (VC); (Gillham and O'Hannesin, 1992; Gillham *et al.*, 1993). One proposed reaction scheme (Figure 14) suggests that the degradation of TCE by Fe⁰ to non-toxic hydrocarbons occurs via concurrent reductive β-elimination and hydrogenolysis reactions (Roberts *et al.*, 1996; Arnold and Roberts, 1997). The reductive β-elimination pathway involves the breakdown of TCE to chloroacetylene and acetylene intermediates. The alternative reductive-dechlorination pathway involves the breakdown of TCE to DCE isomers and VC intermediates. The cis-dichloroethylene (cDCE) and VC intermediates are also of concern as they are carcinogenic and have low MCL values of 70 and 2 µg/L, respectively. However, laboratory experiments indicate that cDCE and VC account for less than 10% of the TCE breakdown products (Orth and Gillham, 1996), and that these chlorinated products are themselves reductively-dechlorinated in the presence of Fe⁰. Laboratory experiments have indicated that the ultimate end-products of both reaction pathways are ethene and ethane, with lesser amounts of other C1 to C4 hydrocarbons (Sivavec and Horney, 1995; Orth and Gillham, 1996).

Batch experiments indicate that the TCE, cDCE and VC degradation reactions are pseudo first-order and dependent on the surface area of iron (Gillham and O'Hannesin, 1994). The first-order rate constant appears to decrease with decreasing degree of chlorination, and each subsequent dechlorination from TCE to cDCE to VC occurs more slowly. A similar surface area and rate dependence was observed in the sequential dehalogenation of chlorinated methanes by Fe⁰ (Matheson and Tratnyek, 1994). Johnson *et al.* (1996) describe a pseudo first-order kinetic model for the dehalogenation of various hydrocarbons by Fe⁰:

$$-\frac{d[P]}{dt} = k_{sa} a_s \rho_m [P] \quad (5)$$

where k_{sa} is the specific reaction rate constant (L h⁻¹ m⁻²), a_s is the surface area of Fe⁰ (m² g⁻¹), and ρ_m is the mass concentration of Fe⁰ (g L⁻¹ of solution). The first-order rate constants for the dehalogenation of TCE, DCE isomers and VC by elemental iron, calculated from various batch and column experiments (Johnson *et al.*, 1996), are given in Table 2.

These rates are significantly greater than those reported for the abiotic hydrolysis of TCE under normal environmental conditions, where half-lives are on the order of years (Vogel *et al.*, 1987). The use of Fe⁰ in subsurface reactive iron walls has also been previously shown to successfully degrade a variety of halogenated organics in ground water (O'Hannesin and Gillham, 1992; Focht *et al.*, 1996).

Design Methodology

Introduction

A series of batch tests were conducted in the laboratory to assess the potential effectiveness of various commercial iron materials in simultaneous removal of both Cr(VI) and TCE from Elizabeth City site water. After identifying suitable iron sources, column tests were undertaken to determine if the organic compounds would degrade under flowing conditions through the various reactive materials. Parameters obtained from the column experiments would ultimately assist in the design of a field treatment system.

Materials

Ground Water

Ground water for the batch and column experiments was collected from monitoring well MW34 at the USCG Support Center. The site water was initially analyzed to determine the concentrations of TCE and Cr(VI) [750 µg/L and 8 mg/L, respectively]. For the batch and column tests, TCE and Cr(VI) concentrations were increased to approximately 2,000 µg/L TCE and 10 mg/L Cr(VI).

Zero Valent Iron

Three different sources of commercially available iron were tested: Ada (batch test only), Master Builders™ (MB) of Cleveland, Ohio, and Peerless™ (PL) Metals and Abrasives of Detroit, Michigan. The grain size of the iron ranged from 0.25 to 1.0 mm for both MB and PL. Ada iron was composed of 0.5 mm shavings of various lengths. The specific surface area measurements were 1.1 and 0.81 m²/g for MB and PL, respectively, determined by the BET method (Brunauer et al., 1938). Particle density measurements were 6.97 and 6.98 g/cm³ for MB and PL, respectively, as determined with an air compression pycnometer (Beckman model 930). Surface area and particle density measurements were not performed for Ada iron due to the large particle size.

Aquifer Materials

Depending on the construction method used (i.e., the width of the excavation) it is often more cost effective to mix sand with the granular iron. Natural sand from the site (AQ) and high purity silica sand (SS) were considered as potential bulking agents. Elizabeth City aquifer material was selected to evaluate the potential benefit and complications associated with using the native aquifer material in the reactive mixture. At the University of Waterloo, the materials were dried and screened through a 2 mm sieve. The washed silica sand that was used ranged between 0.15 to 0.5 mm in diameter. Grain size distribution curves are shown in Appendix A. Hydraulic conductivity measurements were performed on all column mixtures. The column mixtures and hydraulic conductivities are described in the Methodology section of this report. Elemental analysis and toxicity characteristic leaching procedures (TCLP) were conducted on both MB and PL iron sources (Appendix B).

Methodology

Laboratory Batch Tests

Four batch tests were conducted using the three different sources of commercially available iron; Ada, MB, PL and a combination of Elizabeth City aquifer material (AQ) and MB iron.

Each laboratory batch treatability test consisted of 60 samples prepared in 60 mL glass vials. Two types of samples were prepared: blank vials, which contained only spiked site water, and reactive vials containing 6 g of an iron source, 6 g of silica sand (SS) or aquifer material (AQ) along with the spiked site water (Table 3). The mass of iron to volume of solution ratio in the reactive vials was 1 g: 9.4 mL.

For each treatability test, the site water was gravity fed into a 4 L glass bottle with a spigot at the bottom, and was stirred on a magnetic stirrer for 30 minutes. The vials were filled by gravity flow, leaving no headspace, then sealed immediately with aluminum crimp caps with Teflon®-lined septa. The test vials were filled in sequence of one blank and three reactive vials. Sample bottles with no iron or sand were also filled at the beginning, middle and end of the pouring process, to determine initial values of TCE, Cr(VI), redox potential (Eh) and pH. The test vials were then placed on a rotating disc (three complete revolutions per minute), allowing for complete mixing without agitation.

At predetermined time intervals (sampling more frequent at early times), the vials were removed from the rotating disc and samples were extracted for TCE analysis, Eh and pH measurements. Filtered samples (0.2 µm) were collected for alkalinity and inorganic constituent analyses, including Cr(VI). Four vials were sacrificed for each sampling time: one blank and triplicate reactive vials, allowing a maximum of fifteen sampling times. All tests were conducted at room temperature (≅ 25 ° C).

Laboratory Column Tests

Six column tests were conducted to determine the degradability of TCE, cDCE and VC and the removal of Cr(VI) under flowing conditions, using mixtures containing a combination of Elizabeth City aquifer material (AQ), silica sand (SS), MB iron and PL iron. The column mixtures used are listed in Table 4, and the hydraulic characteristics of these columns are described in Table 5.

The columns were constructed of Plexiglas™ with a length of 50 cm (1.64 ft) and an internal diameter of 3.8 cm (1.5 in). Sampling ports were positioned along the length of each column at distances of 2.5, 5, 10, 15, 20, 30 and 40 cm (1, 2, 4, 6, 8, 12 and 16 in) from the inlet end (Figure 15). The columns also allowed for collection of samples from the influent and effluent solutions. Each sampling port consisted of a nylon Swagelok® fitting (0.16 cm) tapped into the side of the column, with a syringe needle (16G) secured by the fitting. Glass wool was placed in the needle to prevent the entry of solid material. The needles were positioned such that the water samples were obtained along the central axis of the column. Each sampling port was fitted with a Luer-Lok™ fitting, such that a glass sampling syringe could be attached to the port to collect a sample. When not in operation the ports were sealed by Luer-Lok™ plugs.

Each column was carefully packed insuring that the mixture was homogeneously distributed. For columns containing the 50% iron and sand mixtures, aliquots of the sand-iron mixtures were packed in lifts, taking care to avoid layering by roughening the surface of the preceding layer before adding the next layer. All measurements were determined gravimetrically and are shown in Table 5. Porosity values ranged from 0.29 to 0.45. Pore volume measurements were determined experimentally by weight and ranged from 166 to 254 mL. Iron mass to volume ratios and surface area to volume ratios are shown in Table 5. The columns were initially flushed with carbon dioxide to avoid air entrapment during wetting. Several pore volumes of distilled water were flushed through each column before the site water was introduced. All column experiments were conducted at room temperature.

An Ismatec™ IPN pump was used to feed the solution from a collapsible Teflon® bag to the bottom influent end of the column. The pump tubing was Viton®; all other tubing was Teflon® (0.33 cm I.D. x 1.52 cm O.D.). The columns were sampled periodically over time until steady-state organic concentration profiles were achieved. After removing stagnant water from a sampling needle, 2.0 or 1.5 mL samples were collected from the sampling ports. Samples for organic analyses were collected from each port.

The first set of column tests was started on March 31, 1995, with a flow velocity range of 0.43 to 0.79 m/day (1.4 to 2.6 ft/day = FV1) (Table 5). The second set of tests, which extended the period of operation of only three of the columns, was conducted with a lower flow velocity of approximately 0.30 m/day (1 ft/day = FV2). Testing at FV2 was started on May 26, 1995. The lower velocity corresponds to the natural ground-water velocity at the site. The higher velocity is about ten times greater, corresponding to the velocity expected in a funnel and gate configuration.

In the first set of tests (0.43 to 0.79 m/day), the five columns were sampled more than ten times for inorganic parameters. Detailed sampling was conducted of the effluent and all column sample ports for Eh, pH, alkalinity, Cr and other ions. Samples were collected in glass syringes to prevent oxidation during collection. A minimum of 8 mL was needed for analysis. Eh and pH measurements were made in sealed containers. Filtered (0.2 µm) samples were analyzed for major ions and trace metals at the University of Waterloo. A detailed column profile was obtained three times during the experiment for each column and the effluent was sampled more often. Additional Cr(VI) profiles were obtained at five different intervals to monitor Cr(VI) movement through the column.

At the lower flow velocity (FV2), sampling was conducted at least 7 times for Cr(VI) concentration. This included two detailed sampling sessions of the column effluent and column ports as described above. Due to the reduced flow rate and the large volume of sample required for analysis, only half of the column ports were sampled at a given sampling session.

Analytical Procedures

Organic Analysis

All organic samples collected from the batch and column experiments were analyzed at the University of Waterloo. Samples were analyzed within two days of collection. The analyses were performed on two types of gas chromatographs. The less volatile halogenated organics such as TCE were extracted from the aqueous phase using pentane with an internal standard of 1, 2-dibromoethane, at a water to pentane ratio of 2.0 to 2.0 mL (Henderson *et al.*, 1976). The samples were placed on a rotary shaker for 10 minutes to allow equilibration between the water and pentane phases. Using a Hewlett Packard 7673 autosampler, a 1.0 µL aliquot of pentane with an internal standard was automatically injected directly onto a Hewlett Packard series II gas chromatograph. The chromatograph was equipped with a ⁶³Ni electron capture detector (ECD) and DB-624 Megabore capillary column (30 m x 0.538 mm ID, film thickness 3 µm). The gas chromatograph had an initial temperature of 50°C, with a temperature time program of 15°C/min reaching a final temperature of 150°C. The detector temperature was 300°C. The carrier gas was helium and makeup gas was 5% methane and 95% argon, with a flow rate of 30 mL/min.

For the more volatile compounds, such as cDCE, tDCE and VC, a headspace was created in the samples with a ratio of 0.5 mL headspace to 1.5 mL aqueous sample. The samples were placed on a rotary shaker for 15 minutes to allow equilibration between the water phase and gas phase. For analysis, a 50 μ L gas sample was injected onto Photovac™, Model 10S50 and/or Model 10S70, gas chromatograph equipped with a photoionization detector (PID). The Model 10S50 chromatograph was fitted with a TFE packed column with 5% SE-30 on Chromosorb G, AW-DMCS (100/120 mesh), with oven temperature of 30°C and carrier gas of ultra-zero with a flow rate of 10 mL/min. The model 10S70 was fitted with a capillary column CP Sil5, with an isothermal oven temperature of 30°C and a flow rate of 3 mL/min.

Method detection limits (MDL) were determined for each compound as the minimum concentration of a substance that can be identified, measured and reported with 99% confidence that the analyte concentration is greater than zero. The MDLs were determined from analysis of samples from a solution matrix containing the analytes of interest. Detection limits for all compounds studied, as given in Table 6, were determined using the EPA procedure for Method Detection Limits (USEPA, 1982).

Standards for TCE and PCE were run at the beginning of each day and an additional set of standards was run later in the day or dispersed throughout the analysis run. Each sample and standard were spiked with an internal 1,2-dibromoethane sample to ensure complete capture by the detector. Calibration curves were run with seven different standards plus a blank. Similar to the VC and DCE analyses, the average of the relative percent differences was calculated to a cutoff limit of 10%. The highest TCE standard run via this pentane extraction method was 2,500 μ g/L. The MDL for TCE and PCE was 1 μ g/L.

Standards for VC and DCE analysis were run twice per day. Approximately 30 samples were run during the day using a gas chromatograph equipped with a photoionization detector (PID). Linear calibration curves were comprised of eight different standards plus a blank. The relative percent difference for each standard was determined and if the average of all the relative differences exceeded 10% then the analyses were repeated. The highest VC and c-DCE standards run via headspace analysis were 700 μ g/L and 1,000 μ g/L respectively. The MDL for VC and DCE was 1 μ g/L.

Inorganic Analysis

Redox potential (Eh) was determined using a combination Ag/AgCl reference electrode with a platinum button (Orion 9678 BN). The electrode was standardized with Zobell and Light solutions (Zobell, 1946; Light, 1972; Nordstrom, 1977). Millivolt readings were converted to Eh using the electrode reading and the standard potential of Ag/AgCl electrode (SHE) at a given temperature. The pH measurements were made using a combination of pH/reference electrode (Orion Models 9172BN and 915600), standardized with the pH buffer 7 and 10 (NIST standard).

Cation analysis for Cr(VI) was determined using a diphenylcarbazide colorimetric technique (Standard Methods, 1992, 3500-Cr D). Other cation analyses, including Al, B, Ca, Cd, Cr(total), Fe, K, Mg, Mn, Na, Ni, Si, Sr, Zn and a suite of other cations, were determined using an inductively coupled plasma Atomic Emission Spectrometer (ICP-AES) instrument (Thermo Jarrell Ash Iris Plasma Spectrometer). The samples were acidified to a pH of 2 with nitric acid and stored at 4°C until analyzed. These samples were analyzed at the Water Quality Laboratory (WQL) at the University of Waterloo. Appendix I describes the analytical procedures used for cation analysis.

Anions including Br, Cl and SO₄ were analyzed using a Dionex System 2000 Ion Chromatograph (IC) or a Waters IC with conductivity detectors. Appendix I describes the analytical procedures used for anion analysis. Alkalinity was measured on filtered subsamples at the time of sample collection using a Hach® Digital Titrator, standardized H₂SO₄ titrant and bromocresol green-methyl red indicator. Because of the low sample volumes available for analysis, the detection limit for alkalinity measurements varied from 2 mg/L CaCO₃ for the batch experiments to between 5 and 8 mg/L CaCO₃ for the column experiments. Detection limits for the inorganic parameters are included in Table 6. The method detection limit for Cr(VI) measured in the lab is between 0.2 and 0.4 mg/L. The MDL for total Cr concentrations on the ICP is 0.02 mg/L. Due to the limited volume of sample available, duplicate measurements of alkalinity could not be conducted.

Geochemical Modeling

The geochemical speciation/mass transfer computer code MINTQA2 (Allison *et al.*, 1990) was used to aid in the interpretation of inorganic aqueous geochemical data. The thermodynamic database of MINTQA2 was adjusted to be consistent with that of WATEQ4F (Ball and Nordstrom, 1991).

Flow and Reactive-Transport Modeling

Model Description

FRAC3D, a three-dimensional finite element computer model designed to simulate saturated-unsaturated ground-water flow and chain-decay solute transport in porous or discretely-fractured porous formations (Therrien and Sudicky, 1996), was used. FRAC3D has been verified and validated against analytical solutions. This model has been used previously

for a number of Funnel-and-Gate™ remediation scenario simulations (Shikaze and Austrins, 1995; Shikaze *et al.*, 1995). FRAC3D was chosen to model the Elizabeth City USCG site because of its versatility and applicability to chain-decay solute transport (Bennett, 1997).

Model Limits and Grid

For the ground-water flow simulations, the model domain was 26 m x 18 m x 18 m (Figure 16). The grid spacing was varied from 0.15 m to 1.5 m, with the finer spacing located near the vertices of the reactive barrier.

For the reactive transport simulations, the model domain was 30 m x 18 m x 18 m. The grid spacing was varied between 0.03 m and 1.5 m, with the finer grid spacing within the vicinity of the reactive barrier. The finer grid spacing within the vicinity of the reactive barrier was chosen to satisfy the grid Peclet number criteria and minimize numerical dispersion.

Hydraulic Parameters

The entire domain was assigned a uniform hydraulic conductivity, which only approximates the heterogeneous nature of the aquifer. For the flow simulations, the hydraulic conductivity was varied between 0.1 and 26 m/day. These values correspond to the lowest and highest hydraulic conductivity values calculated from slug and tracer tests at the site. A uniform hydraulic conductivity was assigned to the domain to facilitate comparison of the hydraulic characteristics of the different reactive barrier designs. This range in hydraulic conductivities was chosen to bracket the anticipated range in calculated ground-water velocities within, and capture areas of, the reactive barriers. A simulation was also conducted with an assigned hydraulic conductivity of 46.4 m/day. This corresponds to the average calculated hydraulic conductivity for the reactive mixtures.

For the reactive transport simulations, the domain was assigned a hydraulic conductivity of 17 m/day. This value was chosen as a realistic estimate of the maximum anticipated hydraulic conductivity. Using the maximum anticipated hydraulic conductivity value will yield a conservative estimate of ground-water velocities and required residence times within the reactive barrier.

Boundary Conditions

The boundary conditions are shown in Figure 17. The top, bottom, east and west boundaries were assigned as no-flow boundaries (Type 2), and the north and south boundaries (Type 1) were assigned constant head values of 18 m and 18.0594 m, respectively. The west no-flow boundary is far enough from the reactive barrier, justifying the no-flow assumption. The bottom no-flow boundary represents the Yorktown confining unit, which is a low hydraulic conductivity confining clay layer. The east boundary represents a symmetry boundary, which runs through the center of the reactive barrier. This configuration results in a uniform flow field from south to north, with a constant horizontal hydraulic gradient of 0.0033. This hydraulic gradient corresponds to the maximum observed hydraulic gradient.

Reactive Barrier Configurations

For the ground-water flow simulations, two pilot-scale barriers composed of equal volumes of reactive material were modeled (Figure 18). These two reactive barrier designs, a Funnel-and-Gate and a continuous wall, differ only in how they are configured to intercept ground-water flow. The Funnel-and-Gate has a gate zone that contains the reactive material, and relies on impermeable funnels to direct ground-water flow through this gate. The continuous permeable wall is composed entirely of reactive material and does not rely on funnels to direct ground-water flow.

The funnels of the simulated Funnel-and-Gate were 6.06 m long, and 9.1 m deep. The simulated gate zone was 3.6 m long, 2 m wide and 9.1 m deep. For efficiency, the funnels were oriented perpendicular to the ground-water flow direction (Starr and Cherry, 1994). The gate zone consists of three zones: an upgradient pea gravel zone; a central granular iron zone; and a downgradient pea gravel zone. The 0.45 m wide pea gravel zones promote an even ground-water velocity distribution and minimize any heterogeneities in ground-water flow through the 1.1 m wide granular iron treatment zone. The total volume of granular iron within this simulated barrier was 35 m³.

The continuous wall configuration simulated was composed entirely of granular iron. It is 10 m long, 7.6 m deep, and 0.5 m wide. The total volume of granular iron in this simulated barrier was also 35 m³. For the reactive-transport simulations, a 36 m by 7.6 m by 0.45 m continuous reactive wall was modeled.

Within the model domain, the reactive barrier was located with the center of its long axis coinciding with the east symmetry/no-flow boundary. The barriers are “hanging” in these simulations, in that they do not intercept an underlying low permeability unit. In this configuration, flow underneath the barriers is possible.

Reactive-Transport Parameters

The goal of the reactive transport simulations was to determine the minimum thickness of a granular iron wall necessary to degrade selected TCE, cDCE and VC concentrations to less than MCL values. Given the sparse TCE characterization at the site, no attempt was made to accurately portray the TCE source zone. Two simulations were conducted in which the anticipated and maximum observed TCE, cDCE, and VC concentrations were assigned to a source zone upgradient of the wall. The source zone was a 12 m by 5 m plane of nodes located at the southern upgradient boundary of the domain.

Longitudinal and transverse dispersivities were assigned values of 1.5 cm in the model, based on laboratory column experiments. A bromide tracer solution was introduced into 50 cm long laboratory columns containing different granular iron reactive mixtures. Longitudinal dispersivities between 0.6 and 1.7 cm were calculated by fitting the effluent concentration vs. time data (Appendix C) to the one-dimensional advection-dispersion equation using CXTFIT (Toride et al., 1995). Although it is generally accepted that laboratory scale dispersivity measurements do not accurately reflect field scale problems, the longitudinal dispersivity value obtained from the 50 cm laboratory granular iron column may reasonably represent the field dispersivity within a 45 to 60 cm granular iron wall. Previous studies have indicated that laboratory values of transverse dispersivity are usually 0.05 to 0.2 times the longitudinal dispersivity (Freeze and Cherry, 1979; Klotz *et al.*, 1980). Thus, assigning equivalent longitudinal and transverse dispersivity values may provide an inaccurate representation of transverse spreading at the fringes of the simulated plume. However, the small value of transverse dispersivity used is not expected to significantly influence declining TCE, cDCE and VC concentrations along the centerline of the plume within the granular iron wall, or significantly bias the estimate of the minimum required thickness of the iron wall.

TCE, cDCE and VC diffusion coefficients at 20°C were assigned values of $10.1 \times 10^{-6} \text{ cm}^2/\text{s}$, $11.4 \times 10^{-6} \text{ cm}^2/\text{s}$, and $13.3 \times 10^{-6} \text{ cm}^2/\text{s}$, respectively. These values were calculated using a semiempirical correlation equation developed for dilute organic solutes in water (Wilke and Chang, 1955). The tortuosity was assigned a value of 0.8 for both aquifer and granular iron media. Tortuosity values between 0.7 and 0.85 are typical for sands.

The distribution coefficient, K_d , was assigned a value of zero. This ignores the partitioning or adsorption of the organic contaminants onto the granular iron or aquifer material within the wall, and results in no retardation of contaminant transport. This assumption will yield conservative estimates of the minimum wall thickness in order to provide the required ground-water residence time within the wall.

The reduction-precipitation reaction of Cr(VI) was not modeled because previous lab experiments indicated it to be the most rapidly reduced contaminant in the granular iron. First-order reaction rates and molar transfer coefficients for the reductive-dechlorination of TCE, cDCE and VC were incorporated into the reactive-transport model. The reactive transport simulation was run for 100 days. This simulation time allows more than 10 pore volumes (PV) to pass through the barrier and establish steady-state conditions.

Results and Discussion

Column and Batch Tests

Batch Results

Organic

The results of the batch tests are plotted as a concentration of TCE in $\mu\text{g/L}$ versus time in hours (Figure 19). The reactive vial concentration values are averaged triplicate values. The concentration of TCE in blanks for all four experiments shows minor fluctuations, but was relatively constant over time. The percent standard deviation for the reaction vial TCE values are generally less than 5% (Table 7).

The reactive vials containing Ada iron and silica sand (AdaSS) showed a gradual decline in TCE concentration from an initial concentration of 2,000 $\mu\text{g/L}$ over the 313 hr duration of the test (Table 7, Figure 19). The reactive vials containing the PLSS iron showed a more rapid decline in TCE concentration, with a concentration of 17 $\mu\text{g/L}$ being reached by the 192 hr sampling. The most rapid loss of TCE was obtained using Master Builders™ (MB) iron. MBAQ and MDSS gave similar results, with losses of about 95% of the initial TCE during the first 50 hours. The degradation rate for MBAQ appeared to be slightly greater than MBSS.

Inorganic

Trends in the dissolved aqueous geochemistry measured during the batch experiments are plotted in Figure 20 and are described in detail in Appendix D. Although the method detection limit for Cr(VI) in the laboratory is fairly high, the similarity of total Cr and Cr(VI) concentrations in the spiked ground water suggest that Cr in this water is dominantly in the Cr(VI) valence for the duration of the experiments. Early time removal of Cr(VI) from the spiked ground water solution is shown in Figure 21. The reaction was rapid for all four batch tests, with complete removal within the first 70 minutes (Table 8). Cr remained below detectable levels (< 0.02 mg/L Cr(VI)) during the remainder of all experiments (200 hours). PLSS showed the fastest reaction (non-detect (nd) at 23 minutes), followed by MBSS (nd at 35 min) and Ada iron (AdaSS) (nd at 70 min). Similar declines in Cr(VI) concentration were observed when natural Elizabeth City aquifer material (MBAQ) was substituted for silica sand in the reactive mixture.

In all four batch tests, the pH increased from an initial value of 5.9 to between pH 7 and 8 (Figure 20; Appendix D) within 5 hours. The final pH was lowest for the AdaSS mixture (pH 7.04). The Eh dropped by at least 500 mV during the experiments and by as much as 1,000 mV for the experiments using MBSS and PLSS. Iron corrosion and the reduction of Cr(VI) by Fe^0 (eqn. 6, 7) are probably responsible for the observed pH-increase and Eh-decrease in the batch flasks.



Over the first 3-6 hours, the alkalinity increased rapidly from an initial value of 30 mg/L CaCO_3 , to near 150 mg/L CaCO_3 . The alkalinity then decreased slowly until the end of the experiment.

Dominant ions in the batch water include Ca, Cl, Cr, Fe, Mg, Na, Si and SO_4 (Appendix D). Analytical charge balance errors of $< 5\%$ were regularly achieved. These species are at concentrations > 1 mg/L at some time during the experiment. Most other dissolved species are present at concentrations < 1 mg/L during the experiment. Dissolved Fe concentrations increased rapidly from < 0.05 mg/L (input) to maximum values between 1 and 64 mg/L within 5 hours, and generally decreased slowly afterwards. The highest Fe concentrations were measured in the PLSS and the lowest in the MBAQ mixture; the MBSS and AdaSS mixtures had mid-range values.

Dissolved Ca, Mn and Na concentrations increase slightly ($\sim 10\%$) from the input water composition during the batch experiments. Dissolved Si concentrations decrease by $\sim 70\%$ from the input water composition of ~ 6 mg/L. Trends for SO_4 concentrations are not evident.

Geochemical Modeling – Inorganic Data

MINTEQA2 was used to calculate the state of saturation of the water with respect to a variety of minerals versus time and batch composition. The results for ferrihydrite [$\text{Fe}(\text{OH})_3$], goethite, amorphous [$\text{Cr}(\text{OH})_3$], crystalline [$\text{Cr}(\text{OH})_3$], calcite [CaCO_3], dolomite [$\text{CaMg}(\text{CO}_3)_2$], siderite [FeCO_3], aragonite [CaCO_3], amakinite [$\text{Fe}(\text{OH})_2$], rhodochrosite [MnCO_3], quartz and amorphous silica are plotted in Figure 22 and are listed in Appendix E. As each batch reacts, similar trends in the state of saturation of the water are observed.

Chemical analyses indicate that the Cr in the input water occurs almost entirely as Cr(VI). High pH and Eh conditions preclude reduction to Cr(III) in the absence of a reductant. MINTEQA2 calculations indicate that the batch input water is undersaturated with respect to Cr(III) bearing solids. This water would only approach saturation with respect to crystalline and amorphous $\text{Cr}(\text{OH})_3$ if the Cr(III) concentration approached 50% of the total Cr concentration.

With the exception of the AdaSS mixture, total Cr concentrations generally reach the detection limit within approximately 0.5 hours (Appendix D). After the detection limit for Cr was reached, Cr was assumed to be 50% of the MDL (i.e., Cr = 0.01 mg/L), with speciation based on the Eh. Using these assumptions, the calculated SI values for Cr(OH)₃ after 0.5 hours indicate moderate supersaturation with respect to Cr(OH)₃.

Between 0 and 0.5 hours, dissolved Cr was speciated with MINTEQA2 based on the measured Eh. During this period the water in each batch experiment is supersaturated (SI ~ 2 to 3) with respect to Cr(OH)₃ (a) and near equilibrium (-0.75 < SI < 1.0) with respect to Cr(OH)₃ (c) (Figure 22). Because of kinetic limitations, however, it is unlikely that amorphous or crystalline Cr(OH)₃ are precipitating and limiting the concentration of dissolved Cr in the short time of the experiments. It is more likely that the Cr(III) is incorporated into a mixed Fe(III)-Cr(III) oxyhydroxide precipitate, similar to those observed in previous studies (Eary and Rai, 1988; Schwertmann, 1989; Powell *et al.*, 1995; Blowes *et al.*, 1997; and Pratt *et al.*, 1997). Although an analysis of solids from the batch flasks was not conducted, the reacted water is supersaturated with respect to goethite.

The reduction of Cr(VI) to Cr(III) is accompanied by the release of dissolved iron, as Fe⁰ is oxidized to Fe³⁺ (eqn. 2). The Fe³⁺ released during the Cr removal reaction may then be reduced to Fe²⁺ by the oxidation of Fe⁰,



Between 0 and ~0.5 hours, while Cr concentrations are measurable, Fe was not detected. The calculated saturation of the water with respect to ferrihydrite, goethite and other Fe-bearing minerals during this time is based on the assumption that the total Fe concentration is 10% of the MDL (i.e., Fe = 0.01 mg/L). Under this assumption, the water is near equilibrium with respect to ferrihydrite (Appendix E). If a solid solution such as (Cr_xFe_{1-x})(OH)₃ controls Cr(III) concentrations during this period, it is probable that this phase also controls Fe(III) concentrations.

After ~0.5 hours, Fe concentrations rise sharply (Appendix D). Based on the measured Eh, this iron is dominantly in the ferrous state. Because Fe(III) concentrations are small and not quantified, predictions about the solubility control for Fe(III) cannot be verified without mineralogical study. As each batch ages (>0.5 hr), the water gradually becomes less undersaturated with respect to amakinite.

Water in each of the batches is initially undersaturated with respect to calcite, dolomite and siderite (Figure 22). As the pH and alkalinity increase during the batch experiments, the water gradually approaches equilibrium with respect to the carbonate minerals calcite, aragonite and siderite. In particular, the water attains and exceeds saturation with respect to siderite, generally within one hour of the start of the experiments. Dissolved Fe(II) concentrations decrease gradually after 3 hours in all but the AdaSS batch mixture. This decrease in Fe concentration possibly results from the precipitation of siderite. Within 24 hours, equilibrium was also attained (SI = -0.20 to + 0.30) with respect to calcite, dolomite and rhodochrosite in the MBAQ batch.

In each of the batch experiments, the water is near equilibrium (SI = -0.02 to 0.35) with respect to quartz (SiO₂), and is undersaturated with respect to amorphous silica at all times (SI = -0.5 to -1.0). Noted decreases in dissolved Si concentrations may be attributed to the precipitation of amorphous silica or coprecipitation of silica with ferrihydrite or goethite. The accumulation of SiO₂ in iron oxyhydroxide coatings (goethite) surrounding zero valent iron grains has been noted previously by Blowes *et al.* (1997). Noted increases in the concentrations of dissolved Ca and Mn may be attributable to ion exchange or the gradual dissolution of trace amounts of minerals in the batch mixtures.

Column Results

Based on the results from the batch tests, the column tests focused on Master Builders™ and Peerless™ iron, with silica sand and Elizabeth City aquifer as the mixing materials.

The site water was siphoned from 4 L amber bottles used for shipping into a collapsible 22 L Telfon® bag. As noted in Appendix F by reservoir number (RN), all the site water could not be held in the collapsible bag and thus the reservoir had to be filled five times over the course of the tests. Reservoirs a-c were used in the first set of tests (high flow velocity, FV1) and reservoirs c-e in the second set (low velocity, FV2).

The main organic compounds detected in the site ground water were TCE, cDCE, trichloromethane (TCM; chloroform) and VC, with concentrations of about 750, 50, 20, and 40 µg/L, respectively. Trace levels of tetrachloroethylene (PCE) and trans-1,2-dichloroethylene (tDCE) were detected (2 µg/L each). The initial Cr(VI) concentration was 8 mg/L. In increase both the initial TCE and Cr(VI) concentrations to approximately 1,600 µg/L and 10 mg/L, respectively, in order to have an adequate amount of time to accurately determine declines in concentrations, the initial TCE and Cr(VI) concentrations were increased to approximately 1,600 µg/L and 10 mg/L, respectively.

Organic

Concentration profiles were measured along the columns at intervals of approximately 5-7 pore volumes. The results are listed in Appendix F. The results, obtained when steady state conditions were reached, are plotted as concentration

($\mu\text{g/L}$) versus distance (cm) along the column. In these columns, the profiles of most interest are the steady-state concentration profiles, reached when the rate at which the contaminants were degrading was equal to the rate at which they were entering the column. If the reaction is indeed first-order, then at steady-state, an exponential decline in concentration along the column would be expected.

High Flow Velocity Tests

Steady-state concentration profiles for the six column tests are shown in Figures 23-26. At a flow velocity of approximately 0.61 m/day (2 ft/day, FV1) a total of 40 to 50 pore volumes of spiked water had passed through the column at the time the profiles shown in Figures 23-27 were determined. In this case, one pore volume corresponds to a residence time ranging from 15 - 28 hours, depending upon the porosity of the particular packing material (Table 5). At steady-state, initial concentrations of 1,600, 23, 50 and 40 $\mu\text{g/L}$ were measured for TCE, TCM, cDCE and VC, respectively.

Figure 23 shows a rapid decline in TCE concentration from an initial value of 1,600 $\mu\text{g/L}$ to non-detectable values between the 15 cm and 30 cm sampling ports for all six columns. As shown in Figure 24, from an initial concentration of 23 $\mu\text{g/L}$ for TCM, a rapid decline in TCM concentration was observed with non-detectable concentrations occurring from 0.15 and 0.20 m (0.5 and 0.66 ft) along the column for all six columns.

The cDCE concentration increased from 50 $\mu\text{g/L}$ to peak concentrations ranging from 65 to 94 $\mu\text{g/L}$ at the 10 cm (0.33 ft) distance for the 100PL, 50PLSSAQ and 48PL/52AQ columns, while the remaining columns peaked at concentrations of approximately 180 $\mu\text{g/L}$ (Figure 25). The cDCE concentration increased due to the dechlorination of TCE. The cDCE concentration then gradually declined to effluent values of 120 and 70 $\mu\text{g/L}$ for 50MBSS and 50MBSSAQ and < 8.4 $\mu\text{g/L}$ for all the other columns.

The VC concentration in the site water was about 40 $\mu\text{g/L}$, with the exception of the water used in the 48PL/52AQ column. The 48PL/52AQ column test was conducted later, with an initial concentration of 12 $\mu\text{g/L}$ VC. The VC concentration declined steadily in four of the six columns (Figure 26). However, with both the 50MBSS and 50MBSSAQ columns, fluctuations in VC concentrations were observed with effluent concentrations of approximately 20 $\mu\text{g/L}$ (Figure 26). These VC concentration fluctuations were attributed to the dechlorination of TCE and cDCE.

Though present at trace levels in the source water, PCE was only detected up to 0.05 m (0.16 ft) distance into the columns. PCE concentrations were non-detectable for the remainder of the profiles for all columns (Appendix F). The tDCE concentrations in the columns fluctuated due to the dechlorination of TCE, and due to the presence of trace levels of tDCE in the source water. However, the highest tDCE concentration observed during the tests was 5.7 $\mu\text{g/L}$, and non-detectable concentrations were observed beyond 0.2 m distance in all of the columns (Appendix F). Though the compounds of greatest interest were TCE and the less chlorinated ethenes, analyses for TCM were performed since it was detected in the water obtained from the site. Though TCM degraded rapidly, a portion of the initial TCM would appear as dichloromethene (DCM). Previous experience indicated that DCM would not degrade in the presence of iron; however, at the low initial TCM concentrations, any DCM that formed would be below the MCL for DCM. DCM analyses were not performed.

Low Flow Velocity Tests

Steady-state concentration profiles of organic concentrations for the three column tests conducted at the low flow velocity are shown in Figures 27-30. At a flow velocity of approximately 0.3 m/day (1 ft/day, FV2) another 35 to 75 pore volumes of site water passed through the columns, giving cumulative pore volumes ranging from 85 to 125. At this flow velocity, one pore volume corresponds to a residence time ranging from 34 -50 hours (Table 5). At steady-state, initial concentrations of 1,400, 23, 75 and 12 $\mu\text{g/L}$ were measured for TCE, TCM, cDCE and VC, respectively.

Because slower treatment of cDCE and VC was observed for both the 50MBSS and 50MBSSAQ columns at the high flow velocity, these two mixtures were not tested at the second slower flow velocity. In addition, further testing of the 48PL/52AQ column at the lower velocity was not conducted because the hydraulic properties could potentially be problematic.

For the three columns (100MB, 100PL and 50PLSSAQ), TCE and TCM showed a steady decline in concentration (degradation) along the column length, with non-detectable concentrations measured between 0.2 and 0.30 m distance, along the columns, as shown in Figures 27 and 28.

The rate of cDCE removal (Figure 29) was slower due to its appearance as an intermediate product of the dechlorination of TCE. Thus the initial cDCE concentration of about 75 $\mu\text{g/L}$ increased to peak concentrations ranging from 80 to 150 $\mu\text{g/L}$, at distances ranging from 0.1 - 0.17 m (0.33 - 0.55 ft) along the column. However, once the concentration peaked, a steady decline in concentration was observed, with all three columns having non-detectable concentrations at the 0.4 and 0.5 m (1.31 and 1.64 ft) distances along the column.

The VC concentration declines steadily for all three columns, with minor fluctuations in concentrations (Figure 30). With initial concentrations ranging from 8 - 11 µg/L, non-detectable concentrations were observed at the effluent end (0.5 m) of the column.

Trace amounts of PCE and tDCE were present in the influent solution, however, declines in concentrations were observed, with non-detectable concentrations beyond a distance of 0.1 m for all three columns (Appendix F).

Inorganic Results

Chromium

Figures 31 to 36 summarize the detailed sampling results for dissolved Cr(VI) for all six columns, including both flow velocities. The first (high flow velocity) is indicated by FV1 in the figure caption, while the second (lower flow velocity) was indicated by FV2. Refer to Table 5 for the calculated flow velocities in each column. Table 9 summarizes the results of the inorganic analyses of samples from the influent and steady-state effluent for all six columns. Detailed column chemistry is listed in Appendix G.

At FV1 (~ 61 cm/day), complete removal of Cr was observed within the first 2.5 cm of each column for more than 40 pore volumes (Figure 31 - 36). Dissolved Cr concentrations dropped from maximum values of 11 mg/L input to non-detectable levels (< 0.02 mg/L) before the 2.5 cm sample port during the first stage of the experiment, along the length of each column. The 48PL/52AQ column was operated for 78 pore volumes at FV1. After 78 PV, measurable Cr was observed only at the 2.5 cm port (Figures 36, 37).

After running all of the columns at FV1, three of the columns (100MB, 100PL and 50PLSSAQ) were operated at a lower flow velocity of 0.3 m/day (1 ft/day = FV2). All columns exhibited similar Cr properties at all of the times, regardless of the solid reactive mixture. The column experiments were terminated after the treatment of 85 - 125 pore volumes. Final cumulative pore volumes for these columns are 98, 115 and 135, respectively. Cr was not detected in the effluent at termination of the experiments, although some Cr was detected at the 2.5 cm port as early as 69 pore volumes (100MB, Figure 37) and as late as 101 pore volumes (50PLSSAQ, Figure 37). The appearance of Cr at the 2.5 cm port, and a total column length of 50 cm, suggests that Cr(VI) could be effectively removed by any of the reactive mixtures in the columns for 1380 - 2020 pore volumes (Table 10). This prediction is preliminary because many factors such as flow rate and input Cr concentration may affect the actual breakthrough of Cr(VI) at the effluent end of the column.

Cations and Anions

Table 9 summarizes the inorganic analyses of samples from the influent and steady-state effluent for all six columns. Appendix G includes all inorganic analytical data, including profile data.

There is little change in the Na, Fe, K, Cl and SO₄ concentrations with passage of the water through the column materials (Appendix G and Table 9). The concentrations of Ca, Mg, Mn, and dissolved Si (as [H₄SiO₄]) decrease along the length of the columns. In contrast, the concentrations of Ca, Mg and Mn in the batch experiments increased over the duration of the experiments.

The Ca concentration decreases by ~ 8-12 mg/L, in all columns except 50MBSSAQ. Mg concentrations decrease significantly (> 25%) in all but the 50MBSS column. Mn concentrations decrease from ~ 0.9 mg/L to < 0.2 mg/L within a short travel distance in all columns. Dissolved H₄SiO₄ concentrations decrease sharply from ~31 mg/L to < 2 mg/L within a short distance in the columns. These results suggest the removal of these dissolved cations through ion exchange or mineral precipitation may be occurring.

Eh, pH and Alkalinity

In all cases, the pH rose from about pH 6.5 to pH 9 within the first 0.1 m of each column (Figures 31-36, Appendix G). The pH values then remained constant throughout the length of the column. In all of the columns, the Eh values declined from influent values of 300 - 400 mV (SHE), to near 0 mV values within the first 0.1 m of the column (Figures 31-36). Pore water alkalinity was maintained near 50 mg/L CaCO₃ with slightly higher values observed near the influent end of the column (Figure 31-36). All columns exhibited similar pH, Eh and alkalinity properties at all sampling times, regardless of solid reactive mixture.

Geochemical Modeling

MINTEQA2 was used to calculate the saturation indices of a variety of minerals (ferrihydrite, goethite, amorphous [Cr(OH)₃], crystalline [Cr(OH)₃], calcite, dolomite, siderite, amakinite, rhodochrosite, quartz, amorphous silica and mackinawite [FeS]), along each of the columns (Figures 38-43, Appendix H). For comparison, the SI values calculated at several pore volumes are plotted together on each figure. The figures show the results for measurements collected at both the fast (FV1, low pore volume measurements) and slow velocities (FV2, high pore volume measurements).

MINTEQA2 calculations suggest that the source water is generally close to equilibrium or undersaturated with respect to amorphous $\text{Cr}(\text{OH})_3$, and undersaturated with respect to crystalline $\text{Cr}(\text{OH})_3$. High pH and Eh conditions limit Cr(III) concentrations in the source input water to low levels, as confirmed by the similarity of total Cr and Cr(VI) values (Appendix D).

Trends in the SI values of crystalline and amorphous $\text{Cr}(\text{OH})_3$ are similar for each column composition and at all pore volumes. However, because Cr concentrations generally are depleted to approximately analytical detection limits beyond the first sampling port, SI values for $\text{Cr}(\text{OH})_3$ beyond the first port are overestimated. In a few cases, however, significant measurable Cr concentrations (>1 mg/L) were detected at the 2.5 cm port (Appendix G). These include the 100MB column at 79 and 98 PV (at FV2), the 100PL column at 100.5 and 114.7 PV (FV2), the 50PLSSAQ column at 135.3 PV (FV2) and the 48PL/52AQ column at 78.4 PV (FV1). Calculated SI values for amorphous $\text{Cr}(\text{OH})_3$ range from 3.2 to 3.9, and for crystalline $\text{Cr}(\text{OH})_3$ range from 0.6 to 1.4.

As with the batch test results, it is not likely that a pure $\text{Cr}(\text{OH})_3$ phase would precipitate within the short duration of the experiments. It is more probable that the Cr is removed by co-precipitation within a mixed Fe(III)-Cr(III) hydroxide solid solution or mixed Fe(III)-Cr(III) (oxy)hydroxide solid, as has been observed previously (Eary and Rai, 1988; Schwertmann, 1989; Powell *et al.*, 1995; Blowes *et al.*, 1997; Pratt *et al.*, 1997). The water samples that contain measurable concentrations of dissolved iron are supersaturated with respect to goethite.

Goethite precipitation may passivate the iron filing surfaces over longer periods of treatment. At FV2 (31 cm/day) and a maximum observed iron concentration of ~ 18 mg/L, the precipitation of goethite (molar volume 20.8 ml/mol) results in a 10% decrease in porosity over the length of the column in about 82 years.

The dissolved Fe concentration is below the analytical detection limit in the input water. Occasionally, higher dissolved Fe concentrations (> 1 mg/L) are detected at the first (2.5 cm) and second (5 cm) sampling ports (Appendix G). This Fe probably results from corrosion of the iron filings by oxygen and by water, and during the reduction of Cr(VI) to Cr(III) (eqn. 6, 7). Dissolved Fe concentrations are otherwise at analytical detection limits in all columns at all times. MINTEQA2 calculations indicate that at the 2.5 cm and 5 cm locations, Fe(II) is the dominant dissolved Fe species. As in the case for Cr, MINTEQA2 saturation index calculations for iron minerals are considered reasonable only at locations where measurable iron concentrations were detected (0-5 cm). At these locations, the water is supersaturated with respect to goethite (SI ~ 6), is near equilibrium with respect to ferrihydrite (SI ~ -0.5 to $+1$); and is undersaturated (SI ~ -2.5 to -4) with respect to amakinite (Appendix H, Figures 38-43).

In parts of the column where the Fe concentrations are below the detection limit, the water along each of the columns would be supersaturated with respect to goethite and would be near equilibrium with respect to ferrihydrite if an Fe concentration of 0.01 mg/L (10% MDL) was assumed to be present. With the same assumption, the water would be slightly undersaturated with respect to amakinite.

The input water for the columns is undersaturated with respect to calcite, aragonite, dolomite and siderite. Within each column, the pH increases significantly downgradient from the source, and the alkalinity decreases slightly. The water approaches equilibrium with respect to calcite and aragonite and becomes supersaturated with respect to dolomite between the first and third sampling ports (10 cm). Precipitation of aragonite or calcite is consistent with the decrease in alkalinity and dissolved Ca concentrations observed along the length of columns 50MBSS, 100MB, 100PL and 48PL/52AQ. Although the water is also slightly supersaturated with respect to calcite and dolomite in the 50MBSSAQ column, dissolved Ca concentrations along the length of these columns remain relatively unchanged. The Ca concentration decreases by approximately 12 mg/L. Assuming that this decrease is due to calcite precipitation (calcite molar volume 35 ml/mol), a 10% decrease in the porosity of the first 10 cm of a column would occur in about 16 years at the slower velocity (31 cm/d) or in about 9 years at the higher velocity (53 cm/d). These calculations suggest that calcite or other carbonate mineral precipitation could adversely affect the permeability or reactivity of the granular iron over longer treatment periods.

Because the behavior of Fe is linked to the geochemical reactions that remove the dissolved Cr, the trends for siderite are unlike those of calcite and dolomite (Ca and Mg are not involved in the Cr removal reactions). In locations where Fe concentrations are measurable, generally within the first 5 cm of the column (Figures 38-43), the water approaches equilibrium with respect to siderite. The precipitation of siderite in this location may limit Fe mobility in the columns. Beyond the first sampling port, calculations of pore-water saturation with respect to siderite assume Fe(II) concentrations that are 10% of the analytical detection limit (*i.e.*, Fe=0.01 mg/L).

The water also approaches and attains equilibrium with respect to magnesite. The observed decrease in Mg concentrations may be due to the precipitation of a magnesium carbonate or hydroxycarbonate.

The water is undersaturated, but approaches equilibrium with respect to rhodochrosite in each of the columns. In each of the columns, equilibrium is reached at the first port of the columns at the slower flow velocity. At the higher flow velocity, equilibrium is attained further along the column, suggesting the precipitation may be rate dependent. It is

possible that precipitation of rhodochrosite or a less crystalline precursor limits dissolved Mn concentrations. The observed sharp decrease in Mn concentrations at the first port is consistent with this conclusion.

The input waters are slightly supersaturated ($SI = 0.58$) with respect to quartz and are undersaturated with respect to amorphous SiO_2 ($SI = -0.4$). With the decreasing H_4SiO_4 concentrations along the length of each column, the water becomes more undersaturated with respect to amorphous SiO_2 ($SI = -1$ to -2). In the downgradient direction, the H_4SiO_4 concentration decreases sharply by the first or second sampling port. Kinetic limitations prevent the direct precipitation of quartz. It is likely, therefore, that H_4SiO_4 concentrations decrease as a result of the coprecipitation of amorphous silica with Cr and Fe bearing solids. The accumulation of SiO_2 within iron oxyhydroxide coatings (goethite) surrounding zero valent iron grains has been noted previously by Blowes et al. (1997). Palmer (1999) confirmed the presence of silica-containing goethite and/or amakinite on the surface of iron filings collected from the downgradient side of the Elizabeth City full-scale barrier. Although a discrete solid silica phase is not expected to form and thereby affect the reactivity of the iron filings, the association of Si with mixed Fe(III)-Cr(III) hydroxide solid solution (eqn. 3) or mixed Fe(III)-Cr(III) (oxy)hydroxide solid indicates that Si may contribute to the passivation of the granular iron surfaces over longer treatment times.

Determination of Reaction Parameters: Cr(VI)

Data from the column tests were used as a basis for the selection of reactive materials for the reactive barrier. Chromium concentrations decrease from approximately 10 mg/L to less than 0.05 mg/L (MCL) at the first sampling port (2.5 cm) for 69 to 101 PV, depending on the column reactive mixture (Table 10, Figure 37). At later times, Cr(VI) concentrations at this port were above MCL. These results suggest that the reaction with Cr(VI) is very rapid and that the Cr front is migrating slowly through some of the columns, possibly as a result of changing reactivity of the Fe^0 surface due to precipitation. Cr(VI) concentrations in the column effluent are predicted to exceed the MCL value of 0.05 mg/L Cr after 1,400 to 2,000 pore volumes (Table 10). At an estimated flow velocity of 10 cm/day at the Elizabeth City site, this would correspond to chromium breakthrough in a 0.5 m granular iron barrier within 19 to 28 years.

Determination of Reaction Parameters: Halogenated Hydrocarbons

Reaction rates for the reductive-dechlorination of TCE, cDCE and VC with various reactive mixtures were calculated from column experiment data (O'Hannesin *et al.*, 1995). The reaction rates were calculated to determine the relative reactivity of different zero-valent iron mixtures, as well as for use in conjunction with reactive-transport modeling.

Concentration profiles along the column were obtained after 40-50 pore volumes had flowed through the column. Rate constants for the reductive-dechlorination of the chlorinated organics were obtained by fitting a consecutive first-order decay model, adapted from Hill (1977), to these profiles. The model assumes that of all the reaction products from TCE degradation, x % of the TCE decays to cDCE, with the other $(1-x)$ % of the TCE degrading to alternative breakdown products such as chloroacetylene. Similarly, only y % of the cDCE decays to VC, with the remaining $(1-y)$ % of the cDCE degrading to alternative breakdown products such as acetylene. The first order rate expressions for the decay of TCE, cDCE and VC are shown in eqn. 9 through 11.

$$\frac{d[TCE]}{dT} = -k_1[TCE] \quad (9)$$

$$\frac{d[cDCE]}{dT} = xk_1[TCE] - k_2[cDCE] \quad (10)$$

$$\frac{d[VC]}{dT} = yk_2[cDCE] - k_3[VC] \quad (11)$$

where k_1 , k_2 , k_3 represent first-order rate constants (d^{-1}), and x , y represent mole transfer coefficients (mole %). The molar transfer coefficients represent the mole percentage of the parent compound that degrades to a daughter product. This model describes the first-order reductive-dechlorination of TCE, including the production or accumulation of cDCE and VC breakdown products and their first-order decay.

Ground-water residence times within the column were calculated by dividing distances along the column by the ground-water velocity. Rate constants and molar transfer coefficients were then calculated from non-linear least squares fit of concentration versus residence time data to analytical solutions for eqn. 9 to 11 (eqn. 12, 13, 14 respectively):

$$[TCE]_t = [TCE]_o e^{-k_1 t} \quad (12)$$

$$[cDCE]_t = [cDCE]_o e^{-k_2 t} + \frac{xk_1 [TCE]_o}{k_2 - k_1} (e^{-k_1 t} - e^{-k_2 t}) \quad (13)$$

$$[VC]_t = [VC]_o e^{-k_3 t} + [cDCE]_o y \left(\frac{k_2 e^{-k_2 t} - k_2 e^{-k_3 t}}{k_3 - k_2} \right) + [TCE]_o xy \left\{ \frac{k_1 k_2 e^{-k_1 t}}{(k_3 - k_1)(k_2 - k_1)} - \frac{k_1 k_2 e^{-k_2 t}}{(k_3 - k_2)(k_2 - k_1)} - \frac{k_1 k_2 e^{-k_3 t}}{(k_3 - k_2)(k_3 - k_1)} \right\} \quad (14)$$

This model neglects the effects of dispersion and diffusion within the columns.

First-order rate constants and molar transfer coefficients for TCE, cDCE and VC are shown in Table 11. TCE concentrations decrease more rapidly than the concentrations of cDCE and VC within the columns. Based on this observation, the selection of the barrier width and reactive material will be based upon the reactivity of the reactive mixtures toward cDCE and VC.

Comparison of the molar transfer coefficients of various reactive mixtures indicates that between 4 and 17% of the TCE mass degrades to cDCE, and between 1 and 100% of the cDCE degrades to VC, with the remaining mass degrading to other products. Previous laboratory experiments indicated that less than 10% of TCE degrades to chlorinated degradation products (Gillham and O'Hannesin, 1994; Orth and Gillham, 1996). It should be noted that reaction rates determined from the filtering procedures can be influenced significantly by one or two data points that fall off the trend. The certainty in the calculated values therefore decreases with increasing scatter in the data. Normally this is the case for compounds that degrade slowly or are present at low concentrations.

There appeared to be no substantial advantage in mixing sand with the iron materials, and there was the further concern of segregation of the sand and iron during installation. Consequently, the sand-iron mixtures were eliminated as potential candidates for the installation. The remaining two reactive materials, 100PL and 100MB, were compared on the basis of reaction rates, hydraulic properties (Table 12) and cost.

TCE, cDCE and VC steady-state concentration profiles within the 100MB and 100PL columns after 40-50 pore volumes, and calculated concentration profiles using least-squares fit parameters, are shown in Figures 44 through 46. The surface area normalized reaction rates for TCE and cDCE were within 20% agreement for 100PL and 100MB, while the normalized rate for VC degradation was significantly greater for 100PL (Table 12). These normalized reaction rates are similar to those reported by Johnson *et al.* (1996), shown previously in Table 2. The 100MB and 100PL columns also have similar hydraulic conductivity and porosity values, which were the highest measured for all reactive materials. These higher values may be advantageous in offsetting potential long-term precipitate formation, which may reduce the hydraulic conductivity and porosity of the barrier. However, the cost of Peerless™ iron (~ \$375 US/ton, 1995) was less than that of Master Builders™ iron (~ \$700 US/ton, 1995). Thus, 100 % Peerless™ iron (100PL) was chosen as the reactive material, based on suitable reaction rates, desirable hydraulic properties and lower cost.

Reactive Barrier Designs

Five three-dimensional numerical flow simulations were performed to assess the relative efficiency of a Funnel-and-Gate versus a continuous wall configuration (Bennett, 1997). In these simulations, the entire model domain was assigned a uniform hydraulic conductivity (Table 13). A range in aquifer hydraulic conductivity values was simulated in order to bracket the anticipated range of ground-water velocities, capture areas and residence times.

The capture area of a reactive barrier is the cross-sectional area of ground water intercepted by the reactive barrier (Figure 47) and which flows through the reactive material. Capture areas were estimated from the ground-water flow pathlines. These pathlines were traced from an upgradient grid of 0.3 m spacing. Pathlines that enter the "gate" zone of a Funnel-and-Gate or the continuous wall were considered to be within the capture area of that barrier. The capture area results are presented as overall capture areas and as values relative to the total area of the front face of the Funnel-and-Gate or continuous wall.

The simulated capture areas of the 15.8 m wide, 9.1 m deep, and 2 m thick Funnel-and-Gate barrier are shown in Table 14. The impermeable funnels of a Funnel-and-Gate increase the capture area of the Gate (reactive material) zone.

However, only a third to a half of the ground-water flow approaching the funnels is directed through the gate. A significant volume of ground-water flows around and underneath the “hanging” Funnel-and-Gate, limiting the increase in capture area (Figures 48, 49). The hydraulic conductivity of the aquifer also has an impact on the capture area of the Funnel-and-Gate. The capture area of the barrier is larger when the hydraulic conductivity of the aquifer is less than that of the gate. Based on the observed aquifer hydraulic conductivities, the capture area is expected to be between 67 and 85 m² for the Funnel-and-Gate configuration simulated.

The simulated capture areas of the 10.3 m wide, 7.6 m deep and 0.45 m thick continuous wall configuration are shown in Table 15. Without funnels to intercept ground-water flow and increase the capture area of the reactive material, the capture area of the wall is equal to or slightly larger than the face of the wall. The capture area of the wall increases by only 14% when the hydraulic conductivity of the reactive material is two orders of magnitude greater than that of the aquifer. Thus, there is only slight preferential ground-water flow through the barrier when the hydraulic conductivity of the wall is much larger than the aquifer. Very little ground-water flow divergence is observed in the vicinity of the barrier (Figure 50). The capture areas of a wall at the site are expected to be between 105% and 114%. This corresponds to a capture area of 82 m² to 89 m² for the simulated pilot-scale configuration. These capture areas are very similar to those obtained with the Funnel-and-Gate. If the hydraulic conductivity of the reactive media comprising the wall falls below that of the aquifer, the capture area of the wall will be less than 100%, indicating that ground water will begin to preferentially flow around it.

Residence times (Table 16) within the reactive material were calculated by averaging the component of the elemental velocity vectors parallel to the shortest path through the barrier. This parameter indicates the minimum period of contact between the contaminant and the reactive material. Similar residence times are calculated for the two barriers. The residence time is expected to be between approximately 2 and 500 days, for the hydraulic conductivity range observed within the aquifer. The similar residence times arise because both barriers have similar capture areas. The similar capture areas indicate that the same volumes of ground water are flowing through both barriers, which have the same volume of reactive material.

The funnels increase the capture area of the reactive material zone 2 to 2.6-fold. As a result, simulated ground water velocities within the Funnel-and-Gate are approximately 2 to 2.6-fold greater than in the aquifer. The calculated ground water velocities within the continuous wall are approximately equal to the velocities within the aquifer. These similar velocities arise because there is only slight preferential ground water flow through the higher hydraulic conductivity reactive material. The increased velocity within the reactive material, relative to the velocity in the aquifer, is similar to the increase in capture area of the reactive material zone. This similarity arises because the ground water velocity within the reactive material is proportional to the volumetric ground water flux through it, and the flux is directly related to the capture area of the reactive material zone.

These results indicate that for the Elizabeth City site, there are no hydraulic advantages of a Funnel-and-Gate over a permeable wall in terms of both increased capture area and increased residence time. Both barrier designs can be configured to achieve similar residence times and capture areas using the same volume of reactive material.

Final Selection of a Reactive Barrier

Final Reactive Barrier Design

The continuous wall was the reactive barrier design chosen for the site, based upon cost and flow modeling results. Flow modeling indicated that, for the Elizabeth City site, there was no hydraulic advantage of a Funnel-and-Gate over a wall, however initial cost estimates suggested that the wall configuration could be more cost-effective for this site.

Reactive transport simulations were conducted to determine whether a 36.4 m long x 7.6 m deep x 0.45 m thick continuous wall composed entirely of granular iron (100PL) would provide a sufficient residence time to remediate TCE, cDCE and VC concentrations similar to those at the site to less than MCL values, and under the maximum anticipated flow conditions. Two simulations were conducted with different hydraulic parameters assigned to the granular iron which comprise the barrier (Table 17).

The maximum anticipated flow conditions arise when the horizontal hydraulic gradient is 0.0033, and hydraulic conductivity is 17 m/day. Under these flow conditions, the simulations indicate that 10,000 µg/L TCE, 900 µg/L cDCE, and 101 µg/L VC will be reduced to MCL values within approximately 0.33 m of travel in the iron (Table 18).

VC requires the longest travel distance within the wall, or longest residence time, before it falls below its MCL value. This is because VC has the lowest MCL value and is the last degradation product produced of the decay of TCE and cDCE. A concentration profile through the center of the reactive wall is shown in Figure 51.

The final dimensions chosen for the reactive barrier were 46 m x 7.3 m x 0.6 m. The 46 m length and 7.3 m depth of the barrier were felt to be sufficient to intercept the Cr(VI) plume, which is approximately 35 m wide and 6.5 m deep. A width of 0.6 m was used to give a slight safety factor for residence time. A reactive medium composed entirely of Peerless™ granular iron was chosen for the barrier based on reactivity, hydraulic properties and cost.

Barrier Installation

Configuration

The subsurface granular iron wall was oriented in an east-west direction, approximately perpendicular to the ground water flow direction. It was installed on June 22, 1996, beneath the parking lot downgradient of the electroplating shop in Hangar 79. The granular iron was installed within a 0.6 m wide trench located between approximately 2 m and 7.3 m depth (Figure 52). The top of the granular iron barrier was planned to coincide with the approximate depth of the water table. The bottom of the barrier was the maximum depth of installation with the trenching machine employed. Approximately 150 m³ of granular iron were required for the barrier. Using the laboratory measured bulk density of 2.72 g/cm³, this volume corresponded to approximately 450 tons of granular iron. Prior to installation, the granular iron was shipped to the Elizabeth City site and stored beneath plastic sheets on the parking lot.

Site Preparation

An 80 m long and 1 m wide cut was made in the concrete parking lot to facilitate the trenching installation. Plastic sheets with covered hay-bail berms were laid out on either side of the cut (Figure 53). The plastic sheets and berms were used to prevent excavated soil from washing into the river. A high capacity pump and large tanker were also kept onsite in the event that excavated materials exceeded the capacity of the bermed area.

A decontamination area was set up with plastic liners and hay-bails for the steam cleaning of all equipment. The parking lot installation area was completely fenced off.

Installation

The installation was performed by Horizontal Technologies Inc. (HTI) using a continuous trenching machine. The trenching machine (Figures 54, 55) used to install the subsurface barrier simultaneously removed aquifer material and deposited the granular iron. Excavated aquifer material was brought to the surface by an excavating belt and then conveyed to one side of the machine. A 0.6 m wide rectangular box, located behind the excavating belt, kept the trench open while granular iron was poured in. A total of 280 tons of granular iron was placed into the trench. The mass of granular iron used was significantly less than the 450 ton mass calculated using the laboratory bulk density for granular iron. The lower mass of granular iron within the trench suggests that emplaced density may be less than the laboratory density, and that the granular iron may not occupy the entire volume of the trench. The actual volume and shape occupied by the granular iron is irregular, due to the compaction and slumping of aquifer material into the trench. Studies using borehole radar, electromagnetics, and other geophysical techniques are planned to confirm the extent of the granular iron zone.

The lower mass of granular iron within the wall is expected to have an impact on the surface area dependent reductive-dechlorination rates. An emplaced granular iron density of 1.69 g/cm³, which is approximately 60% of the laboratory measured bulk density, is calculated assuming that the granular iron fills the entire trench. At this density, the overall surface-area dependent reaction rates may be as low as 60% of the laboratory measured values. Lower reaction rates at this lower emplacement density, however, may be offset by an increase in porosity to as high as 0.62 and decrease in ground water velocity within the granular iron. Alternatively, the granular iron thickness within the trench may be as low as 37 cm at an emplaced density of 2.72 g/cm³. Under this extreme case, residence times would be only approximately 60% of the design value.

The aquifer material that was excavated by the trenching machine liquefied, forming a soil slurry on either side of the trench (Figure 56). In addition, aquifer soils within the trench slumped in as the excavation proceeded. This simultaneously loaded and undermined the concrete pavement and led to the collapse of approximately 3 m of pavement on either side of the trench (Figure 57).

Post-Installation Work

The concrete removed from the initial 80 m by 1 m trench cut was tested for VOCs and chromium. None was detected, and this concrete was disposed of in the local landfill (Parsons Engineering Science, 1997). Excavated soils from the trench were stockpiled on the site. Four samples and one duplicate were collected the day after installation and analyzed for VOCs and Cr. Total Cr concentrations were found to be at background levels. However, TCE concentrations in the soil exceeded MCL values, and therefore required additional management before disposal. The excavated soils were taken to a Corrective Action Management Unit (CAMU). The CAMU consisted of a plastic liner surrounded by concrete barriers. The soils were worked with earth moving equipment and then covered by plastic. Approximately one month later, additional samples were taken and analyzed. TCE concentrations were found to be below the laboratory quantitative limits. The USCG was then permitted to use the soil as a clean backfill at the Support Center. The trench was backfilled with the natural excavated soils, followed by a coarse aggregate. This formed the subbase, which was subsequently paved with asphalt.

Barrier Costs and Performance

The total cost of the barrier installation, including the initial design work, soil treatment and follow-up work, was approximately \$985,000 U.S. (Table 19). The actual installation and granular iron costs are estimated to be approximately \$350,000 U.S. This corresponds to an installation and materials cost of approximately \$7550 U.S./linear meter for the 5.3 m thick and 0.6 m wide continuous reactive wall.

An internal USCG report indicates that this reactive wall will lead to a cost savings of \$4,000,000 U.S. over a 20 year span compared to a traditional pump-and-treat system (USCG, Pers. Comm.). The report states that the installation costs for the reactive barrier and a pump-and-treat system were comparable, however a cost savings results from the lower monitoring and maintenance costs associated with the continuous reactive wall barrier. Annual costs are estimated to be approximately \$32,000 U.S. for the reactive wall compared to \$200,000 U.S. for a comparable pump-and-treat system. A similar cost analysis conducted by Manz and Quinn (1997) indicates that permeable treatment walls can result in significant cost savings over a comparable ground-water extraction and treatment system. In their study of two sites, they indicate that while capital costs vary, the annual estimated operation and maintenance costs for a treatment wall were \$20,000 and \$27,120 U.S., as opposed to between \$55,000 and \$100,000 U.S. for a pump-and-treat system.

The long-term cost savings associated with a reactive barrier result from its lower operation and maintenance costs, compared to a pump-and-treat system. However, the actual savings also depend on the initial capital costs for the barrier installation and the estimated longevity of the reactive barrier. Previous studies with granular iron indicate that carbonate and hydroxide minerals precipitate on the iron surfaces from anaerobic high alkalinity ground waters (Reardon, 1995; Schuhmacher *et al.*, 1997; Mackenzie *et al.*, 1997). These precipitates can influence the long-term performance of the barrier by potentially altering both the reactivity towards contaminants, and the hydraulic conductivity and porosity of the barrier. Granular iron column experiments indicated minimal loss in reactivity toward Cr(VI) or TCE, even after more than 100 pore volumes passed through the columns (Blowes *et al.*, 1992; O'Hannesin *et al.*, 1995; Blowes *et al.*, 1997; Cippolone *et al.*, 1997). Based on laboratory column data in this report, the extrapolated breakthrough of Cr(VI) is not expected to occur for 19-28 years at ground water velocities of 10 cm/day. Other laboratory studies to assess the impact of precipitate formation on ground water flow hydraulics within granular iron media indicated porosity losses that levelled off at 5-15% (Mackenzie *et al.*, 1997). These porosity losses were attributed mainly to H₂ gas formation, and mineral precipitation was suggested to have a more significant impact on porosity at later times. In future studies, cores will be collected from the granular iron zone to assess the extent of precipitate formation.

Conclusions

Ground-water flow simulations indicate that a Funnel-and-Gate and a continuous wall can be configured to achieve the same capture area and residence time, with the same volume of reactive material. Therefore, there is no hydraulic advantage in using a Funnel-and-Gate over a continuous wall. The choice of barrier design then depends on the logistics and cost of the site-specific situation. For the Elizabeth City site, the wall configuration was selected.

The selection of the granular iron mixture that the reactive barrier would be composed of was based on reactivity, hydraulic properties and cost. Fast reaction rates were desirable to minimize the amount of granular iron required and high hydraulic conductivity and porosity are desirable to ensure that ground water preferentially flows through the barrier. Of the reactive mixtures tested in laboratory batch and column experiments, the ones containing 100% granular iron had the most rapid reaction rates for Cr(VI), TCE, cDCE and VC removal and the highest hydraulic conductivity and porosity values. In the column tests, input concentrations of 11-12 mg/L Cr were depleted to < 0.02 mg/L over less than 10 cm travel distance in the columns. Input TCE concentrations of 1,500-2,000 µg/L were reduced to non-detectable concentrations (<1.7 µg/L) before reaching the half-way point (30 cm) in the columns. The PL and MB granular iron materials tested had similar surface-area normalized reaction rates and hydraulic properties. A reactive material composed entirely of Peerless™ brand granular iron was chosen for the reactive barrier, with the final choice of granular iron source based on reactivity, hydraulic properties and cost.

Contaminant reactive transport simulations indicate that 10,000 µg/L TCE, 900 µg/L cDCE, and 101 µg/L VC would be reduced to less than MCL values in 0.33 m of travel within a reactive wall composed of this granular iron at a density of 2.72 g/cm³ and under the maximum anticipated ground-water velocity conditions. The final barrier width of 60 cm was chosen to provide a safety factor for the treatment of TCE, cDCE, and VC contaminated ground water that is intercepted by the barrier. The length and depth of the barrier were chosen to intercept the entire Cr(VI) plume.

The full-scale granular iron reactive wall was installed quickly and relatively inexpensively using a trenching technique, although the maximum width and depth were dictated by the trenching machine configuration. The installation was completed in 6 hours, with the only complication arising from the failure of the concrete pavement alongside the trench. The speed and relatively low cost of the installation is attributed to the effectiveness of the trenching machine, which simultaneously removed aquifer sediments and emplaced granular iron. The emplaced mass of the granular iron was approximately 60% of that calculated, suggesting a lower emplacement density and smaller volume of granular iron within the 60 cm trench. This lower iron density may result in slower reaction rates, due to decreased available mass and surface area of granular iron. Alternatively, greater porosity in the wall may lower ground water velocities within the wall, increasing the available reaction time. The extent or distribution of granular iron within the trench and the impact of the lower mass of granular iron on reaction rates will be assessed in future studies.

References

- Allison, J.D., Brown, D.S. and Nova-Gradac, K.J., 1990. MINTEQA2/PRODEFA2, A geochemical assessment model for environmental systems: Version 3.0 user's manual. Environmental Research Laboratory, Office of Research and Development, U.S.EPA., Athens, Ga. 106p.
- Arnold, W.A., and Roberts, A.L. 1997. Development of a quantitative model for chlorinated ethylene reduction by zero-valent metals. In *Proc. 213th American Chemical Society National Meeting, Environmental Chemistry Division*, San Francisco, CA, April 13-17, Vol. 37, No. 1, pp. 76-77.
- Ball, J.W. and Nordstrom, D.K. 1991. User's manual for WATEQ4F, with revised thermodynamic database and test cases for calculating speciation of major, trace and redox elements in natural waters. *U.S. Geological Survey, Open-File Report 91-183*.
- Bennett, T.A., 1997. An in-situ reactive barrier for the treatment of hexavalent chromium and trichloroethylene in groundwater. M.Sc. Thesis, University of Waterloo. 203p.
- Blowes, D.W., and Ptacek, C.J. 1992. Geochemical remediation of groundwater by permeable reactive walls: removal of chromate by reaction with iron-bearing solids. In *Proc. Subsurface Restoration Conference, Third International Conference of Ground water Quality Research*, Dallas, Texas, June 21-24, 1992. pp. 214-216.
- Blowes, D.W., Ptacek, C.J., Cherry, J.A., Gillham, R.W., and Robertson, W.D. 1995. Passive remediation of groundwater using in situ treatment curtains. In Acer, Y.B. and Daniel, D.E. (Eds), *Geoenvironment 2000, Characterization, Containment, Remediation, and Performance in Environmental Geotechnics*, Geotechnical Special Publication No. 46, Vol. 2, American Society of Civil Engineers, New York, pp. 1588-1607.
- Blowes, D.W., Ptacek, C.J. and Jambor, J.L. 1997. In-Situ remediation of chromate contaminated groundwater using permeable reactive walls: Laboratory Studies. *Environ. Sci. Technol.*, 31 (12), 3348-3357.
- Brunauer, S., Emmett, P.H. and Teller, E., 1938. Adsorption of gases, in multimolecular layers. *J. American Chemical Society*, 60, 309-319.
- Buerge, I.J., and Hug, S.J. 1997. Kinetics and pH dependence of chromium(VI) reduction by iron(II). *Environ. Sci. Technol.*, 31, 1426- 1432.
- Dennis, J.K. and Such, T.E. 1972. *Nickel and Chromium Plating*. Butterworth & Co. (Canada), Toronto, 325 pp.
- Eary, L.E., and Rai, D. 1988. Chromate removal from aqueous wastes by reduction with ferrous ion. *Environ. Sci. Technol.*, 22, 972-977.
- Eary, L.E., and Rai, D. 1989. Kinetics of chromate reduction by ferrous ions derived from hematite and biotite at 25°C. *Am. J. Sci.*, 289, 180-213.
- Eary, L.E., and Rai, D. 1991. Chromate reduction by subsurface soils under acidic conditions. *Soil Sci. Soc. Am. J.*, 55, 576-683.
- Focht, R., Vogan, J., and O'Hannesin, S. 1996. Field application of reactive iron walls for in-situ degradation of volatile organic compounds in groundwater. *Remediation*, 6 (3), 81-94.
- Freeze, R.A., and Cherry, J.A. 1979. *Groundwater*. Prentice-Hall, Englewood Cliffs, J.J. 604 pp.
- Glaze, W.H., Rawley, R., Burleson, J.L., Mapel, D. and Scott, D.R., 1981. Further optimization of the pentane liquid-liquid extraction method for the analysis of trace organic compounds in water. In: *Advances in the identification and analysis of organic pollutants in water*. Vol. 1, Keith, L.H. ed, Ann Arbor Pub. Inc., Ann Arbor, MI.
- Gillham, R.W., and Burris, D.R. 1992. Recent developments in permeable in situ treatment walls for remediation of contaminated ground water. In *Subsurface Restoration Conference, 3rd International Conference on Ground Water Quality Research*, Dallas, Texas, June 21-24. pp. 66-68.
- Gillham, R.W., and O'Hannesin, S.F. 1992. Metal-catalysed abiotic degradation of halogenated organic compounds. In *Proc. 1992 IAH Conference "Modern Trends in Hydrogeology"*, Hamilton, Ont., May 10-13.
- Gillham, R.W., and O'Hannesin, S.F. 1994. Enhanced degradation of halogenated aliphatics by zero-valent iron. *Ground Water*, 32 (6), 958-967.
- Gillham, O'Hannesin, S.F., Orth, W.S., 1993. Metal enhanced abiotic degradation of halogenated aliphatics: Laboratory tests and field trials. Proceedings of the 6th Annual Environmental Management and Technical Conference/HazMat Central Conference, Rosemont, Illinois, 440-461.
- Gould, J.P. 1982. The kinetics of hexavalent chromium reduction by metallic iron. *Water Res.*, 16, 871-877.
- Greenwood, J.D. 1971. *Hard Chromium Plating*. 2nd edition. Clare o'Molesey Ltd., Surrey, GB, 217 pp.
- Hem, J.D. 1977. Reactions of metal ions at surfaces of hydrous iron oxide. *Geochim. Cosmochim. Acta*, 41, 527-538.

-
- Henderson, J.E., Peyton, G.R. and Glaze, W.H., 1976. A convenient liquid-liquid extraction method for the determination of halomethanes in water at the parts-per-billion level. In *Identification and Analysis of Organic Pollutants in Water*. L.H. Keith, Ed., Ann Arbor Science Publishers Inc., Ann Arbor, MI, p. 105.
- Hill, C.G. Jr. 1977. *An Introduction to Chemical Engineering Kinetics and Reactor Design*. John Wiley & Sons, NY, pp. 150-153.
- Johnson, T., Scherer, M.M., and Tratnyek, P.G. 1996. Kinetics of halogenated organic compound degradation by iron metal. *Environ. Sci. Technol.*, 30, 2634-2640.
- Klotz, D., Seiler, K.P., Moser, H., and Neumaier, F. 1980. Dispersivity and velocity relationship from laboratory and field experiments. *J. Hydrol.*, 45 (3), 169-184.
- Light, T.S., 1972. Standard solution for redox potential measurements. *Analytical Chemistry*, 44(6), 1038-1039.
- Mackay, D.M., and Cherry, J.A. 1989. Ground water contamination: Pump-and-treat remediation. *Environ. Sci. Technol.*, 23 (6), 630-636.
- Mackay, D.M., Feenstra, S., and Cherry, J.A. 1993. Alternative goals and approaches for ground water remediation. In *Proc. Workshop of "Contaminated Soils - Risks and Remedies."* Stockholm, October 26-28. Neretnieks, I. Ed., pp. 35-47.
- Manz, C., and Quinn, K. 1997. Permeable treatment wall design and cost analysis. In *International Containment Technology Conference*. St. Petersburg, Florida, Feb. 9-12. pp. 788-793.
- Matheson, L.J., and Tratnyek, P.G. 1994. Reductive dehalogenation of chlorinated methanes by iron metal. *Environ. Sci. Technol.*, 28, 2045-2053.
- McMurtry, D.C., and Elton, R.O. 1985. New approach to in-situ treatment of contaminated groundwaters. *Environ. Prog.*, 4 (3), 168-170.
- Nordstrom, D.K., 1977. Thermochemical redox equilibria of ZoBell's Solution. *Geochim. Cosmochim. Acta.*, 41, 1835-1841.
- O'Hannesin, S.F. 1993. A field demonstration of a permeable reaction wall for the in situ abiotic degradation of halogenated aliphatic organic compounds. M.Sc. Thesis, University of Waterloo, Waterloo, Ontario, Canada.
- O'Hannesin, S.F., and Gillham, R.W. 1992. A permeable reaction wall for in situ degradation of halogenated organic compounds. In *Proc. 1992 Canadian Geotechnical Society Conference*, Toronto, Ont., Oct. 25-28.
- O'Hannesin, S.F., Hanton-Fong, C.J., Blowes, D.W., Gillham, R.W., and Ptacek, C.J. 1995. Remediation of groundwater contaminated with chromium and TCE using reactive barriers: Laboratory batch and column testing. *Progress Report II*, 10 June 1995.
- Orth, W.S., and Gillham, R.W. 1996. Dechlorination of trichloroethylene in aqueous solution using Fe⁰. *Environ. Sci. Technol.*, 30, 66-71.
- Palmer, C.D., 1999. Ground water remediation using reactive barriers, Elizabeth City, NC Site. Final Report to EPA. Department of Geology, Portland State University.
- Palmer, C.D., and Puls, R.W. 1994. Natural attenuation of hexavalent chromium in ground water and soils. U.S. EPA/540/S-94/505 October 1994.
- Palmer, C.D., and Wittbrodt, P.R. 1991. Processes affecting the remediation of chromium-contaminated sites. *Environ. Health Perspect.*, 92, 25-40.
- Pankow, J.F., and Cherry, J.A. 1996. *Dense Chlorinated Solvents and other DNAPLs in Ground water: History, Behaviour, and Remediation*. Waterloo Press, OR. p. 362.
- Parsons Engineering Science, 1993. *RCRA Facility Investigation Work Plan*, Rev. 0, October 1993.
- Parsons Engineering Science, 1994. *RCRA Facility Investigation Work Plan*, Rev. 0, November 1994.
- Parsons Engineering Science, 1995. *Interim Measures Work Plan*, Rev. 1, December 1995.
- Parsons Engineering Science, 1997. *Interim Measures Baseline Report*, Rev. 1, March 1997.
- Powell, R.M., Puls, R.W., Hightower, S.K. and Sabatini, D.A. 1995. Coupled iron corrosion and chromate reduction: Mechanisms for subsurface remediation. *Environ. Sci. Technol.*, 29 (8), 1913-1922.
- Pratt, A.R., Blowes, D.W., and Ptacek, C.J. 1997. Remediation of groundwater chromate contamination: Mineralogy and mineral chemistry. *Environ. Sci. Technol.*, 31, 2492-2498.
- Puls, R.W., Clark, D.A., Paul, C.J., and Vardy, J. 1994. Transport and transformation of hexavalent chromium through soils and into ground water. *J. Soil Contam.*, 3 (2), 203-224.

-
- Puls, R.W., Powell, R.M., and Paul, C.J. 1995. In situ remediation of ground water contaminated with chromate and chlorinated solvents using zero-valent iron: A field study. In *Proc. Div. Environ. Chem., Am. Chem. Soc.*, Anaheim, CA, April 2-7, 1995.
- Rai, D., Sass, B.M., and Moore, D.A. 1987. Chromium(III) hydrolysis constants and solubility of chromium(III) hydroxide. *Inorg. Chem.*, 26, 345-349.
- Roberts, A.L., Totten, L.A., Arnold, W., Burris, D.R., and Campbell, T. 1996. Reductive elimination of chlorinated ethylenes by zero-valent metals. *Environ. Sci. Technol.*, 30, 2655-2659.
- Sass, B.M., and Rai, D. 1987. Solubility of amorphous chromium(III)-iron(III) hydroxide solid solutions. *Inorg. Chem.*, 26, 2228-2232.
- Schroeder, D.C., and Lee, G.F. 1975. Potential transformations of chromium in natural waters. *Water, Air, Soil Poll.*, 4, 355-365.
- Schumacher, T., Odziemkowski, M.S., Reardon, E.J. and Gillham, R.W., 1997. Identification of precipitates formed on zero-valent iron in anaerobic solutions. In: International Containment Technology Conference, St. Petersburg, FL, Feb. 9-12:801-805.
- Schwertmann, U., Gasser, U., and Sticher, H. 1989. Chromium-for-iron substitution in synthetic goethites. *Geochim. Cosmochim. Acta*, 53, 1293-1297.
- Shikaze, S.G., and Austrins, C.D. 1995. A 3-D numerical investigation of groundwater flow in the vicinity of a Funnel-and-Gate System. In *Proc. 1995 5th Annual Symposium on Groundwater and Soil Remediation*. Toronto, Ontario, October 2-6, 1995.
- Shikaze, S.G., Austrins, C.D., Smyth, D.J.A., Cherry, J.A., Barker, J.F., and Sudicky, E.A. 1995. The hydraulics of a Funnel-and-Gate System: A three-dimensional numerical analysis. In *Proc. 1995 IAHR Conference*, Edmonton, Alberta, July 1995 (distributed on CD-ROM).
- Sivavec, T.M., and Horney, D.P. 1995. Reductive dechlorination of chlorinated ethenes by iron metal. In *Proc. 209th Am. Chem. Soc. Natl. Mtg., Environ. Chem. Div.*, Anaheim, CA, April 2-7, Vol. 35, pp. 695-698.
- Standard methods for the examination of water and wastewater, 1992. A.E. Greenberg, L.S. Clesceri and A.D. Eaton, Editors. American Public Health Association, Washington, D.C.. Eighth Edition.
- Starr, R.C., and Cherry, J.A. 1994. In situ remediation of contaminated ground water: the funnel-and-gate system. *Ground Water*, 32, 465-477.
- Therrien, R., and Sudicky, E.A. 1996. Three dimensional analysis of variably-saturated flow and solute transport in discretely-fractured porous media. *J. Contam. Hydrol.*, 23, 1-44.
- Toride, N., Leij, F.J., and vanGenuchten, M.Th., 1995. The CXTFIT code for estimating transport parameters from laboratory or field tracer experiments, Version 2.0. Research Report No. 137, U.S. Salinity Laboratory, USDA, ARS, Riverside, CA.
- United States Environmental Protection Agency, 1982. Methods for organic chemical analysis of municipal and industrial wastewater; EPA-600/4-82-057, J.E. Longbottom and J.J. Lichtenberg (eds.); Cincinnati, Ohio; Appendix A.
- Vogel, T.M., Criddle, C.S., and McCarty, P.L. 1987. Transformations of halogenated aliphatic compounds, *Environ. Sci. Technol.*, 21, 722-736.
- Wilke, C.R., and Chang, P. 1955. Correlation of diffusion coefficients in dilute solutions. *A.I.Ch.E. Journal*, 1, 264-270.
- Wittbrodt, P.R. and Palmer, C.D. 1997. Reduction of Cr(VI) by soil humic acids. *Eur. J. Soil Sci.*, 48, 151-162.
- Zobell, C.E., 1946. Studies on redox potential of marine sediments. *Bull. Am. Petrol Geologists*, 30: 477-509.



Tables

Table 1. Horizontal Hydraulic Gradients and Water Levels Observed in Monitoring Wells Screened Between 3 and 4.5 m Below Ground Surface

Water level measurement date	Range in observed water levels (meters below top of well casing)	Range in observed water levels (meters above sea level)	Approximate horizontal hydraulic gradient (m/m)
October 1994	1.57 - 2.06	0.18 - 0.25	0.0029
October 1993	1.61 - 2.10	0.15 - 0.21	0.0011
March 1993	1.53 - 2.03	0.23 - 0.37	0.0033
April 1992	1.59 - 2.04	0.18 - 0.31	0.0012
September 1991	1.47 - 1.91	0.31 - 0.46	0.0025

Table 2. First-order Rate Constants for the Dehalogenation of TCE, DCE Isomers, and VC (after Johnson *et al.*, 1996)

<i>Halocarbon</i>	K_{SA} (L m ⁻² h ⁻¹)
TCE	$(3.9 \pm 3.6) \times 10^{-4}$
1,1 DCE	$(6.4 \pm 5.5) \times 10^{-5}$
Trans 1,2-DCE	$(1.2 \pm 0.4) \times 10^{-4}$
cis 1,2-DCE	$(4.1 \pm 1.7) \times 10^{-5}$
VC	$(5 \pm 1.5) \times 10^{-5}$

Table 3. Reactive Mixtures Used in Batch Experiments

<i>Batch name</i>	<i>Iron</i>	<i>Silica Sand</i>	<i>Aquifer Material</i>
AdaSS	6 g Ada	6 g	0 g
MBSS	6 g MB	6 g	0 g
PLSS	6 g PL	6 g	0 g
MBAQ	6 g MB	0	6 g

Table 4. Reactive Mixtures Used in Column Experiments

<i>Column name</i>	<i>Peerless Iron</i>	<i>Master Builders Iron</i>	<i>Silica Sand</i>	<i>Elizabeth City Aquifer Material</i>
100PL	100 %			
100MB		100 %		
48PL/52AQ	48 %			52 %
50MBSSAQ		50 %	25 %	25 %
50PLSSAQ	50 %		25 %	25 %
50MBSS		50 %	50 %	

Table 5. Column Flow Velocities and Hydraulic Properties of Reactive Mixtures Used (after O'Hannesin *et al.*, 1995)

Column Name	<i>50MBSS</i>	<i>50MBSSAQ</i>	<i>48PL/52AQ</i>	<i>50PLSSAQ</i>		<i>100MB</i>		<i>100PL</i>	
Mixture	<i>50% MB Iron 50% Silica</i>	<i>50% MB Iron 25% Silica 25% ECAQ</i>	<i>48% PL Iron 52% ECAQ</i>	<i>50% PL Iron 25% Silica 25% ECAQ</i>		<i>100% MB Iron</i>		<i>100% PL Iron</i>	
	FV1	FV1	FV1	FV1	FV2	FV1	FV2	FV1	FV2
Flow Velocity (FV) (ft/day) (cm/day)	1.8 55	2.2 68	2.3 71	2.6 79	1.2 36	1.4 43	0.8 24	1.8 53	1.0 31
Residence Time (hours)	21.6	17.7	17	15.3	34	27.7	0.8	22.5	39
Pore Volume (mL)	233	201	189	166		254		245	
Porosity	0.41	0.35	0.33	0.29		0.45		0.43	
Hydraulic Conductivity (cm/sec)	6.7E-02	2.6E-02	8.9E-03	3.6E-02		8.6E-02		9.8E-02	
Bulk Density (g/cm ³)	2.17	2.33	2.21	2.20		3.09		2.72	
Iron to Volume of Solution Ratio (g:mL)	2.7 : 1	3.3 : 1	3.2 : 1	3.78 : 1		6.9 : 1		6.4 : 1	
Surface Area to Volume of Solution Ratio (m ² :mL)	2.97 : 1	3.63 : 1	2.59 : 1	3.06 : 1		7.6 : 1		5.18 : 1	

FV1 = First flow velocity, Mar 31 - May 17, 1995

FV2 = Second flow velocity, May 26 - Aug 12, 1995

FV1 = First flow velocity, June 28 - Aug 12, 1995*

Table 6. Method Detection Limits (MDL)

<i>Organic Compounds</i>	<i>MDL (µg/L)</i>
Trichloroethene (TCE)	1.7
Chloroform (TCM)	2.7
Tetrachloroethene (PCE)	2.2
cis 1,2-Dichloroethene (cDCE)	1.2
trans 1,2-Dichloroethene (tDCE)	1.5
1,1-Dichloroethene (1,1-DCE)	1.0
Vinyl Chloride (VC)	0.8
<i>Inorganic Compounds</i>	<i>MDL (mg/L)</i>
Chromium VI [Cr(VI)]*	0.20-0.40
Chromium (total)	0.02
Iron (Fe)	0.10
Sodium (Na)	1.00
Magnesium (Mg)	0.05
Calcium (Ca)	0.02
Potassium (K)	1.00
Manganese (Mn)	0.02
Chloride (Cl)	0.05
Sulphate (SO ₄)	0.05
Alkalinity (as CaCO ₃)*	2-10

*MDL varied due to small sample volumes available for analysis

Table 7. Changes in TCE Concentration in Batch Experiments Over Time, for Reaction and Control Vials. Three Reaction Vials and One Control Vial Were Sampled at Each Time. Only TCE Was Analyzed

MBSS		Reaction Vial			AdaSS		Reaction Vial		
<i>Control</i>					<i>Control</i>				
<i>Time</i>	<i>TCE</i>	<i>Average</i>	<i>Standard</i>	<i>% Standard</i>	<i>Time</i>	<i>TCE</i>	<i>Average</i>	<i>Standard</i>	<i>% Standard</i>
<i>(h)</i>	<i>(µg/L)</i>	<i>TCE</i>	<i>Deviation</i>	<i>Deviation</i>	<i>(h)</i>	<i>(µg/L)</i>	<i>TCE</i>	<i>Deviation</i>	<i>Deviation</i>
		<i>(µg/L)</i>	<i>(µg/L)</i>				<i>(µg/L)</i>	<i>(µg/L)</i>	
0		1948	134	6.9	0		1800	83	4.6
0.20	1839	1489	16	1.1	0.25	1614	1546	71	4.6
0.50	1970	1114	61	5.5	0.50	1658	1565	17	1.1
0.77	1962	1113	40	3.6	0.75	1704	1724	14	0.8
1.0	1900	954	23	2.5	1.0	1812	1744	22	1.2
1.5	1670	845	18	2.1	1.5	1821	1758	50	2.8
3.0	1786	705	23	3.3	3.0	1786	1775	20	1.1
6.0	1849	597	22	3.6	5.7	1813	1763	71	4.0
10.8	1798	474	20	4.3	10.8	1665	1646	37	2.2
24.1	1678	268	13	4.8	23.9	1696	1520	10	0.7
48.0	1670	96	2	1.8	120.9	1519	1307	91	7.0
120.9	1463	24	2	7.2	192.3	1609	655	43	6.6
192.8	1652	9.1	1	14.9	313.3	1467	45	43	95.4
313.4	1543	2	0	0.0					

PLSS		Reaction Vial			MBAQ		Reaction Vial		
<i>Control</i>					<i>Control</i>				
<i>Time</i>	<i>TCE</i>	<i>Average</i>	<i>Standard</i>	<i>% Standard</i>	<i>Time</i>	<i>TCE</i>	<i>Average</i>	<i>Standard</i>	<i>% Standard</i>
<i>(h)</i>	<i>(µg/L)</i>	<i>TCE</i>	<i>Deviation</i>	<i>Deviation</i>	<i>(h)</i>	<i>(µg/L)</i>	<i>TCE</i>	<i>Deviation</i>	<i>Deviation</i>
		<i>(µg/L)</i>	<i>(µg/L)</i>				<i>(µg/L)</i>	<i>(µg/L)</i>	
0		1393	415	29.8	0	1618	1561	114	7.3
0.10	1517	1588	29	1.8	0.10	1602	1416	59	4.1
0.23	1505	1514	120	7.9	0.27	1572	1250	35	2.8
0.36	1824	1393	239	17.2	0.42	1635	1084	18	1.6
0.50	1812	1483	3	0.2	0.58	1606	1003	21	2.1
0.75	1839.1	1415	35	2.4	0.75	1589	913	16	1.8
1.1	1726	1403	12	0.8	1.0	1538	879	40	4.5
3.0	1796	1213	18	1.5	3.0	1648	636	8	1.2
6.0	1740	1160	82	7.0	6.0	1552	482	34	7.0
11.8	1778	1040	33	3.2	11.5	1573	299	17	5.6
23.9	1575	782	18	2.4	24.0	1561	149	13	8.9
48.2	1815	528	8	1.4	48.0	1624	48	7	14.4
72.2	1678	298	19	6.4	96.2	1540	11	2	16.9
97.2	1588	131	15	11.1	167.9	1417	3.2	1	40.6

Table 8. Summary of Cr Removal in Batch Tests

<i>Batch ID</i>	<i>Cr(VI) Co (mg/L)</i>	<i>Time to Non-detect (min)</i>
AdaSS	11.4	70
PLSS	12.1	23
MBSS	11.4	35
MBAQ	12.0	43

Co = Initial Concentration

Table 9. Inorganic Concentrations of All Columns for Both Influent and Effluent Samples at Steady-state Conditions

	<i>FV</i>	<i>Influent Conc.</i>	<i>50MBSS</i>	<i>50MBSSAQ</i>	<i>50PLSSAQ</i>	<i>48PL52AQ</i>	<i>100MB</i>	<i>100PL</i>
<i>Cations</i>	<i>mg/L</i>							
Chromium	FV1	8.4	bd	bd	bd	bd	bd	bd
Cr(total)	FV2	7.6	NA	NA	bd	NA	bd	bd
Iron	FV1	<0.1	bd	bd	bd	bd	bd	bd
(Fe)	FV2	<0.1	NA	NA	bd	NA	bd	bd
Sodium	FV1	104	107	106	100	88	101	104
(Na)	FV2	104	NA	NA	102	NA	104	104
Magnesium	FV1	15	15	12	12.6	0.8	11	12
(Mg)	FV2	15	NA	NA	8.9	NA	6.8	6.9
Calcium	FV1	24	12	19	20	7.7	11	16
(Ca)	FV2	22	NA	NA	15	NA	9	9.4
Potassium	FV1	5.2	4.4	4.4	4.8	4.1	4.4	4.8
(K)	FV2	4.7	NA	NA	4.8	NA	3.8	4.1
Manganese	FV1	0.89	0.10	0.06	0.09	0.1	0.12	0.09
(Mn)	FV2	0.88	NA	NA	0.02	NA	0.06	0.06
Silica	FV1	9.0	0.51	0.57	0.39	0.7	0.25	0.32
(Si)	FV2	9.4	NA	NA	0.37	NA	0.23	0.12
<i>Anions</i>								
Chloride	FV1	121	117	123	118	110	119	116
(Cl)	FV2	113	NA	NA	106	NA	118	110
Sulphate	FV1	99	95	102	100	81	97	99
(SO ₄)	FV2	89	NA	NA	95	NA	92	90
Alkalinity	FV1	55	31	57	58	56	39	52
(as HCO ₃)	FV2	59	NA	NA	55	NA	33	31

Table 10. First Detection of Cr at the 2.5 cm Sample Port in Each Column. Predicted Breakthrough Volumes Calculated from these Data Are Shown

Column	First detection of Cr at 2.5 cm port (Pore Volumes)	Cr(VI) or Cr(tot) (mg/L)	Predicted Breakthrough at Column Effluent (Pore Volumes)
100MB	69	0.53	1380
100PL	82	0.09	1640
50PLSSAQ	101	0.11	2020
48PL/52AQ	78	3.77	1560

Table 11. First Order Rate Constants in Various Reactive Iron Mixtures (Rate Constants Not Normalized to Surface Area)

REACTIVE MIXTURE	TCE RATE CONSTANT 1/D ($T_{1/2}$ HRS)	MOLAR TRANSFER COEFF. ($TCE \Rightarrow CDCE$)	CDCE RATE CONSTANT [1/D] ($T_{1/2}$ HRS)	MOLAR TRANSFER COEFF. ($CDCE \Rightarrow VC$)	VC RATE CONSTANT [1/D] ($T_{1/2}$ HRS)
100% Master Builders iron	16.27	17%	5.83	27%	6.31
50% Master Builders iron 50% Silica sand	9.81	8%	0.15	100%	1.27
50% Master Builders 25% Silica sand 25% Aquifer sed.	15.71	9%	1.02	1%	1.08
100% Peerless iron	9.62	7%	3.40	100%	10.61
50% Peerless iron 25% Silica sand 25% Aquifer sed.	13.17	4%	4.23	100%	10.99
AVERAGE	12.92	9%	2.93		6.06

Table 12. Hydraulic Properties and First-order Rate Constants for Peerless™ and Master Builders™ Granular Iron

	UNITS	100PL	100MB
Hydraulic Conductivity	m/day	84.7	74.3
Porosity		0.43	0.45
Surface Area	m ² /g	0.81	1.1
bulk density	g/cm ³	2.72	3.09
TCE degradation rate, k_1	d ⁻¹	9.62	16.27
cDCE degradation rate, k_2	d ⁻¹	3.40	5.83
VC degradation rate, k_3	d ⁻¹	10.61	6.31
TCE degradation rate, k_1^{SA}	L hr ⁻¹ m ⁻²	7.82×10^{-5}	8.98×10^{-5}
cDCE degradation rate, k_2^{SA}	L hr ⁻¹ m ⁻²	2.76×10^{-5}	3.22×10^{-5}
VC degradation rate, k_3^{SA}	L hr ⁻¹ m ⁻²	8.63×10^{-5}	3.48×10^{-5}

k_x^{SA} : Surface area normalized reaction rate constants

Table 13. Hydraulic Conductivity Values Used in Ground-water Flow Simulations to Compare Relative Capture Areas and Residence Times of Two Barrier Designs

SIMULATION	V_{AQUIFER} cm/day	K_{AQUIFER} m/day
1	0.09	0.1
2	4.17	4.8
3	14.5	16.7
4	22.6	26.0
5	40.3	46.4

Pea gravel: porosity 0.35; hydraulic conductivity 864 m/day
 Granular iron: porosity 0.38; hydraulic conductivity 46.4 m/day

Table 14. Capture Areas for the Funnel-and-Gate Under Varying Aquifer Hydraulic Conductivity Conditions

Simulation	$\frac{K_{\text{iron}}}{K_{\text{aquifer}}}$	Capture Area (m ²)	Capture Area (% of total FUNNEL-AND- GATE area)	Area of Groundwater directed to GATE (% of FUNNEL area)	Capture Area (relative to GATE area)
1	464	85	59%	45%	2.6 x
2	10	83	58%	44%	2.5 x
3	3	79	55%	41%	2.4 x
4	2	70	49%	35%	2.1 x
5	1	67	47%	34%	2.0 x

Total FUNNEL-AND-GATE™ area: 143 m²
 Area of each (6.1 m wide by 9.1 m deep) FUNNEL: 55.2 m²
 Area of (3.6 m wide by 9.1 m deep by 2m thick) GATE: 32.76 m²

Table 15. Capture Areas for the Continuous Wall Configuration Under Varying Aquifer Hydraulic Conductivity Conditions

Simulation	$\frac{K_{\text{iron}}}{K_{\text{aquifer}}}$	Capture Area (m ²)	Capture Area (% of total WALL area)	Capture Area (relative to WALL area)
1	464	89	114%	1.1 x
2	10	87	111%	1.1 x
3	3	84	108%	1.1 x
4	2	82	105%	1.1 x
5	1	78	100%	1.0 x

Total area of (10.3 m wide by 7.6 m deep by 0.45 m thick) WALL: 78 m²

Table 16. Ground-water Velocities and Residence Times within the Reactive Material Zones of the Funnel-and-Gate and the continuous Wall

SIMULATION	<i>Funnel-and-Gate</i> TM			<i>Wall</i>		
	Velocity (m/day)	Velocity relative to aquifer	Residence Time (days)	Velocity (m/day)	Velocity relative to aquifer	Residence Time (days)
1	2.02 x 10 ⁻³	2.6	525	9.18 x 10 ⁻⁴	1.2	495
2	1.03 x 10 ⁻¹	2.5	10.29	4.74 x 10 ⁻²	1.1	9.59
3	3.24 x 10 ⁻¹	2.2	3.27	1.57 x 10 ⁻¹	1.1	2.90
4	4.76 x 10 ⁻¹	2.1	2.23	2.38 x 10 ⁻¹	1.1	1.91
5	7.52 x 10 ⁻¹	1.9	1.41	4.03 x 10 ⁻¹	1.0	1.13

Table 17. Hydraulic Parameters (Source of Values Indicated in Brackets) Used in Ground-water Flow Modelling to Determine Minimum Barrier Dimensions

PARAMETER	RANGE OBSERVED	SIMULATION 1	SIMULATION 2
Aquifer hydraulic conductivity (Field estimates)	0.1 to 26 m/day	17 m/day	17 m/day
Aquifer porosity (Estimated)		0.38	0.38
Granular iron hydraulic Conductivity (Lab estimates)	7.7 to 84.7 m/day	43.0 m/day	84.7 m/day
Granular iron porosity (Lab estimates)	0.29 to 0.45	0.40	0.43
Horizontal hydraulic gradient (Field estimates)	0.0011 to 0.0033	0.0033	0.0033

Table 18. Reactive-transport Parameters, Source Concentrations, and Minimum Distance Within Reactive Barrier Before Contaminant Falls Below MCL

	<i>COMPOUND</i>		
	TCE	cDCE	VC
MODEL PARAMETERS			
Diffusion coefficient, D _o (cm ² /s)	10.1 x 10 ⁻⁶	11.4 x 10 ⁻⁶	13.3 x 10 ⁻⁶
Rate Constant, k (day ⁻¹)	9.62	3.40	10.61
Transfer coefficient (%)	7%	100%	N/A
Source Concentration (µg/L)	10,000	900	101
MINIMUM DISTANCE WITHIN BARRIER			
Simulation 1	24 cm	21 cm	33 cm
Simulation 2	23 cm	20 cm	32 cm

Table 19. Barrier Installation Project Costs in U.S. Dollars (USCG, Pers. Comm.)

	DESCRIPTION	COST
Preliminary work	Site Assessment	\$60,000
	RFI Workplan	\$40,000
	RFI Implementation	\$ 50,000
Barrier Design	Model	\$10,000
	Bench Test	\$25,000
	Pilot Study	\$75,000
	Design	\$35,000
Barrier Construction	Granular iron	\$200,000
	Trenching Installation	\$150,000
	Setup/cleanup	\$150,000
Post Installation work Reports	CAMU	\$40,000
	RFI Report	\$60,000
	CMS/Interim Report	\$50,000
	Baseline Report	\$40,000
	TOTAL	\$985,000

FIGURES

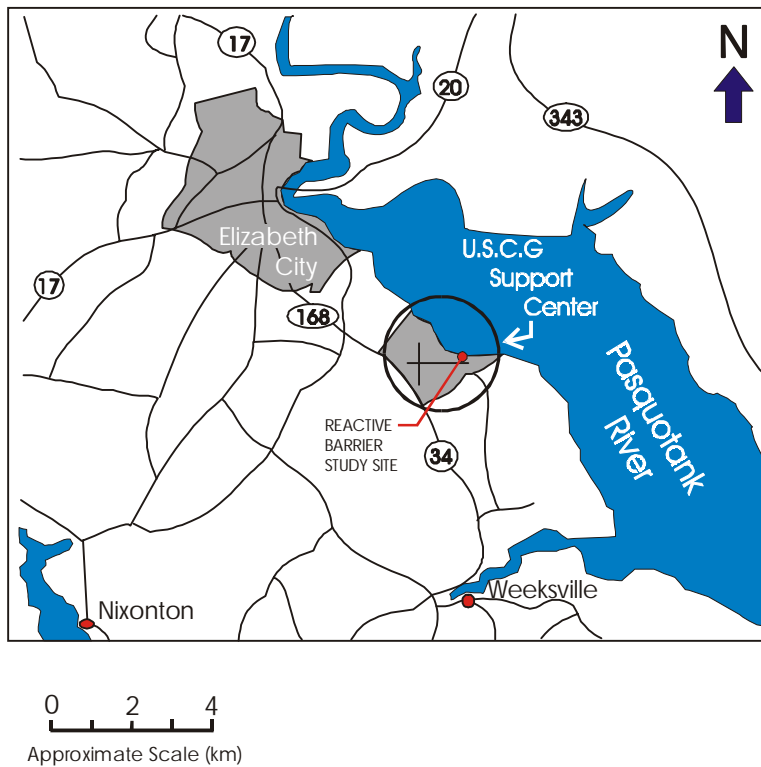


Figure 1. Location map showing U.S. Coast Guard Support Center, Elizabeth City, North Carolina.

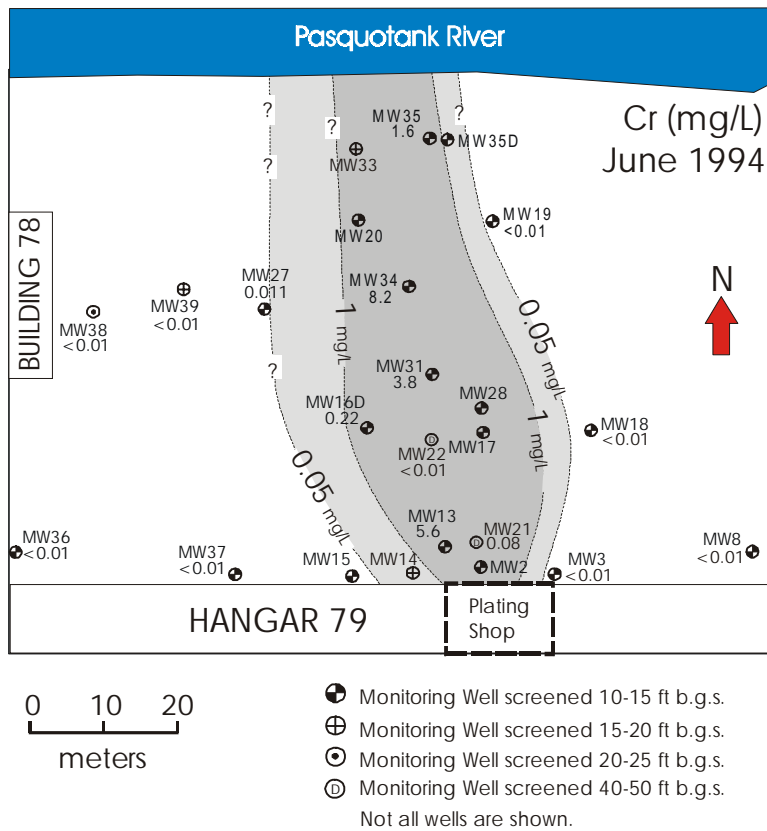


Figure 2. Plan view map showing total Cr concentrations (mg/L), and inferred 0.05 and 1 mg/L contours.

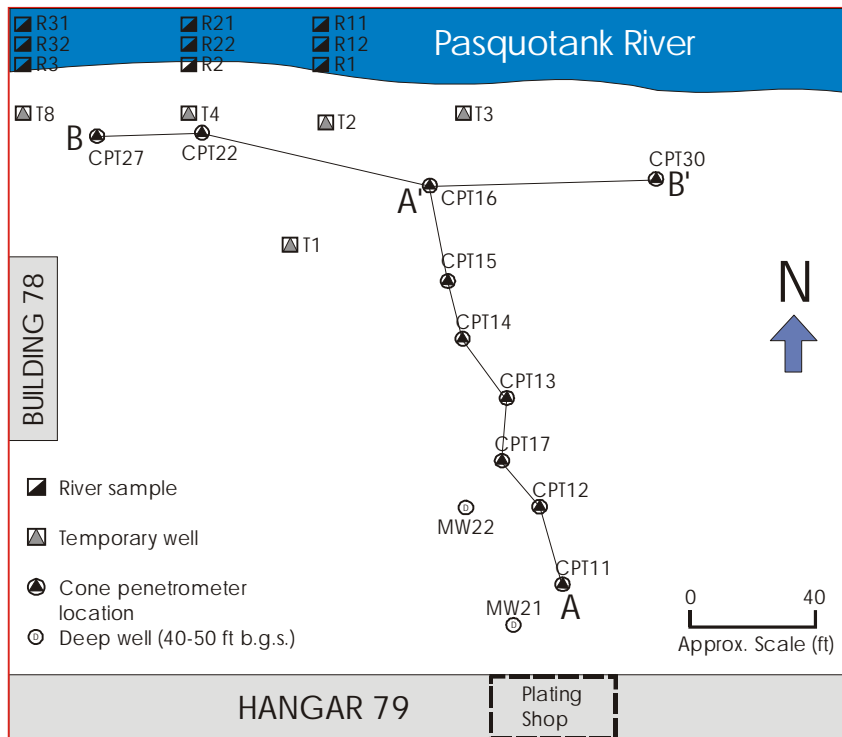


Figure 3. Plan view map showing approximate locations of temporary wells, cone penetrometer tests, river sampling, and deep wells (after Parsons Engineering Science, 1994).

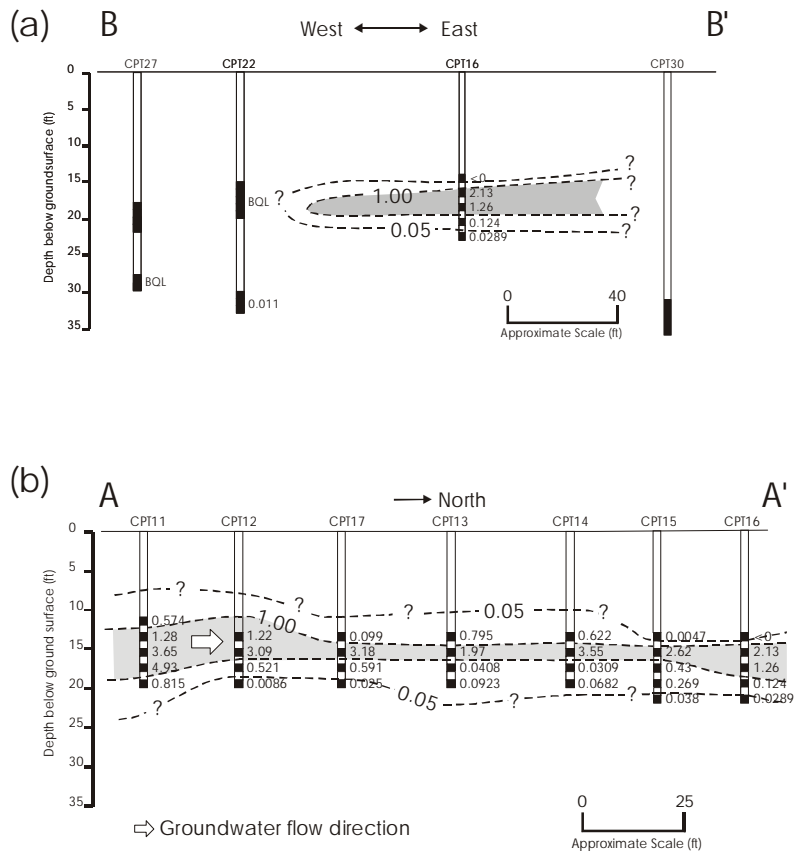


Figure 4. (a) Cross-section B-B', and (b) cross-section A-A' indicating total chromium concentrations (mg/L), and inferred 0.05 mg/L and 1.00 mg/L contours in June 1994.

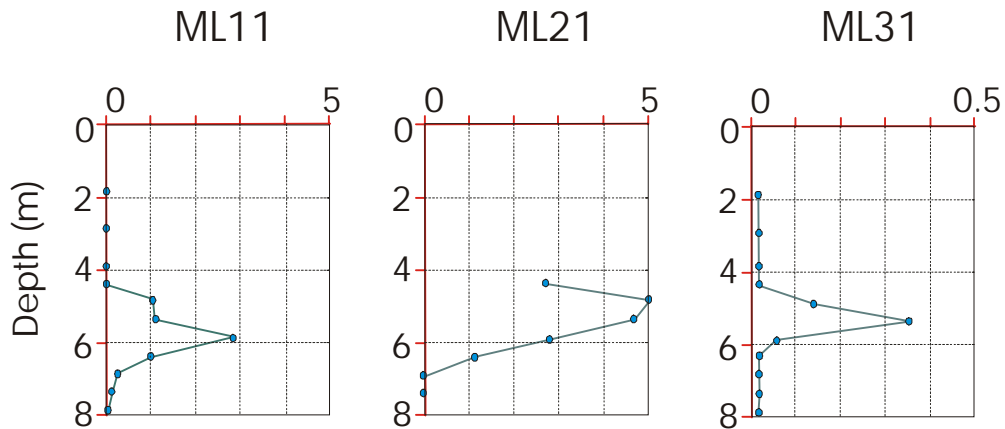


Figure 5. Cr concentration profiles (mg/L) at multilevel samplers in the approximate locations of piezometer bundles ML11, ML21, and ML31, upgradient of proposed Reactive Barrier (April 1996).

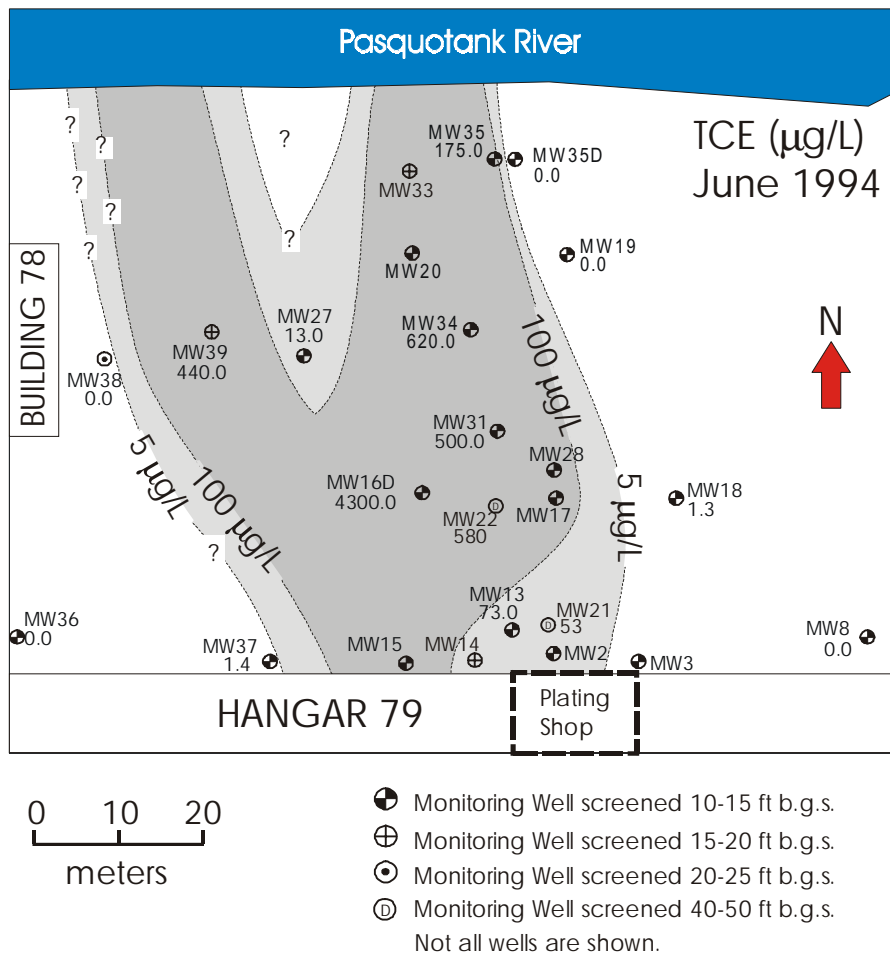


Figure 6. Plan view map showing TCE concentrations (µg/L), and inferred 5 and 100 µg/L contours.

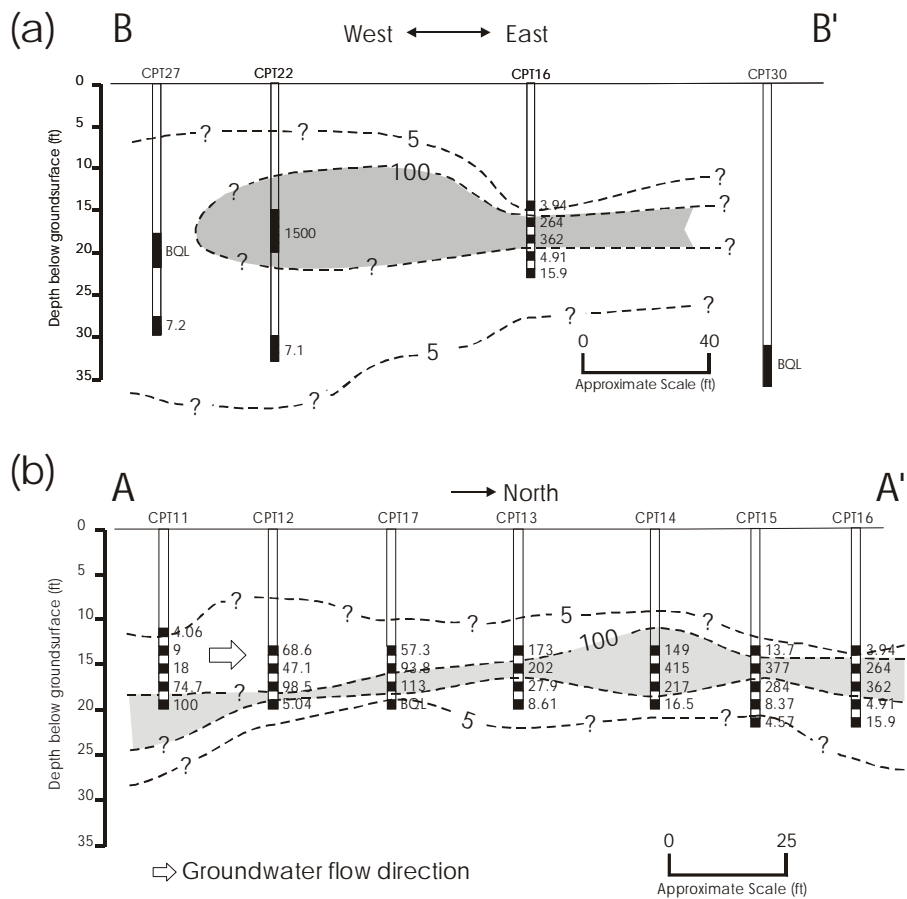


Figure 7. (a) Cross-section B-B', and (b) cross-section A-A' indicating TCE concentrations (µg/L), and inferred 5 µg/L and 100 µg/L contours in June 1994.

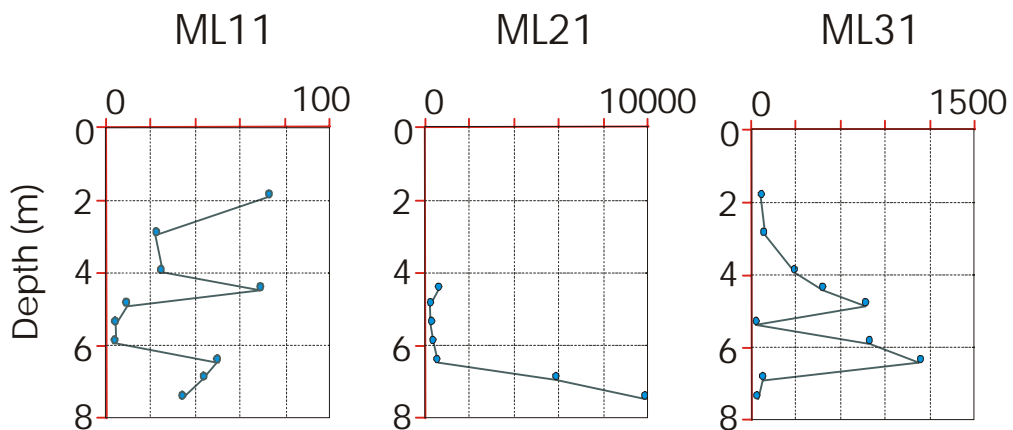


Figure 8. TCE concentration profiles (µg/L) at multilevel samplers in the approximate locations of piezometer bundles ML11, ML21, and ML31, upgradient of proposed Reactive Barrier (April 1996).

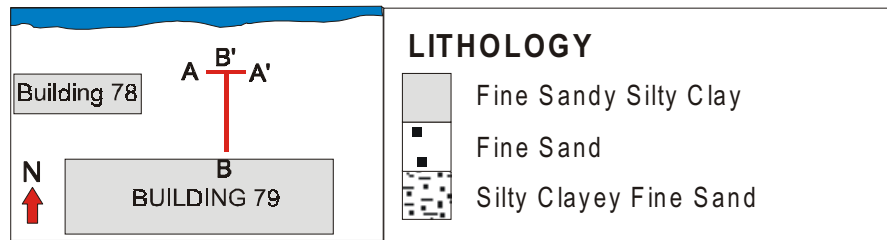
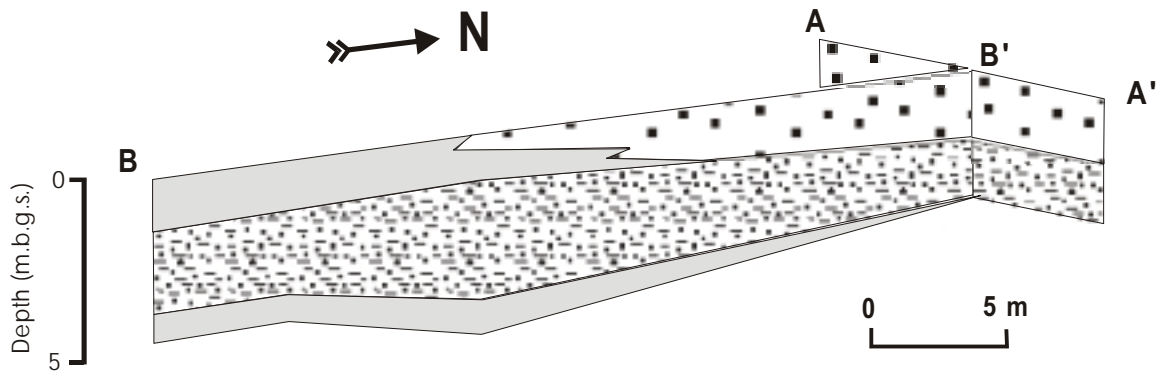


Figure 9. Cross-sections extrapolated from borehole log data.

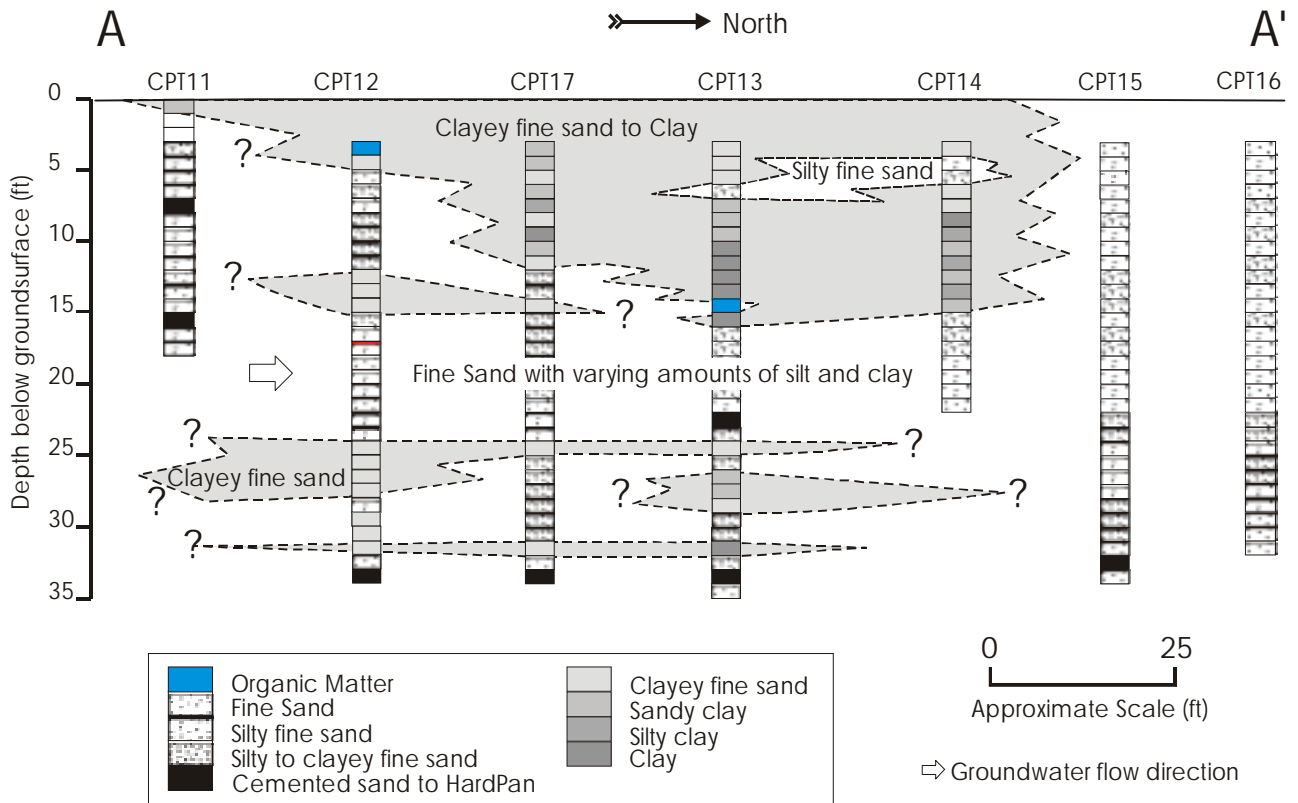


Figure 10. Geologic cross-section A-A' extrapolated from cone penetrometer test data.

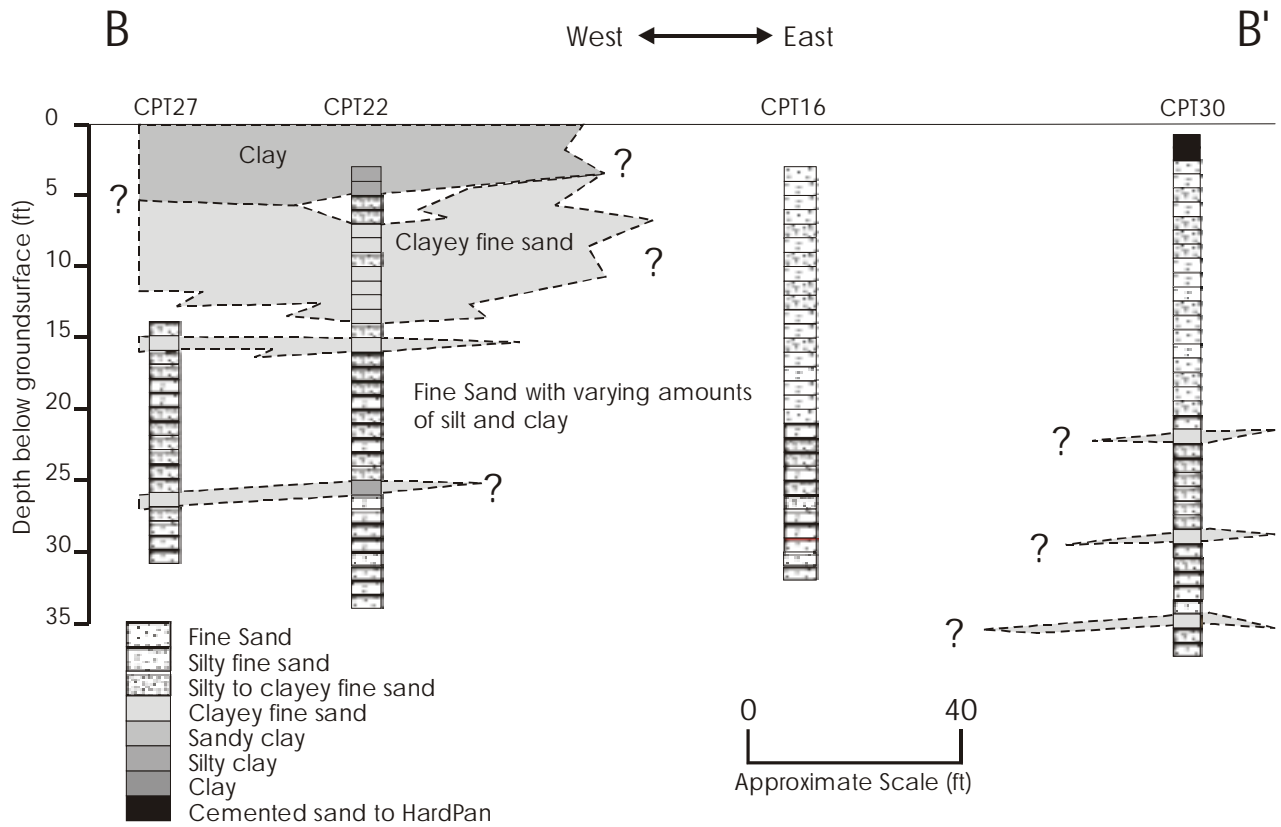
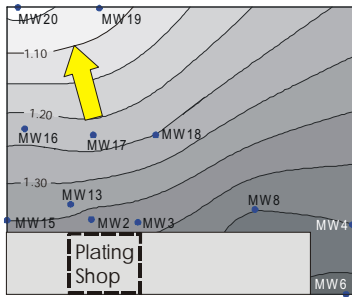
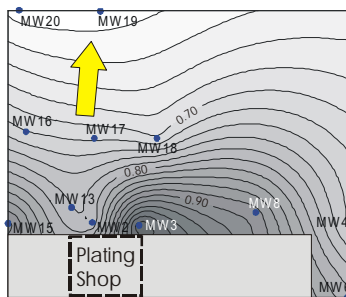


Figure 11. Geologic cross-section B-B' extrapolated from cone penetrometer test data.

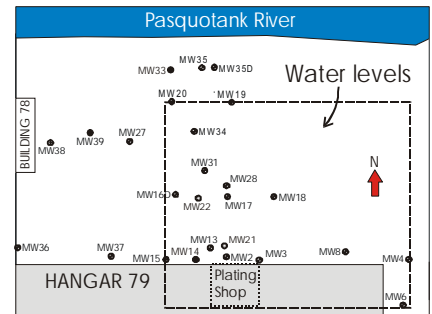
September 1991



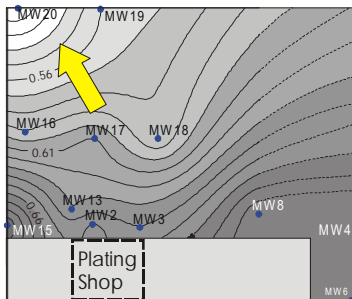
April 1992



Site map



October 1993



October 1994

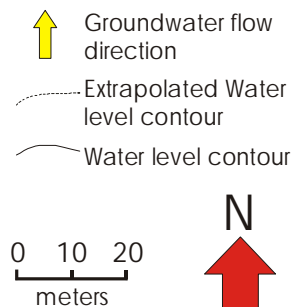
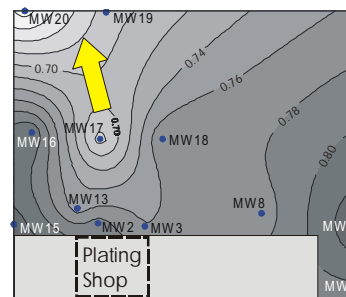


Figure 12. Water levels in wells screened 3 to 4.5 m below ground surface (ft.a.s.l.).

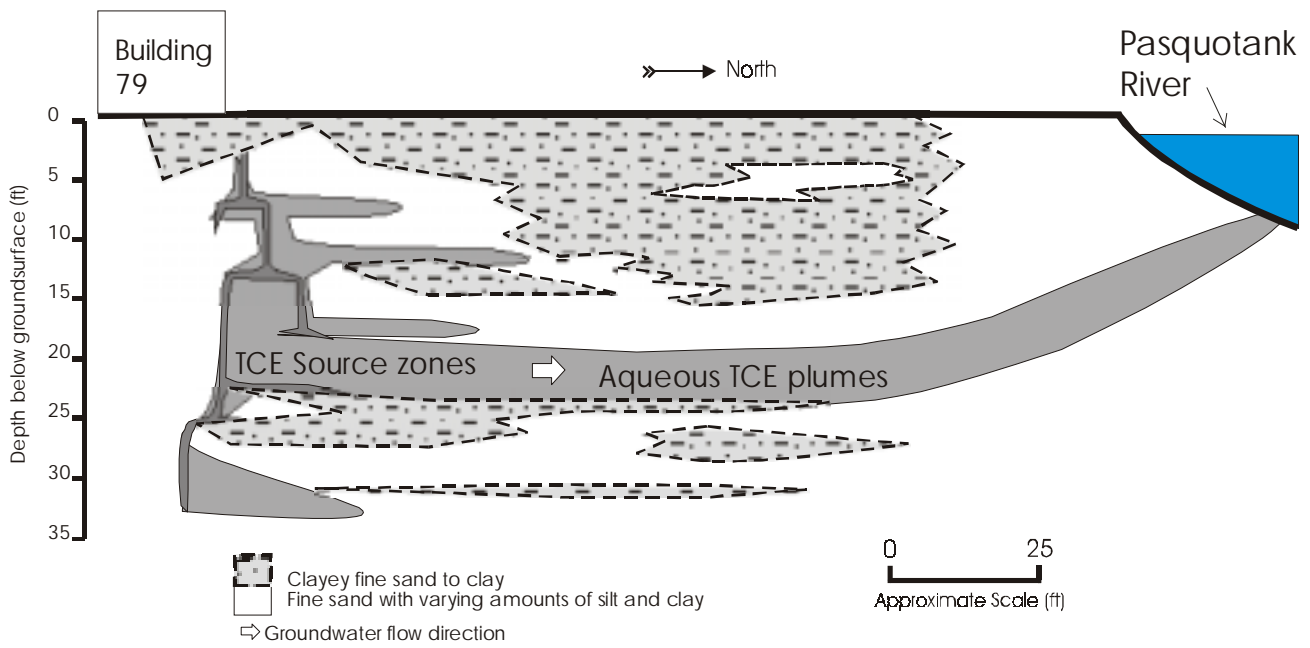
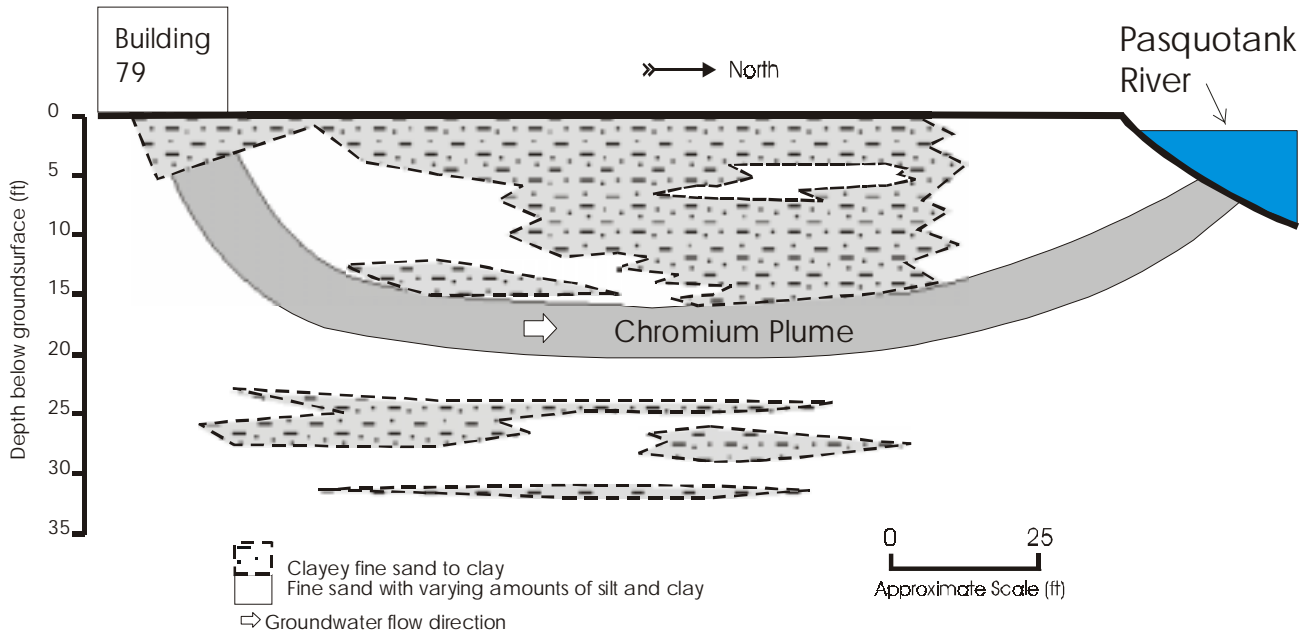


Figure 13. Diagram of conceptual model Cr(VI) and TCE plume development.

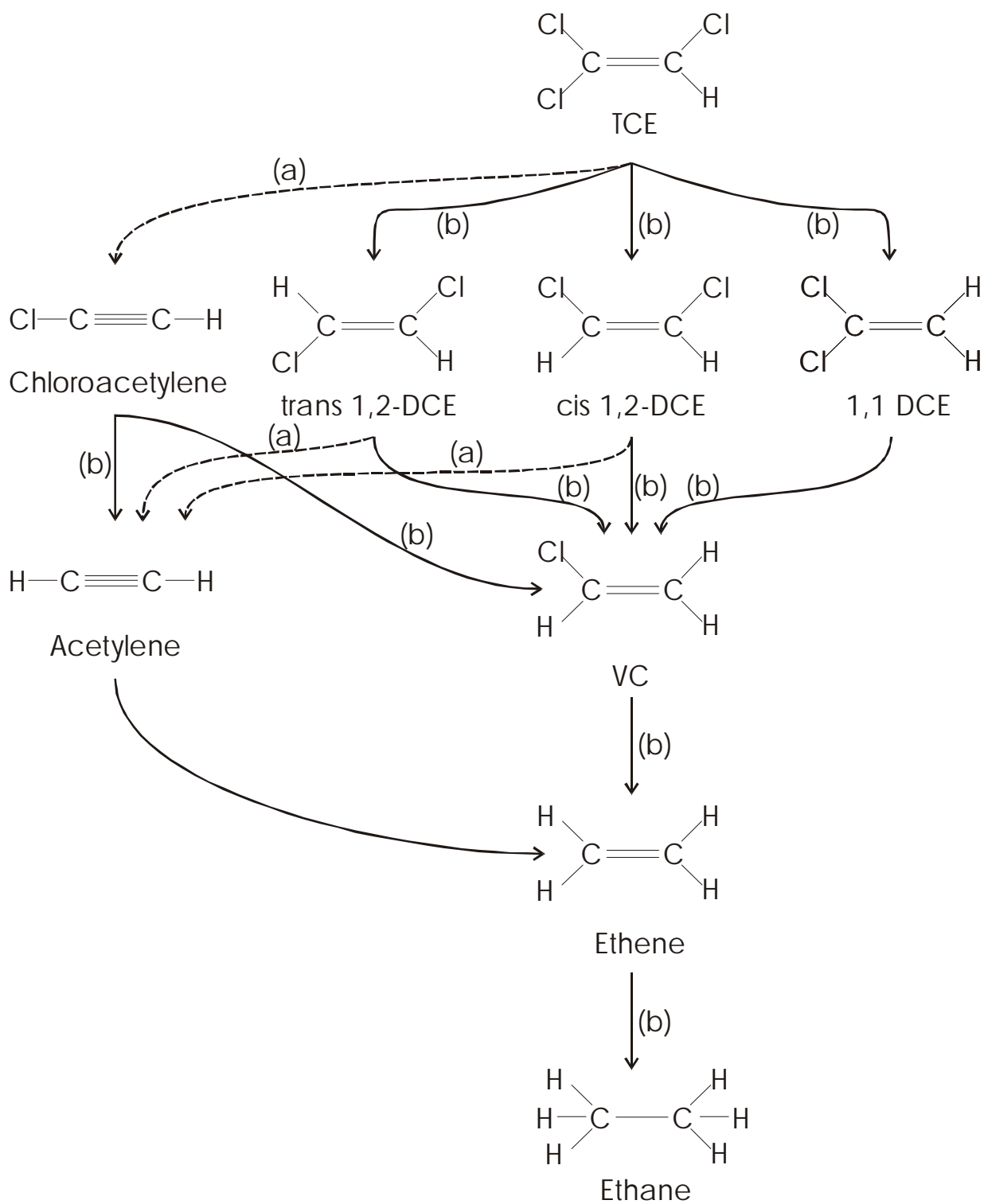


Figure 14. (a) Reductive β -elimination, and (b) hydrogenolysis reaction steps in degradation of TCE (after Arnold and Roberts, 1997).

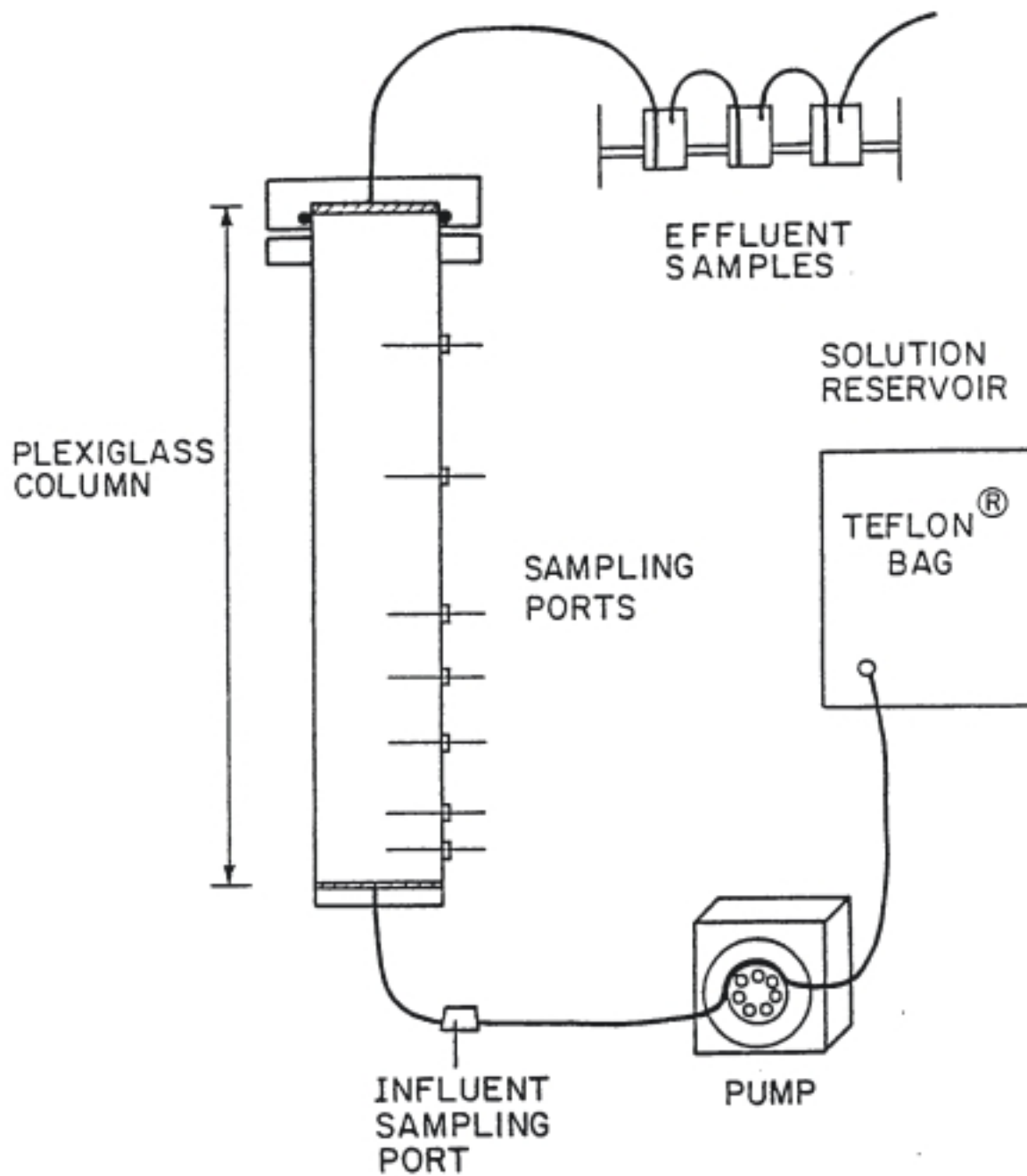


Figure 15. Schematic of the apparatus used in the column experiments.

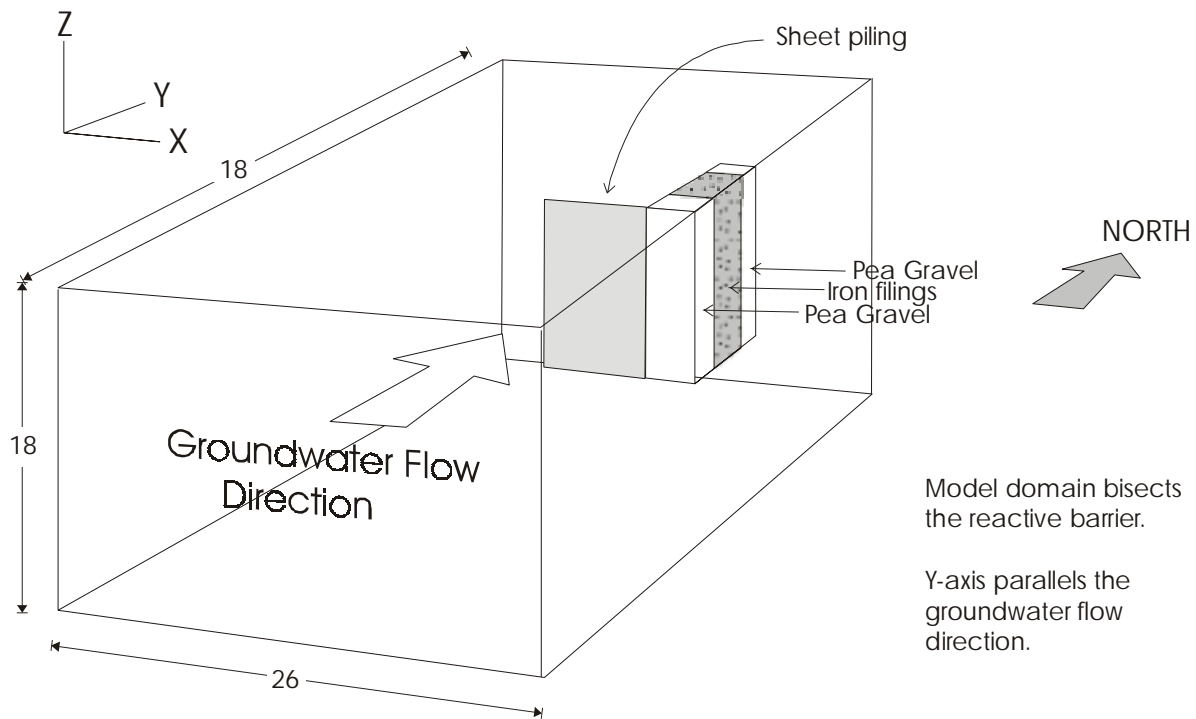


Figure 16. Model domain dimensions, with Funnel-and-Gate barrier shown (all dimensions in m).

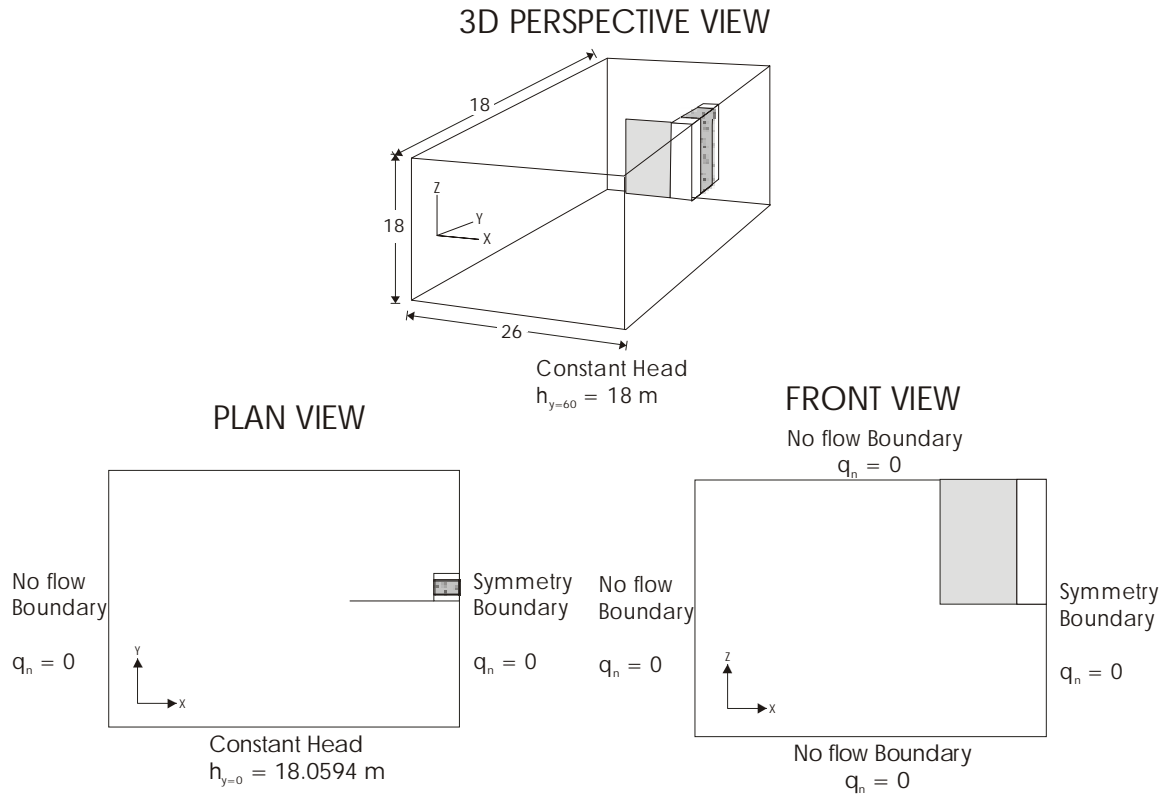


Figure 17. Model boundary conditions, with Funnel-and-Gate barrier shown.

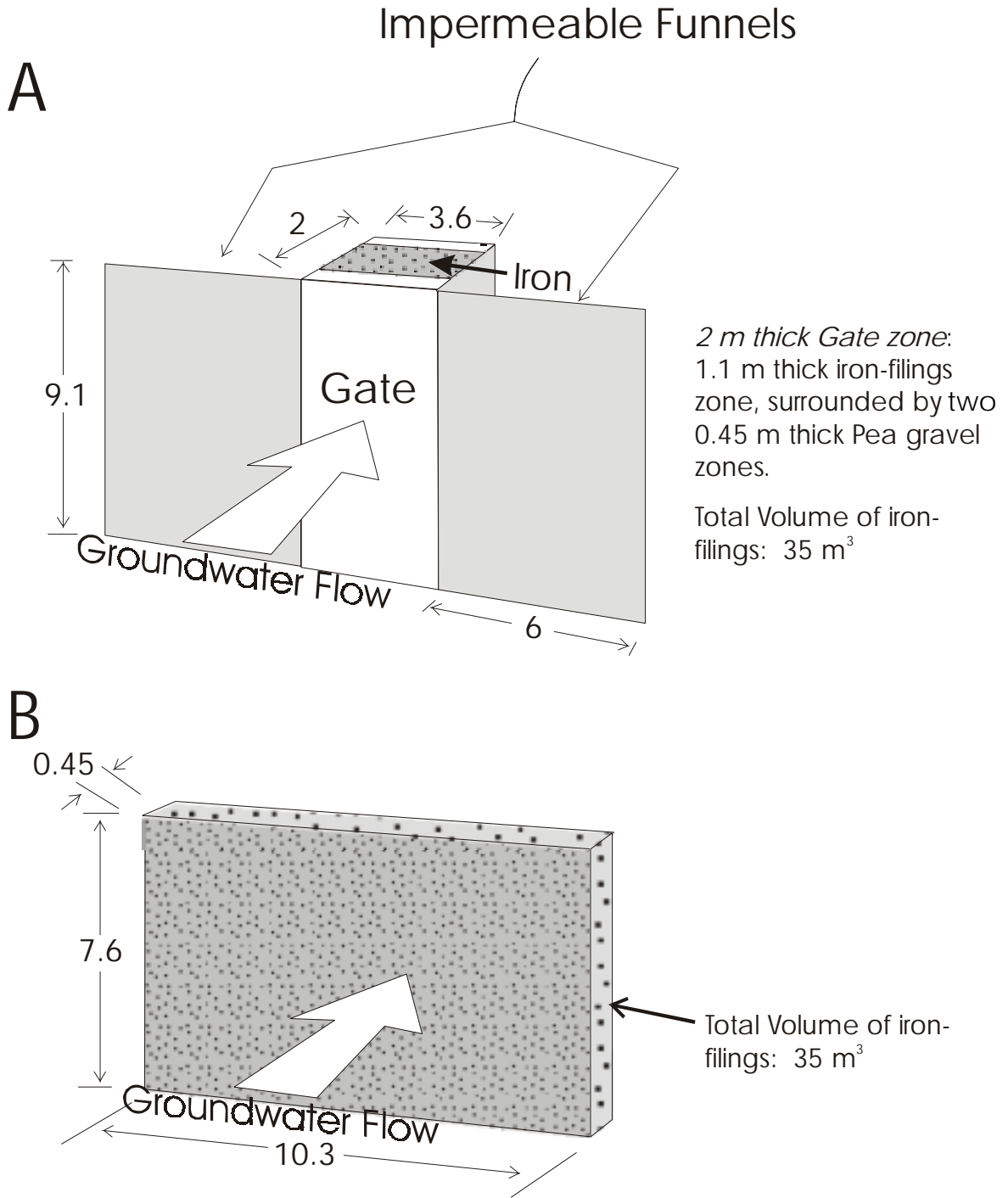


Figure 18. (A) Funnel-and-Gate, and (B) permeable wall configurations used in flow simulations [all dimensions in meters].

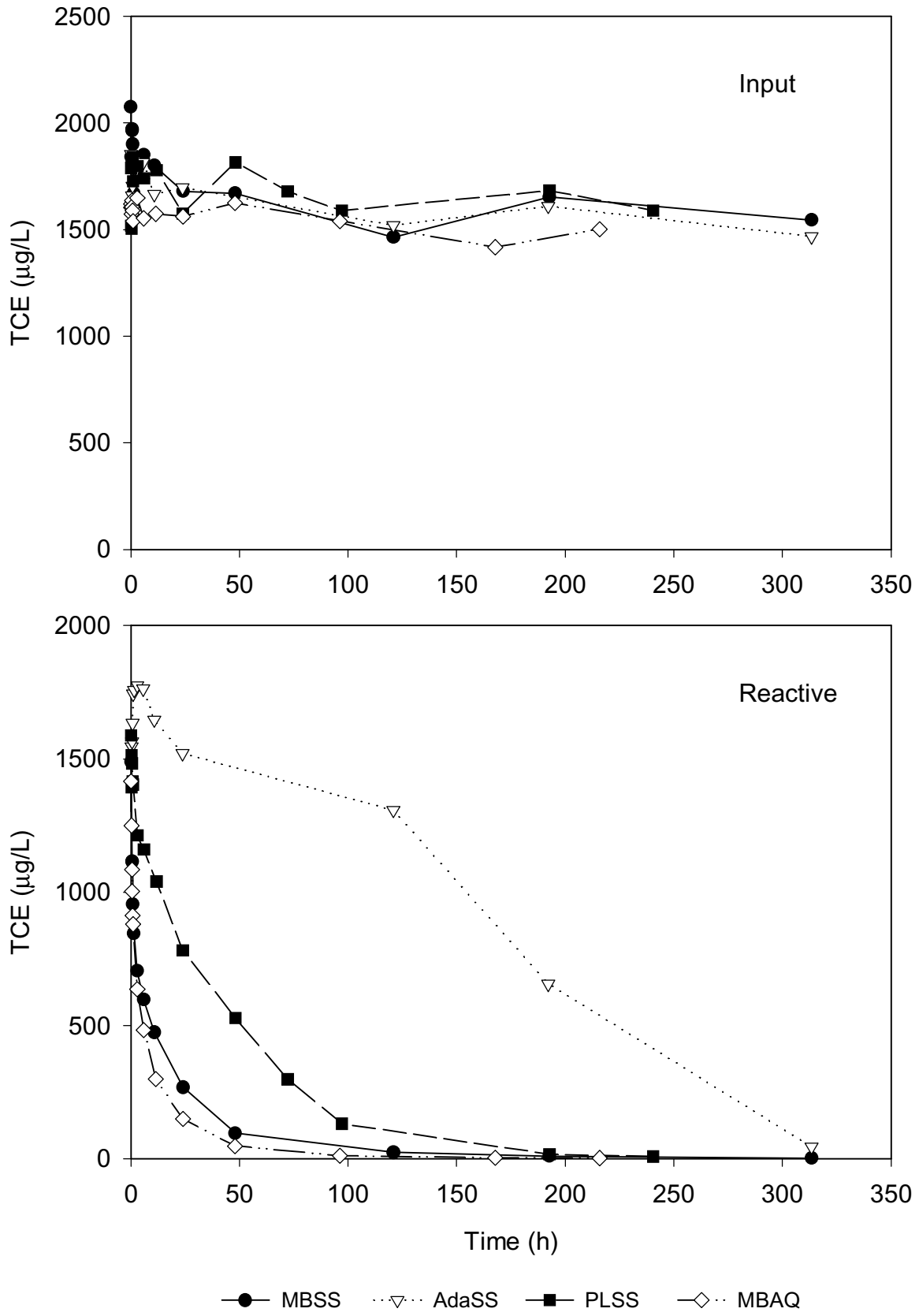


Figure 19. TCE concentration versus time in each of the four batch test mixtures.

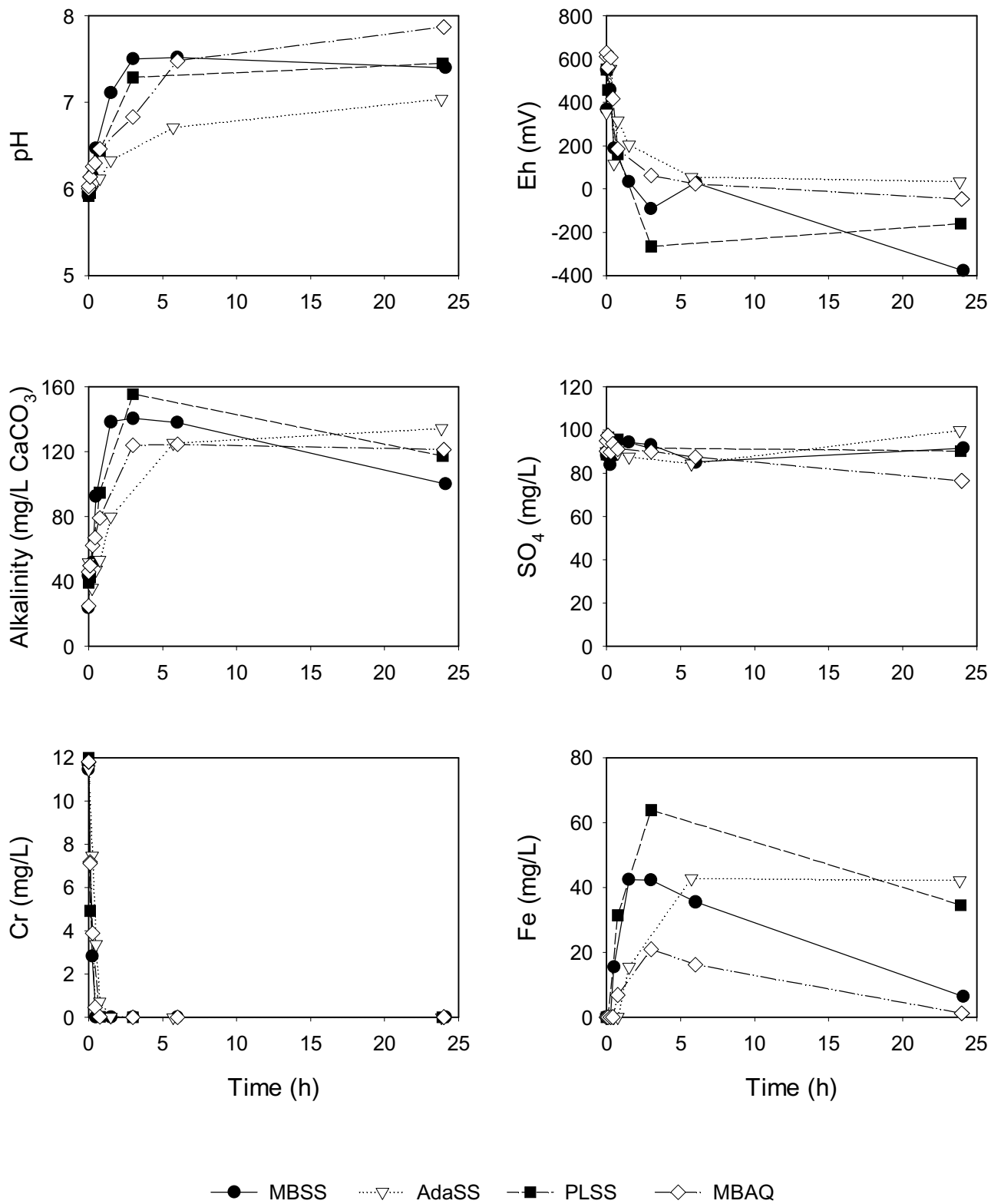


Figure 20. Batch test inorganic geochemistry for all mixtures, versus time.

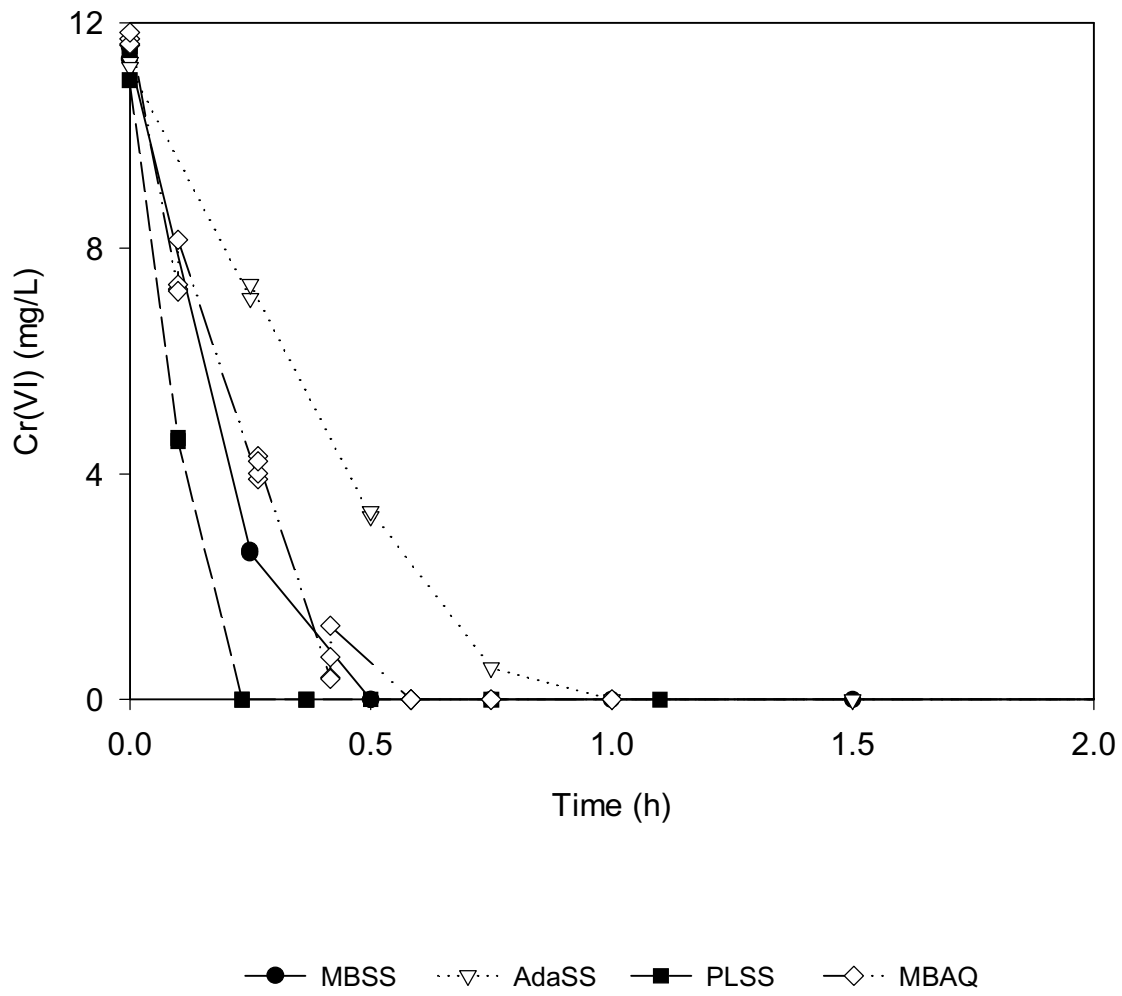


Figure 21. Cr(VI) concentration vs. time in each of the four batch test mixtures.

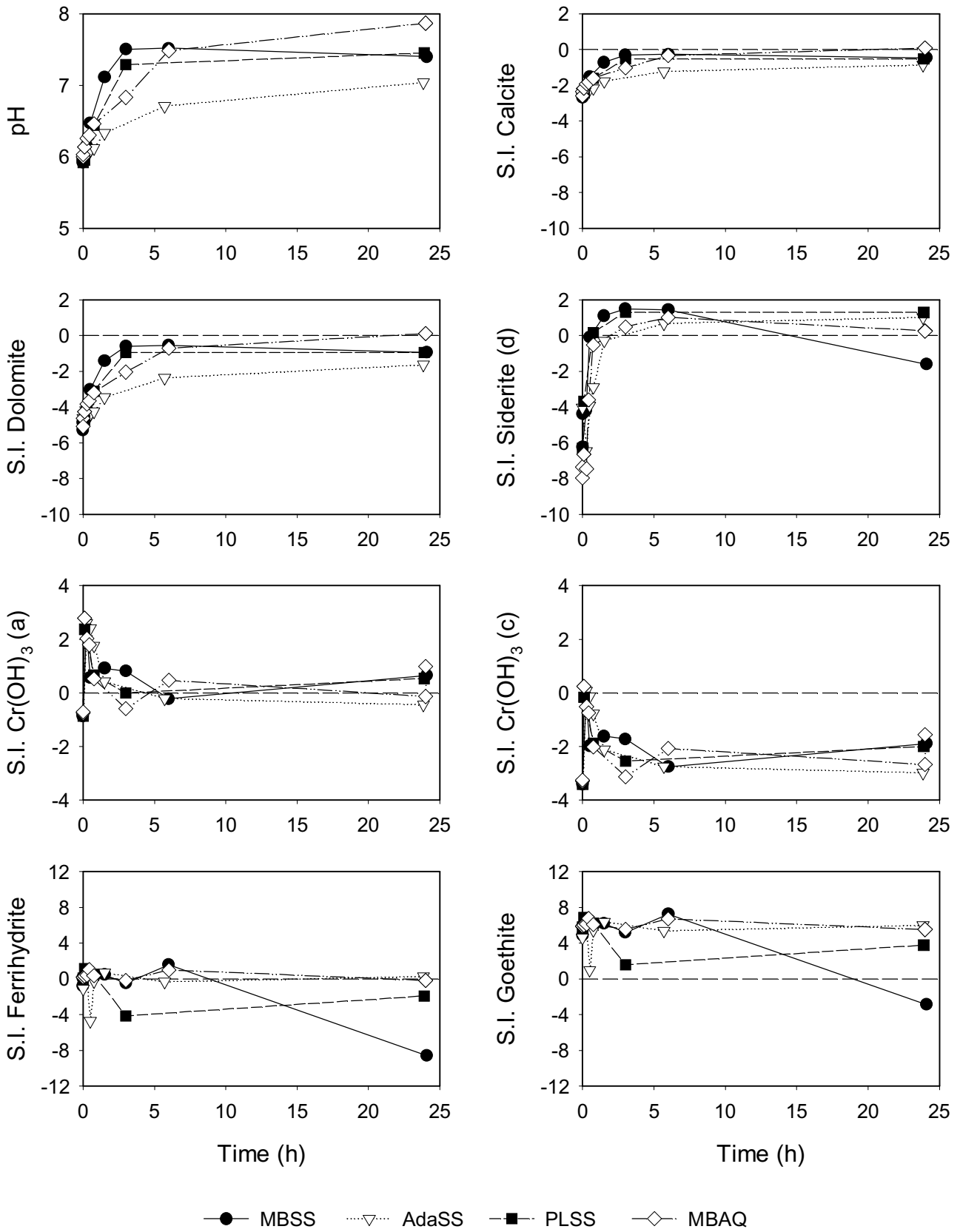


Figure 22. Mineral saturation indices for batch tests, calculated with MINTEQA2.

Trichloroethene (TCE)

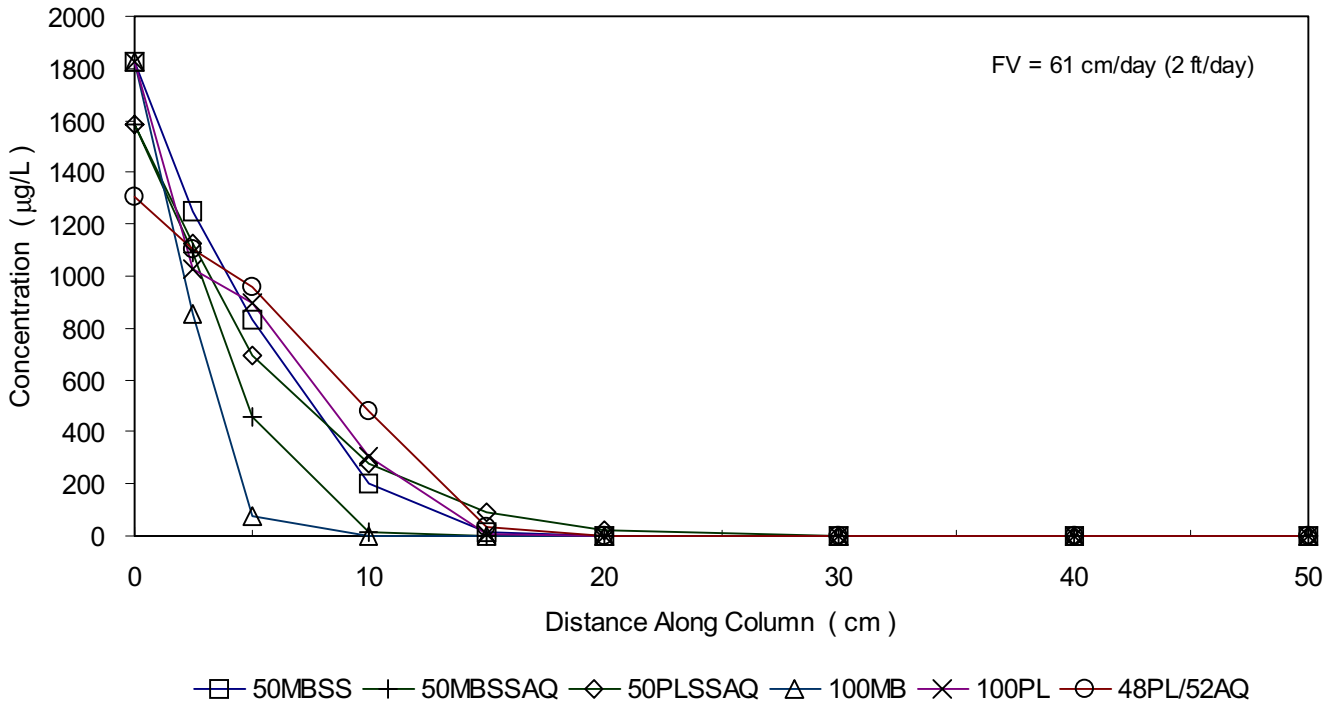


Figure 23. TCE concentration versus distance along all six columns at the first flow velocity (FV1), approximately 61 cm/day (2 ft/day).

Chloroform (TCM)

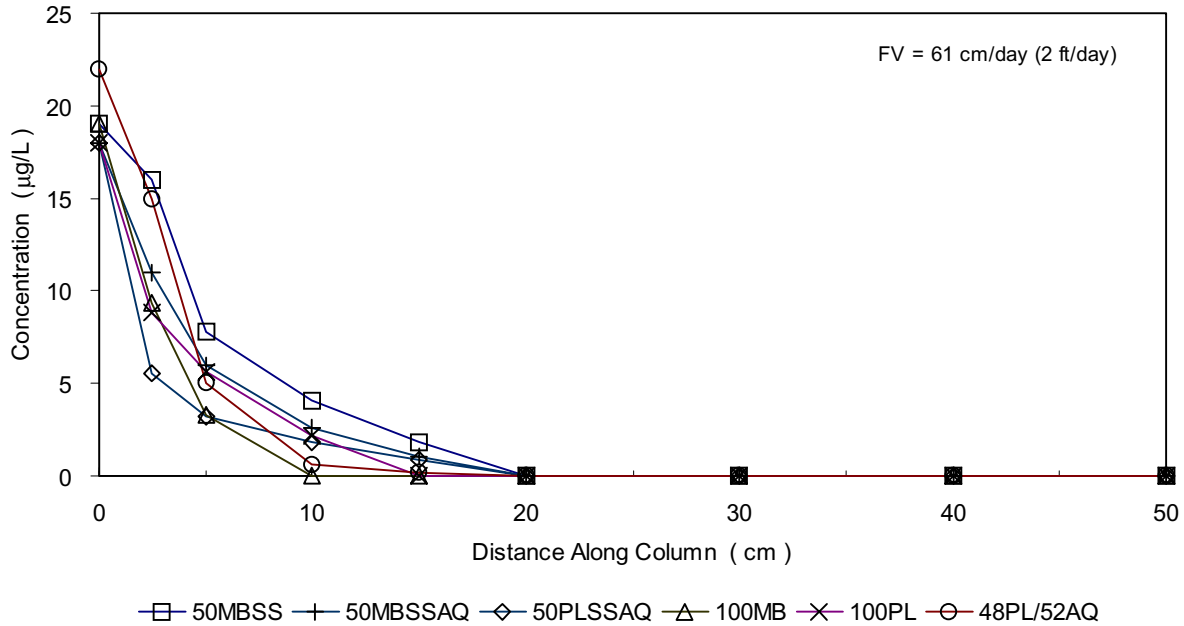


Figure 24. TCM concentration versus distance along all six columns at the first flow velocity (FV1), approximately 61 cm/day (2 ft/day).

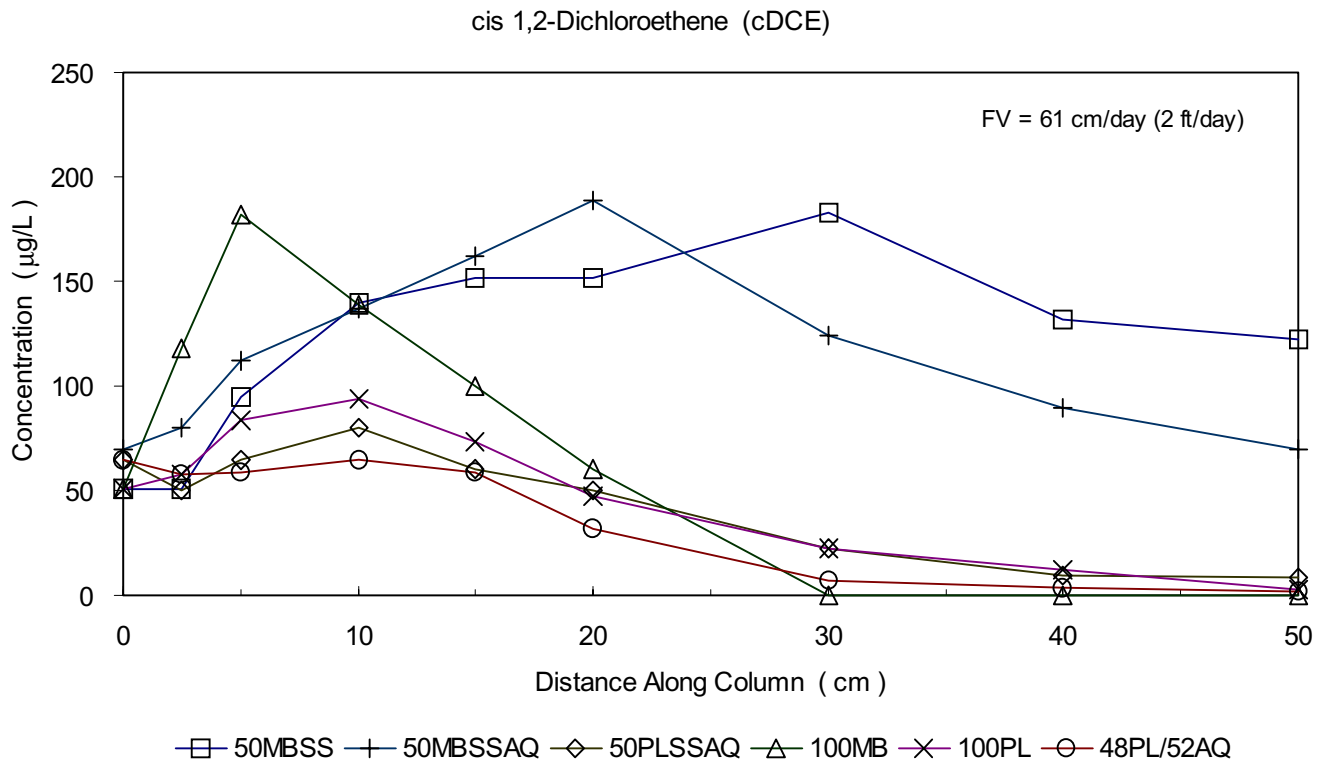


Figure 25. cDCE concentration versus distance along all six columns at the first flow velocity (FV1), approximately 61 cm/day (2 ft/day).

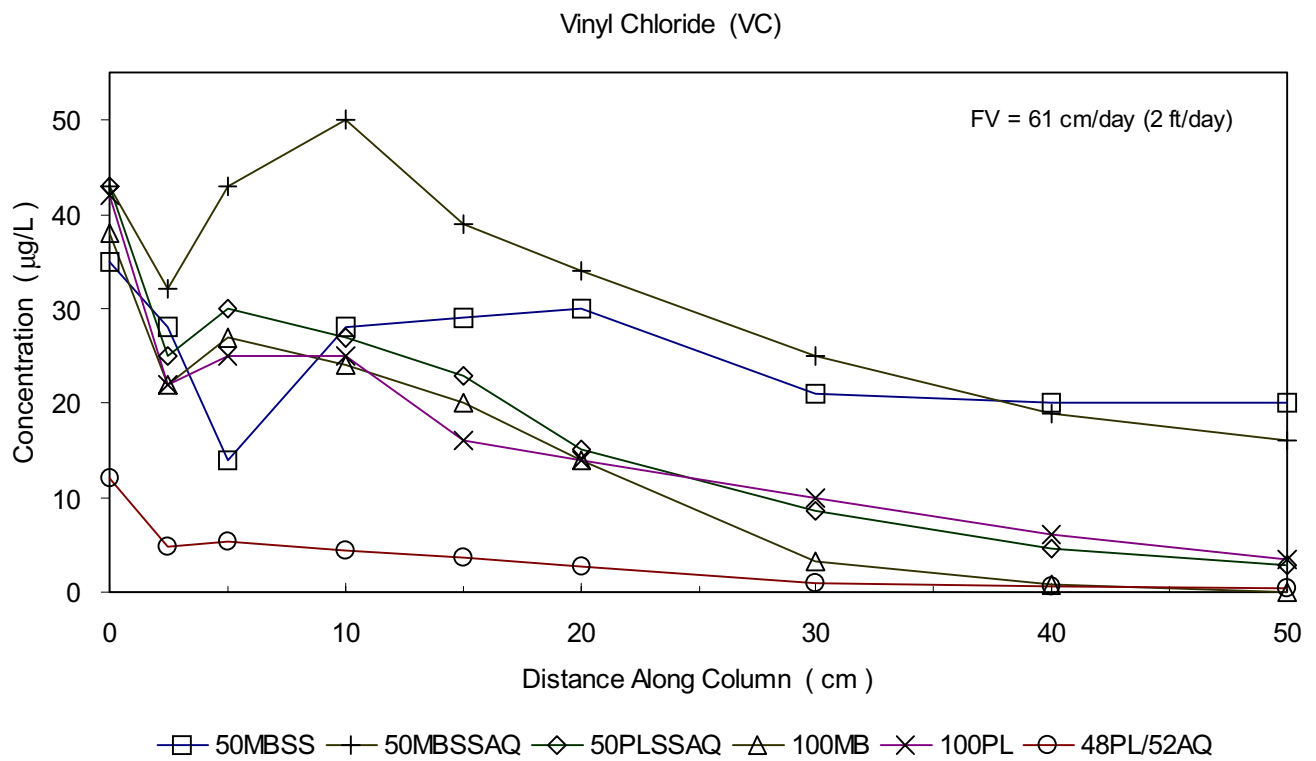


Figure 26. VC concentration versus distance along all six columns at the first flow velocity (FV1), approximately 61 cm/day (2 ft/day).

Trichloroethene (TCE)

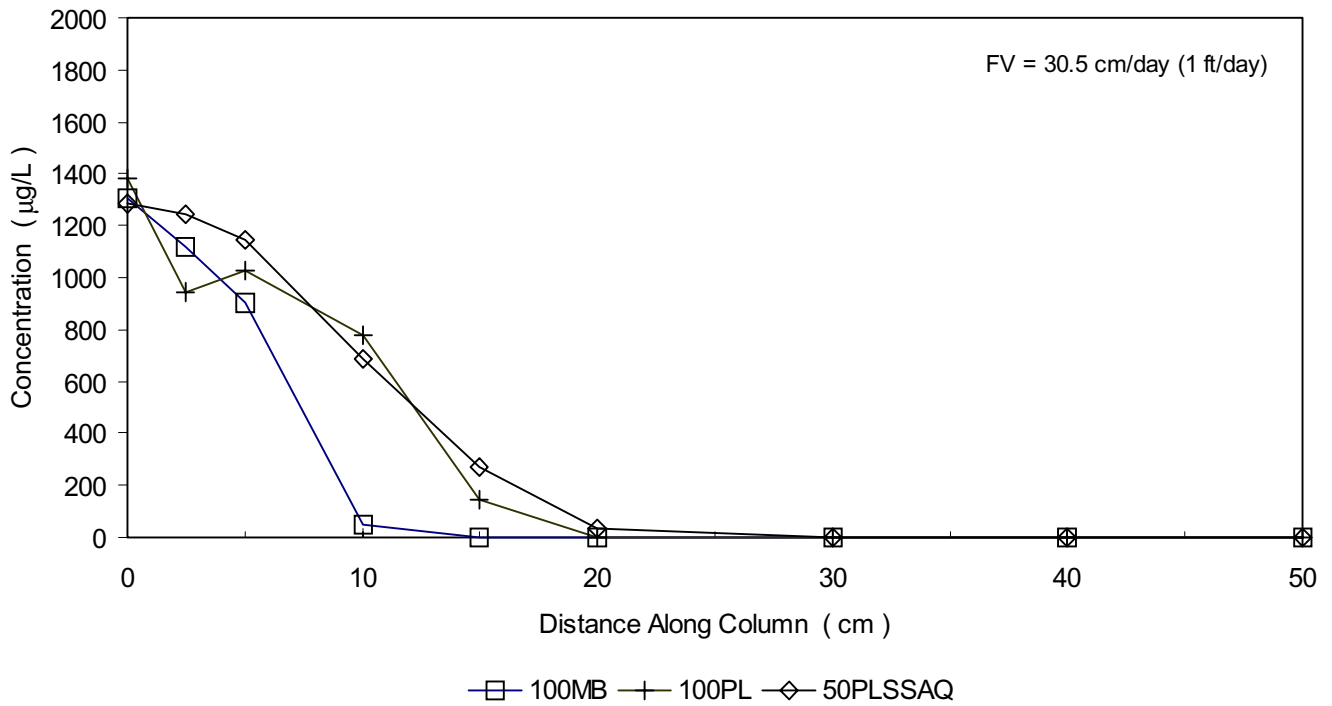


Figure 27. TCE concentration versus distance along three columns at the second flow velocity (FV2), approximately 30 cm/day (1 ft/day).

Chloroform (TCM)

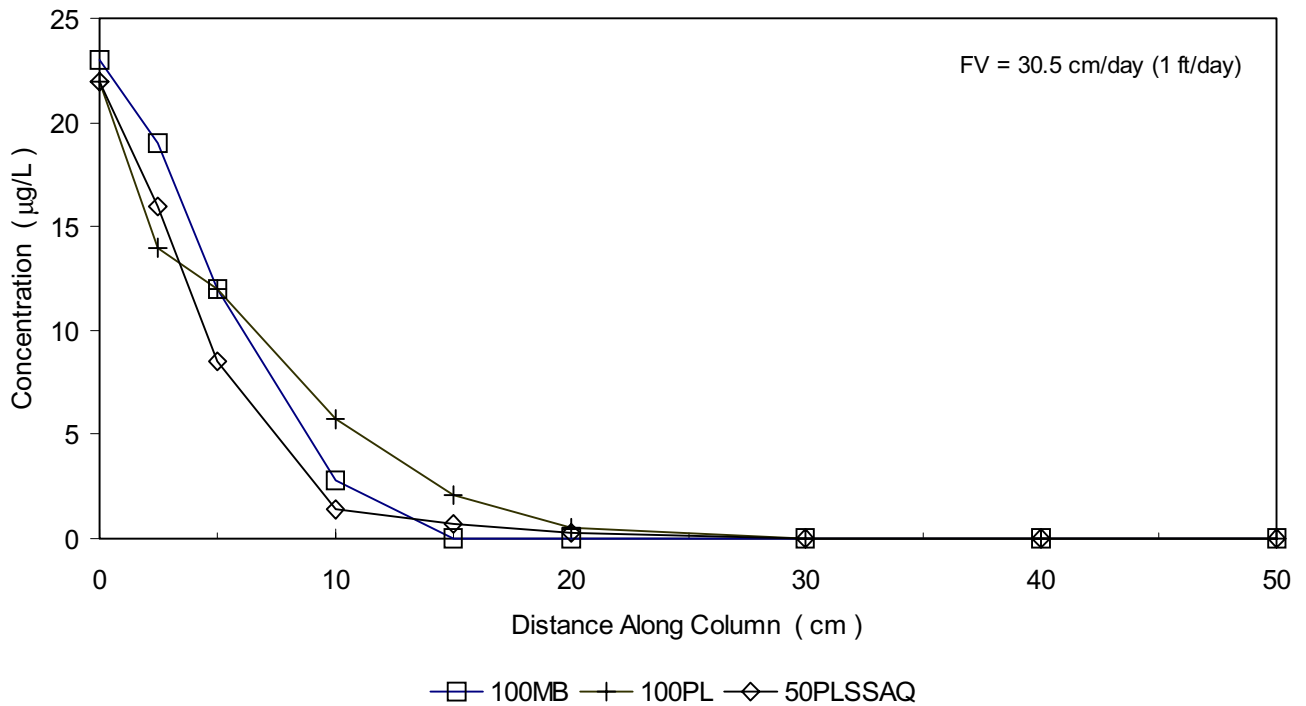


Figure 28. TCM concentration versus distance along three columns at the second flow velocity (FV2), approximately 30 cm/day (1 ft/day).

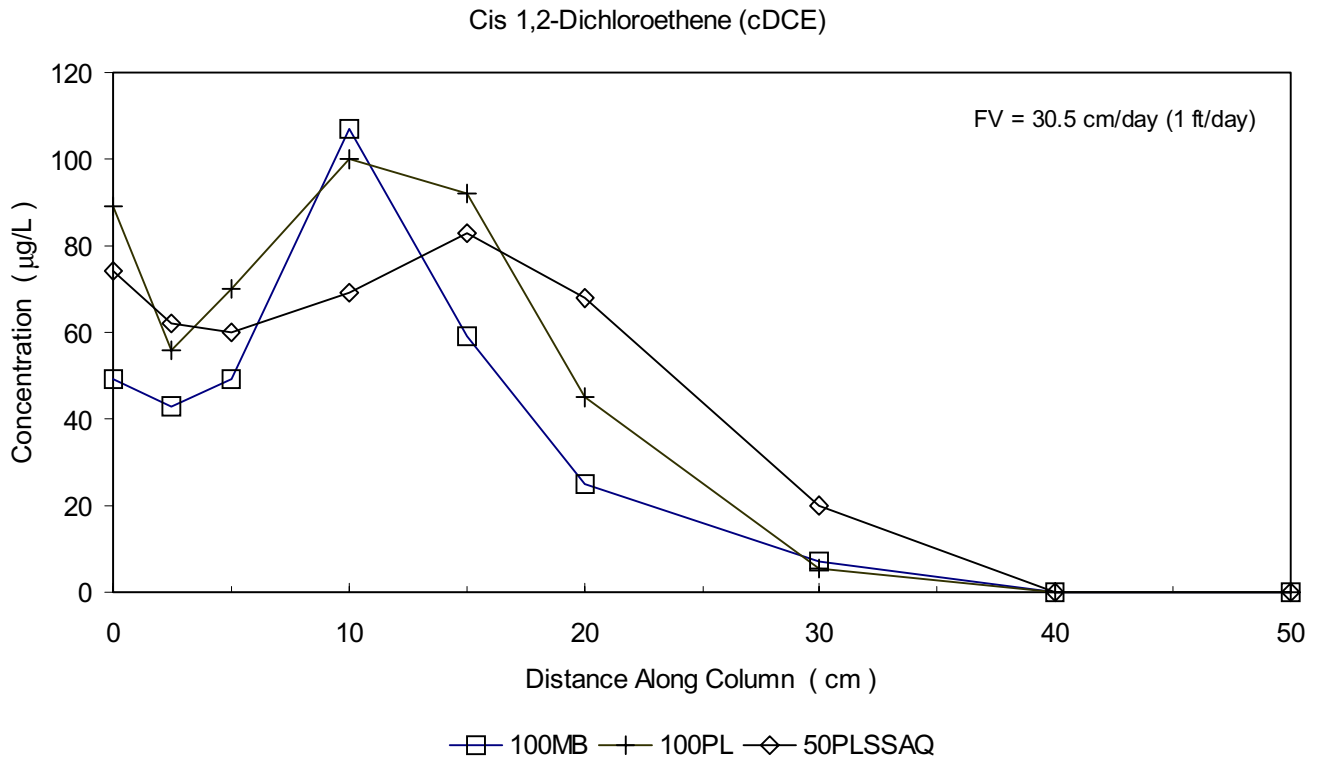


Figure 29. cDCE concentration versus distance along three columns at the second flow velocity (FV2), approximately 30 cm/day (1 ft/day).

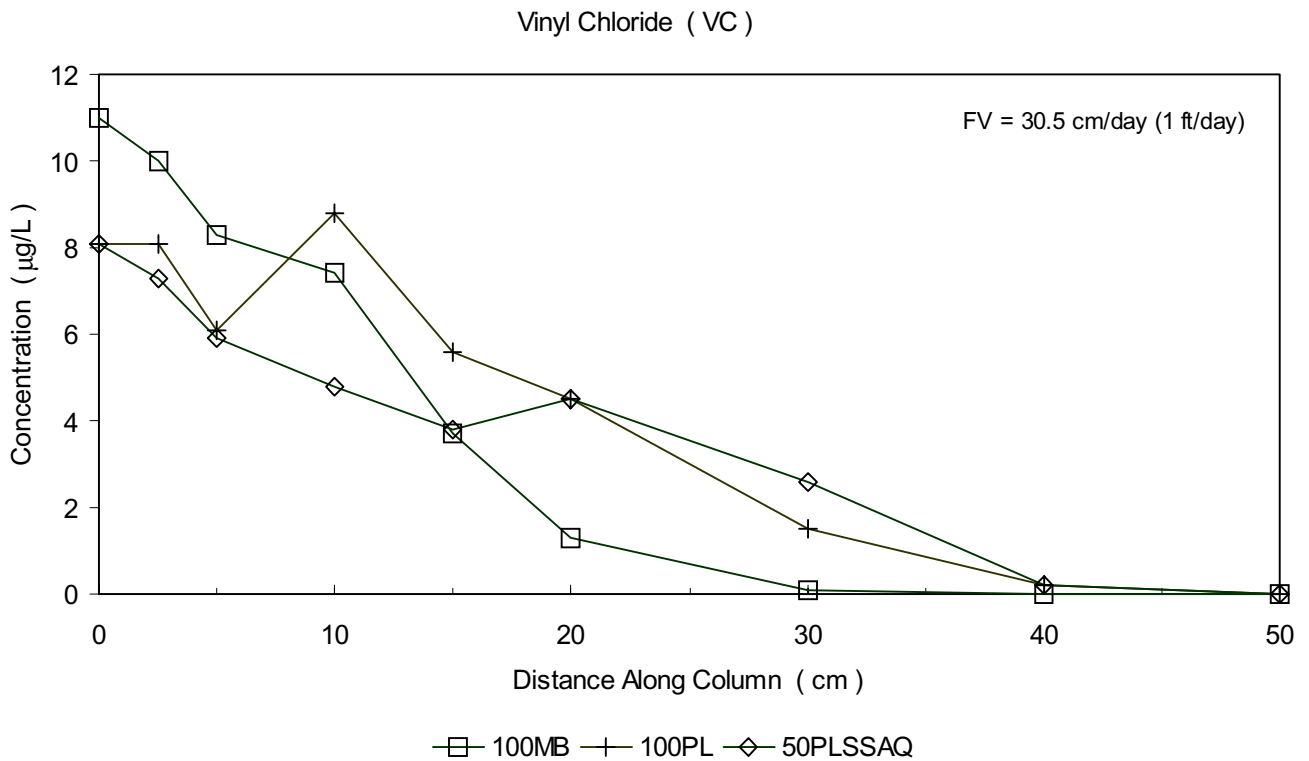


Figure 30. VC concentration versus distance along three columns at the second flow velocity (FV2), approximately 30 cm/day (1 ft/day).

50% MB Fe + 25% EC aquifer material + 25% sand

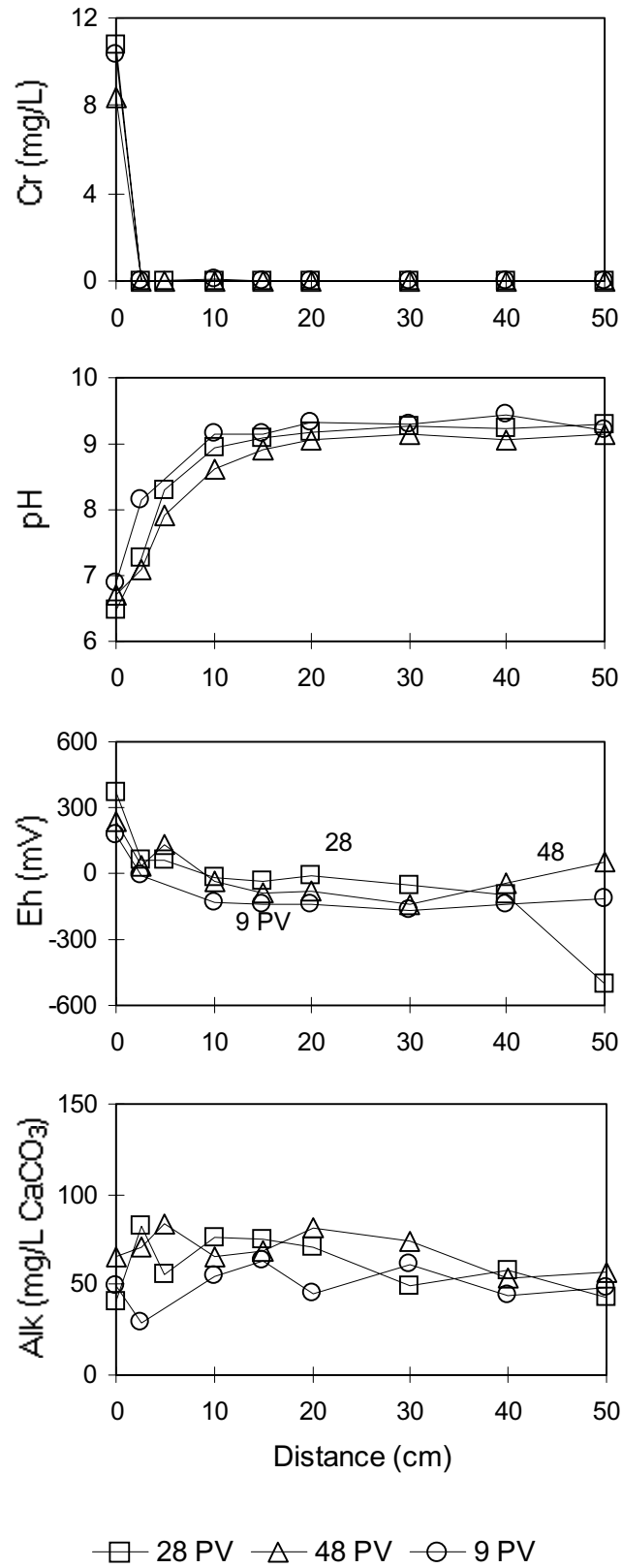


Figure 31. Inorganic results for column 50MBSSAQ at FV1.

50% MB Fe + 50% sand

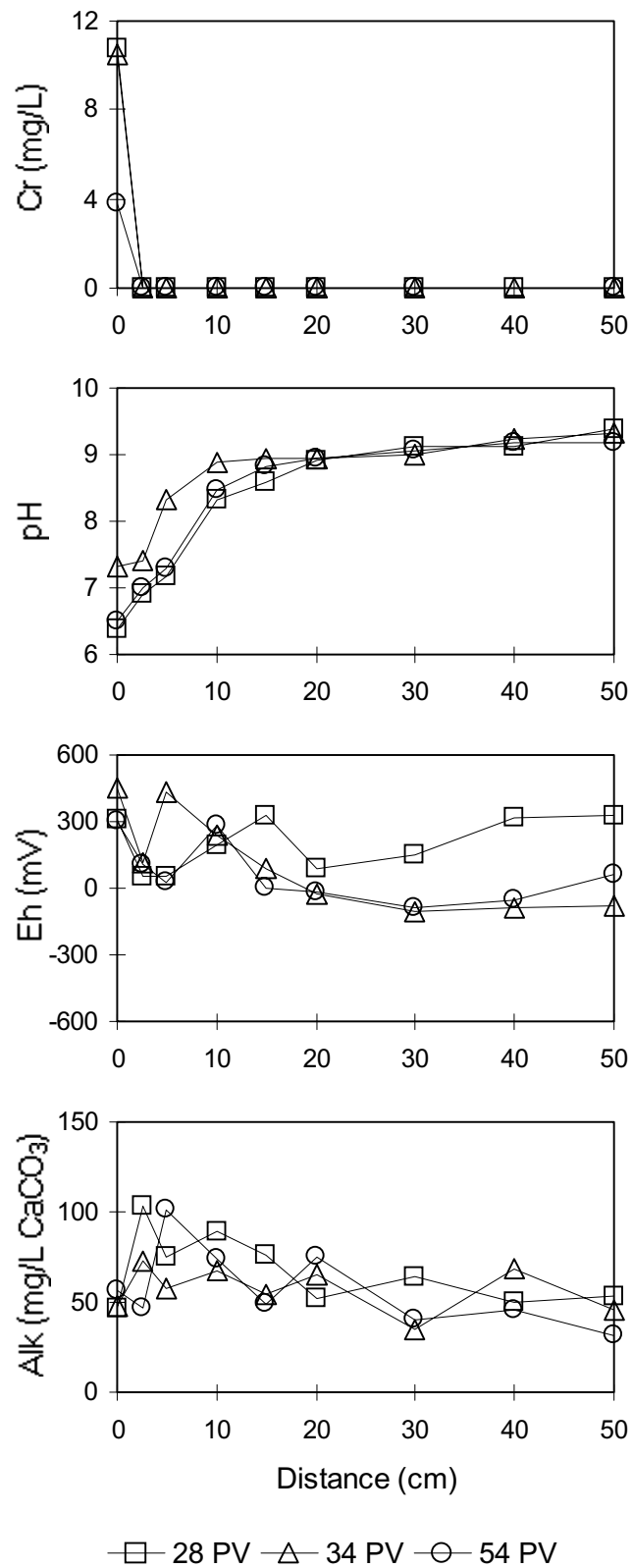


Figure 32. Inorganic results for column 50MBSS at FV1.

100% MB Fe

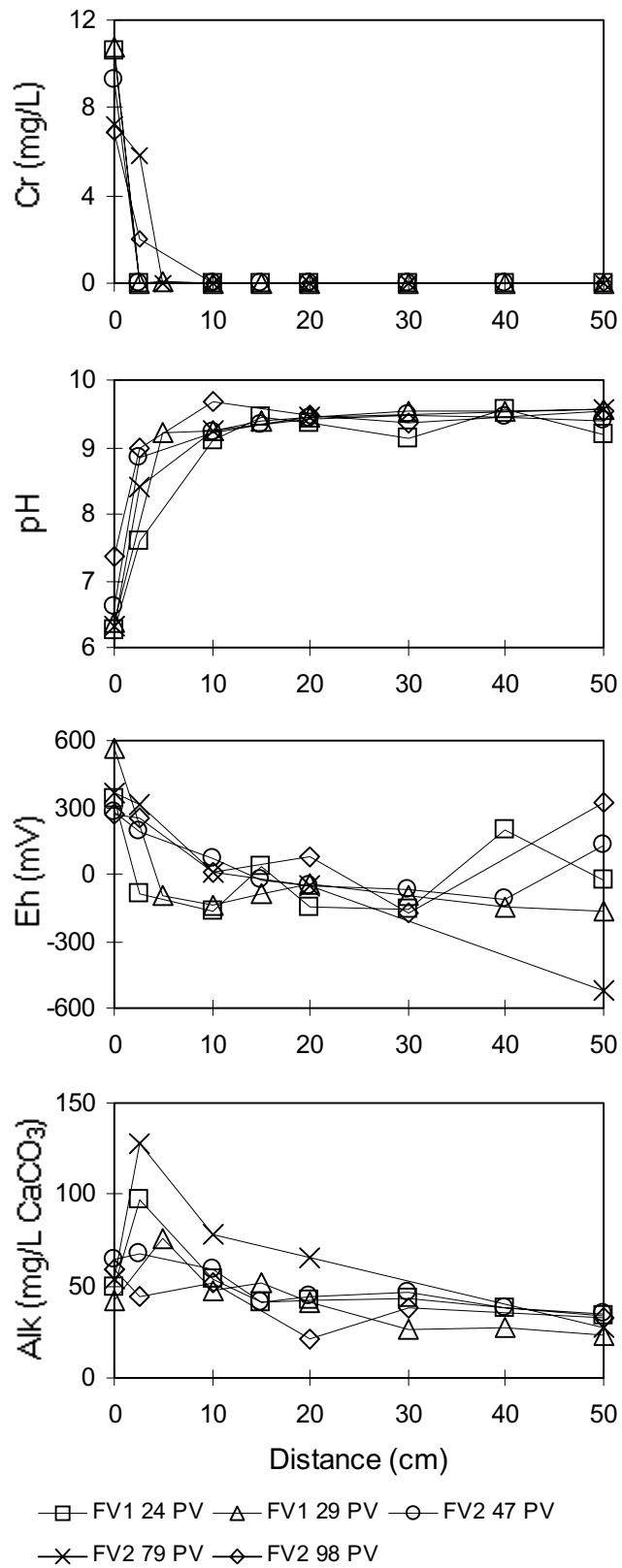


Figure 33. Inorganic results for column 100MB at FV1 and FV2.

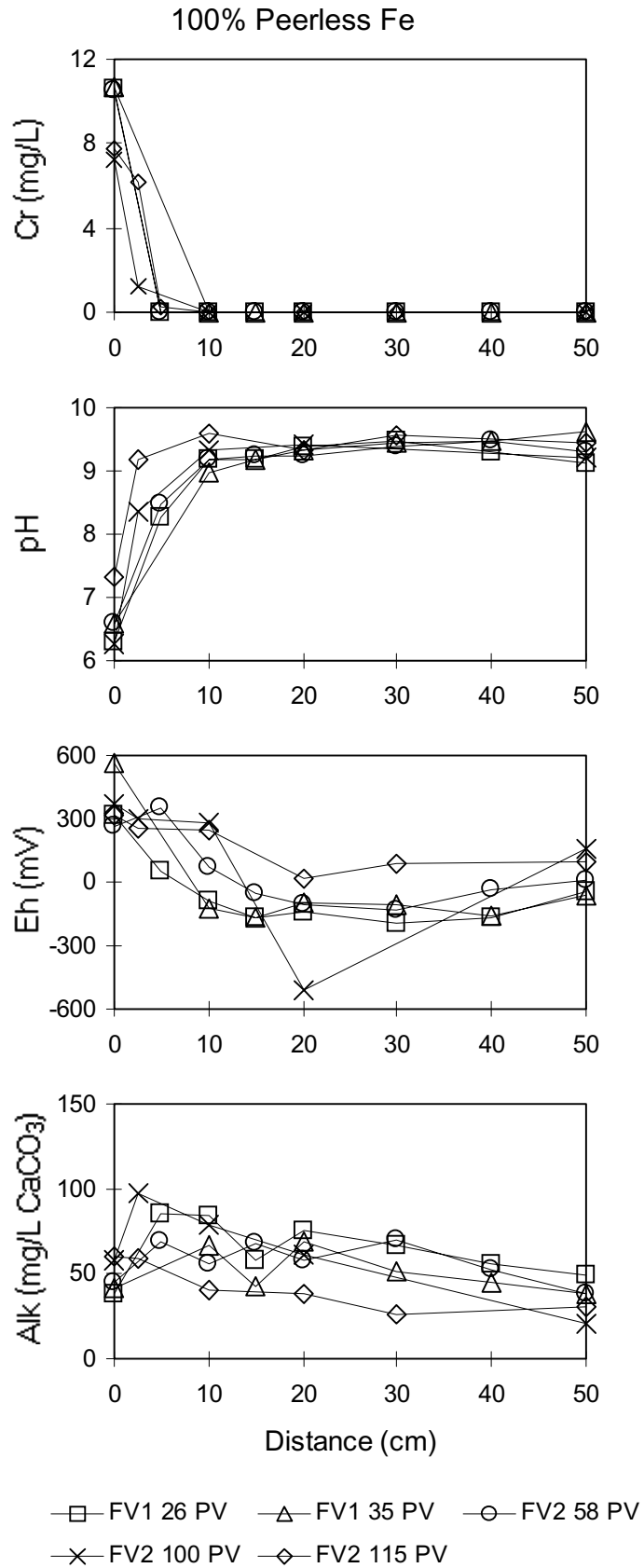


Figure 34. Inorganic results for column 100PL at FV1 and FV2.

50% Peerless Fe + 25% EC aquifer material + 25% sand

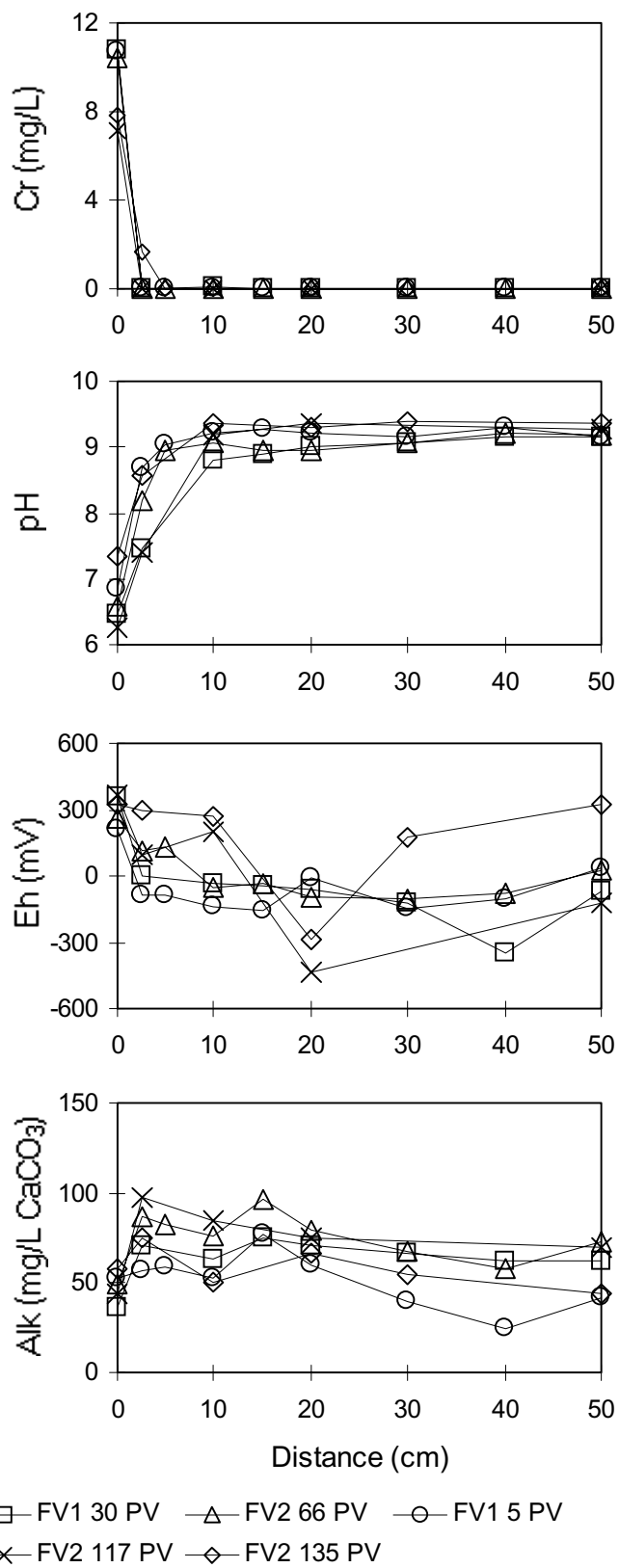


Figure 35. Inorganic results for column 50PLSSAQ at FV1 and FV2.

48% Peerless Fe + 52% EC aquifer material

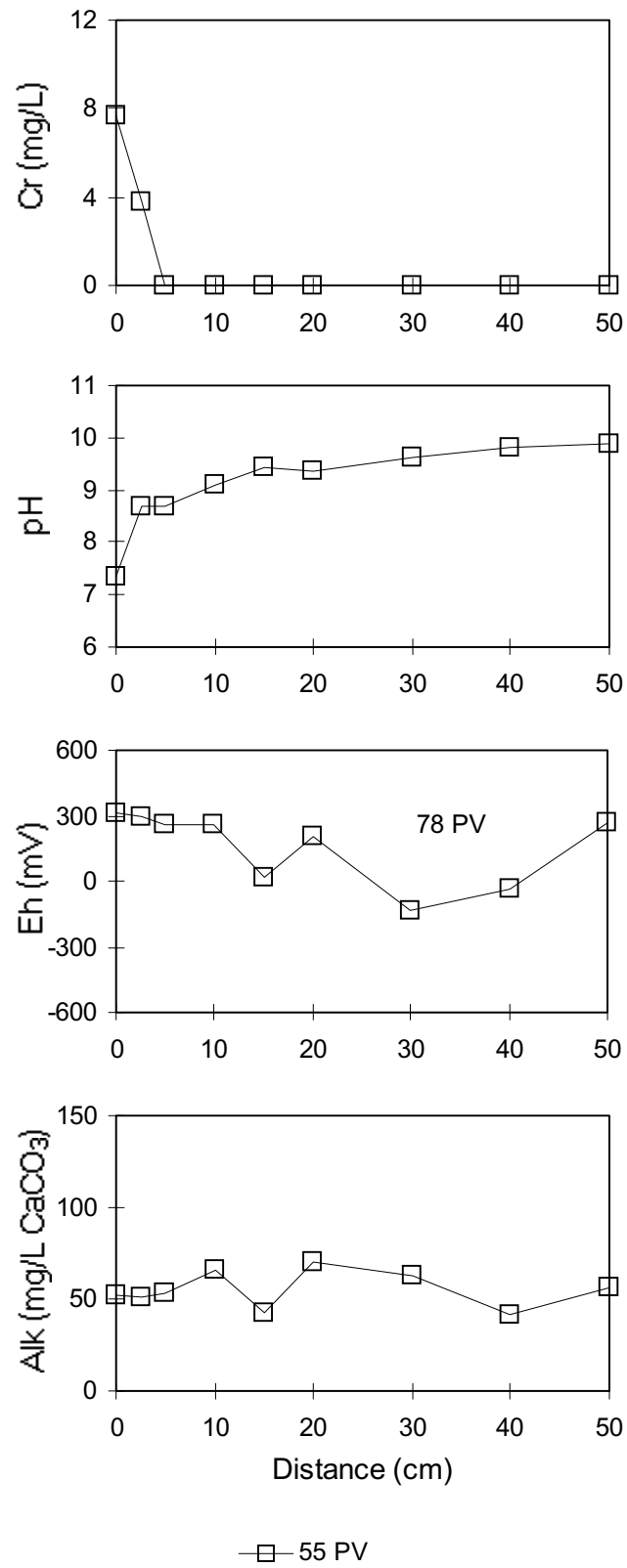


Figure 36. Inorganic results for column 48PL/52AQ at FV1.

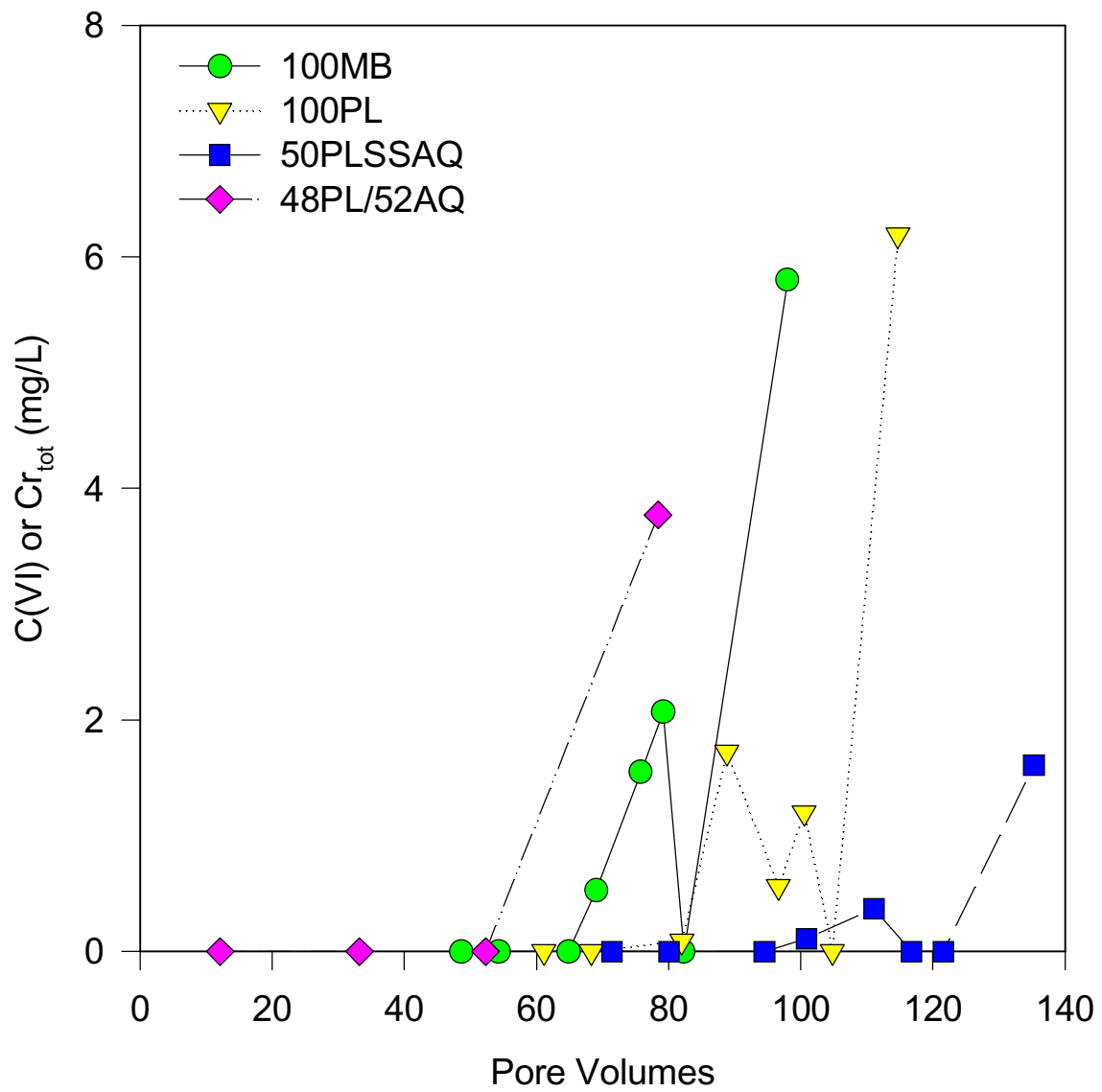


Figure 37. Cr detection at the 2.5 cm sample port.

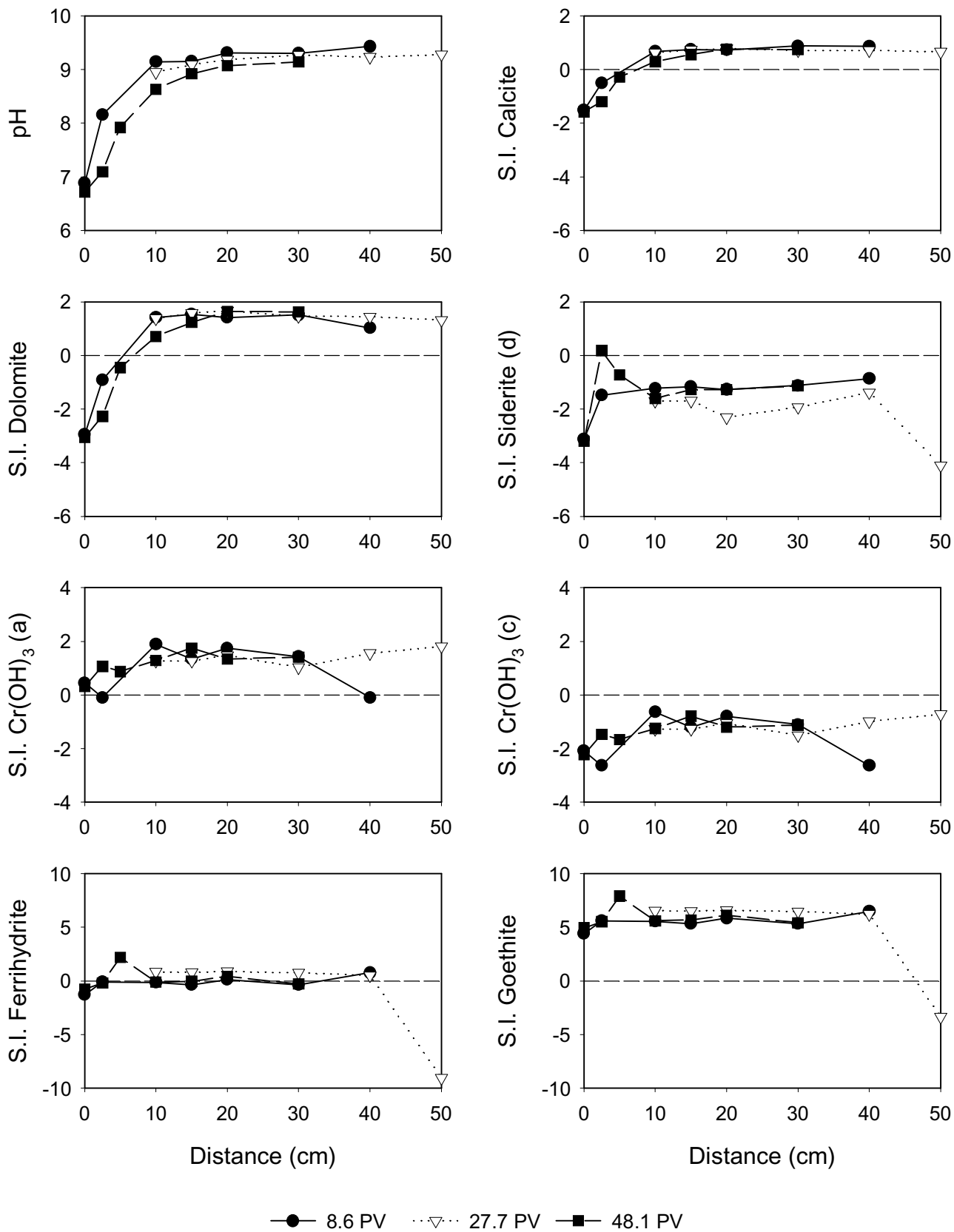


Figure 38. Mineral saturation indices for column 50MBSSAQ at FV1.

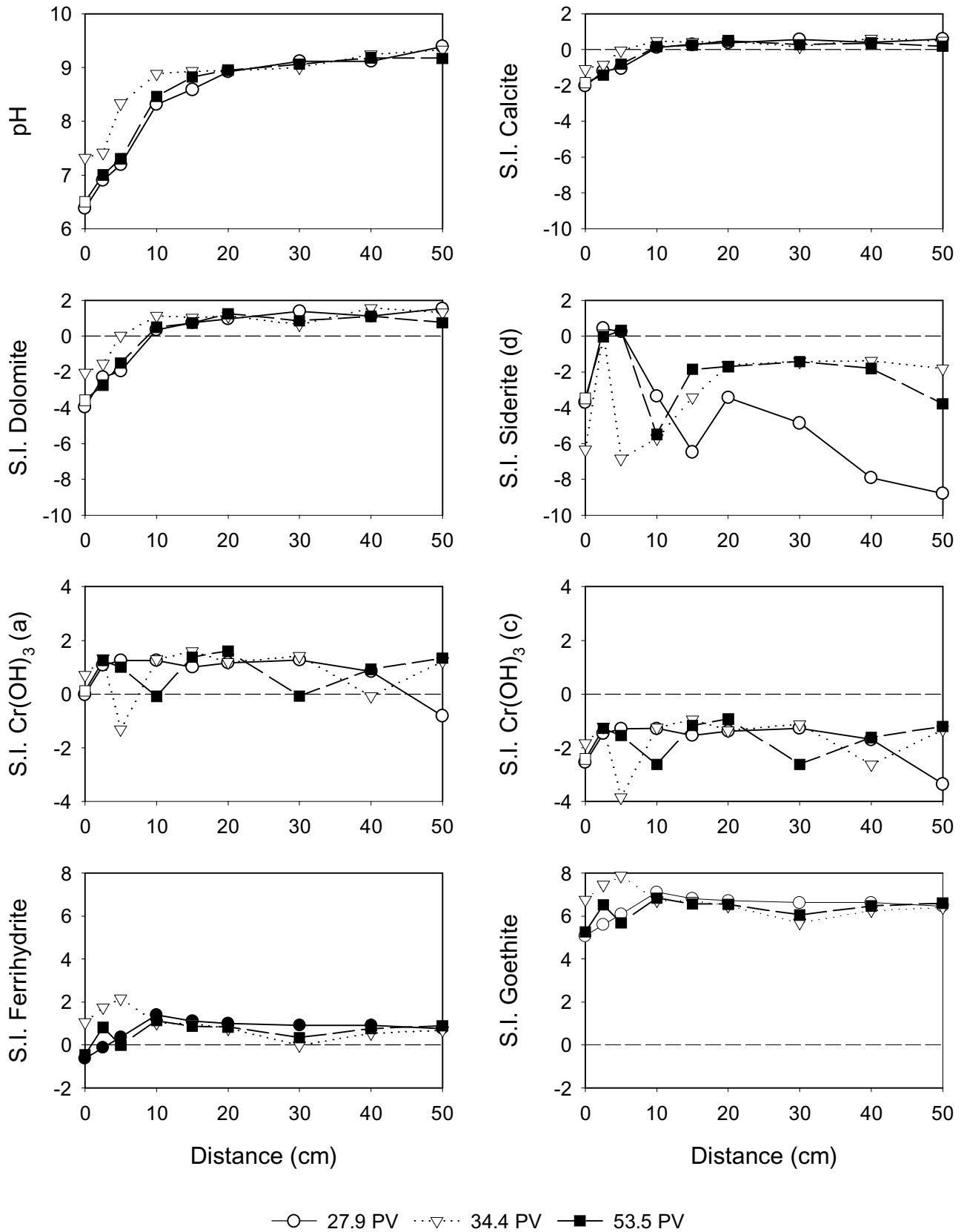


Figure 39. Mineral saturation indices for column 50MBSS at FV1.

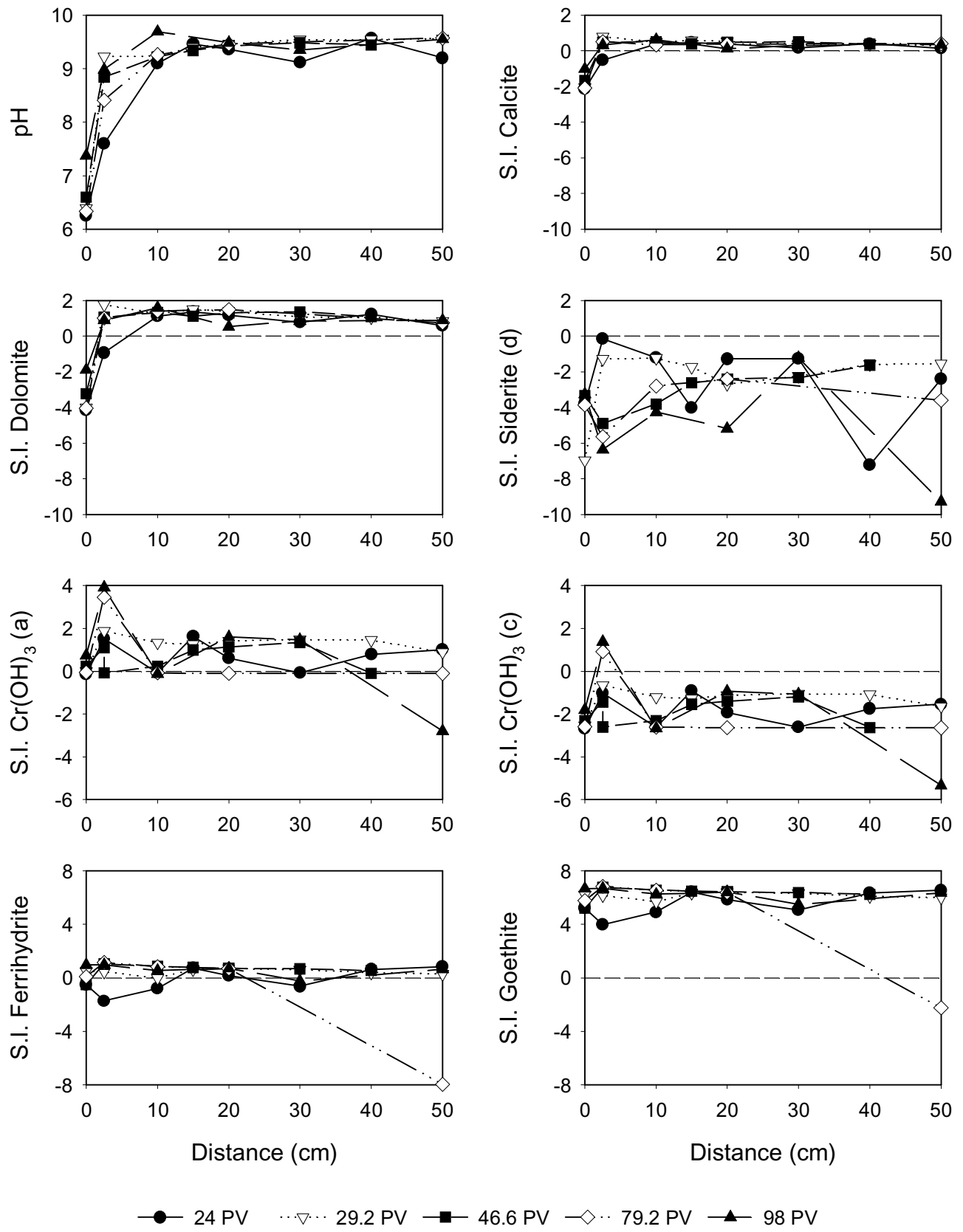


Figure 40. Mineral saturation indices for column 100MB at FV1 and FV2.

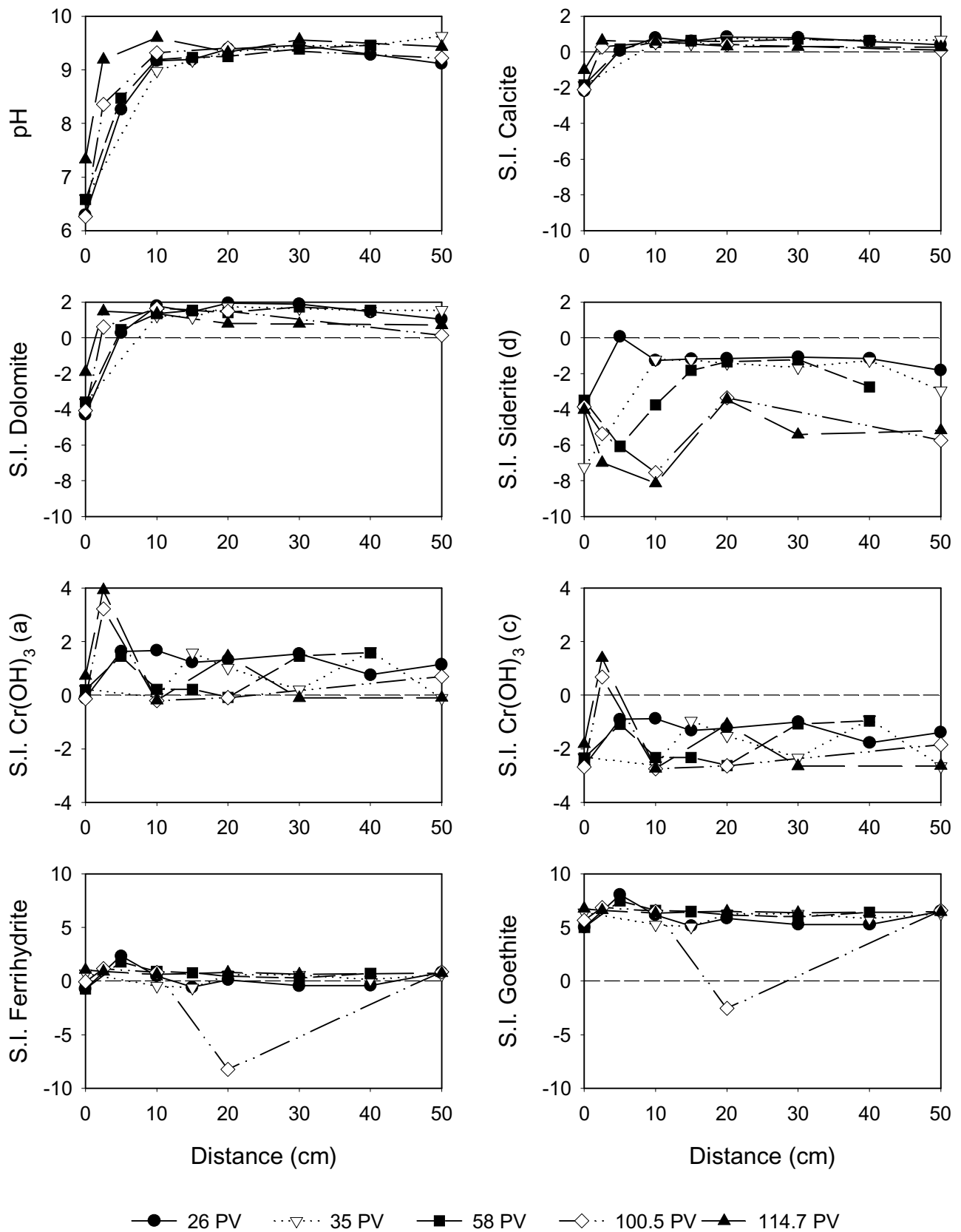


Figure 41. Mineral saturation indices for column 100PL at FV1 and FV2.

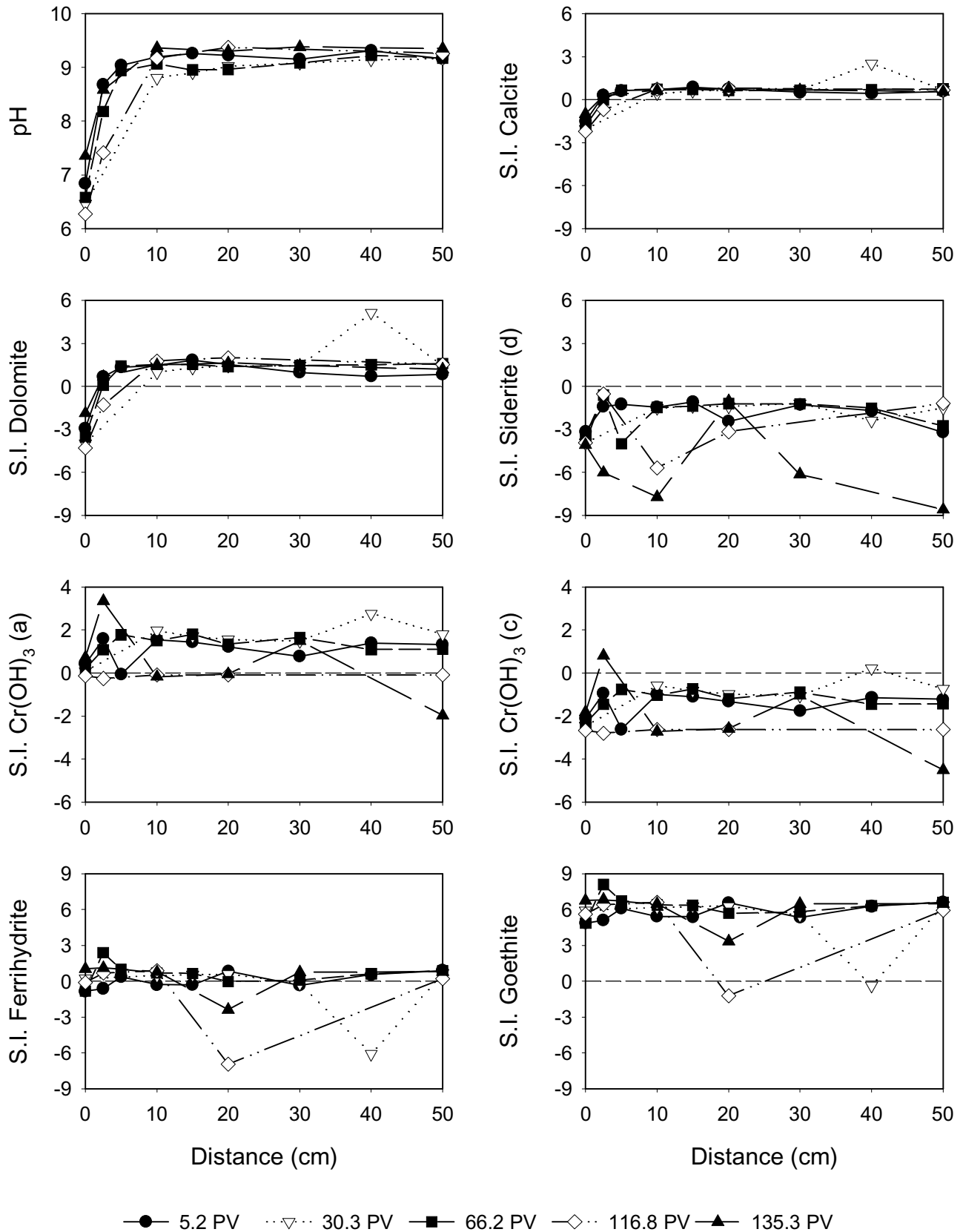


Figure 42. Mineral saturation indices for column 50PLSSAQ at FV1 and FV2.

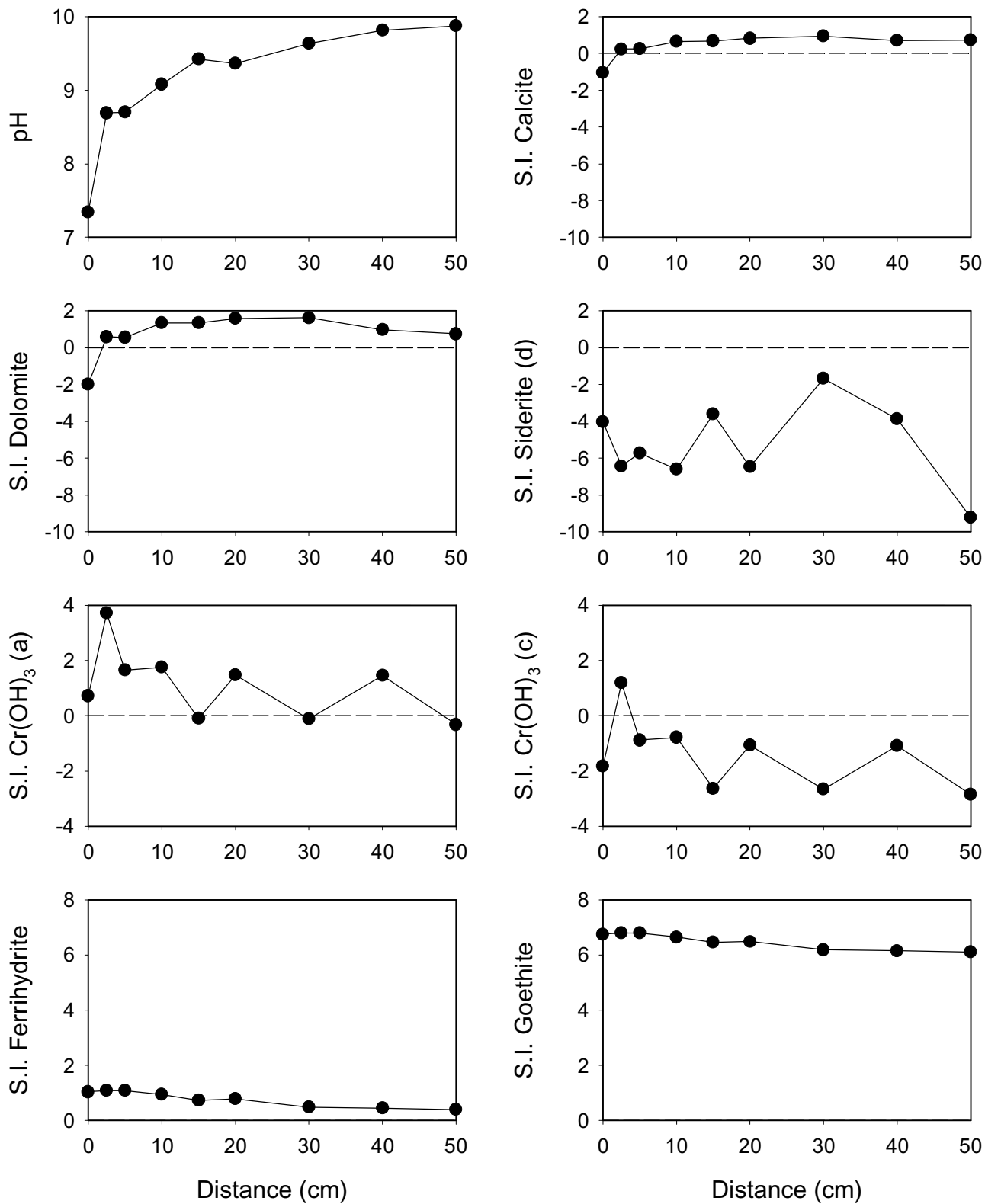


Figure 43. Mineral saturation indices for column 48PL/52AQ at 78.4 PV and FV1.

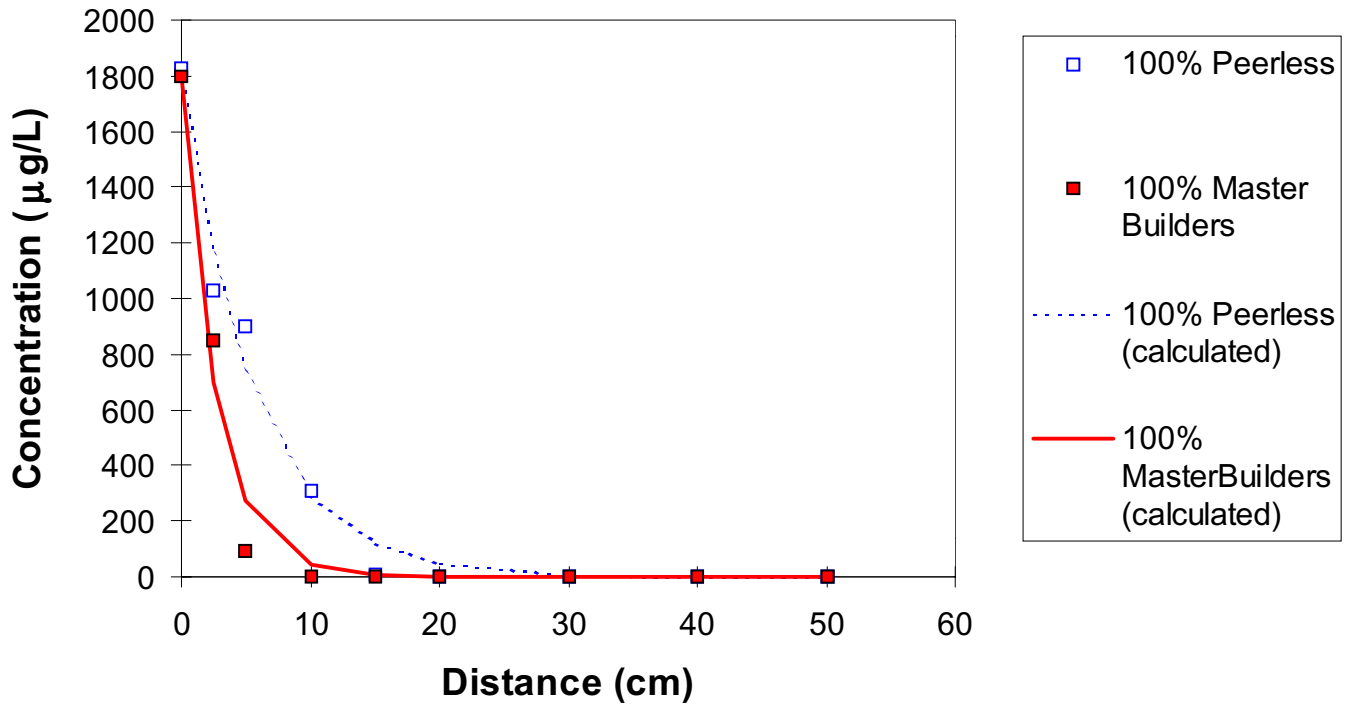


Figure 44. Experimental and calculated TCE concentration profiles in column.

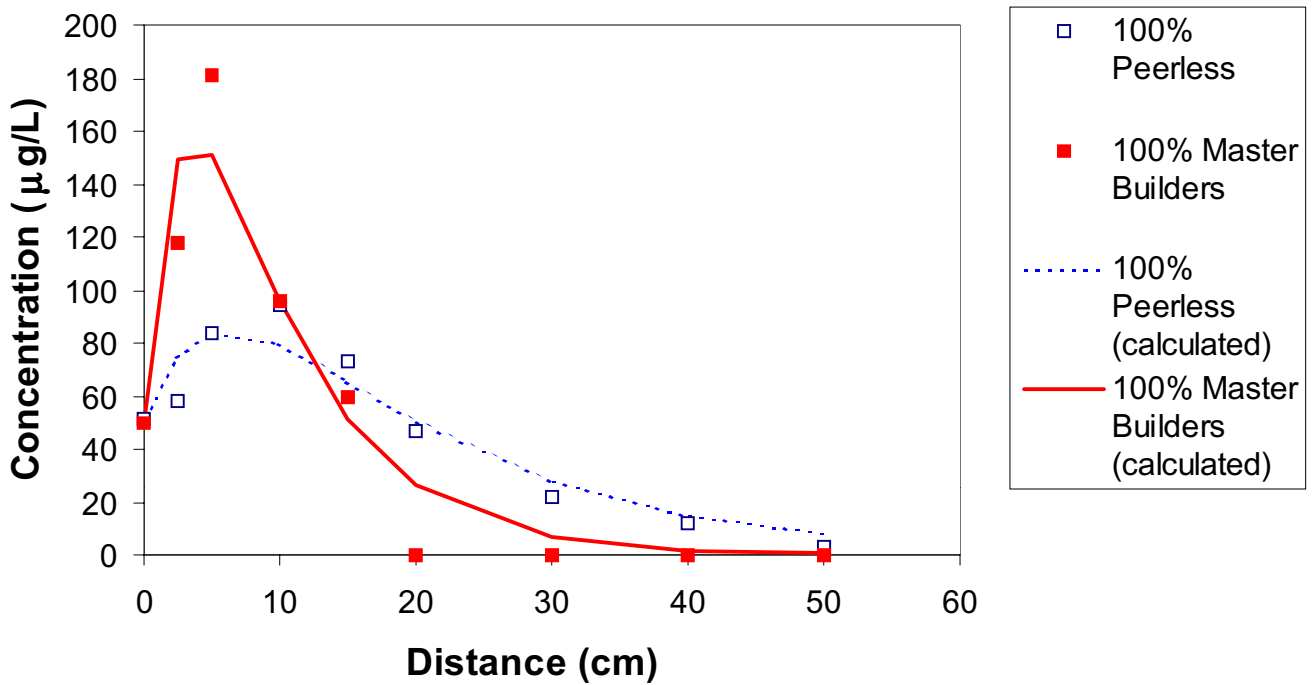


Figure 45. Experimental and calculated cDCE concentration profiles in column.

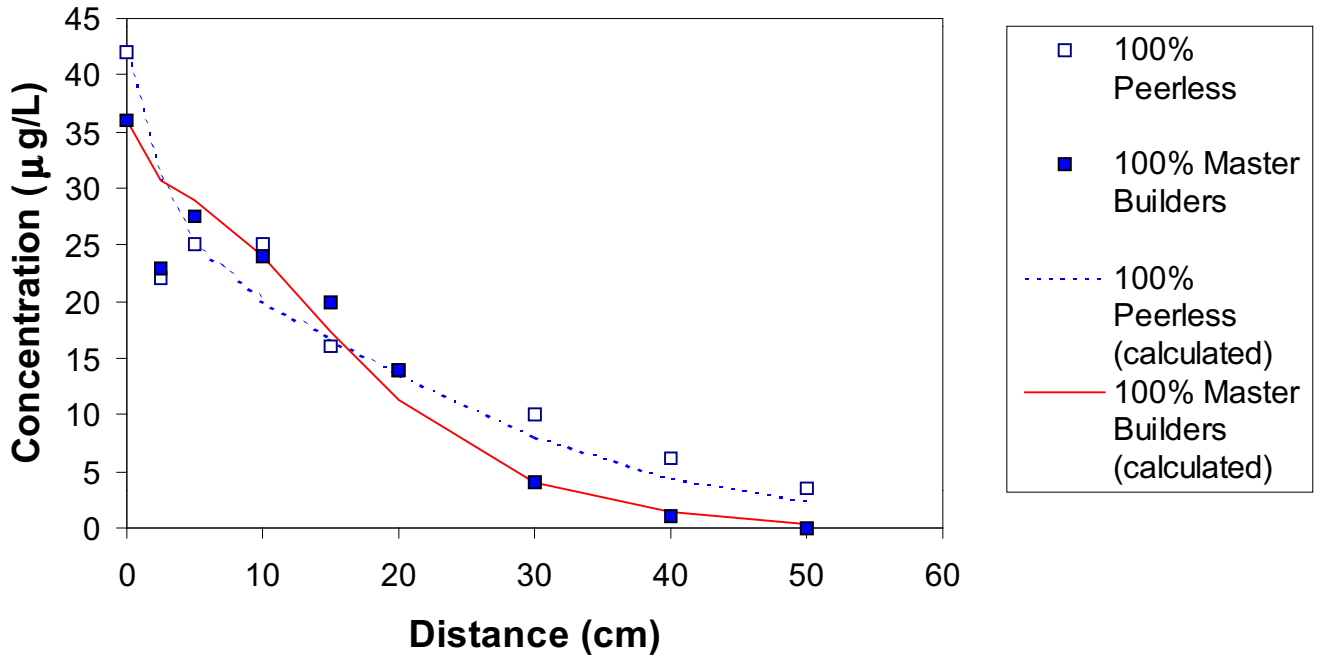
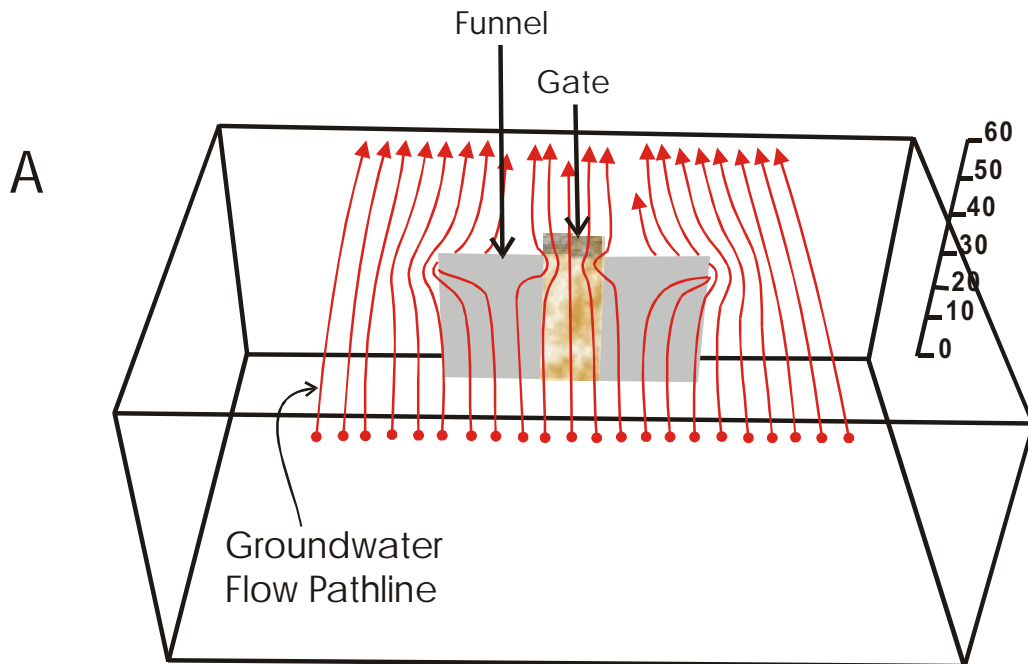
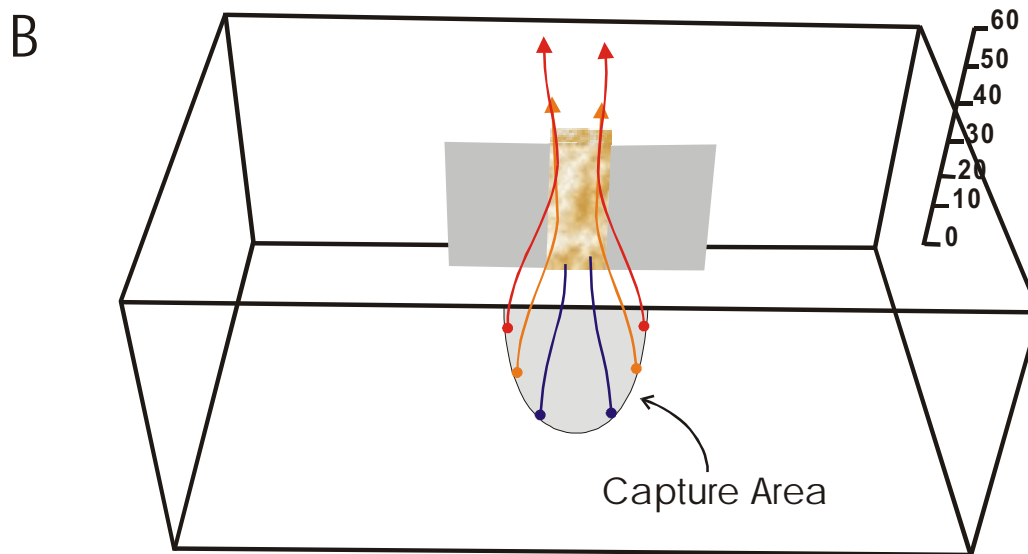


Figure 46. Experimental and calculated VC concentration profiles in column.



Groundwater flow is diverted both through and around the Gate by the Impermeable Funnel.



Groundwater within the Capture Area flows through the Gate zone.

Figure 47. (A) Groundwater flow divergence in vicinity of a Funnel-and-Gate, and (B) Capture area.

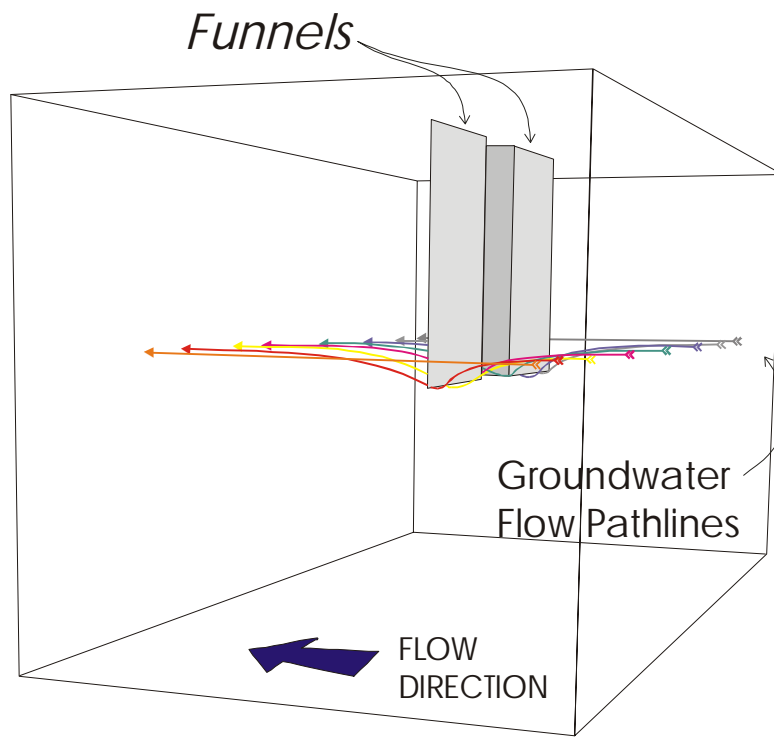


Figure 48. Vertical groundwater flow divergence around a Funnel-and-Gate.

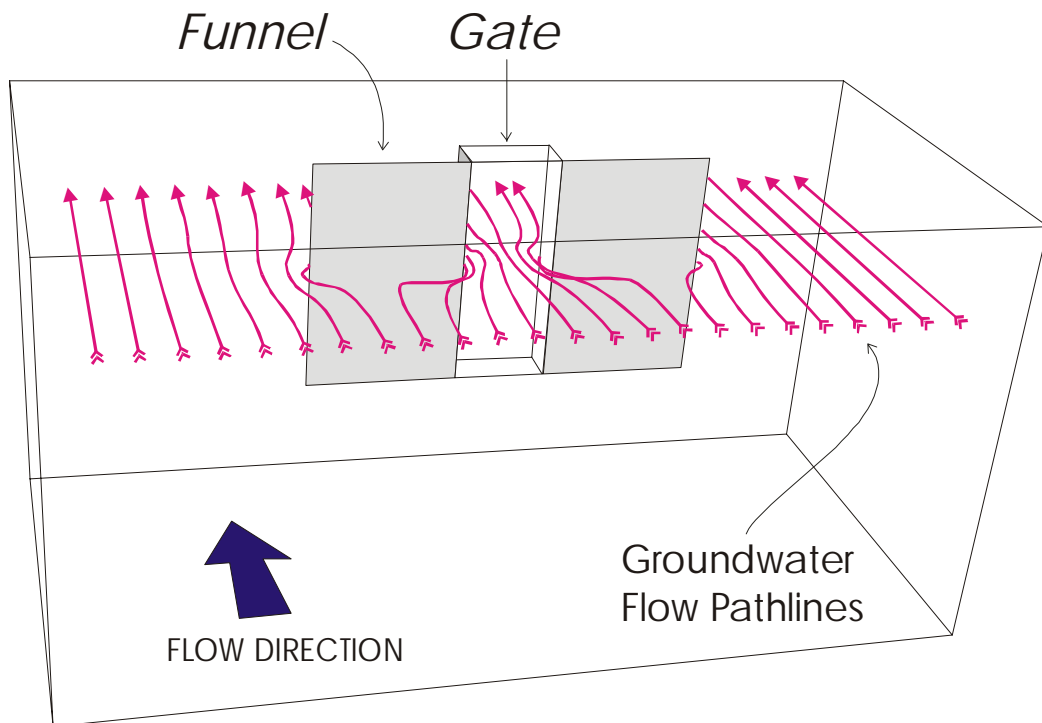


Figure 49. Horizontal groundwater flow divergence around a Funnel-and-Gate.

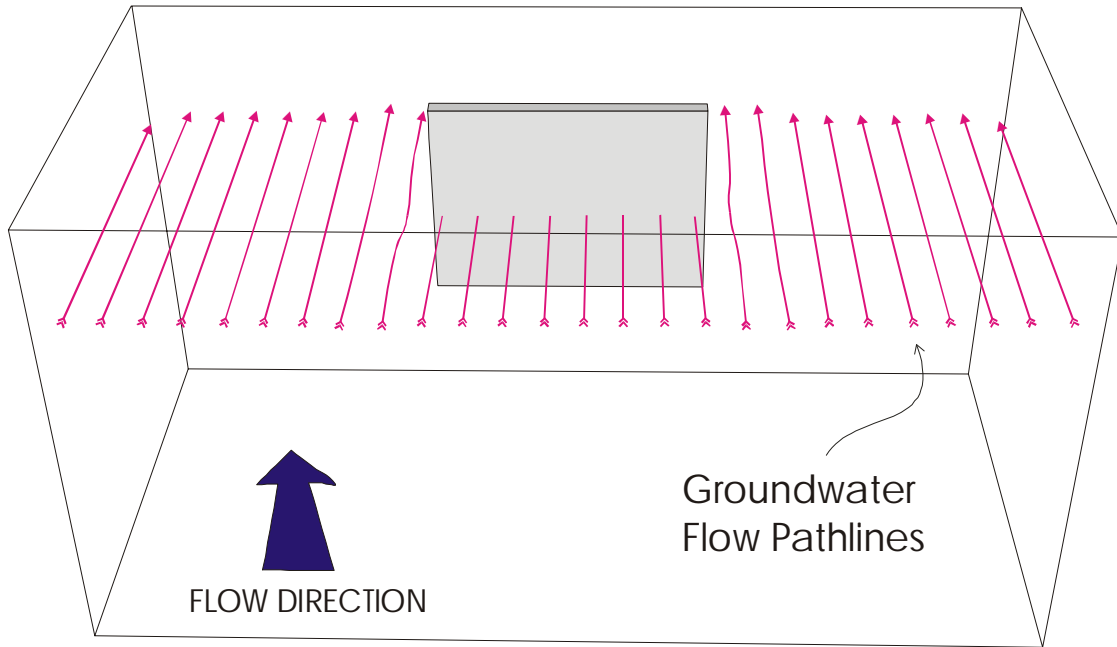


Figure 50. Groundwater flow divergence around a continuous wall.

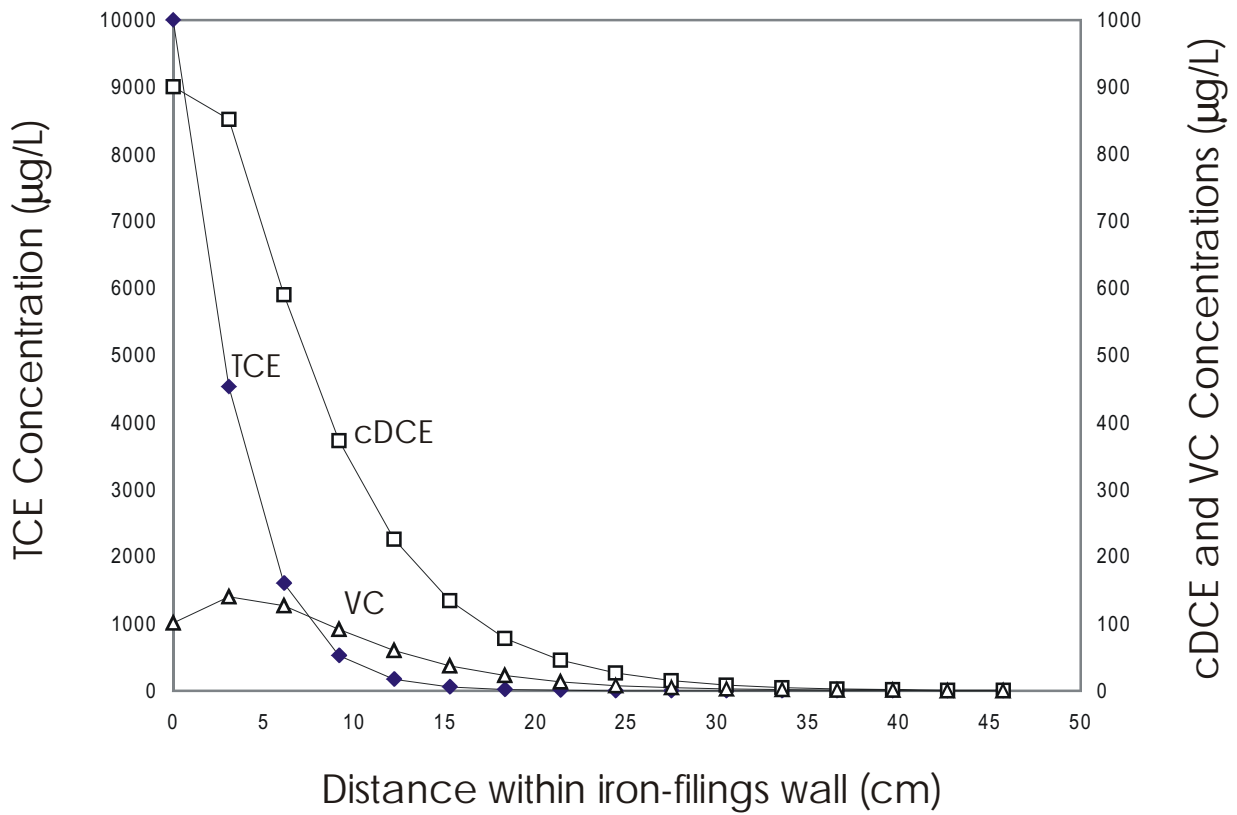
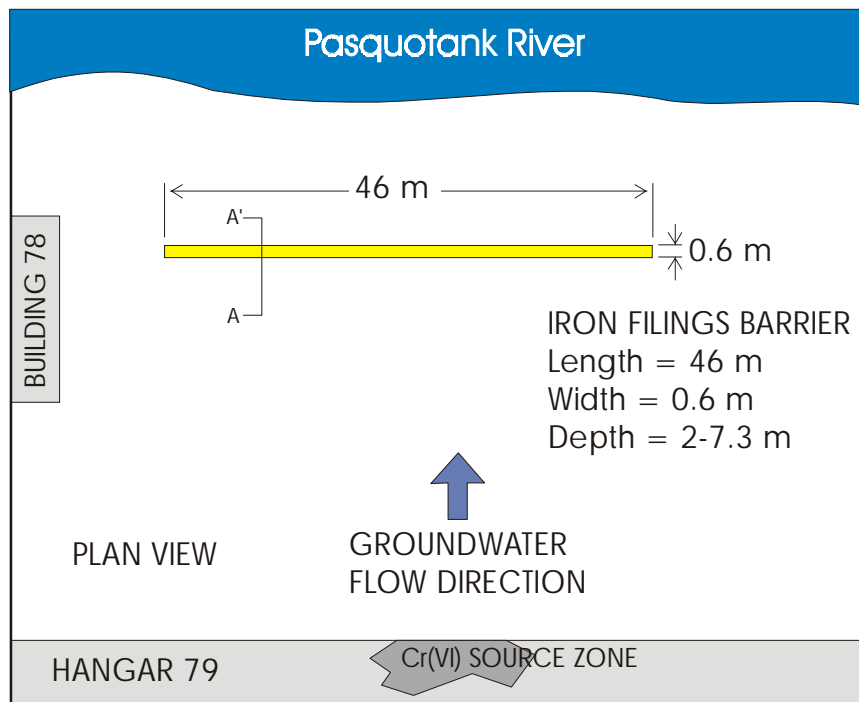


Figure 51. Predicted TCE, cDCE, and VC concentration profiles through the iron-filings wall.

(A)



(B)

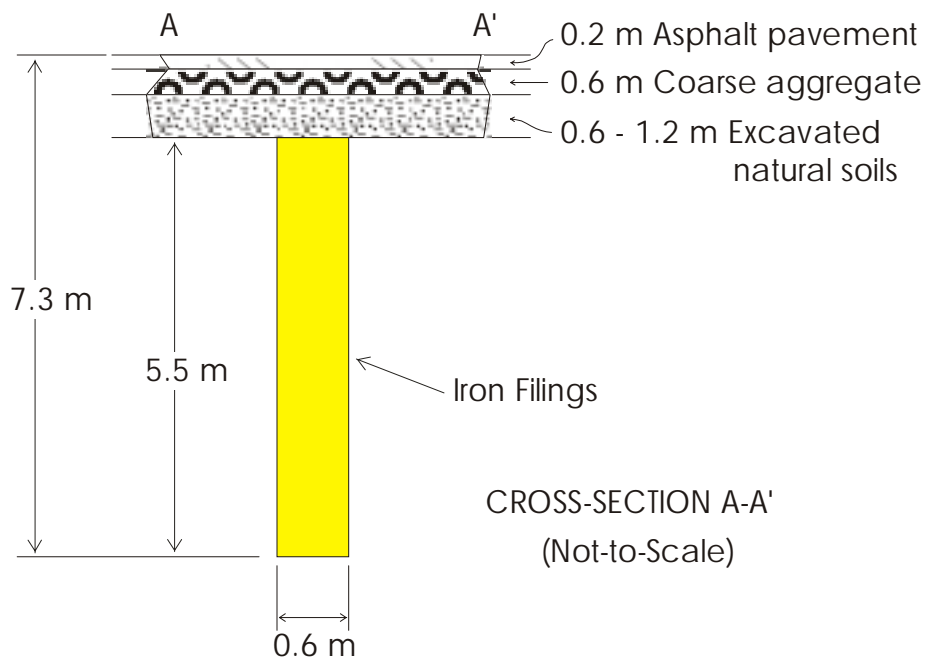


Figure 52. (a) Plan view, and (b) cross-sectional view of reactive barrier.



Figure 53. Peerless™ iron filings stored on site.



Figure 54. Plastic sheets laid down around trench for erosion control.



Figure 55. Trenching machine used to install the 7.3 m deep, 0.6 m wide granular iron barrier.



Figure 56. Excavated aquifer sediments on either side of the trench.



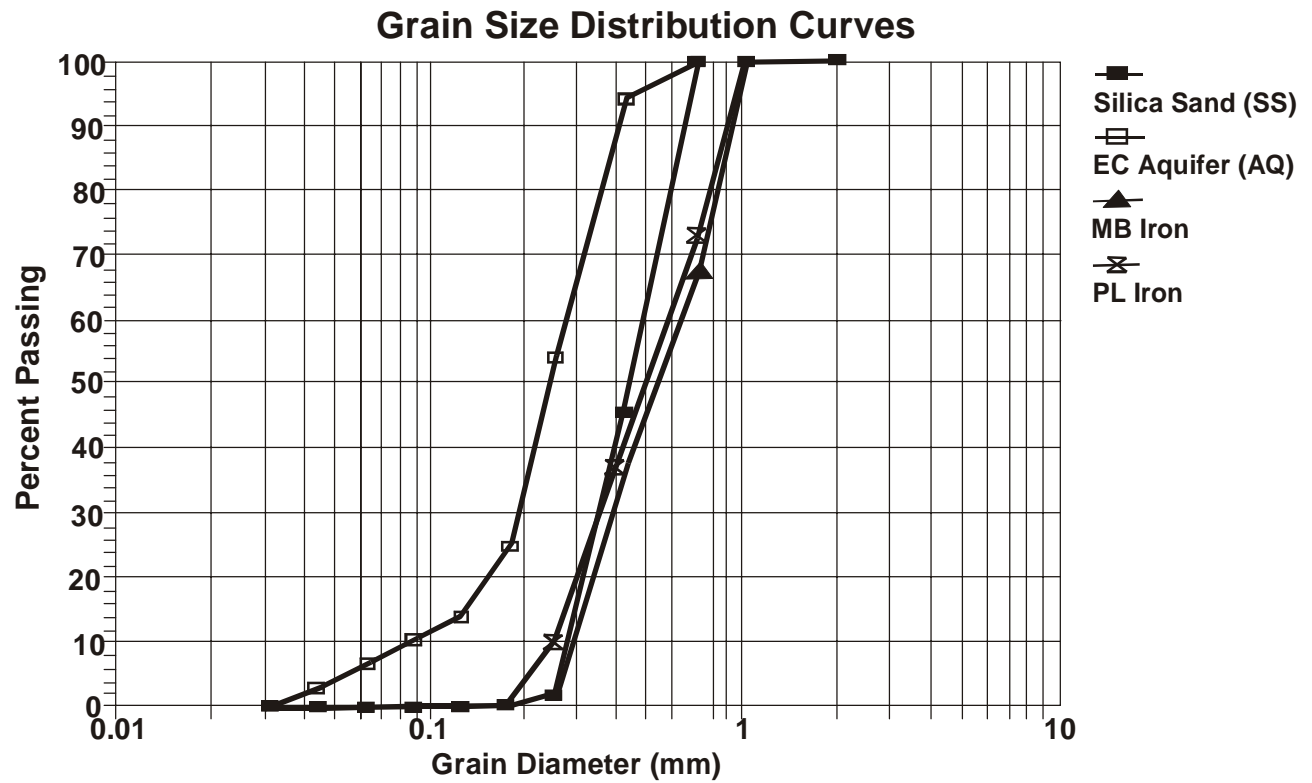
Figure 57. Picture showing collapse of concrete pavement on either side of the trench.

LIST OF APPENDICES

- Appendix A:** Grain size distribution curves
- Appendix B:** Elemental and TCLP analyses
- Appendix C:** Bromide tracer test data (lab columns)
- Appendix D:** Batch test inorganic data
- Appendix E:** Batch test mineral saturation indices
- Appendix F:** Reactive column organic data
- Appendix G:** Reactive column inorganic data
- Appendix H:** Reactive column mineral saturation indices
- Appendix I:** Analytical laboratory procedures

This page intentionally left "BLANK."

Appendix A: Grain size distribution curves



Appendix B: Elemental and TCLP analyses

Element	Master (MB)	Peerless (PL)	MDL
	GX-27		
	wt%	wt%	wt%
Al	0.0036	0.0019	0.00050
B	0.2910	0.1420	0.00025
Ba	0.0001	0.0002	0.00005
Be	0.0001	<	0.00005
Cd	0.0000	<	0.00010
Ca	1.0043	<	0.00025
Cr	0.1970	0.1700	0.00010
Co	0.0058	<	0.00045
Cu	0.2850	0.2500	0.00010
Fe	88.2000	82.7000	0.00025
Pb	0.0044	<	0.00100
Mg	0.0030	0.0013	0.00005
Mn	0.5060	0.5570	0.00005
V	0.0159	<	0.00010
Zn	0.0064	0.0073	0.00005
Ni	0.0577	0.0700	0.00030
P	0.0737	0.0750	0.00160
Ag	0.0004	<	0.00010
Sr	0.0000	<	0.00005
Na	0.0000	<	0.01000
Mo	0.0152	0.0210	0.00020
Ti	0.0149	0.0156	0.00005
Zr	0.0022	<	0.00010
S	0.1400	0.1100	0.01000
C	2.4717	3.2440	0.00100
Si	1.7400	2.3400	0.01000
Total %	95.0384	89.7052	

< = less than MDL

%Wt = ((mg/Kg)/1000000) *100

Appendix B: Elemental and TCLP analyses
Toxicity Characteristic Leaching Procedure (TCLP)

Client ID	MasterBuilder	Peerless	Leach Blank	Leach Blank	Regulatory
Volatiles (mg/L)					
Benzene	<0.05	<0.05	<0.05		0.05
Carbon Tetrachloride	<0.05	<0.05	<0.05		1.0
Chlorobenzene	<0.05	<0.05	<0.05		100
Chloroform	<0.05	<0.05	<0.05		6.0
Methyl Ethyl Ketone	<0.10	<0.10	<0.10		200
Tetrachloroethylene	<0.05	<0.05	<0.05		0.7
Trichloroethylene	<0.05	<0.05	<0.05		0.5
VinylChloride	<0.10	<0.10	<0.10		0.2
1,2-Dichloroethane	<0.05	<0.05	<0.05		0.5
1,1-Dichlorethylene	<0.05	<0.05	<0.05		0.7
Semi-Volatiles (mg/L)					
1,4-Dichlorobenzene	<0.04	<0.04		<0.04	7.5
Hexachloroethane	<0.04	<0.04		<0.04	3.0
Nitrobenzene	<0.04	<0.04		<0.04	2.0
Hexachlorbutadiene	<0.04	<0.04		<0.04	0.5
2,4,6-Trichlorophenol	<0.04	<0.04		<0.04	2.0
2,4,5-Trichlorophenol	<0.08	<0.08		<0.08	400
2,4-Dinitrotoluene	<0.04	<0.04		<0.04	0.13
Hexachlorobenzene	<0.04	<0.04		<0.04	0.13
Pentachlorophenol	<0.20	<0.20		<0.20	100
Total Cresols	<0.12	<0.12		<0.12	200
Pyridine	<0.04	<0.04		<0.04	5.0
Pesticides (mg/L)					
Chlordane	<0.01	<0.01		<0.01	0.03
Endrin	<0.001	<0.001		<0.001	0.02
Heptachlor	<0.0005	<0.0005		<0.0005	0.008
Heptachlor Epoxide	<0.0005	<0.0005		<0.0005	0.008
Lindane	<0.005	<0.005		<0.005	0.4
Methoxychlor	<0.005	<0.005		<0.005	10.0
Toxaphene	<0.025	<0.025		<0.025	0.5
Metals (mg/L)					
Antimony	<0.100	<0.100		<0.100	0.10
Arsenic	<0.200	<0.200		<0.200	0.20
Barium	1.07	0.431		0.281	0.20
Beryllium	<0.025	<0.025		<0.025	0.025
Cadmium	<0.025	<0.025		<0.025	0.025
Chromium	<0.100	<0.100		<0.100	0.10
Copper	<0.025	0.038		<0.025	0.025
Lead	<0.100	<0.100		<0.100	0.10
Mercury	<0.0002	<0.0002		<0.0002	0.0002
Nickel	<0.040	<0.040		<0.040	0.04
Selenium	<0.200	<0.200		<0.200	0.20
Silver	<0.025	<0.025		<0.025	0.025
Thallium	<0.100	<0.100		NA	0.10
Zinc	0.084	0.153		0.063	0.05

Appendix C: Bromide tracer test data (lab columns)

TABLE H-1. Bromide concentrations (mg/L) during tracer tests.

COLUMN 101					COLUMN 102					COLUMN 110			
Date analyzed					Date analyzed					Date analyzed			
S.N.	1	2	3	4	S.N.	1	2	3	4	S.N.	1	2	3
10	0				10	0.4				10	0.37		
20	0.38				20	0.48				20	0.53		
30	0				30	0.35				25		0.36	
40	1.28				40	0.58				30	11.5		0.4
44		12			45		8.63			33			0.41
46		25.9			50	30.2				35		1.67	
48		41.6			53		46.3			37			7.45
50	56.6	<i>L.F. (0.15)</i>			55		57.2			40	33.7		
55		75			57		63.5			42		55.1	
60	85.7				60	75.4				44		72.7	
66			88.1		64		<i>H.F.(0.24)</i>	75.4		46		79.7	
68				110	68		<i>L.F.(0.13)</i>	75.5		48		83.3	
70	83.8		98.2		69	80.6				50	87.1		
73				104	70			78.4		60	89.1		
75			89.3		72				82.2	70	92.5		
76				104	75		94.7			80		92.8	
77				104	78				82.4	90		92	
80	98.2				79			106		100		91.6	
90	98.2				80	110							
93				107	82				91.8				
97			112		85			91.9					
98	111	<i>L.F.(0.12)</i>			90	99							
103				102	100	98.8							
110	102	<i>New Pump</i>			110	103							
120	99.5	<i>New Pump</i>			115				91.1				
130	99.7	<i>New Pump</i>			120	110			97				
140	93.7	<i>New Pump</i>			130				96.8				
					139				100				
					140	119							
					150	101							
					160	102							

Column		101	102	110
Stock solution concentration	µg/L	104, 100	104, 100	93.8
Average flow rate	mL/min	0.19	0.16	0.17
Composition		100% MB	100% PL	52% PL/48% AQ
<i>(MB: Master Builders, PL: Peerless; AQ: Aquifer sediments)</i>				

COMMENTS

S.N. indicates Sample Number (samples were taken every 30 minutes)

L.F. indicates Low Flow rate **H.F.** indicates High Flow rate

Column 101: Low flow in S.N. 98, Pump stops and is replaced, New pumping rate slightly lower

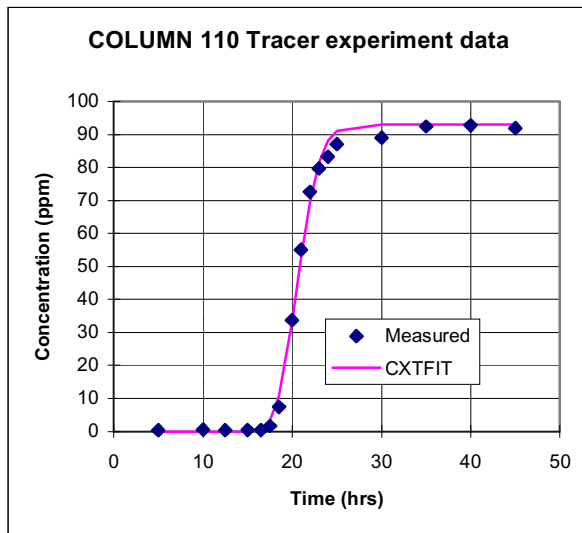
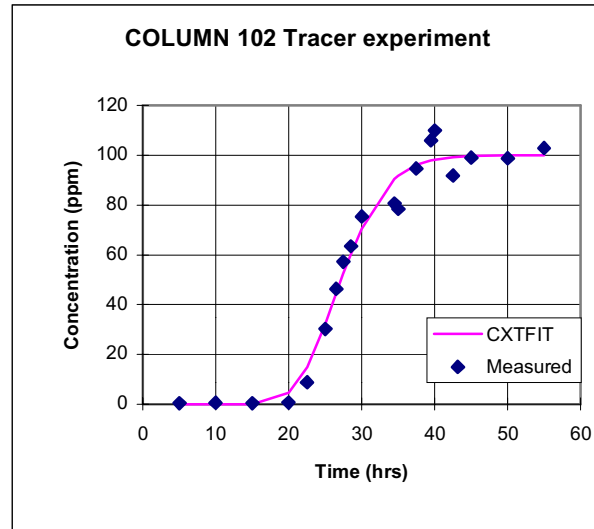
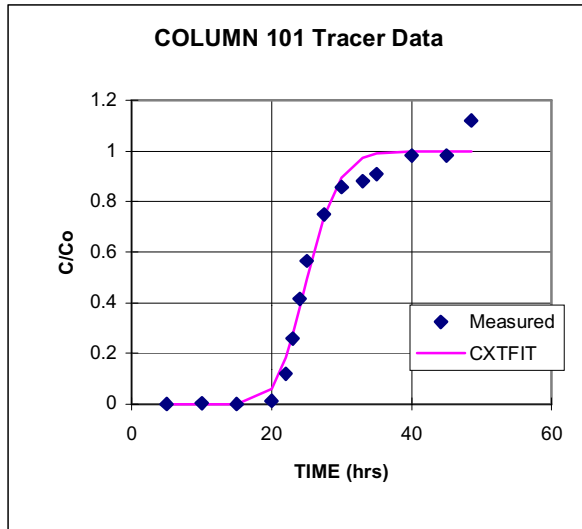
Column 102: No Flow in Samples 65, 66, 67

Date Analyzed: (1) 10/26/95; (2) 11/17/95; (3) 12/8/95; (4) 1/17/96

Appendix C: Bromide tracer test data (lab columns)

Bromide tracer results

Final Results (April 1996)



COLUMN	MATERIAL*
101	100% Master Builders (100 MB)
102	100% Peerless (100 PL)
110	48% Peerless/ (48 PL52AQ) 52% Aquifer material

* Master Builders™ and Peerless™ are Iron

RESULTS

	CASE 1		CASE 2		Calculated (see (1) below)		Measured results		
	V	D	D	R	porosity	Pore vol.	V	porosity	Pore vol.
column	[cm/hr]	[cm]	[cm]		[calc]	[mL]	[cm/hr]	[lab]	[mL]
101	1.98	1.03	1.15	1.11	0.51	288	2.20	0.45	254
102	1.81	1.51	1.66	1.09	0.47	264	1.97	0.43	245
110	2.41	0.51	0.58	1.13	0.37	211	2.73	0.33	189
	fixed R (R=1)		using lab velocity		calc. from CXTFIT Velocity		from effluent flux		

CASE 1: Finding unknowns (velocity, V, and dispersivity, D) assuming a known retardation of R=1.

CASE 2: Finding unknowns (dispersivity, D, and retardation, R) using lab. measured velocities

(1): Calculated porosity, and pore volume from CASE 1 velocity and lab. measured effluent flux.

Concentrations in mg/L analysed at U.W. Water Quality Lab

Time (h)	pH	Eh (mV)	CaCO ₃	Al	As	Ba	Ca	Cd	Co	Cr	Cr(VI)	Cu	Fe	K	Mg	Mn	Mo	Na	Ni	Pb	Si	Sr	Zn	Cl	SO ₄		
Composition: MB+SS																											
0	5.96	368	23.7	0.12	<0.5	0.09	27.7	<0.02	0.027	11.69	11.6	0.00	<0.05	<0.2	17.6	0.94	0.01	96.3	<0.01	<0.01	5.92	0.48	0.10	123	89.7		
0	5.92	551	43.4	0.03	<0.5	0.09	27.1	<0.02	0.03	11.45	11.4	0.01	<0.05	20.1	17.3	0.91	0.00	94.4	<0.01	0.01	5.84	0.48	0.10	126	88.3		
0.25	6.15	459	51.7	0.16	<0.5	0.07	32.7	<0.02	0.03	2.81	2.6	0.01	<0.05	<0.2	18.0	1.17	0.01	98.8	<0.01	<0.01	5.51	0.47	0.03	107	84		
0.5	6.47	188	92.6	0.16	<0.5	0.07	33.3	<0.02	0.04	0.02	0	0.01	15.39	<0.2	17.9	1.71	<0.01	97.6	<0.01	0.05	5.33	0.47	0.01	107	88.2		
1.5	7.11	34	138.4	0.15	<0.5	0.07	35.4	<0.02	0.05	0.01	0	0.01	42.43	15.76	18.3	2.51	<0.01	99.5	<0.01	<0.01	5.12	0.48	0.01	106	94.3		
3	7.5	-92	140.5	0.19	<0.5	0.08	36.6	<0.02	0.06	0.01	0	0.01	42.31	4.38	18.4	2.98	<0.01	100.4	<0.01	<0.01	4.49	0.49	0.00	107	93.1		
6	7.52	29	137.8	0.18	<0.5	0.09	38.4	<0.02	0.05	0.00	0	0.02	35.55	<0.2	18.4	2.88	<0.01	100.5	<0.01	0.02	3.93	0.51	0.00	112	85.1		
24.12	7.4	-378	100.2	0.08	<0.5	0.08	38.3	<0.02	0.06	0.01	0	0.02	6.39	<0.2	17.6	2.01	0.00	97.6	<0.01	<0.01	1.00	0.49	0.00	110	91.5		
Composition: Ada+SS																											
0	5.96	352	51.8	0.14	<0.5	0.08	26.9	<0.02	0.07	11.45	11.3	0.00	<0.05	<0.2	17.3	0.92	0.01	93.9	0.03	-0.03	5.77	0.47	0.09	122	90.1		
0.25	5.99	554	36.0	0.13	<0.5	0.07	29.7	<0.02	0.07	7.47	7.2	0.00	<0.05	<0.2	18.2	1.04	0.02	98.2	0.13	0.00	5.61	0.47	0.07	125	93.4		
0.5	6.09	116	47.0	0.12	<0.5	0.06	28.9	<0.02	0.06	3.37	3.3	0.02	<0.05	<0.2	17.9	1.11	0.01	96.9	0.25	0.00	5.28	0.44	0.04	106	92.3		
0.75	6.12	315	53.1	0.14	<0.5	0.06	28.6	<0.02	0.05	0.71	0.6	0.01	0.09	<0.2	17.6	1.21	0.04	95.6	0.34	0.02	4.95	0.44	0.01	118	89.4		
1.5	6.33	204	80.0	0.17	<0.5	0.06	29.5	<0.02	0.06	0.02	0	0.01	15.52	<0.2	18.3	1.76	0.05	98.4	0.66	0.06	4.80	0.45	0.01	101	87.6		
5.72	6.71	55	125.2	0.14	<0.5	0.06	29.7	<0.02	0.08	0.00	0	0.00	42.70	<0.2	17.9	2.33	0.16	97.0	1.27	<0.01	4.01	0.44	0.00	115	84.4		
23.85	7.04	34	134.3	0.21	<0.5	0.07	30.6	<0.02	0.12	0.00	0	0.01	42.14	<0.2	18.5	2.76	0.24	101.1	0.56	<0.01	2.35	0.47	0.00	130	99.9		
Composition: PL+SS																											
0	5.92	552	39.1	0.12	<0.5	0.08	28.0	<0.02	0.03	11.99	12.1	0.02	<0.05	<0.2	18.0	0.96	<0.01	101.6	<0.01	<0.01	6.14	0.49	0.10	130	88.6		
0.1	5.95	458	42.4	0.12	<0.5	0.08	29.6	<0.02	0.03	4.92	4.9	0.02	0.13	<0.2	18.5	1.22	<0.01	104.2	<0.01	<0.01	5.98	0.48	0.05	129	96.5		
0.75	6.44	159	94.7	0.14	<0.5	0.10	30.0	<0.02	0.08	0.02	0	0.01	31.43	<0.2	18.7	2.39	<0.01	106.9	<0.01	<0.01	6.10	0.48	0.01	128	95.6		
3	7.29	-266	155.5	0.07	<0.5	0.08	29.9	<0.02	0.13	0.00	0	0.00	63.84	<0.2	18.7	3.67	<0.01	107.4	<0.01	0.03	5.76	0.48	0.02	130	91.6		
23.92	7.45	-161	117.4	0.15	<0.5	0.08	29.5	<0.02	0.08	0.00	0	0.00	34.55	<0.2	18.3	3.66	<0.01	106.3	<0.01	0.02	1.88	0.48	0.00	131	90.3		
Composition: MB+AQ																											
0	6	611	45.9	0.11	<0.5	0.08	28.0	<0.02	<0.1	11.79	11.6	0.01	<0.05	8.991	17.3	0.96	0.04	101.1	<0.01	0.13	6.13	0.49	0.17	126	90.2		
0	6.03	630	25.0	0.06	<0.5	0.08	28.0	<0.02	<0.1	11.82	11.7	0.02	<0.05	10.39	17.4	0.96	0.03	101.1	0.01	0.22	6.14	0.49	0.16	124	95.1		
0.1	6.14	563	49.7	0.13	<0.5	0.10	30.6	<0.02	<0.1	7.17	7.4	0.02	<0.05	15.04	16.7	1.05	0.05	100.7	<0.01	0.08	5.86	0.46	0.11	125	97.5		
0.1	6.14	563	49.7	0.11	<0.5	0.10	30.5	<0.02	<0.1	7.11	7.2	0.02	<0.05	10.74	16.7	1.03	0.04	103.7	0.02	0.08	5.79	0.45	0.11	125	97.5		
0.27	6.26	608	62.3	0.09	<0.5	0.09	30.7	<0.02	<0.1	3.88	3.9	0.01	<0.05	10.28	16.5	1.20	0.00	105.9	<0.01	0.16	5.69	0.45	0.05	119	89.7		
0.42	6.3	418	67.0	0.05	<0.5	0.09	32.8	<0.02	<0.1	0.46	0.4	0.01	0.05	<10	17.0	1.48	0.02	112.3	<0.01	0.25	5.64	0.47	0.02	120	93.7		
0.75	6.46	184	79.2	0.06	<0.5	0.08	33.3	<0.02	<0.1	0.02	0	0.00	6.90	11.92	16.9	2.02	0.01	112.6	<0.01	0.26	5.47	0.47	0.01	122	91.2		
3	6.83	62	123.8	0.17	<0.5	0.07	36.3	<0.02	<0.1	0.00	0	0.01	20.98	11.56	17.7	2.98	0.03	112.5	<0.01	0.31	4.40	0.49	0.00	122	90.1		
6	7.48	23	124.5	0.09	<0.5	0.06	38.6	<0.02	<0.1	0.00	0	0.01	16.20	11.96	17.7	2.88	<0.01	113.7	<0.01	0.25	3.66	0.49	0.02	125	87.5		
24	7.87	-47	121.3	0.13	<0.5	0.04	42.2	<0.02	<0.1	0.00	0	0.01	1.21	12.5	18.4	1.59	0.02	115.0	<0.01	0.32	1.51	0.50	0.00	121	76.5		
24	7.87	-47	121.3	0.11	<0.5	0.04	41.8	<0.02	<0.1	0.008	0	0.00	1.20	12.97	18.2	1.58	0.05	114.4	<0.01	0.21	1.52	0.49	0.00	121	76.5		

Elizabeth City batch experiments
 Saturation indices calculated by MINTEQA2
 Based on UW Water Quality Lab data

Composition: MB+SS

Time (h)	Ferrihydrite	Goethite	Cr(OH) ₃ (a)	Cr(OH) ₃ (c)	Calcite	Dolomite	Siderite (d)	Amakinite	Aragonite	Rhodochrosite	Quartz	SiO ₂
0	-0.844	4.866	-0.521	-3.060	-2.690	-5.280	-4.396	-8.384	-2.844	-2.370	0.379	-0.603
0	0.087	5.797	-0.867	-3.407	-2.479	-4.856	-6.263	-10.554	-2.633	-2.170	0.374	-0.607
0.25	0.960	6.670	2.397	-0.143	-2.090	-4.143	-4.197	-8.332	-2.245	-1.757	0.347	-0.634
0.5	0.794	6.504	0.566	-1.973	-1.526	-3.025	-0.106	-4.166	-1.680	-1.053	0.333	-0.648
1.5	0.477	6.187	0.920	-1.619	-0.714	-1.417	1.099	-2.480	-0.868	-0.133	0.316	-0.665
3	-0.527	5.183	0.816	-1.724	-0.307	-0.615	1.479	-1.712	-0.461	0.302	0.260	-0.722
6	1.537	7.247	-0.219	-2.759	-0.268	-0.558	1.421	-1.745	-0.422	0.303	0.199	-0.782
24.1	-8.610	-2.899	0.644	-1.896	-0.459	-0.957	-1.616	-4.786	-0.613	-0.021	-0.395	-1.376

Composition: Ada+SS

0	-1.110	4.600	-0.521	-3.061	-2.366	-4.626	-4.048	-8.377	-2.520	-2.051	0.368	-0.614
0.25	0.153	5.863	2.608	0.069	-2.453	-4.821	-6.471	-10.610	-2.607	-2.122	0.357	-0.625
0.5	-4.742	0.968	2.398	-0.142	-2.246	-4.404	-3.932	-8.087	-2.401	-1.880	0.328	-0.653
0.75	-0.279	5.431	1.760	-0.780	-2.169	-4.252	-2.893	-7.070	-2.323	-1.763	0.301	-0.680
1.5	0.660	6.370	0.417	-2.122	-1.779	-3.468	-0.298	-4.435	-1.933	-1.234	0.288	-0.693
5.7	-0.344	5.366	-0.210	-2.750	-1.225	-2.371	0.677	-3.262	-1.379	-0.581	0.210	-0.771
23.85	0.265	5.975	-0.444	-2.984	-0.861	-1.644	1.015	-2.622	-1.015	-0.171	-0.021	-1.002

Composition: PL+SS

0	0.087	5.797	-0.578	-3.117	-2.511	-4.916	-6.326	-10.571	-2.665	-2.191	0.396	-0.586
0.1	1.138	6.848	2.37	-0.169	-2.426	-4.759	-3.687	-7.937	-2.580	-2.027	0.383	-0.598
0.75	0.509	6.219	0.657	-1.882	-1.608	-3.125	0.167	-3.924	-1.763	-0.944	0.391	-0.590
3	-4.154	1.556	-0.006	-2.545	-0.52	-0.946	1.308	-2.143	-0.674	0.268	0.367	-0.614
23.9	-1.934	3.776	0.535	-2.004	-0.52	-0.951	1.283	-1.884	-0.675	0.289	-0.119	-1.100

Composition: MB+AQ

0	0.164	5.874	-0.468	-3.007	-2.363	-4.637	-7.352	-11.587	-2.517	-2.046	0.396	-0.586
0	0.191	5.901	-0.428	-2.968	-2.597	-5.103	-7.975	-11.915	-2.751	-2.271	0.396	-0.586
0.1	0.289	5.999	2.783	0.244	-2.155	-4.276	-6.650	-10.778	-2.310	-1.839	0.374	-0.607
0.1	0.289	5.999	2.78	0.24	-2.157	-4.278	-6.650	-10.778	-2.311	-1.847	0.370	-0.611
0.27	0.395	6.105	2.03	-0.509	-1.934	-3.84	-7.458	-11.564	-2.089	-1.566	0.361	-0.620
0.42	1.049	6.759	1.789	-0.75	-1.837	-3.663	-3.593	-7.689	-1.991	-1.409	0.359	-0.622
0.75	0.35	6.06	0.525	-2.015	-1.604	-3.205	-0.527	-4.532	-1.758	-1.053	0.345	-0.636
3	-0.176	5.534	-0.591	-3.13	-1.018	-2.05	0.486	-3.334	-1.172	-0.358	0.249	-0.732
6	0.979	6.689	0.467	-2.073	-0.341	-0.723	1.011	-2.160	-0.495	0.239	0.169	-0.812
24	-0.197	5.513	-0.135	-2.675	0.085	0.108	0.249	-2.524	-0.069	0.306	-0.214	-1.195
24	-0.201	5.509	0.979	-1.561	0.082	0.099	0.246		-0.073	0.304	-0.214	-1.195

These calculations assume that the t=0 Cr composition is dominantly Cr(VI) and that the Cr(III) concentration (0.01 mg/L) is one half the analytical detection limit.

Notes: (c) = crystalline (a) = amorphous (d) = disordered, or freshly precipitated

Appendix F: Reactive column organic data

REACTIVE COLUMN
99
50MBSSAQ

Column Composition:

50 % Granular Iron - MasterBuilder
25 % Elizabeth City Aquifer Material
25 % Silica Sand

Pore Volume (PV):

201 mL

Porosity:

0.35

Flow Velocity 1 (FV1):

2.2 ft/day (68 cm/day)

Residence Time (FV1):

17.7 hr

		Distance Along Column (ft)									
		0.00	0.08	0.16	0.33	0.50	0.66	1.00	1.31	1.64	
	PV	RN	Influent	Organic Concentration ($\mu\text{g/L}$)							Effluent
TCE											
FV1	6.8	a	1553	888	136	14	nd	nd	nd	nd	nd
	12.4	a	1464	992	256	14	nd	nd	nd	nd	nd
	20.3	b	1588	1104	383	10	nd	nd	nd	nd	nd
	30.2	b	1795	1160	673	46	nd	nd	nd	nd	nd
	38.2	b	1393	1048	446	35	nd	nd	nd	nd	nd
	45.3	c	1580	1090	460	11	nd	nd	nd	nd	nd
PCE											
FV1	6.8	a	1.6	0.9	nd	nd	nd	nd	nd	0.3	2.2
	12.4	a	1.8	nd	nd	nd	nd	nd	nd	8.6	2.4
	20.3	b	2.4	3.1	2.0	nd	nd	nd	nd	nd	3.0
	30.2	b	2.3	4.3	4.1	2.8	nd	nd	nd	2.9	4.4
	38.2	b	2.8	4.3	3.7	2.9	nd	nd	nd	nd	nd
	45.3	c	1.7	4.2	3.6	1.7	nd	nd	nd	nd	nd
TCM											
FV1	6.8	a	25	13	4.1	0.2	nd	nd	nd	nd	nd
	12.4	a	21	15	6.5	0.4	nd	nd	nd	nd	nd
	20.3	b	22	16	6.4	2.4	nd	nd	nd	nd	nd
	30.2	b	26	17	11	4.2	0.4	nd	nd	nd	nd
	38.2	b	18	14	8.1	2.9	nd	nd	nd	nd	nd
	45.3	c	18	11	6.0	2.6	1.0	nd	nd	nd	nd
cDCE											
FV1	8.1	a	61	167	221	204	14	nd	nd	nd	nd
	16.2	b	58	113	208	198	104	83	nd	nd	nd
	18.9	b	69	122	136	222	173	99	8.2	nd	nd
	25.9	b	55	68	101	155	134	155	64	4.7	nd
	39.5	c	50	79	103	145	132	112	103	50	41
	47.7	c	70	80	112	137	162	189	124	90	70

nd = not detected

RN = reservoir number

Appendix F: Reactive column organic data

REACTIVE COLUMN 99 50MBSSAQ	Column Composition: Pore Volume (PV): Porosity: Flow Velocity 1 (FV1): Residence Time (FV1):	50 % Granular Iron - MasterBuilder 25 % Elizabeth City Aquifer Material 25 % Silica Sand 201 mL 0.35 2.2 ft/day (68 cm/day) 17.7 hr
-----------------------------------	--	---

		Distance Along Column (ft)										
		0.00	0.08	0.16	0.33	0.50	0.66	1.00	1.31	1.64		
	PV	RN	Influent	Organic Concentration (µg/L)								Effluent
iDCE												
FV1	8.1	a	1.2	0.2	nd							
	16.2	b	2.1	1.8	1.1	nd	nd	nd	nd	nd	nd	
	18.9	b	1.9	1.5	0.9	nd	nd	nd	nd	nd	nd	
	25.9	b	nd	nd	nd	nd	nd	nd	nd	nd	nd	
	39.5	c	1.7	1.7	nd							
	47.7	c	1.2	0.8	nd							
VC												
FV1	8.1	a	17	15	15	13	13	12	3.0	0.3	nd	
	16.2	b	41	36	34	40	27	29	19	11	4.5	
	18.9	b	39	34	31	31	31	28	22	10	7.3	
	25.9	b	38	32	26	29	24	26	20	17	nd	
	39.5	c	28	24	25	22	24	19	12	7.4	9.2	
	47.7	c	43	32	43	50	39	34	25	19	16	
pH Along Column												
pH												
FV1	1.2	a	6.9	8.0	9.0	9.1	9.2	9.2	9.0	8.8	9.0	
	10.8	a	7.8	8.6	8.3	9.3	9.3	9.4	9.4	9.4	9.5	
	17.6	b	6.5	7.4	8.1	8.9	9.2	9.2	9.2	9.2	9.0	
	37.1	b	7.0	8.9	9.1	9.4	9.3	9.2	9.3	9.0	9.3	
	39.8	c	6.3	7.2	9.0	9.3	9.3	9.2	9.3	9.2	9.3	
Redox Potential Along Column (mV)												
Eh												
FV1	1.2	a	386	-47	-139	-157	-168	-205	-278	-269	-38	
	10.8	a	350	-168	-191	-231	-218	-229	-260	-281	274	
	17.6	b	369	-144	-16	-132	-149	-126	-216	-150	-157	
	37.1	b	275	218	317	-26	-44	-63	-67	61	294	
	39.8	c	354	-203	-217	-256	-217	-140	-275	-242	-42	

nd = not detected
RN = reservoir number

Appendix F: Reactive column organic data

REACTIVE COLUMN 100 50MBSS	Column Composition: Pore Volume (PV): Porosity: Flow Velocity I (FV1): Residence Time (FV1):	50 % Granular Iron - MasterBuilder 50 % Silica Sand 233 mL 0.41 1.8 ft/day (55 cm/day) 21.6 hr
----------------------------------	--	---

Distance Along Column (ft)											
			0.00	0.08	0.16	0.33	0.50	0.66	1.00	1.31	1.64
	PV	RN	Influent	Organic Concentration (µg/L)							Effluent
TCE											
FV1	4.2	a	1584	835	328	13	0.7	nd	35	nd	7.9
	10.7	a	1671	899	538	85	4.4	1.0	14	nd	7.6
	18.3	a	1538	1185	798	172	8.2	nd	18	nd	5.6
	26.4	b	1830	846	634	197	31	nd	15	nd	nd
	33.9	b	1621	1246	943	260	30	2.3	13	nd	1.9
	42.9	b	1825	1250	835	204	16	nd	nd	nd	nd
PCE											
FV1	4.2	a	2.2	11.0	0.9	nd	nd	nd	nd	nd	nd
	10.7	a	1.6	6.3	0.6	nd	nd	nd	nd	nd	0.4
	18.3	a	1.8	11.0	0.9	0.3	nd	nd	nd	nd	nd
	26.4	b	2.7	2.9	nd						
	33.9	b	1.6	2.3	1.0	nd	nd	nd	nd	nd	nd
	42.9	b	1.6	3.5	1.5	nd	nd	nd	nd	nd	nd
TCM											
FV1	4.2	a	20	11	8.0	1.7	0.4	nd	nd	nd	0.4
	10.7	a	20	12	11	5.9	1.8	0.5	nd	nd	nd
	18.3	a	23	15	13	5.9	2.8	1.2	nd	nd	nd
	26.4	b	23	8.0	6.0	3.5	3.5	1.8	nd	nd	nd
	33.9	b	22	15	8.5	4.0	2.6	nd	nd	nd	nd
	42.9	b	19	16	7.8	4.1	1.8	nd	nd	nd	nd
cDCE											
FV1	7.2	a	62	96	209	251	167	134	8.2	nd	nd
	12.8	a	60	80	108	173	205	163	119	69	12
	19.4	a	61	37	154	170	204	187	204	168	137
	27.5	b	46	69	96	136	146	156	127	98	62
	38.4	b	51	51	95	140	152	152	183	132	122

nd = not detected
RN = reservoir number

Appendix F: Reactive column organic data

REACTIVE COLUMN 100 50MBSS	Column Composition: Pore Volume (PV): Porosity: Flow Velocity I (FV1): Residence Time (FV1):	50 % Granular Iron - MasterBuilder 50 % Silica Sand 233 mL 0.41 1.8 ft/day (55 cm/day) 21.6 hr
----------------------------------	--	---

			Distance Along Column (ft)											
			0.00	0.08	0.16	0.33	0.50	0.66	1.00	1.31	1.64			
tDCE	PV	RN	Influent	Organic Concentration (µg/L)								Effluent		
FV1	7.2	a	2.0	1.0	1.0	nd	nd							
	12.8	a	2.0	1.1	1.0	0.4	nd	nd	nd	nd	nd	nd	nd	
	19.4	a	0.9	1.1	0.9	0.4	nd	nd	nd	nd	nd	nd	nd	
	27.5	b	1.7	1.5	1.4	0.7	0.2	0.1	nd	nd	nd	nd	nd	
	38.4	b	nd	nd	nd	nd	nd	nd	nd	nd	nd	nd	nd	
	49.8	c	1.3	1.9	0.4	0.4	nd	nd	nd	nd	nd	nd	nd	
VC	7.2	a	32	22	29	30	25	24	20	16	12			
	12.8	a	37	20	32	28	29	24	23	22	26			
	19.4	a	15	20	17	17	19	18	16	17	16			
	27.5	b	37	27	28	27	31	32	28	27	20			
	38.4	b	40	26	28	27	28	24	24	21	21			
	49.8	c	35	28	14	28	29	30	21	20	20			
			pH Along Column											
FV1	5.1	a	6.5	7.8	8.4	9.0	9.1	9.0	8.5	8.6	9.3			
	13.8	a	6.6	7.9	8.7	9.2	9.3	9.3	9.4	9.4	9.3			
	21.8	a	7.3	9.0	9.2	9.4	9.3	9.4	9.4	9.4	9.5			
	29.8	b	6.5	7.5	7.8	8.7	8.9	9.0	9.2	9.2	9.3			
	44.0	b	7.0	8.8	9.1	9.2	9.3	9.2	9.2	9.2	9.3			
			Redox Potential Along Column (mV)											
FV1	5.1	a	344	-77	-218	-204	-221	-223	-197	-171	82			
	13.8	a	371	-120	-121	-175	-152	-206	-228	-310	28			
	21.8	a	354	9	65	-187	-265	-250	-201	-244	229			
	29.8	b	360	31	-9	-207	-200	-239	-309	-279	-181			
	44.0	b	360	159	85	129	-7	-103	-201	-175	156			

nd = not detected
RN = reservoir number

Appendix F: Reactive column organic data

REACTIVE COLUMN 101 100MB	Column Composition: Pore Volume (PV): Porosity: Flow Velocity 1 (FV1): Residence Time (FV1): Flow Velocity 2 (FV2): Residence Time (FV2):	100 % Granular Iron Master Builders 254 mL 0.45 1.4 ft/day (43 cm/day) 27.7 hr 0.8 ft/day (24 cm/day) 50 hr
---------------------------------	---	--

		Distance Along Column (ft)										
		0.00	0.08	0.16	0.33	0.50	0.66	1.00	1.31	1.64		
	PV	RN	Influent	Organic Concentration (µg/L)								Effluent
TCE												
FV1	4.3	a	1697	1.2	nd	nd	nd	nd	nd	nd	nd	nd
	10.2	a	1634	177	2.6	8.5	nd	nd	nd	nd	nd	nd
	16.6	a	1541	378	48	3.7	nd	nd	nd	nd	nd	nd
	22.9	b	1691	649	6.8	5.9	nd	nd	nd	nd	nd	nd
	29.1	b	1596	602	16	2.9	nd	nd	nd	nd	nd	nd
	35.1	b	1825	857	78	nd	nd	nd	nd	nd	nd	nd
FV2	51.7	c	1288	713	95	1.4	nd	nd	nd	nd	nd	nd
	57.9	d	1462	848	212	nd	nd	nd	nd	nd	nd	nd
	61.4	d	1295	386	265	nd	nd	nd	nd	nd	nd	nd
	64.9	d	1214	975	465	nd	nd	nd	nd	nd	nd	nd
	68.2	d	1227	1018	691	1.2	nd	nd	nd	nd	nd	nd
	71.4	d	1069	1016	746	2.4	nd	nd	nd	nd	nd	nd
	74.7	d	861	791	674	1.0	nd	nd	nd	nd	nd	nd
	77.4	e	1734	1184	890	0.8	nd	nd	nd	nd	nd	nd
	80.3	e	1436	1203	1019	6.2	nd	nd	nd	nd	nd	nd
	84.5	e	1309	1116	904	46	nd	nd	nd	nd	nd	nd
PCE												
FV1	4.3	a	1.6	nd	nd	nd	nd	nd	nd	nd	nd	nd
	10.2	a	1.6	0.4	2.0	2.4	nd	nd	nd	nd	nd	nd
	16.6	a	1.8	0.7	1.5	1.9	nd	nd	nd	nd	nd	nd
	22.9	b	2.7	nd	11.5	5.3	nd	nd	nd	nd	nd	nd
	29.1	b	1.6	0.6	7.7	0.4	nd	nd	nd	nd	nd	nd
	31.5	b	2.1	1.1	1.0	nd	nd	nd	nd	nd	nd	nd
FV2	51.7	c	2.8	nd	nd	nd	nd	nd	nd	nd	nd	nd
	57.9	d	2.2	0.7	0.5	nd	nd	nd	nd	nd	nd	nd
	61.4	d	1.4	nd	nd	nd	nd	nd	nd	nd	nd	nd
	64.9	d	1.3	1.2	nd	nd	nd	nd	nd	nd	nd	nd
	68.2	d	1.4	1.4	1.4	0.1	nd	nd	nd	nd	nd	nd
	71.4	d	1.3	1.4	1.3	nd	nd	nd	nd	nd	nd	nd
	74.7	d	1.1	1.2	1.2	0.5	nd	nd	nd	nd	nd	nd
	77.4	e	1.5	1.0	1.0	nd	nd	nd	nd	nd	nd	nd
	80.3	e	1.2	1.3	1.7	nd	nd	nd	nd	nd	nd	nd
	84.5	e	1.0	1.0	nd	nd	nd	nd	nd	nd	nd	nd

nd = not detected
RN = reservoir number

Appendix F: Reactive column organic data

REACTIVE COLUMN
101
100MB

Column Composition: 100 % Granular Iron
Master Builders
Pore Volume (PV): 254 mL
Porosity: 0.45
Flow Velocity 1 (FV1): 1.4 ft/day (43 cm/day)
Residence Time (FV1): 27.7 hr
Flow Velocity 2 (FV2): 0.8 ft/day (24 cm/day)
Residence Time (FV2): 50 hr

		Distance Along Column (ft)									
		0.00	0.08	0.16	0.33	0.50	0.66	1.00	1.31	1.64	
	PV	RN	Influent	Organic Concentration (µg/L)							Effluent
TCM FV1	4.3	a	20	1.7	0.2	nd	nd	nd	nd	nd	nd
	10.2	a	23	7.0	nd						
	16.6	a	22	8.0	0.8	nd	nd	nd	nd	nd	nd
	22.9	b	22	11.0	1.9	nd	nd	nd	nd	nd	nd
	29.1	b	20	7.4	1.9	nd	nd	nd	nd	nd	nd
	35.1	b	19	9.3	3.3	nd	nd	nd	nd	nd	nd
FV2	51.7	c	20	9.4	3.3	nd	nd	nd	nd	nd	nd
	57.9	d	23	11	4.6	nd	nd	nd	nd	nd	nd
	61.4	d	24	5.7	4.4	nd	nd	nd	nd	nd	nd
	64.9	d	19	15	6.4	nd	nd	nd	nd	nd	nd
	68.2	d	22	18	9.2	nd	nd	nd	nd	nd	nd
	71.4	d	22	20	11	nd	nd	nd	nd	nd	nd
	74.7	d	19	16	12	1.0	nd	nd	nd	nd	nd
	77.4	e	28	17	6.9	1.3	nd	nd	nd	nd	nd
	80.4	e	23	19	12	1.8	nd	nd	nd	nd	nd
84.5	e	23	19	12	2.8	nd	nd	nd	nd	nd	
cDCE FV1	7.1	a	62	243	209	nd	nd	nd	nd	nd	nd
	12.1	a	68	216	242	2.4	nd	nd	nd	nd	nd
	17.4	a	68	204	256	111	nd	nd	nd	nd	nd
	23.7	b	59	127	156	107	37	nd	nd	nd	nd
	32.4	b	51	112	228	183	81	22	nd	nd	nd
	39.0	c	51	118	182	139	100	60	nd	nd	nd
FV2	53.7	c	58	53	130	130	88	53	3	nd	nd
	55.1	c	56	62	118	101	73	45	nd	nd	nd
	58.8	d	67	73	118	84	78	53	3.5	nd	nd
	62.3	d	48	57	145	140	67	43	5.8	nd	nd
	65.7	d	61	56	129	142	57	51	7.8	nd	nd
	69.0	d	39	81	47	73	49	34	6.4	nd	nd
	72.0	d	46	43	56	83	53	30	5.1	nd	nd
	75.7	d	76	61	74	144	81	53	5.6	nd	nd
	78.7	e	65	63	59	101	59	35	7.4	nd	nd

Appendix F: Reactive column organic data

REACTIVE COLUMN
101
100MB

Column Composition: 100 % Granular Iron
Master Builders
Pore Volume (PV): 254 mL
Porosity: 0.45
Flow Velocity 1 (FV1): 1.4 ft/day (43 cm/day)
Residence Time (FV1): 27.7 hr
Flow Velocity 2 (FV2): 0.8 ft/day (24 cm/day)
Residence Time (FV2): 50 hr

			Distance Along Column (ft)								
			0.00	0.08	0.16	0.33	0.50	0.66	1.00	1.31	1.64
	PV	RN	Influent	Organic Concentration (µg/L)							Effluent
tDCE FV1	7.1	a	2.0	nd	nd	nd	nd	nd	nd	nd	nd
	12.1	a	2.0	0.6	nd						
	17.4	a	1.1	0.5	nd						
	23.7	b	1.9	0.9	nd						
	32.4	b	nd	nd	nd	nd	nd	nd	nd	nd	nd
	39.0	c	1.3	0.6	nd						
FV2	53.7	c	nd	nd	nd	nd	nd	nd	nd	nd	nd
	55.1	c	0.6	0.2	nd						
	58.8	d	1.4	1.0	0.1	nd	nd	nd	nd	nd	nd
	62.3	d	0.8	0.5	0.4	nd	nd	nd	nd	nd	nd
	65.7	d	1.4	0.7	0.9	nd	nd	nd	nd	nd	nd
	69.0	d	3.9	13.0	1.6	nd	nd	nd	nd	nd	nd
	72.0	d	2.8	2.5	1.4	nd	nd	nd	nd	nd	nd
	75.7	d	1.8	1.2	0.7	nd	nd	nd	nd	nd	nd
	78.7	e	5.7	1.8	0.8	nd	nd	nd	nd	nd	nd
	81.8	e	1.0	0.4	0.5	nd	nd	nd	nd	nd	nd
85.5	e	1.3	0.8	0.7	0.3	nd	nd	nd	nd	nd	
VC FV1	7.1	a	34	29	26	12	7.5	2.1	nd	nd	nd
	12.1	a	37	26	29	25	15	10	1.8	nd	nd
	17.4	a	15	12	12	13	9.1	5.2	1.9	0.2	nd
	23.7	b	38	30	26	25	20	12	4.1	0.7	nd
	32.4	b	40	26	28	32	22	14	4.6	0.9	2.9
	39.0	c	38	22	27	24	20	14	3.3	0.7	nd
FV2	53.7	c	17	12	12	15	10	3.4	1.4	nd	nd
	55.1	c	15	13	12	14	8.2	5.8	0.6	nd	nd
	58.8	d	33	22	22	18	12	8.1	0.5	nd	nd
	62.3	d	28	11	19	16	7.8	7.2	1.0	nd	nd
	65.7	d	26	21	26	15	7.9	6.5	0.7	nd	nd
	69.0	d	10	10	3.3	5.5	3.7	2.1	0.3	nd	nd
	72.0	d	6.9	8.3	3.8	6.6	3.6	2.0	nd	nd	nd
	78.7	e	12	5.1	5.8	5.3	2.8	1.3	0.1	nd	nd
	81.8	e	9	5.3	5.9	7.3	6.1	2.5	0.1	nd	nd
	85.5	e	11	10	8.3	7.4	3.7	1.3	0.1	nd	nd

Appendix F: Reactive column organic data

REACTIVE COLUMN 101 100MB	Column Composition: Pore Volume (PV): Porosity: Flow Velocity 1 (FV1): Residence Time (FV1): Flow Velocity 2 (FV2): Residence Time (FV2):	100 % Granular Iron Master Builders 254 mL 0.45 1.4 ft/day (43 cm/day) 27.7 hr 0.8 ft/day (24 cm/day) 50 hr
---------------------------------	---	--

		Distance Along Column (ft)										
		0.00	0.08	0.16	0.33	0.50	0.66	1.00	1.31	1.64		
	PV	RN	Influent	Organic Concentration (µg/L)								Effluent
			pH Along Column									
pH FV1	5.2	a	7.2	8.7	9.0	9.2	9.2	9.1	8.9	8.3	8.3	
	12.9	a	6.6	9.0	9.3	9.5	9.6	9.5	9.6	9.6	9.5	
	19.5	a	7.3	9.0	9.4	9.6	9.6	9.7	9.6	9.4	9.3	
	25.4	b	6.2	8.0	9.1	9.2	9.4	9.5	9.5	9.5	9.5	
	36.1	b	7.1	9.0	9.2	9.2	9.2	9.4	9.5	9.6	9.6	
FV2	54.2	c	7.8	9.3	9.3	9.4	9.3	9.4	9.4	9.5	9.6	
	57.2	d	6.8	9.1	9.4	9.7	9.8	9.7	9.8	9.8	9.6	
	60.9	d	6.7	8.8	9.1	9.3	9.4	9.4	9.5	9.5	9.1	
	64.4	d	6.7	8.2	8.5	9.1	9.0	9.2	9.2	9.3	9.4	
	68.6	d	7.2	9.2	9.3	9.5	9.5	9.6	9.6	9.7	9.7	
	71.0	d	7.7	9.3	9.4	9.6	9.6	9.6	9.7	9.7	9.7	
	74.3	d	8.3	9.4	9.4	9.6	9.4	9.6	9.6	9.5	9.6	
	77.8	e	6.3	7.8	9.1	9.3	9.5	9.5	9.6	9.5	9.2	
	80.8	e	6.7	8.1	8.6	9.4	9.3	9.5	9.5	9.5	9.5	
	85.1	e	7.3	8.9	8.9	9.5	9.5	9.5	9.6	9.5	9.6	
			Redox Potential Along Column (mV)									
Eh FV1	5.2	a	351	-213	-289	-256	-297	-274	-222	-197	127	
	12.9	a	386	-206	-196	-205	-269	-293	-296	-290	112	
	19.5	a	332	-159	-268	-329	-437	-380	-432	-447	-443	
	25.4	b	336	-327	-287	-345	-221	-272	-307	-375	-11	
	36.1	b	366	198	137	-168	-347	-265	-349	-254	126	
FV2	54.2	c	278	309	296	-31	-92	-123	-31	-94	293	
	57.2	d	315	202	135	-7	-14	-129	-37	-107	256	
	60.9	d	309	186	133	-208	-272	-181	-311	-367	263	
	68.6	d	286	174	147	-137	-174	-257	-347	-290	205	
	71.0	d	284	194	-97	-302	-204	-241	-204	-270	265	
	74.3	d	272	184	164	-195	-108	-145	-282	-196	241	
	77.8	e	291	129	-27	-72	-215	-306	-312	-349	240	
	80.8	e	289	260	170	-100	-145	-232	-199	-209	73	
85.1	e	245	1	72	-153	-229	-315	-328	-311	258		

nd = not detected

RN = reservoir number

Appendix F: Reactive column organic data

REACTIVE COLUMN 102 100PL	Column Composition: Pore Volume (PV): Porosity: Flow Velocity 1 (FV1): Residence Time (FV1): Flow Velocity 2 (FV2): Residence Time (FV2):	100 % Granular Iron Peerless (-8 to 50 mesh) 245 mL 0.43 1.8 ft/day (53 cm/day) 22.5 hr 1.0 ft/day (31 cm/day) 39 hr
---------------------------------	---	---

		Distance Along Column (ft)										
		0.00	0.08	0.16	0.33	0.50	0.66	1.00	1.31	1.64		
	PV	RN	Influent	Organic Concentration (µg/L)								Effluent
TCE												
FV1	4.0	a	1697	245	53	nd	nd	nd	nd	nd	nd	nd
	10.3	a	1750	471	190	24	15	12	nd	nd	nd	nd
	16.9	a	1533	1159	473	15	5.1	3.5	nd	nd	nd	nd
	24.5	b	1830	1256	931	123	13	4.4	nd	nd	nd	nd
	32.6	b	1691	1263	1020	153	5.3	1.0	nd	nd	nd	nd
	41.0	b	1825	1031	897	306	7.9	0.8	nd	nd	nd	nd
FV2	65.2	c	1288	652	894	303	18	2.4	nd	nd	nd	nd
	72.2	d	1462	623	861	287	6.7	2.2	nd	nd	nd	nd
	77.8	d	1442	223	971	270	6.6	nd	nd	nd	nd	nd
	81.9	d	1214	1010	1041	559	9.2	nd	nd	nd	nd	nd
	85.8	d	1227	1038	975	745	22	1.1	nd	nd	nd	nd
	91.2	d	1069	1035	1016	718	56	0.7	nd	nd	nd	nd
	95.2	d	815	639	821	730	76	1.2	nd	nd	nd	nd
	98.7	e	1734	837	1026	836	97	1.2	nd	nd	nd	nd
	102.5	e	1436	1000	1002	739	95	1.7	nd	nd	nd	nd
	107.1	e	1385	941	1025	781	147	2.4	nd	nd	nd	nd
PCE												
FV1	4.0	a	1.6	0.6	0.2	nd	nd	nd	nd	nd	nd	nd
	10.3	a	3.7	0.5	2.1	nd	nd	nd	nd	nd	nd	nd
	16.9	a	3.7	1.6	1.7	0.3	nd	nd	nd	nd	nd	nd
	24.5	b	2.7	nd	nd	nd	nd	nd	nd	nd	nd	nd
	32.6	b	1.7	1.2	1.0	nd	nd	nd	nd	nd	nd	nd
	41.0	b	1.6	1.0	0.8	nd	nd	nd	nd	nd	nd	nd
FV2	65.2	c	2.8	nd	nd	nd	nd	nd	nd	nd	nd	nd
	72.2	d	2.2	1.2	1.9	1.2	nd	nd	nd	nd	nd	nd
	77.8	d	1.3	nd	0.9	nd	nd	nd	nd	nd	nd	nd
	81.9	d	1.3	2.6	1.9	1.3	nd	nd	nd	nd	nd	nd
	85.8	d	1.4	6.7	1.7	1.6	nd	nd	nd	nd	nd	nd
	91.2	d	1.3	1.9	1.7	1.8	nd	nd	nd	nd	nd	nd
	95.2	d	1.0	1.0	1.6	2.0	nd	nd	nd	nd	nd	nd
	98.7	e	1.5	1.1	1.5	1.6	nd	nd	nd	nd	nd	nd
	102.5	e	1.2	1.4	1.6	1.9	nd	nd	nd	nd	nd	nd
	107.1	e	1.1	1.0	1.5	1.8	nd	nd	nd	nd	nd	nd

nd = not detected

RN = reservoir number

Appendix F: Reactive column organic data

REACTIVE COLUMN
102
100PL

Column Composition: 100 % Granular Iron
Peerless (-8 to 50 mesh)
Pore Volume (PV): 245 mL
Porosity: 0.43
Flow Velocity 1 (FV1): 1.8 ft/day (53 cm/day)
Residence Time (FV1): 22.5 hr
Flow Velocity 2 (FV2): 1.0 ft/day (31 cm/day)
Residence Time (FV2): 39 hr

		Distance Along Column (ft)									
		0.00	0.08	0.16	0.33	0.50	0.66	1.00	1.31	1.64	
	PV	RN	Influent	Organic Concentration (µg/L)							Effluent
TCM FV1	4.0	a	20	2.1	0.2	nd	nd	nd	nd	nd	nd
	10.3	a	25	5.0	2.0	0.3	7.0	nd	nd	nd	nd
	16.9	a	21	12	4.6	0.7	0.3	nd	nd	nd	nd
	24.5	b	23	12	6.7	2.0	0.4	nd	nd	nd	nd
	32.6	b	23	8.9	5.0	1.2	nd	nd	nd	nd	nd
	41.0	b	18	8.8	5.6	2.2	nd	nd	nd	nd	nd
FV2	65.2	c	20	6.6	6.8	2.7	0.4	nd	nd	nd	nd
	72.2	d	23	4.8	5.6	2.5	0.6	nd	nd	nd	nd
	77.8	d	22	2.6	8.9	2.3	0.4	nd	nd	nd	nd
	81.9	d	21	13	14	3.5	0.8	nd	nd	nd	nd
	85.8	d	22	17	12	6.1	1.2	nd	nd	nd	nd
	91.2	d	25	19	15	6.0	1.8	nd	nd	nd	nd
	95.2	d	18	12	12	6.5	2.1	0.6	nd	nd	nd
	98.7	e	28	6.1	8.8	5.6	2.4	0.9	nd	nd	nd
	102.5	e	23	11	10	4.9	2.2	0.6	nd	nd	nd
107.1	e	22	14	13	5.7	2.1	0.5	nd	nd	nd	
cDCE FV1	7.1	a	67	167	181	94	38	8.4	nd	nd	nd
	12.2	a	56	108	130	108	71	38	6.9	nd	nd
	17.9	a	66	93	148	136	96	58	14	nd	nd
	25.7	b	62	60	78	98	76	38	15	3.8	1.8
	36.6	b	51	54	96	107	75	52	22	8.7	7.1
	47.9	c	51	58	84	94	73	47	22	12	2.7
FV2	67.5	c	53	46	48	59	35	18	5.1	nd	nd
	69.1	c	56	62	53	78	34	17	nd	nd	nd
	73.3	d	73	55	67	84	56	30	5.3	nd	nd
	79.0	d	52	52	67	109	52	25	7.6	nd	nd
	82.8	d	57	57	78	93	67	24	0.9	nd	nd
	88.3	d	39	45	20	51	54	21	2.7	nd	nd
	92.3	d	49	43	46	53	62	25	3.6	nd	nd
	96.5	d	59	81	68	97	101	57	8.7	nd	nd
	100.3	e	65	59	59	71	65	42	5.4	nd	nd
104.2	e	89	56	70	100	92	45	5.5	nd	nd	

Appendix F: Reactive column organic data

REACTIVE COLUMN 105 50PLSSAQ	Column Composition: Pore Volume (PV): Porosity: Flow Velocity 1 (FV1): Residence Time (FV1): Flow Velocity 2 (FV2): Residence Time (FV2):	50 % Granular Iron - Peerless 25 % Elizabeth City Aquifer Material 25 % Silica Sand 166 mL 0.29 2.6 ft/day (79 cm/day) 15.3 hr 1.2 ft/day (36 cm/day) 34 hr
------------------------------------	---	---

		Distance Along Column (ft)										
		0.00	0.08	0.16	0.33	0.50	0.66	1.00	1.31	1.64		
	PV	RN	Influent	Organic Concentration (µg/L)								Effluent
TCE												
FV1	3.5	a	1553	1141	676	167	19	5.4	2.4	9.2	4.3	
	9.5	b	1560	1205	716	225	39	12	4.9	7.9	7.1	
	21.9	b	1724	1200	812	289	51	12	nd	nd	nd	
	33.8	b	1795	1216	680	241	44	13	nd	nd	nd	
	42.0	b	1524	1220	981	473	136	14	nd	nd	nd	
	51.4	c	1580	1123	696	278	93	22	nd	nd	nd	
FV2	76.0	c	1288	838	403	45	21	nd	nd	nd	nd	
	84.3	d	1462	1134	936	168	24	4.1	1.6	1.6	3.0	
	89.6	d	1246	683	648	133	14	3.0	nd	nd	nd	
	94.4	d	1214	1242	1020	328	26	3.8	nd	nd	nd	
	99.4	d	1227	1022	916	435	63	5.1	1.2	nd	nd	
	104.3	d	1069	1056	1056	525	145	2.8	0.9	nd	nd	
	109.5	d	905	912	896	591	211	16	nd	nd	nd	
	113.8	e	1734	1231	1112	706	256	20	1.2	1.2	2.8	
	119.0	e	1436	1177	1134	608	272	27	1.2	1.5	nd	
	124.5	e	1282	1245	1144	688	270	34	nd	nd	nd	
PCE												
FV1	3.5	a	1.6	7.3	1.2	0.6	0.8	0.8	1.6	1.0	19	
	9.5	b	4.2	3.0	nd	1.2	nd	nd	nd	nd	21	
	21.9	b	6.4	3.0	3.9	nd	nd	nd	nd	nd	14	
	33.8	b	4.5	6.4	4.9	nd	nd	nd	nd	nd	11	
	42.0	b	6.7	12	5.1	1.5	0.8	0.8	nd	nd	nd	
	51.4	c	2.1	2.1	1.4	nd	nd	nd	nd	nd	nd	
FV2	76.0	c	2.8	2.2	1.3	nd	nd	nd	nd	nd	nd	
	84.3	d	2.2	2.2	2.1	1.0	nd	nd	nd	nd	nd	
	89.6	d	1.3	1.5	1.2	nd	nd	nd	nd	nd	nd	
	94.4	d	1.3	1.7	1.6	1.1	nd	nd	nd	nd	nd	
	99.4	d	1.4	1.9	1.7	1.1	0.4	0.3	nd	nd	nd	
	104.3	d	1.3	1.6	2.6	1.3	0.9	0.3	nd	nd	nd	
	109.5	d	1.2	1.4	2.5	1.4	1.1	nd	nd	nd	nd	
	113.8	e	1.5	1.5	1.7	nd	nd	nd	nd	nd	nd	
	119.0	e	2.0	1.5	2.0	1.9	nd	nd	nd	nd	nd	
	124.5	e	2.3	1.6	2.2	1.4	nd	nd	nd	nd	nd	

nd = not detected
 RN = reservoir number

Appendix F: Reactive column organic data

REACTIVE COLUMN
105
50PLSSAQ

Column Composition:

50 % Granular Iron - Peerless
25 % Elizabeth City Aquifer Material
25 % Silica Sand

Pore Volume (PV):

166 mL

Porosity:

0.29

Flow Velocity 1 (FV1):

2.6 ft/day (79 cm/day)

Residence Time (FV1):

15.3 hr

Flow Velocity 2 (FV2):

1.2 ft/day (36 cm/day)

Residence Time (FV2):

34 hr

		Distance Along Column (ft)									
		0.00	0.08	0.16	0.33	0.50	0.66	1.00	1.31	1.64	
	PV	RN	Influent	Organic Concentration (µg/L)							Effluent
TCM FV1	3.5	a	20	10	4.8	1.3	0.3	nd	nd	nd	nd
	9.5	b	23	12	7.3	2.1	0.4	nd	nd	nd	nd
	21.9	b	23	9.3	4.7	1.9	nd	nd	nd	nd	nd
	33.8	b	26	10	4.3	2.4	0.8	1.0	nd	nd	nd
	42.0	b	22	10	5.4	2.5	0.6	nd	nd	nd	nd
	51.4	c	18	5.5	3.2	1.8	0.9	nd	nd	nd	nd
FV2	76.0	c	20	5.2	1.3	0.4	nd	nd	nd	nd	nd
	84.3	d	23	10	3.4	1.1	0.5	nd	nd	nd	nd
	89.6	d	18	4.7	1.9	0.6	nd	nd	nd	nd	nd
	94.4	d	19	13	4.6	1.7	0.8	nd	nd	nd	nd
	99.4	d	22	13	4.7	1.7	0.7	nd	nd	nd	nd
	104.3	d	20	18	7.4	2.6	1.3	nd	nd	nd	nd
	109.5	d	21	16	7.9	3.2	1.7	0.6	nd	nd	nd
	113.8	e	28	15	4.3	1.5	1.2	0.8	0.6	nd	nd
	119.0	e	23	13	3.3	1.3	0.8	0.6	0.2	nd	nd
124.5	e	22	16	8.5	1.4	0.7	0.3	nd	nd	nd	
cDCE FV1	4.6	a	61	86	138	137	110	104	39	16	6.1
	16.3	b	58	54	72	93	94	60	29	16	8.7
	20.2	b	54	67	99	99	81	38	30	17	18
	28.5	b	49	47	59	86	51	34	22	19	4.6
	43.6	c	50	46	58	58	54	36	17	8.3	3.7
	54.4	c	65	50	65	80	60	50	22	9.3	8.4
FV2	78.3	c	51	55	44	42	47	34	4.3	nd	nd
	80.1	c	56	47	67	67	51	22	0.6	nd	nd
	85.7	d	67	56	51	62	46	31	9.2	nd	nd
	90.8	d	49	57	52	40	31	12	6.1	nd	nd
	95.5	d	51	52	45	57	57	32	6.7	nd	nd
	100.8	d	39	32	34	47	51	28	6.7	nd	nd
	105.7	d	37	34	37	59	71	59	14	nd	nd
	110.9	d	66	77	64	90	88	105	27	nd	nd
	116.0	e	65	59	56	71	50	43	21	3.5	nd
120.7	e	74	62	60	69	83	68	20	nd	nd	

Appendix F: Reactive column organic data

REACTIVE COLUMN
105
50PLSSAQ

Column Composition: 50 % Granular Iron - Peerless
25 % Elizabeth City Aquifer Material
25 % Silica Sand

Pore Volume (PV): 166 mL
Porosity: 0.29
Flow Velocity 1 (FV1): 2.6 ft/day (79 cm/day)
Residence Time (FV1): 15.3 hr
Flow Velocity 2 (FV2): 1.2 ft/day (36 cm/day)
Residence Time (FV2): 34 hr

		Distance Along Column (ft)										
		0.00	0.08	0.16	0.33	0.50	0.66	1.00	1.31	1.64		
	PV	RN	Influent	Organic Concentration (µg/L)								Effluent
tDCE												
FV1	4.6	a	1.1	1.1	1.0	0.1	nd	nd	nd	nd	nd	
	16.3	b	2.1	1.2	1.0	0.5	nd	nd	nd	nd	nd	
	20.2	b	1.7	1.3	1.3	0.6	nd	nd	nd	nd	nd	
	28.5	b	nd	nd	nd	nd	nd	nd	nd	nd	nd	
	43.6	c	1.7	1.2	0.9	nd	nd	nd	nd	nd	nd	
	54.4	c	1.2	0.3	0.2	nd	nd	nd	nd	nd	nd	
FV2	78.3	c	nd	nd	nd	nd	nd	nd	nd	nd	nd	
	80.1	c	0.6	0.1	nd	nd	nd	nd	nd	nd	nd	
	85.7	d	1.3	1.3	0.6	nd	nd	nd	nd	nd	nd	
	90.8	d	0.8	1.0	0.7	0.1	nd	nd	nd	nd	nd	
	95.5	d	1.4	1.3	1.0	0.5	0.6	0.2	nd	nd	nd	
	100.8	d	1.3	2.0	2.1	1.4	0.8	nd	nd	nd	nd	
	105.7	d	1.7	1.7	1.8	1.6	1.1	nd	nd	nd	nd	
	110.9	d	0.9	1.9	1.2	1.1	0.7	0.3	nd	nd	nd	
	116.0	e	5.7	3.5	2.2	1.4	0.1	nd	nd	nd	nd	
	120.7	e	1.2	0.7	0.5	0.3	nd	nd	nd	nd	nd	
VC												
FV1	4.6	a	16	19	19	15	14	12	7.7	5.4	3.4	
	16.3	b	41	27	28	26	21	15	12	7.5	6.3	
	20.2	b	39	28	28	24	18	8.3	10	6.8	6.2	
	28.5	b	36	24	24	22	17	13	6.6	6.7	2.9	
	43.6	c	27	20	16	21	12	12	5.8	3.2	1.8	
	54.4	c	43	25	30	27	23	15	8.6	4.6	2.8	
FV2	78.3	c	17	16	12	4.7	9.1	5.4	2.2	nd	nd	
	80.1	c	15	14	14	13	8.9	3.7	1.5	nd	nd	
	85.7	d	33	22	17	17	13	8.4	4.1	nd	nd	
	90.8	d	28	19	14	6.7	6.0	0.9	2.4	nd	nd	
	95.5	d	26	26	21	12	17	10	3.5	0.2	nd	
	100.8	d	10	7.5	6.0	5.0	2.4	1.3	0.1	nd	nd	
	105.7	d	6.6	4.7	6.0	6.9	4.9	3.9	1.9	nd	nd	
	116.0	e	12	6.9	5.8	5.8	4.2	2.4	2.4	0.5	nd	
	120.7	e	8.1	7.3	5.9	4.8	3.8	4.5	2.6	0.2	nd	

Appendix F: Reactive column organic data

REACTIVE COLUMN
105
50PLSSAQ

Column Composition:

50 % Granular Iron - Peerless
25 % Elizabeth City Aquifer Material
25 % Silica Sand

Pore Volume (PV):

166 mL

Porosity:

0.29

Flow Velocity 1 (FV1):

2.6 ft/day (79 cm/day)

Residence Time (FV1):

15.3 hr

Flow Velocity 2 (FV2):

1.2 ft/day (36 cm/day)

Residence Time (FV2):

34 hr

		Distance Along Column (ft)									
		0.00	0.08	0.16	0.33	0.50	0.66	1.00	1.31	1.64	
	PV	RN	Influent		Organic Concentration (µg/L)						Effluent
pH Along Column											
pH											
FV1	1.5	a	6.6	8.2	9.0	9.1	9.1	9.1	9.1	8.7	8.5
	8.3	a	7.2	9.0	9.3	9.3	9.4	9.4	9.4	9.3	9.2
	18.1	b	6.5	6.8	7.1	7.3	8.7	8.8	9.2	9.2	9.0
	40.6	b	7.0	9.3	9.1	9.1	9.3	9.1	9.2	9.2	9.2
	44.0	c	6.1	7.2	8.5	9.3	9.3	9.1	9.1	9.2	9.2
FV2	79.3	c	7.9	9.1	9.3	9.2	9.4	9.2	9.3	9.3	9.2
	83.4	d	6.7	9.0	9.3	9.7	9.7	9.6	9.6	9.6	9.4
	88.9	d	6.6	8.0	9.0	9.2	9.3	9.1	9.0	9.2	9.1
	93.7	d	6.9	8.2	9.0	8.9	9.0	8.2	7.9	6.5	9.2
	100.1	d	7.1	9.0	8.6	9.6	9.5	9.4	9.4	9.4	9.4
	103.7	d	7.9	9.2	8.9	9.6	9.3	9.6	9.5	9.5	9.4
	108.9	d	8.1	9.2	9.5	9.4	9.6	9.5	9.5	9.4	9.4
	114.7	e	6.1	7.8	8.4	9.2	9.4	9.4	9.4	9.4	9.1
	119.4	e	6.5	7.3	7.5	9.0	8.3	9.3	9.3	9.3	9.3
	125.4	e	7.3	8.4	8.5	9.3	9.3	9.2	9.4	9.3	9.4
Redox Potential Along Column (mV)											
Eh											
FV1	1.5	a	386	-264	-102	-244	-281	-325	-271	-295	-59
	8.3	a	340	-129	-226	-224	-273	-265	-296	-304	188
	18.1	b	312	-191	-247	-311	-349	-136	-143	-218	-211
	40.6	b	275	19	51	-116	-279	-204	-250	-214	104
	44.0	c	345	-195	129	-209	-192	-272	-275	-232	25
FV2	79.3	c	257	229	239	260	-78	73	-167	-86	306
	83.4	d	334	182	171	80	-44	18	-84	23	123
	88.9	d	266	230	227	254	-125	84	-409	-362	217
	93.7	d	317	211	79	3	27	76	-8	-2	79
	100.1	d	293	192	191	72	-187	-117	250	-212	-83
	103.7	d	329	222	207	-152	-156	-206	-233	-279	256
	108.9	d	281	175	147	-142	-265	-224	-225	-202	245
	114.7	e	233	133	35	-186	-301	-287	-282	-242	156
	119.4	e	293	188	253	-84	8	-158	-247	-346	77
	125.4	e	257	246	259	52	-290	-248	-282	-347	138

nd = not detected

RN = reservoir number

Appendix F: Reactive column organic data

REACTIVE COLUMN
110
48PL/52AQ

Column Composition: 48 % Granular Iron - Peerless
52 % Elizabeth City Aquifer Material
Pore Volume (PV): 189 mL
Porosity: 0.33
Flow Velocity I (FV1): 2.3 ft/day (71 cm/day)
Residence Time (FV1): 17 hr

		Distance Along Column (ft)										
		0.00	0.08	0.16	0.33	0.50	0.66	1.00	1.31	1.64		
	PV	RN	Influent	Organic Concentration (µg/L)							Effluent	
TCE												
FV1	3.2	d	1219	803	424	29	nd	nd	nd	nd	nd	
	9.2	d	1227	864	568	103	nd	nd	nd	nd	nd	
	18.8	d	1166	1005	803	357	50	2.1	nd	nd	nd	
	28.7	d	916	892	723	383	82	5.3	nd	nd	nd	
	33.0	d	538	323	227	179	25	3.5	nd	nd	nd	
	36.7	e	1734	1231	1039	492	32	3.7	nd	nd	nd	
	46.7	e	1436	1090	848	342	13	1.1	nd	nd	nd	
	58.0	e	1309	1105	955	480	33	1.5	nd	nd	nd	
PCE												
FV1	3.2	d	1.3	0.4	nd							
	9.2	d	1.4	0.8	0.4	nd	nd	nd	nd	nd	nd	
	18.8	d	1.3	1.1	nd							
	28.7	d	1.2	1.1	nd							
	33.0	d	2.2	nd	nd	nd	nd	nd	nd	nd	nd	
	36.7	e	2.2	nd	nd	nd	nd	nd	nd	nd	nd	
	46.7	e	1.4	1.0	nd							
	58.0	e	1.5	nd	nd	nd	nd	nd	nd	nd	nd	
TCM												
FV1	3.2	d	21	10	3.8	nd	nd	nd	nd	nd	nd	
	9.2	d	22	12	5.7	2.3	nd	nd	nd	nd	nd	
	18.8	d	26	18	11	5.2	2.4	nd	nd	nd	nd	
	28.7	d	22	18	9.2	4.8	2.1	0.9	nd	nd	nd	
	33.0	d	8.2	4.6	2.5	2.0	1.0	nd	nd	nd	nd	
	36.7	e	28	16	6.5	3.2	0.8	nd	nd	nd	nd	
	46.7	e	24	16	3.7	1.0	0.4	0.4	nd	nd	nd	
	58.0	e	22	15	5.0	0.6	0.2	nd	nd	nd	nd	

nd = not detected
RN = reservoir number

Appendix F: Reactive column organic data

REACTIVE COLUMN
110
48PL/52AQ

Column Composition:

48 % Granular Iron - Peerless
52 % Elizabeth City Aquifer Material

Pore Volume (PV):

189 mL

Porosity:

0.33

Flow Velocity I (FV1):

2.3 ft/day (71 cm/day)

Residence Time (FV1):

17 hr

		Distance Along Column (ft)										
		0.00	0.08	0.16	0.33	0.50	0.66	1.00	1.31	1.64		
	PV	RN	Influent	Organic Concentration (µg/L)								Effluent
cDCE												
FV1	12.0	d	41	51	41	26	11	0.2	nd	nd	nd	
	17.6	d	41	41	55	65	38	23	2.3	nd	nd	
	21.7	d	37	37	37	34	24	21	3.5	nd	nd	
	31.3	d	36	76	80	77	73	64	13	5.0	6.5	
	38.4	e	57	73	52	94	72	51	11	5.2	3.9	
	41.1	e	65	58	59	65	59	32	6.6	3.1	2.1	
tDCE												
FV1	12.0	d	3.9	1.6	1.7	0.8	nd	nd	nd	nd	nd	
	17.6	d	1.8	1.5	1.9	1.3	0.1	nd	nd	nd	nd	
	21.7	d	1.6	1.4	0.9	0.6	nd	nd	nd	nd	nd	
	31.3	d	nd	0.5	nd	nd	nd	nd	nd	nd	nd	
	38.4	e	2.9	2.3	1.4	1.8	1.1	0.7	nd	nd	nd	
	41.1	e	5.7	2.2	2.9	0.2	1.2	nd	nd	nd	nd	
VC												
FV1	12.0	d	10.0	9.5	8.0	6.5	4.8	3.0	0.7	nd	nd	
	17.6	d	9.0	9.0	6.4	6.4	8.4	4.1	1.5	0.2	nd	
	21.7	d	6.6	5.7	4.8	4.0	3.9	2.9	1.3	0.2	0.1	
	38.4	e	12.0	11.0	6.8	8.1	5.9	4.2	1.9	1.3	1.2	
	41.1	e	12.0	4.7	5.3	4.3	3.7	2.7	1.0	0.5	0.4	

nd = not detected

RN = reservoir number

Appendix F: Reactive column organic data

REACTIVE COLUMN
110
48PL/52AQ

Column Composition:

48 % Granular Iron - Peerless
52 % Elizabeth City Aquifer Material

Pore Volume (PV):

189 mL

Porosity:

0.33

Flow Velocity I (FV1):

2.3 ft/day (71 cm/day)

Residence Time (FV1):

17 hr

		Distance Along Column (ft)										
		0.00	0.08	0.16	0.33	0.50	0.66	1.00	1.31	1.64		
	PV	RN	Influent		Organic Concentration (µg/L)						Effluent	
			pH Along Column									
pH FV1	1.9	d	6.7	8.4	8.3	7.8	7.2	7.2	7.4	7.2	6.4	
	10.7	d	7.2	9.1	9.3	9.2	9.0	9.0	8.9	9.0	8.9	
	19.1	d	7.5	9.1	9.4	9.5	9.4	9.1	8.9	8.0	9.2	
	23.4	d	8.1	9.1	9.3	9.4	9.3	9.2	9.0	9.1	9.1	
	27.5	d	8.5	9.2	9.4	9.4	9.6	9.2	9.3	9.3	9.4	
	39.9	e	6.4	7.2	8.5	9.1	9.1	9.1	9.1	9.1	9.1	9.3
	42.5	e	6.4	7.3	8.2	9.0	9.1	9.1	9.1	9.1	9.1	9.3
	48.2	e	6.7	7.9	8.7	9.0	8.9	9.0	9.1	9.0	9.0	9.3
Redox Potential Along Column (mV)												
Eh FV1	1.9	d	344	68	-15	-29	22	192	166	127	273	
	10.7	d	298	149	93	-115	-155	-35	-159	-225	226	
	19.1	d	264	136	121	74	-49	-205	-146	-153	275	
	23.4	d	256	194	175	155	86	-10	-24	-86	252	
	27.5	d	298	134	51	-51	-293	-139	-172	-219	266	
	39.9	e	322	74	150	-295	-404	-310	-455	-418	229	
	42.5	e	294	123	115	-213	-211	-361	-395	-399	32	
	48.2	e	313	140	103	-132	-176	-208	-170	-146	41	

nd = not detected

RN = reservoir number

Appendix G: Reactive column inorganic data

Elizabeth City reactive columns
 Concentrations in mg/L, determined at UW Water Quality Lab

Distance along column (cm)	pH	Eh (mV)	CO ₃	SO ₄	Al	Ba	Ca	Cr	Fe	K	Mg	Mn	Na	Ni	Sr	H ₄ SiO ₄	Zn	Cl	
50MBSSAQ at 8.6 PV			FV1 = 68 cm/d																
0	6.88	178	29.4	101.0	<0.2	0.07	24	10.300	<0.1	3.51	15.3	0.84	96.8	<0.1	0.47	31.41	0.149	119	
2.5	8.15	-10	17.4	98.3	<0.2	0.08	22.4	0.001	<0.1	2.44	14.5	0.28	94.2	<0.1	0.43	6.45	<0.05	116	
10	9.14	-132	32.7	99.9	<0.2	0.04	23.5	0.057	<0.1	2.83	14.3	0.13	95.4	<0.1	0.44	1.85	<0.05	121	
15	9.15	-145	38.1	102.0	<0.2	0.02	24.4	0.016	<0.1	3.52	13.2	0.09	101	<0.1	0.45	1.89	<0.05	122	
20	9.31	-140	27.0	90.3	<0.2	0.04	23.9	0.041	<0.1	2.84	11	0.07	94.6	<0.1	0.43	2.38	<0.05	127	
30	9.3	-169	36.9	100.0	<0.2	0.02	25.6	0.020	<0.1	4.06	7.16	0.07	96.7	<0.1	0.31	2.00	<0.05	119	
40	9.43	-143	26.3	114.0	0.33	0.03	28.5	0.001	<0.1	3.94	2.82	0.04	98.9	<0.1	0.18	3.33	<0.05	144	
50MBSSAQ at 27.7 PV																			
0	6.48	367	24.3	105.0	<0.2	0.08	24	10.8	<0.1	7.01	16.4	0.87	105	<0.1	0.43	32.6	0.073	119	
2.5	7.27	60	49.6	112.0	<0.2	0.053	22.6	0.032	8.24	7	15.9	0.79	104	<0.1	0.40	13.5	<0.05	119	
5	8.29	62	33.3	106.0	<0.2	0.051	22.9	0.014	0.307	6.28	15.9	0.49	103	<0.1	0.40	3.66	<0.05	120	
10	8.95	-14	45.7	104.0	<0.2	0.06	22.5	0.013	<0.1	6.59	15.4	0.45	119	<0.1	0.40	1.56	<0.05	122	
15	9.09	-35	44.9	102.0	<0.2	0.03	22.2	0.013	<0.1	7.35	14.7	0.38	104	<0.1	0.39	1.30	<0.05	126	
20	9.18	-8	42.5	104.0	<0.2	0.02	22.2	0.022	<0.1	6.83	14.1	0.16	103	<0.1	0.40	1.93	<0.05	132	
30	9.27	-57	29.5	93.2	0.207	0.02	22.9	0.008	<0.1	5.43	12.4	0.08	101	<0.1	0.41	1.80	<0.05	125	
40	9.23	-94	34.7	94.8	<0.2	0.02	20.7	0.026	<0.1	5.4	10.9	0.08	99.7	<0.1	0.41	2.26	<0.05	123	
50	9.28	-506	26.0	94.0	0.617	0.06	19.9	0.048	<0.1	6.94	10	0.06	97.9	<0.1	0.39	1.42	<0.05	125	
50MBSSAQ at 48.1 PV																			
0	6.71	241	38.9	101.0	<0.2	0.07	23.5	8.370	<0.1	5.23	15	0.84	103	<0.1	0.41	28.51	0.179	120	
2.5	7.09	35	42.7	104.0	<0.2	0.05	22.2	0.018	9.08	5.53	14.7	0.76	102	<0.1	0.38	14.83	<0.05	118	
5	7.92	134	50.0	105.0	<0.2	0.10	23.1	0.006	0.26	7.81	15	0.47	97.6	<0.1	0.40	4.04	<0.05	123	
10	8.63	-39	39.5	102.0	<0.2	0.07	22.8	0.014	<0.1	4.72	15	0.46	102	<0.1	0.39	1.15	<0.05	119	
15	8.92	-89	40.9	103.0	<0.2	0.06	22.6	0.040	<0.1	4.61	14.7	0.38	103	<0.1	0.40	1.31	<0.05	120	
20	9.07	-76	49.0	104.0	<0.2	0.03	22.8	0.016	<0.1	4.08	14.9	0.20	103	<0.1	0.40	1.46	<0.05	121	
30	9.14	-137	44.4	104.0	<0.2	0.02	21.3	0.019	<0.1	4.46	14.2	0.10	103	<0.1	0.42	1.50	<0.05	124	
50MBSS at 27.9 PV			FV1 = 55 cm/d																
0	6.38	307	27.8	105	<0.2	0.08	25	10.800	<0.1	4.02	16	0.86	100	<0.1	0.48	32.61	0.108	128	
2.5	6.9	56	61.9	99	<0.2	0.06	23.3	0.025	18.4	3	15.3	0.94	100	0.202	0.47	23.82	<0.05	120	
5	7.19	54	45.2	99	<0.2	0.06	24	0.024	7.95	3.55	15.4	0.64	97.5	0.124	0.45	15.18	<0.05	121	
10	8.31	196	53.2	101	<0.2	0.05	22.8	0.013	<0.1	4.42	15	0.28	95.2	<0.1	0.42	2.95	<0.05	117	
15	8.59	324	45.8	101	<0.2	0.05	21.3	0.007	<0.1	3.71	15.3	0.38	97.6	<0.1	0.38	1.60	<0.05	118	
20	8.92	91	31.2	101	<0.2	0.04	19.9	0.010	<0.1	3.83	15.2	0.61	97.1	<0.1	0.34	1.45	<0.05	118	
30	9.12	149	38.4	104	<0.2	0.03	16.6	0.013	<0.1	4.38	14.9	0.41	96.8	<0.1	0.26	1.28	<0.05	133	
40	9.12	321	30.0	108	<0.2	0.07	14.5	0.034	<0.1	4.25	15	0.19	101	<0.1	0.21	1.16	<0.05	136	
50	9.39	330	31.8	99	<0.2	0.04	12.9	0.040	<0.1	4.49	14.5	0.12	98.5	<0.1	0.18	1.35	<0.05	122	
50MBSS at 34.4 PV																			
0	7.32	451	28.7	100	0.25	0.08	24.3	10.500	<0.1	5.56	15.9	0.85	99	<0.1	0.41	32.28	0.062	121	
2.5	7.41	113	43.8	97	0.943	0.06	23	0.023	4.11	7.31	15.6	0.71	100	<0.1	0.39	20.61	<0.05	125	
5	8.33	431	34.3	93	0.166	0.04	22.6	0.010	0.103	5.66	15.1	0.28	104	<0.1	0.38	6.81	<0.05	122	
10	8.88	237	40.5	94	0.255	0.04	20.2	0.014	<0.1	5.08	15.2	0.08	98.5	<0.1	0.32	2.53	<0.05	122	
15	8.93	90	32.3	101	<0.2	0.04	19.3	0.028	<0.1	3.62	16.1	0.12	108	<0.1	0.31	1.59	<0.05	121	
20	8.94	-25	39.0	100	<0.2	0.03	17	0.011	<0.1	4.42	15.2	0.24	101	<0.1	0.26	1.44	<0.05	120	
30	9	-105	21.1	102	0.638	0.04	14.7	0.019	<0.1	6.56	15.1	0.34	106	<0.1	0.20	3.32	<0.05	122	
40	9.24	-88	41.0	100	0.265	0.03	13.9	0.001	<0.1	3.7	14.7	0.17	102	<0.1	0.19	1.37	<0.05	117	
50	9.33	-77	27.3	100	<0.2	0.03	13.1	0.012	<0.1	4.21	14.1	0.10	100	<0.1	0.18	1.14	<0.05	118	
50MBSS at 53.5 PV																			
0	6.5	297	34.1	85	<0.2	0.06	23.2	3.800	<0.1	5.14	15.3	0.92	103	<0.1	0.40	24.97	<0.05	148	
2.5	7	107	28.1	99	<0.2	0.06	24.5	0.032	9.83	4.94	15.8	1.05	115	0.155	0.42	25.36	<0.05	128	
5	7.3	23	60.9	98	<0.2	0.06	23.3	0.012	5.4	5.01	15.3	0.60	111	<0.1	0.40	10.70	<0.05	123	
10	8.46	283	44.1	102	<0.2	0.13	22.6	0.001	<0.1	5.88	15.6	0.10	102	<0.1	0.38	2.97	<0.05	126	
15	8.82	2	29.5	100	<0.2	0.04	18.5	0.017	<0.1	4.44	15.5	0.06	107	<0.1	0.29	1.73	<0.05	122	
20	8.95	-14	44.7	98	<0.2	0.04	16.6	0.029	<0.1	4.23	15.2	0.11	105	<0.1	0.25	1.68	<0.05	122	
30	9.06	-88	24.4	97	0	0.04	14.2	0.001	<0.1	4.66	14.8	0.17	104	<0.1	0.20	1.46	<0.05	120	
40	9.18	-53	27.3	101		0.06	13		<0.1	3.41	15	0.12	104	<0.1	0.18	1.86	<0.05	129	
50	9.17	61	19.0	95	<0.2	0.03	12.4	0.016	<0.1	4.36	14.6	0.10	107	<0.1	0.17	1.71	<0.05	117	

Appendix G: Reactive column inorganic data

Distance along column (cm)	Alkalinity																	
	pH	Eh (mV)	CO ₃	SO ₄	Al	Ba	Ca	Cr(OH) ₂ ⁺	Fe	K	Mg	Mn	Na	Ni	Sr	H ₄ SiO ₄	Zn	Cl
100MB at 24 PV			FV1 = 43 cm/d															
0	6.26	338	29.6	106	<0.2	0.08	24.7	10.600	<0.1	4.69	15.8	0.85	101	<0.1	0.46	32.54	0.113	125
2.5	7.6	-86	58.2	106	0.209	0.07	24	0.030	1.01	5.85	15.3	0.39	97.5	0.101	0.44	9.30	<0.05	129
10	9.1	-165	32.1	104	<0.2	0.03	13.2	0.001	<0.1	5.3	15	0.26	97.9	<0.1	0.19	1.10	<0.05	125
15	9.46	33	24.6	98	<0.2	0.02	11.2	0.032	<0.1	4.09	14.7	0.25	101	<0.1	0.14	0.73	<0.05	122
20	9.36	-145	25.4	108	0.26	0.03	10.2	0.003	<0.1	5.62	14.1	0.15	98.1	<0.1	0.13	0.84	<0.05	132
30	9.12	-160	25.9	103	0.238	0.03	9.31	0.001	<0.1	6.41	13	0.14	97.6	<0.1	0.10	0.65	<0.05	123
40	9.56	201	23.1	103	<0.2	0.02	<9	0.005	<0.1	4.57	12	0.17	102	<0.1	0.11	0.75	<0.05	120
50	9.2	-24	20.0	100	<0.2	0.03	9.88	0.007	<0.1	4.12	9.85	0.16	103	<0.1	0.13	0.65	<0.05	118
100MB at 29.2 PV																		
0	6.39	561	25.1	103	0.32	0.08	25.9	10.800	<0.1	3.68	16	0.84	99.9	<0.1	0.44	32.52	0.092	123
2.5					0.707	0.18	25.9	0.019	<0.1	6.14	14.6	0.06	94.7	<0.1	0.37	9.41	<0.05	
5	9.22	-94	45.6	99	<0.2	0.04	20.2	0.056	<0.1	5.73	14.6	0.06	97.2	<0.1	0.26	1.28	<0.05	121
10	9.24	-139	28.6	97	<0.2	0.02	14.4	0.016	<0.1	4.81	13.9	0.20	98.3	<0.1	0.16	0.70	<0.05	117
15	9.4	-90	31.0	99	<0.2	0.03	13	0.013	<0.1	6.05	13.8	0.23	97.2	<0.1	0.14	0.70	<0.05	119
20	9.46	-45	24.8	98	<0.2	0.02	12.9	0.020	<0.1	3.94	13.7	0.15	101	<0.1	0.13	0.93	<0.05	122
30	9.54	-99	16.0	98	<0.2	0.02	12.6	0.023	<0.1	4.3	12.7	0.14	101	<0.1	0.12	0.67	<0.05	123
40	9.54	-149	16.5	104	<0.2	0.02	12.3	0.022	<0.1	4.98	11.7	0.14	101	<0.1	0.12	0.95	<0.05	126
50	9.56	-165	13.6	98	<0.2	0.03	11.4	0.006	<0.1	4.35	10.5	0.11	101	<0.1	0.11	0.39	<0.05	124
100MB at 46.6 PV																		
0	6.6	276	38.4	102	<0.2	0.08	25.1	9.270	<0.1	5.6	16.2	0.86	108	<0.1	0.44	32.32	0.097	121
2.5	8.84	195	40.5	100	0.369	0.06	21.6	0.009	<0.1	6.21	13.7	0.08	102	<0.1	0.37	15.82	<0.05	119
2.5	8.84	195	40.5	100	0.662	0.13	21.8	0.033	<0.1	8.61	13.8	0.09	107	<0.1	0.36	17.20	<0.05	119
10	9.22	71	35.5	100	<0.2	0.02	12.5	0.001	<0.1	5.38	12.8	0.08	103	<0.1	0.17	0.98	<0.05	116
15	9.34	-29	24.4	103	<0.2	0.02	11.4	0.007	<0.1	4.9	12.6	0.15	101	<0.1	0.15	0.78	<0.05	121
20	9.42	-53	26.7	100	<0.2	0.02	11.1	0.010	<0.1	5.04	12.5	0.12	103	<0.1	0.14	0.53	<0.05	116
30	9.48	-67	28.0	107	<0.2	0.02	10.4	0.017	<0.1	4.87	11.8	0.12	102	<0.1	0.13	0.92	<0.05	127
40	9.44	-115	23.1	104	<0.2	0.02	9.78	0.001	<0.1	5.05	10.9	0.13	99.6	<0.1	0.12	0.87	<0.05	123
100MB at 79.2 PV			FV2 = 24 cm/d															
0	6.33	369	32	98.1	<0.20	0.07	21.3	6.844	<0.10	5.0	14.1	0.78	110	<0.20	0.388	30.7	0.010	115
2.5	8.41	312	77.0	93.8	<0.20	0.14	32.0	2.077	<0.10	5.8	15.6	1.41	111	<0.20	0.602	30.4	0.010	115
10	9.26	12	47.0	91.4	<0.20	0.01	6.0	0.001	<0.10	5.1	16.3	<0.01	108	<0.20	0.060	1.4	0.010	111
20	9.46	-49	39.5	94.2	<0.20	0.01	5.8	0.001	<0.10	5.3	15.1	<0.01	107	<0.20	0.062	1.1	0.010	115
50	9.57	-521	16.3	98.1	<0.20	0.02	10.6	0.001	<0.10	5.2	4.4	<0.01	105	<0.20	0.143	1.4	0.010	115
100MB at 98 PV																		
0	7.37	266	35.4	95.5	<0.20	0.07	20.6	7.270	<0.10	5.4	14.1	0.86	99.3	<0.20	0.38	31.4	0.138	116
2.5	8.98	250	26.7	85.7	<0.20	0.04	17.1	5.800	<0.10	5.5	14.5	0.13	102	<0.20	0.30	28.6	0.088	113
5					<0.20	0.03	12.5	0.030	<0.10	5.6	10.0	<0.01	102	<0.20	0.23	15.4	0.017	
10	9.69	12	31.1	85.2	<0.20	<0.20	9.0	0.001	<0.10	5.2	9.8	<0.01	100	<0.20	0.11	3.1	0.049	113
20	9.48	81	12.7	90.0	<0.20	<0.20	9.1	0.030	<0.10	4.2	8.9	0.06	106	<0.20	0.12	0.4	0.137	120
30	9.35	-171	23.1	89.6	<0.20	<0.20	9.1	0.022	<0.10	4.0	8.2	0.06	105	<0.20	0.12	0.8	0.081	113
50	9.55	318	19.5	91.6	<0.20	0.03	9.0	0.001	<0.10	3.8	6.8	0.06	104	<0.20	0.12	0.8	0.013	118
100PL at 26 PV			FV1 = 53 cm/d															
0	6.29	317	23.0	98	<0.2	0.08	25.1	10.600	<0.1	5.07	16.1	0.87	102	<0.1	0.47	32.63	0.121	110
5	8.26	57	51.4	104	<0.2	0.05	24.3	0.032	0.629	5.05	15.7	0.38	101	<0.1	0.44	5.69	<0.05	123
10	9.17	-87	50.8	102	<0.2	0.04	20	0.034	<0.1	5.02	15.7	0.28	99.8	<0.1	0.33	1.21	<0.05	122
15	9.19	-165	34.5	99	<0.2	0.04	18	0.012	<0.1	4.96	15.7	0.23	102	<0.1	0.29	1.01	<0.05	118
20	9.39	-145	45.2	102	<0.2	0.03	16.9	0.015	<0.1	4.82	15.4	0.12	100	<0.1	0.26	0.90	<0.05	122
30	9.46	-194	40.2	96	<0.2	0.04	15.8	0.026	<0.1	4.84	14.6	0.10	99.8	<0.1	0.25	1.56	<0.05	110
40	9.29	-171	33.3	97	<0.2	0.05	15.1	0.004	<0.1	5.37	13.4	0.12	101	<0.1	0.23	0.71	<0.05	114
50	9.12	-42	29.8	99	<0.2	0.06	14.6	0.010	<0.1	4.83	12.1	0.11	100	<0.1	0.23	0.81	<0.05	111
100PL at 35 PV																		
0	6.6	561	24.9	92	<0.2	0.08	25	10.700	<0.1	4.83	15.8	0.87	99.3	<0.1	0.43	32.92	0.086	124
10	8.98	-124	39.8	100	0.219	0.03	18.7	0.001	<0.1	4.41	14.8	0.13	101	<0.1	0.28	1.24	<0.05	121
15	9.18	-170	25.8	100	<0.2	0.03	17.1	0.028	<0.1	4.73	14.7	0.21	102	<0.1	0.25	1.01	<0.05	121
20	9.33	-97	41.5	102	<0.2	0.03	16.3	0.008	<0.1	4.52	14.3	0.15	101	<0.1	0.23	1.23	<0.05	124
30	9.45	-107	30.7	99	<0.2	0.04	16	0.001	<0.1	4.66	14.1	0.11	104	<0.1	0.23	1.01	<0.05	124
40	9.46	-160	26.8	102	<0.2	0.04	16.2	0.033	<0.1	4.7	13.3	0.11	105	<0.1	0.24	0.85	<0.05	124
50	9.63	-63	23.1	101	<0.2	0.05	16.1	0.001	<0.1	4.75	12	0.10	104	<0.1	0.24	1.00	<0.05	123

Appendix G: Reactive column inorganic data

Distance along column (cm)	pH	Eh (mV)	Alkalinity		Al	Ba	Ca	Cr(OH) ₂ ⁺	Fe	K	Mg	Mn	Na	Ni	Sr	H ₄ SiO ₄	Zn	Cl
			CO ₃	SO ₄														
100PL at 58 PV																		
0	6.58	266	27.0	101	<0.2	0.08	24.5	10.500	<0.1	5.13	15.7	0.86	101	<0.1	0.43	32.47	0.133	118
5	8.47	351	41.7	96	<0.2	0.04	22.9	0.023	<0.1	5.8	14.5	0.16	107	<0.1	0.41	8.82	<0.05	116
10	9.19	70	33.2	96	<0.2	0.02	16.3	0.001	<0.1	5.24	14.3	0.05	107	<0.1	0.26	1.99	<0.05	115
15	9.23	-49	40.4	98	<0.2	0.02	14.8	0.001	<0.1	5.17	14	0.07	107	<0.1	0.22	1.36	<0.05	116
20	9.25	-102	34.5	97	<0.2	0.03	14.6	0.001	<0.1	4.4	13.8	0.08	107	<0.1	0.21	1.29	<0.05	119
30	9.39	-133	41.7	101	<0.2	0.03	13.9	0.022	<0.1	4.75	13.2	0.10	104	<0.1	0.20	1.24	<0.05	119
40	9.46	-36	31.5	100	<0.2	0.03	13.2	0.029	<0.1	4.11	12	0.08	104	<0.1	0.19	1.24	<0.05	122
100PL at 100.5 PV																		
			FV2 = 31 cm/d															
0	6.26	370	34.5	99.6	<0.20	0.08	22.9	7.255	<0.10	6.0	14.9	0.84	113	<0.20	0.401	31.8	0.010	117
2.5	8.36	296	58.6	95.1	<0.20	0.10	27.4	1.203	<0.10	5.1	14.9	1.05	107	<0.20	0.494	21.6	0.010	113
10	9.32	278	47.0	92.4	<0.20	0.03	9.1	0.001	<0.10	5.5	15.8	<0.01	111	<0.20	0.141	7.5	0.010	109
20	9.41	-512	36.6	95.9	<0.20	0.02	6.5	0.001	<0.10	5.0	15.1	<0.01	109	<0.20	0.085	1.2	0.010	114
50	9.22	156	12.3	109.0	<0.20	0.03	14.1	0.004	<0.10	4.4	6.0	<0.01	107	<0.20	0.227	1.4	0.010	115
100PL at 114.7 PV																		
0	7.33	319	35.9	93.9	<0.20	0.07	22.7	7.790	<0.10	4.1	14.9	0.89	107	<0.20	0.40	32.5	0.279	117
2.5	9.19	260	35.2	87.3	<0.20	0.04	18.8	6.190	<0.10	4.3	15.0	0.09	105	<0.20	0.31	29.6	0.081	113
5					<0.20	<0.20	6.6	0.136	<0.10	2.1	5.7	0.01	54.4	<0.20	0.11	11.4	0.189	
10	9.60	248	24.2	84.6	<0.20	<0.20	11.5	0.001	<0.10	4.8	9.2	<0.01	106	<0.20	0.18	8.3	0.016	109
20	9.33	21	23.1	90.9	<0.20	<0.20	9.7	0.021	<0.10	4.3	7.4	0.02	105	<0.20	0.13	2.9	0.022	118
30	9.56	86	16.0	89.6	<0.20	0.02	9.5	0.001	<0.10	4.5	7.4	0.02	104	<0.20	0.13	2.1	0.034	107
50	9.43	99	18.6	88.9	<0.20	0.03	9.4	0.001	<0.10	4.1	6.9	0.06	104	<0.20	0.14	0.4	0.083	110
50PLSSAQ at 5.2 PV																		
			FV1 = 79 cm/d															
0	6.84	213	31.4	95	<0.2	0.08	25.2	10.700	<0.1	4.57	15.8	0.86	98.3	<0.1	0.46	31.93	0.166	110
2.5	8.68	-88	34.0	100	<0.2	0.04	23.1	0.028	<0.1	5.43	14.6	0.31	97.1	<0.1	0.41	3.18	v	113
5	9.04	-85	35.4	116	<0.2	0.13	23.9	0.001	<0.1	4.35	15.1	0.35	101	<0.1	0.41	2.24	<0.05	118
10	9.2	-135	31.4	105	<0.2	0.03	23.2	0.026	<0.1	4.89	14.4	0.14	99.7	<0.1	0.41	1.89	<0.05	114
15	9.26	-155	46.5	101	<0.2	0.05	22.1	0.020	<0.1	3.56	12.6	0.10	96.9	<0.1	0.38	2.06	<0.05	113
20	9.22	-11	36.0	101	<0.2	0.02	22.2	0.012	<0.1	4.7	11.8	0.09	98	<0.1	0.39	2.10	<0.05	115
30	9.15	-149	23.8	100	<0.2	0.04	21.8	0.004	<0.1	3.5	9.41	0.08	97.3	<0.1	0.35	2.59	<0.05	116
40	9.31	-104	14.9	96	<0.2	0.03	21.3	0.018	<0.1	5.07	7.64	0.13	93.9	<0.1	0.28	1.40	<0.05	116
50	9.16	36	25.0	101	<0.2	0.02	22.5	0.015	<0.1	5.4	5.85	0.09	98.9	<0.1	0.21	1.34	<0.05	121
50PLSSAQ at 30.3 PV																		
0	6.46	355	21.7	100	<0.2	0.08	25.3	10.800	<0.1	4.49	16.2	0.85	100	<0.1	0.44	32.54	0.261	118
10	8.8	-33	37.8	99	0.232	0.06	22.9	0.066	<0.1	4.62	14.8	0.33	98.2	<0.1	0.41	1.42	<0.05	120
15	8.9	-44	45.2	96	<0.2	0.06	22.9	0.036	<0.1	5.15	14.5	0.52	97.3	<0.1	0.38	1.70	<0.05	113
20	9.02	-57	42.5	93	<0.2	0.04	22.6	0.026	<0.1	4.13	14.1	0.41	96.4	<0.1	0.37	1.81	<0.05	115
30	9.08	-124	39.9	98	<0.2	0.03	22.4	0.022	<0.1	4.35	13.3	0.14	95.2	<0.1	0.38	1.84	<0.05	118
40	9.14	-348	37.2	99	<0.2	0.02	21.9	0.025	<0.1	4.88	12.6	0.14	94.7	<0.1	0.39	1.67	<0.05	121
50	9.16	-68	37.2	97	<0.2	0.03	20.9	0.046	<0.1	4.91	11.8	0.09	95.5	<0.1	0.39	1.88	<0.05	120
50PLSSAQ at 66.2 PV																		
0	6.58	259	29.7	104	<0.2	0.08	24.2	10.400	<0.1	5.12	15.4	0.86	100	<0.1	0.43	32.06	0.103	114
2.5	8.18	109	51.9	106	<0.2	0.04	23	0.009	0.286	5.7	14.7	0.39	99.9	<0.1	0.40	13.27	<0.05	119
5	8.94	133	49.6	104	<0.2	0.03	22.3	0.043	<0.1	4.48	14.1	0.05	100	<0.1	0.38	1.85	<0.05	117
10	9.06	-50	45.9	105	<0.2	0.04	22.2	0.023	<0.1	5.03	14	0.07	100	<0.1	0.38	1.44	<0.05	116
15	8.95	-38	57.6	99	<0.2	0.05	21.9	0.045	<0.1	5.22	13.6	0.18	99.8	<0.1	0.37	1.63	<0.05	115
20	8.96	-93	47.3	105	<0.2	0.06	21.8	0.016	<0.1	5.18	13.4	0.30	101	<0.1	0.37	1.23	<0.05	120
30	9.08	-105	40.6	102	<0.2	0.03	21.6	0.032	<0.1	5.33	13.4	0.17	102	<0.1	0.38	1.08	<0.05	118
40	9.22	-78	34.9	100	<0.2	0.03	21.2	0.009	<0.1	4.82	13	0.12	101	<0.1	0.38	2.02	<0.05	118
50	9.17	22	43.8	100	<0.2	0.03	19.9	0.009	<0.1	4.77	12.6	0.09	99.7	<0.1	0.38	1.28	<0.05	118
50PLSSAQ at 116.8 PV																		
			FV2 = 36 cm/d															
0	6.27	364	26.3	99.0	<0.20	0.08	22.1	7.128	0.01	5.4	14.6	0.82	108	<0.02	0.383	30.6	0.010	117
2.5	7.41	99	58.6	95.6	<0.20	0.12	23.8	0.001	0.62	5.6	15.5	2.93	105	<0.02	0.428	25.7	0.010	114
10	9.17	197	50.7	92.3	<0.20	0.03	16.6	0.001	0.01	5.2	17.5	<0.01	106	<0.02	0.319	1.8	0.010	115
20	9.37	-436	44.8	82.5	<0.20	0.03	14.5	0.001	0.01	5.4	18.1	0.03	105	<0.02	0.280	1.7	0.010	114
50	9.26	-121	41.9	87.7	<0.20	0.03	14.9	0.001	0.01	6.2	11.1	<0.01	105	<0.02	0.302	1.7	0.010	111

Appendix H: Reactive column mineral saturation indices

Elizabeth City reactive columns
 Saturation indices calculated by MINTEQA2
 Based on UW Water Quality Lab data

Distance along

column (cm)	Ferrihydrite	Goethite	Cr(OH) ₃ (a)	Cr(OH) ₃ (c)	Calcite	Dolomite	Siderite (d)	Mackinawite	Magnesite	Rhodochro	Aragonite	Amakinite	SiO ₂ (a)	pH	Eh (mV)
50MBSSAQ at 8.6 PV			FV1 = 68 cm/d												
0	-1.317	4.393	0.450	-2.089	-1.523	-2.944	-3.133	-50.583	-1.996	-1.204	-1.677	-6.516	-0.411	6.88	178
2.5	-0.124	5.586	-0.099	-2.639	-0.516	-0.923	-1.491	-34.324	-0.982	-0.696	-0.670	-3.367	-1.108	8.15	-10
10	-0.161	5.549	1.893	-0.646	0.663	1.412	-1.227	-26.399	0.175	-0.294	0.509	-2.299	-1.686	9.14	-132
15	-0.371	5.339	1.335	-1.204	0.750	1.534	-1.169	-24.703	0.211	-0.433	0.595	-2.296	-1.687	9.15	-145
20	0.117	5.827	1.744	-0.795	0.725	1.414	-1.272	-26.792	0.115	-0.556	0.570	-2.054	-1.609	9.31	-140
30	-0.397	5.313	1.431	-1.108	0.878	1.505	-1.124	-22.668	0.054	-0.517	0.723	-2.060	-1.686	9.30	-169
40	0.757	6.467	-0.097	-2.637	0.863	1.024	-0.864	-26.902	-0.413	-0.834	0.709	-1.482	-1.493	9.43	-143
50MBSSAQ at 27.7 PV															
10	0.833	6.543	1.268	-1.272	0.622	1.381	-1.703	-41.534					-1.741	8.95	-14
15	0.790	6.500	1.264	-1.275	0.727	1.577	-1.693	-39.877					-1.845	9.09	-35
20	0.854	6.564	1.475	-1.065	0.774	1.654	-2.314	-44.964					-1.691	9.18	-8
30	0.750	6.460	1.028	-1.511	0.712	1.460	-1.934	-38.531					-1.727	9.27	-57
40	0.499	6.209	1.550	-0.990	0.710	1.444	-1.386	-32.613					-1.615	9.23	-94
50	-9.057	-3.347	1.811	-0.728	0.656	1.316	-4.107	0.713					-1.838	9.28	-506
50MBSSAQ at 48.1 PV															
0	-0.765	4.945	0.314	-2.225	-1.583	-3.065	-3.201	-57.894						6.71	241
2.5	-0.196	5.514	1.066	-1.474	-1.195	-2.272	0.179	-29.674						7.09	35
5	2.184	7.894	0.873	-1.666	-0.283	-0.456	-0.733	-51.708						7.92	134
10	-0.117	5.594	1.287	-1.253	0.291	0.700	-1.613	-35.106						8.63	-39
15	-0.041	5.669	1.745	-0.794	0.558	1.229	-1.273	-30.492						8.92	-89
20	0.423	6.133	1.338	-1.202	0.759	1.635	-1.275	-33.683						9.07	-76
30	-0.295	5.415	1.412	-1.128	0.746	1.618	-1.140	-25.745						9.14	-137

Notes: Calculations assume that the t=0 Cr composition is dominantly Cr(VI), and that the Cr(III) concentration is one half the analytical detection limit (0.01 mg/L)

- (a) = amorphous
- (c) = crystalline
- (d) = disordered, or freshly precipitated

Appendix H: Reactive column mineral saturation indices

Elizabeth City reactive columns
 Saturation indices calculated by MINTEQA2
 Based on UW Water Quality Lab data

Distance along column (cm)	Ferrihydrite	Goethite	Cr(OH) ₃ (a)	Cr(OH) ₃ (c)	Calcite	Dolomite	Siderite (d)	Mackinawite	Magnesite	Rhodochro	Aragonite	Amakinite	SiO ₂ (a)	pH	Eh (mV)
50MBSS at 27.9 PV															
	FV1 = 55 cm/d														
0	-0.634	5.076	-0.007	-2.546	-2.033	-3.963	-3.689	-64.316	-2.504	-1.715	-2.187	-7.547	-0.395	6.38	307
2.5	-0.114	5.596	1.076	-1.463	-1.210	-2.305	0.438	-30.776	-1.670	-0.852	-1.364	-3.239	-0.532	6.90	56
5	0.370	6.080	1.246	-1.293	-1.034	-1.964	0.244	-33.167	-1.504	-0.852	-1.189	-3.010	-0.727	7.19	54
10	1.398	7.108	1.255	-1.284	0.120	0.355	-3.345	-66.376	-0.339	-0.227	-0.035	-5.540	-1.454	8.31	196
15	1.104	6.814	0.996	-1.544	0.290	0.734	-6.474	-89.520	-0.129	0.022	0.135	-8.311	-1.721	8.59	324
20	1.002	6.712	1.156	-1.383	0.392	0.966	-3.437	-57.258		0.293	0.238	-4.744	-1.767	8.92	91
30	0.914	6.624	1.263	-1.276	0.565	1.384	-4.857	-68.489	0.245	0.210	0.410	-6.027	-1.848	9.12	149
40	0.914	6.624	0.853	-1.686	0.403	1.121	-7.915	-95.041	0.144	-0.156	0.249	-8.979	-1.883	9.12	321
50	0.755	6.465	-0.813	-3.353	0.584	1.522	-8.803	-99.594	0.364	-0.289	0.429	-9.563	-1.890	9.39	330
50MBSS at 34.4 PV															
0	1.049	6.759	0.707	-1.833	-1.090	-2.067	-6.345	-95.235	-1.551	-0.778	-1.244		-0.400	7.32	451
2.5	1.749	7.459	1.323	-1.216	-0.845	-1.562	0.157	-43.329	-1.291	-0.609	-0.999		-0.595	7.41	113
5	2.158	7.868	-1.312	-3.852	-0.050	0.022	-6.851	-102.174	-0.502	-0.330	-0.204		-1.085	8.33	431
10	1.020	6.730	1.288	-1.252	0.478	1.133	-5.723	-79.383	0.080	-0.559	0.324		-1.542	8.88	237
15	0.997	6.707	1.588	-0.951	0.401	1.023	-3.429	-57.221	0.048	-0.404	0.247		-1.740	8.93	90
20	0.769	6.479	1.181	-1.359	0.438	1.127	-1.620	-39.794	0.115	-0.068	0.283		-1.798	8.94	-25
30	-0.018	5.692	1.416	-1.124	0.164	0.639	-1.431	-28.872	-0.099	-0.003	0.010		-1.431	9.00	-105
40	0.546	6.256	-0.084	-2.624	0.613	1.553	-1.389	-33.581	0.366	-0.139	0.458		-1.832	9.24	-88
50	0.686	6.396	1.211	-1.328	0.486	1.306	-1.817	-36.126	0.246	-0.395	0.332		-1.951	9.33	-77
50MBSS at 53.5 PV															
0	-0.453	5.257	0.121	-2.418	-1.850	-3.584	-3.487	-63.999	-2.308	-1.477	-2.004		6.50	297	
2.5	0.816	6.526	1.257	-1.283	-1.424	-2.741	-0.047	-38.822	-1.891	-1.016	-1.578		7.00	107	
5	-0.018	5.692	0.998	-1.541	-0.812	-1.510	0.297	-29.982	-1.272	-0.666	-0.966		7.30	23	
10	1.128	6.838	-0.080	-2.619	0.176	0.489	-5.496	-81.733	-0.261	-0.634	0.022		8.46	283	
15	0.863	6.573	1.374	-1.166	0.253	0.728	-1.856	-42.554	-0.099	-0.763	0.098		8.82	2	
20	0.835	6.545	1.607	-0.933	0.493	1.249	-1.705	-41.548	0.182	-0.385	0.339		8.95	-14	
30	0.341	6.051	-0.077	-2.617	0.266	0.849	-1.428	-31.818	0.009	-0.252	0.111		9.06	-88	
40	0.759	6.469	0.919	-1.621	0.368	1.099	-1.823	-38.110	0.157	-0.351	0.214		9.18	-53	
50	0.887	6.597	1.334	-1.205	0.191	0.752	-3.788	-55.504	-0.013	-0.489	0.036		9.17	61	

Appendix H: Reactive column mineral saturation indices

Elizabeth City reactive columns
 Saturation indices calculated by MINTEQA2
 Based on UW Water Quality Lab data

Distance along

column (cm)	Ferrihydrite	Goethite	Cr(OH) ₃ (a)	Cr(OH) ₃ (c)	Calcite	Dolomite	Siderite (d)	Mackinawite	Magnesite	Rhodochro	Aragonite	Amakinite	SiO ₂ (a)	pH	Eh (mV)
100MB at 24 PV															
	FV1 = 43 cm/d														
0	-0.491	5.220	-0.142	-2.682	-2.132	-4.160	-3.810	-67.637	-2.603	-1.814	-2.286	-7.816	-0.396	6.26	338
2.5	-1.725	3.985	1.505	-1.035	-0.520	-0.938	-0.158	-18.113	-0.993	-0.596	-0.674	-3.113	-0.941	7.60	-86
10	-0.801	4.909	-0.078	-2.617	0.380	1.116	-1.214	-21.475	0.162	-0.014	0.225	-2.333	-1.918	9.10	-165
15	0.707	6.417	1.624	-0.915	0.462	1.344	-4.029	-54.533	0.308	0.015	0.307	-4.583	-2.155	9.46	33
20	0.146	5.856	0.607	-1.932	0.366	1.175	-1.287	-26.457	0.234	-0.222	0.212	-1.989	-2.074	9.36	-145
30	-0.634	5.076	-0.079	-2.618	0.162	0.769	-1.264	-22.297	0.033	-0.305	0.008	-2.272	-2.149	9.12	-160
40	0.636	6.346	0.793	-1.747	0.393	1.230	-7.239	-81.627	0.263	-0.142	0.239	-7.638	-2.168	9.56	201
50	0.838	6.548	0.997	-1.543	0.146	0.590	-2.413	-42.720	-0.130	-0.263	-0.009	-3.214	-2.159	9.20	-24
100MB at 29.2 PV															
0	0.504	6.214	0.005	-2.535	-2.050	-4.013	-6.975	-102.532	-2.537	-1.756	-2.205		-0.396	6.39	561
2.5	0.454	6.164	1.885	-0.654	0.798	1.759	-1.292	-32.535	0.387	-0.586	0.644		-1.868	9.22	-94
10	-0.023	5.687	1.331	-1.209	0.482	1.249	-1.241	-26.281	0.194	-0.107	0.327		-2.133	9.24	-139
15	0.636	6.346	1.248	-1.292	0.584	1.497	-1.748	-34.942	0.339	-0.007	0.430		-2.161	9.40	-90
20	0.695	6.405	1.419	-1.121	0.526	1.382	-2.699	-42.496	0.281	-0.206	0.372		-2.050	9.46	-45
30	0.603	6.314	1.472	-1.067	0.379	1.062	-2.249	-35.125	0.109	-0.277	0.225		-2.212	9.54	-99
40	0.386	6.096	1.449	-1.091	0.382	1.042	-1.591	-27.592	0.086	-0.272	0.227		-2.060	9.54	-149
50	0.280	5.990	0.890	-1.649	0.283	0.831	-1.556	-25.469	-0.027	-0.399	0.129		-2.451	9.56	-165
100MB at 46.6 PV															
0	-0.512	5.198	0.215	-2.324	-1.673	-3.239	-3.335	-61.839						6.60	276
2.5	1.034	6.744	1.102	-1.437	0.470	1.042	-4.904	-72.418						8.84	195
2.5	1.034	6.744	-0.074	-2.613	0.473	1.046	-4.905	-72.420						8.84	195
10	0.859	6.570	0.218	-2.322	0.497	1.307	-3.819	-57.604						9.22	71
15	0.772	6.482	0.989	-1.551	0.388	1.120	-2.624	-43.548						9.34	-29
20	0.712	6.422	1.134	-1.405	0.471	1.296	-2.414	-40.792						9.42	-53
30	0.667	6.377	1.345	-1.194	0.499	1.357	-2.336	-39.306						9.48	-67
40	0.538	6.248	-0.098	-2.637	0.371	1.091	-1.631	-31.588						9.44	-115
100MB at 79.2 PV															
	FV2 = 24 cm/d														
0	0.078	5.788	-0.060	-2.600	-2.082	-4.046	-3.874	-72.653	-2.539	-1.739	-2.236	-7.850	-0.421	6.33	369
2.5	1.135	6.845	3.454	0.915	0.509	1.004	-5.648	-85.706	-0.079	0.604	0.354	-7.894	-0.436	8.41	312
10	0.829	6.539	-0.085	-2.625	0.329	1.396	-2.800	-48.998	0.493	-1.352	0.174	-3.901	-1.835	9.26	12
20	0.689	6.399	-0.100	-2.639	0.381	1.485	-2.421	-41.899	0.529	-1.338	0.227	-3.194	-1.989	9.46	-49
50	-7.967	-2.257	-0.111	-2.650	0.406	0.734	-3.615	1.502	-0.246	-1.394	0.252	-3.859	-1.886	9.57	-521
100MB, 98 PV															
0	0.966	6.676	0.728	-1.810	-1.017	-1.902	-3.260	-67.301	-1.460	-0.642	-1.173	-6.233	-0.412	7.37	266
2.5	0.980	6.691	3.907	1.367	0.322	0.873	-6.379	-82.565	-0.024	-0.366	0.168	-7.554	-0.491	8.98	250
10	0.536	6.246	-0.127	-2.667	0.618	1.581	-4.268	-54.038	0.389	-1.330	0.463	-4.624	-1.590	9.69	12
20	0.695	6.405	1.597	-0.942	0.118	0.524	-5.197	-62.202	-0.168	-0.717	-0.036	-5.439	-2.421	9.48	81
30	-0.235	5.475	1.466	-1.074	0.293	0.841	-1.230	-22.777	-0.026	-0.656	0.138	-1.914	-2.092	9.35	-171
50	0.644	6.354	-2.806	-5.346	0.350	0.881	-9.280	-99.621	-0.044	-0.625	0.196	-9.628	-2.137	9.55	318

Appendix H: Reactive column mineral saturation indices

Elizabeth City reactive columns
Saturation indices calculated by MINTEQA2
Based on UW Water Quality Lab data

Distance along

column (cm)	Ferrihydrite	Goethite	Cr(OH) ₃ (a)	Cr(OH) ₃ (c)	Calcite	Dolomite	Siderite (d)	Mackinawite	Magnesite	Rhodochro	Aragonite	Amakinite	SiO ₂ (a)	pH	Eh (mV)
50PLSSAQ at 5.2 PV															
	FV1 = 79 cm/d														
0	-0.842	4.868	0.420	-2.119	-1.511	-2.927	-3.150	-55.102	-1.991	-1.203	-1.666	-6.602	-0.405	6.84	213
2.5	-0.615	5.095	1.588	-0.951	0.283	0.665	-1.438	-28.593	-0.192	-0.085	0.128	-3.049	-1.426	8.68	-88
5	0.377	6.087	-0.077	-2.616	0.614	1.330	-1.245	-31.962	0.141	0.107	0.460	-2.468	-1.603	9.04	-85
10	-0.286	5.424	1.551	-0.988	0.684	1.462	-1.452	-26.700	0.204	-0.263	0.530	-2.433	-1.696	9.20	-135
15	-0.311	5.399	1.433	-1.106	0.875	1.811	-1.090	-24.308	0.362	-0.355	0.721	-2.175	-1.667	9.26	-155
20	0.838	6.548	1.218	-1.322	0.744	1.515	-2.435	-44.961	0.197	-0.433	0.589	-3.457	-1.653	9.22	-11
30	-0.363	5.347	0.765	-1.774	0.514	0.964	-1.291	-24.075	-0.125	-0.555	0.360	-2.220	-1.552	9.15	-149
40	0.558	6.268	1.389	-1.151	0.427	0.709	-1.706	-31.874	-0.293	-0.374	0.273	-2.231	-1.843	9.31	-104
50	0.889	6.599	1.317	-1.222	0.559	0.833	-3.212	-51.499	-0.300	-0.492	0.404	-4.153	-1.840	9.16	36
50PLSSAQ at 30.3 PV															
0	0.213	5.923	0.079	-2.460	-2.051	-3.998	-3.933	-71.785	-2.522	-1.739	-2.205	-7.604	-0.396	6.46	355
10	0.460	6.170	1.964	-0.576	0.430	0.969	-1.513	-37.336	-0.035	0.014	0.275	-3.038	-1.782	8.80	-33
15	0.531	6.241	1.704	-0.835	0.593	1.287	-1.386	-36.678	0.121	0.276	0.438	-2.878	-1.711	8.90	-44
20	0.577	6.287	1.557	-0.982	0.664	1.424	-1.400	-35.956	0.186	0.199	0.509	-2.728	-1.694	9.02	-57
30	-0.208	5.502	1.479	-1.061	0.682	1.438	-1.191	-27.026	0.183	-0.261	0.527	-2.424	-1.693	9.08	-124
40	-6.086	-0.374	2.756	0.216	2.520	5.124	-2.402	1.740	2.030	1.074	2.366	-4.516	-0.523	9.14	-348
50	0.644	6.354	1.800	-0.739	0.689	1.432	-1.502	-35.705	0.169	-0.441	0.535	-2.612	-1.693	9.16	-68
50PLSSAQ at 66.2 PV															
0	-0.839	4.872	0.197	-2.342	-1.816	-3.532	-3.440	-59.306	-2.290	-1.486	-1.971			6.58	259
2.5	2.386	8.096	1.079	-1.460	-0.016	0.071	-0.611	-50.500	-0.487	-0.174	-0.170			8.18	109
5	0.996	6.706	1.777	-0.763	0.651	1.405	-4.002	-63.961	0.179	-0.718	0.497			8.94	133
10	0.676	6.386	1.503	-1.037	0.715	1.532	-1.472	-37.327	0.243	-0.551	0.561			9.06	-50
15	0.638	6.348	1.795	-0.745	0.716	1.526	-1.381	-38.034	0.237	-0.141	0.561			8.95	-38
20	-0.033	5.677	1.340	-1.199	0.638	1.365	-1.215	-30.294	0.153	0.059	0.483			8.96	-93
30	0.080	5.790	1.647	-0.893	0.670	1.435	-1.221	-29.658	0.191	-0.175	0.516			9.08	-105
40	0.623	6.333	1.093	-1.447	0.710	1.509	-1.515	-34.833	0.225	-0.312	0.555			9.22	-78
50	0.878	6.588	1.095	-1.444	0.741	1.586	-2.764	-49.475	0.271	-0.422	0.586			9.17	22
50PLSSAQ at 116.8 PV															
0	-0.107	5.603	-0.129	-2.668	-2.216	-4.315	-3.943	-71.403	-2.673		-2.370	-7.889	-0.422	6.27	364
2.5	0.678	6.388	-0.257	-2.796	-0.706	-1.301	-0.547	-42.243	-1.169	-0.860	-3.695	-0.499	7.41	99	
10	0.887	6.598	-0.081	-2.620	0.721	1.768	-5.697	-76.537	0.473	0.566	-6.928	-1.713	9.17	197	
20	-6.943	-1.232	-0.092	-2.632	0.795	1.994	-3.164	1.387	0.625	0.640	-4.093	-1.769	9.37	-436	
50	0.209	5.919	-0.085	-2.625	0.677	1.530	-1.190	-29.090	0.279	0.523	-2.238	-1.750	9.26	-121	
50PLSSAQ, 135.3 PV															
0	1.044	6.754	0.720	-1.820	-1.002	-1.886	-4.082	-75.392	-1.460	-0.658	-1.158	-7.062	-0.399	7.35	320
2.5	1.106	6.817	3.348	0.809	0.263	0.668	-6.012	-85.437	-0.169	-0.249	0.108	-7.852	-0.521	8.58	298
10	0.775	6.485	-0.179	-2.719	0.657	1.475	-7.728	-90.157	0.243	-1.378	0.503	-8.500	-1.618	9.36	271
20	-2.379	3.331	-0.051	-2.590	0.755	1.635	-1.025	-6.546	0.306	-0.774	0.600	-2.034	-1.553	9.30	-286
30	0.762	6.472	1.487	-1.053	0.677	1.447	-6.146	-75.998	0.196	-0.985	0.522	-6.937	-1.483	9.38	178
50	0.782	6.492	-1.969	-4.508	0.545	1.180	-8.604	-97.742	0.060	-1.161	0.391	-9.341	-1.882	9.35	321
48PL/52AQ at 78.4 PV															
0	1.037	6.747	0.716	-1.824	-1.050	-1.999	-4.025	-74.463	-1.524	-0.710	-1.206	-6.974	-0.408	7.34	315
2.5	1.080	6.790	3.720	1.180	0.240	0.594	-6.436	-86.660	-0.220	-0.808	0.085	-7.988	-0.482	8.69	298
5	1.078	6.788	1.650	-0.889	0.242	0.560	-5.722	-80.315	-0.256	-0.925	0.088	-7.280	-0.750	8.70	256
10	0.935	6.645	1.754	-0.785	0.631	1.343	-6.602	-84.922	0.138	-1.007	0.477	-7.838	-1.827	9.08	258
15	0.734	6.444	-0.096	-2.636	0.672	1.354	-3.603	-51.466	0.108	-0.894	0.518	-4.224	-2.037	9.42	16
20	0.775	6.485	1.465	-1.075	0.824	1.591	-6.477	-80.235	0.192	-1.268	0.670	-7.402	-1.852	9.36	207
30	0.473	6.183	-0.119	-2.658	0.927	1.625	-1.666	-31.547	0.125	-1.146	0.772	-2.189	-1.736	9.63	-130
40	0.439	6.149	1.455	-1.085	0.689	0.972	-3.881	-47.858	-0.292	-1.252	0.535	-3.983	-1.926	9.81	-38
50	0.390	6.100	-0.323	-2.862	0.721	0.758	-9.235	-96.377	-0.536	-1.265	0.566	-9.395	-1.785	9.87	271

Appendix I: Analytical laboratory procedures

Cations

Ion analyses of the lab treatability samples were performed at the Water Quality Lab (WQL), University of Waterloo. Analytical charge balance errors of < 5% were regularly achieved.

Cations were determined using an Inductively Coupled Plasma Atomic Emission Spectrometer (ICP-AES) instrument (Thermo Jarrell Ash IRIS Plasma Spectrometer). The instrument conditions were set according to the manufacturer's instructions. Prepared mixed standards, with element concentrations of 10 mg/L, were run after every five to ten samples. A commercial mixed standard was used to verify the prepared standards on a regular basis. Samples were run in duplicate and were usually diluted due to the small sample volume available from the batch and column tests. Sample analyses were repeated if the relative difference on the prepared standards exceeded 5%.

Anions

Anions including Br, Cl and SO₄ were analyzed using a Dionex System 2000 Ion Chromatograph (IC) or a Waters IC with a conductivity detector. The Dionex IC was capable of running 55 samples per day plus standards and the Waters IC could run 33 samples per day plus standards. Samples were run a minimum of two times and at different dilution ratios to verify sample reproducibility and linearity of the calibration.

The IC instrument was evaluated daily for calibration linearity. Three sets of standards were run at regular intervals:

1. A prepared mixed standard containing 2 mg/L Cl, 5 mg/L Br, 10 mg/L SO₄, 5 mg/L NO₃ and 10 mg/L PO₄
2. an additional prepared mixed standard containing 0.4 mg/L Cl, 1 mg/L Br, 2 mg/L SO₄, 1 mg/L NO₃, and 2 mg/L PO₄
3. a commercial setpoint mixed standard at ion concentrations similar to standard #1

The two in-house standards were run after every eleven samples. The setpoint standard was run at least twice per day as were blanks. Sample analyses were repeated if the relative difference on the setpoint standard exceeded 5%.